METEOR-Berichte 02-2

North Atlantic 2001

Cruise No. 50

7 May – 12 August 2001

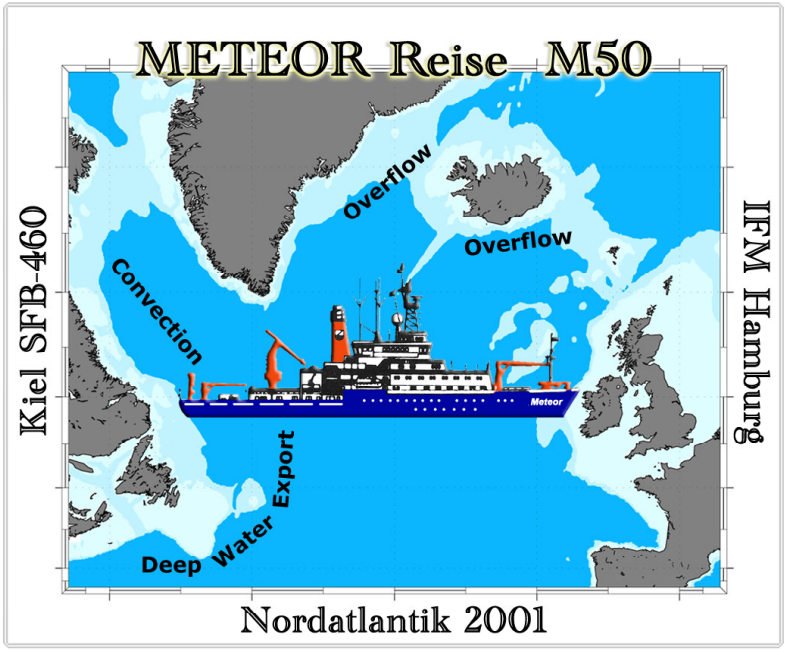

Friedrich Schott, Jürgen Fischer, Jürgen Holfort and Walter Zenk

Editorial Assistance:

Frank Schmieder
Fachbereich Geowissenschaften, Universität Bremen

Leitstelle METEOR
Institut für Meereskunde der Universität Hamburg

2002

The METEOR-Berichte are published at irregular time intervals. They are working papers for people who are occupied with the respective expedition and are intended as reports for the funding institutions. The opinions expressed in the METEOR-Berichte are only those of the authors. The reports can be obtained from:

Leitstelle METEOR
Institut für Meereskunde
Troplowitzstr. 7
22529 Hamburg
Germany

The reports are available in PDF format (with colored figures) from www.marum.de.
The METEOR expeditions are funded by the *Deutsche Forschungsgemeinschaft* and the *Bundesministerium für Bildung und Forschung*.

Addresses of the editors:

Prof. Dr. F. Schott, Dr. J. Fischer, Dr. W. Zenk
Institut für Meereskunde
Düsternbrooker Weg 20
24105 Kiel

Dr. J. Holfort
Institut für Meereskunde
an der Universität Hamburg
Troplowitzstraße 7
22529 Hamburg

Quotation:

Schott, F., J. Fischer, J. Holfort and W. Zenk (2002). North Atlantic, Cruise No. 50, 7 May – 12 August 2001. METEOR-Berichte, Universität Hamburg, 02-2, 123 pp.

ISSN 0 9 3 6 - 8 9 5 7

Table of Contents

Table of Contents, Part 1 (M 50/1)

Table of Contents, Part 2 (M 50/2)

Table of Contents, Part 3 (M 50/3)

Table of Contents, Part 4 (M 50/4)

Abstract

METEOR-cruise 50 took place in the North Atlantic Ocean with measurements north of 40°N (Figure 1). The cruise began on 7 May 2001 in Halifax and ended on 12 August 2001 at the shipyard in Rendsburg. METEOR-cruise 50 consisted of four legs with activities in Physical Oceanography and Marine Chemistry.

During the first leg (Halifax - St. John's) the changes of the deep circulation and water mass distribution were investigated in the Irminger Sea within the context of the SFB 460 of IfM Kiel. The southern zonal section was a repeat survey of the western part of the WOCE A2 section. For measuring water mass transports a deep reaching profiling Acoustic Doppler current meter (Ocean Surveyor) was used for the first time. Another ADCP was lowered with the CTD (LADCP). To characterize the water masses, CTD hydrography and tracer measurements (Freon) were carried out. The Deep Water Export Array located within the western boundary current off the Grand Banks as well as moorings at 53°N and the Mid-Atlantic Ridge at about 45°N were recovered and redeployed.

The second leg (St. John's - St. John's), also operated by IfM Kiel, was dedicated to mooring work and hydrographic measurements in the Labrador Sea and at the 53°N mooring array, again within the context of the SFB 460. The hydrographic measurements were a continuation of annual repeat surveys since 1996 to investigate the variability of water mass transformation and its relation to the large scale deep circulation. In the Labrador Sea, a number of tomography and convection moorings were recovered and redeployed.

During the third leg, (St.Johns – Reykjavik) mooring work and hydrographic measurements were carried out by IfM Hamburg along sections normal to the southeastern slope of Greenland. The scientific objectives were the long-term description of the composition of the Denmark Strait Overflow and its temporal variability, in continuation of the work of the EU Project VEINS on the Variability of Exchanges in the Northern Seas.

The return leg (Reykjavik - Germany) took place in the overflow regions around Iceland and particularly in the eastern basin of the subpolar North Atlantic. The investigation concentrated primarily on the spreading and mixing of water masses of the region. The field program was part of research initiatives of IfM Kiel (SFB 460) and BSH Hamburg (repeat of WOCE section A1). Observations of the deep circulation and of mass distributions included meaasurements of current, nutrients, CO_2 and tracers. In addition, a research group from GEOMAR Kiel investigated methane sources that were detected during an earlier cruise at the Mid-Atlantic Ridge.

Zusammenfassung

Die METEOR-Reise M50 fand im Nordatlantischen Ozean statt, nördlich von 40°N (Abbildung 1). Die Reise begann am 7. Mai 2001 in Halifax und endete am 12. August 2001 in der Werft Rendsburg. Die METEOR-Fahrt 50 setzte sich aus vier Fahrtabschnitten zusammen, die physikalisch-ozeanographische und meereschemische Arbeiten beinhalteten.

Im ersten Abschnitt (Halifax - St. John's) wurden im Rahmen des SFB 460 der Universität Kiel die Änderungen der Tiefenzirkulation und Wassermassenverteilung in der Irminger See untersucht. Dabei stellte der südliche Zonalschnitt eine wiederholte Aufnahme des westlichen WOCE A2-Schnittes dar. Zum Einsatz für die Bestimmung von Wassermassentransporten kamen erstmalig ein neuer tiefreichender Schiffs-ADCP (ocean surveyor) sowie ein an der CTD-

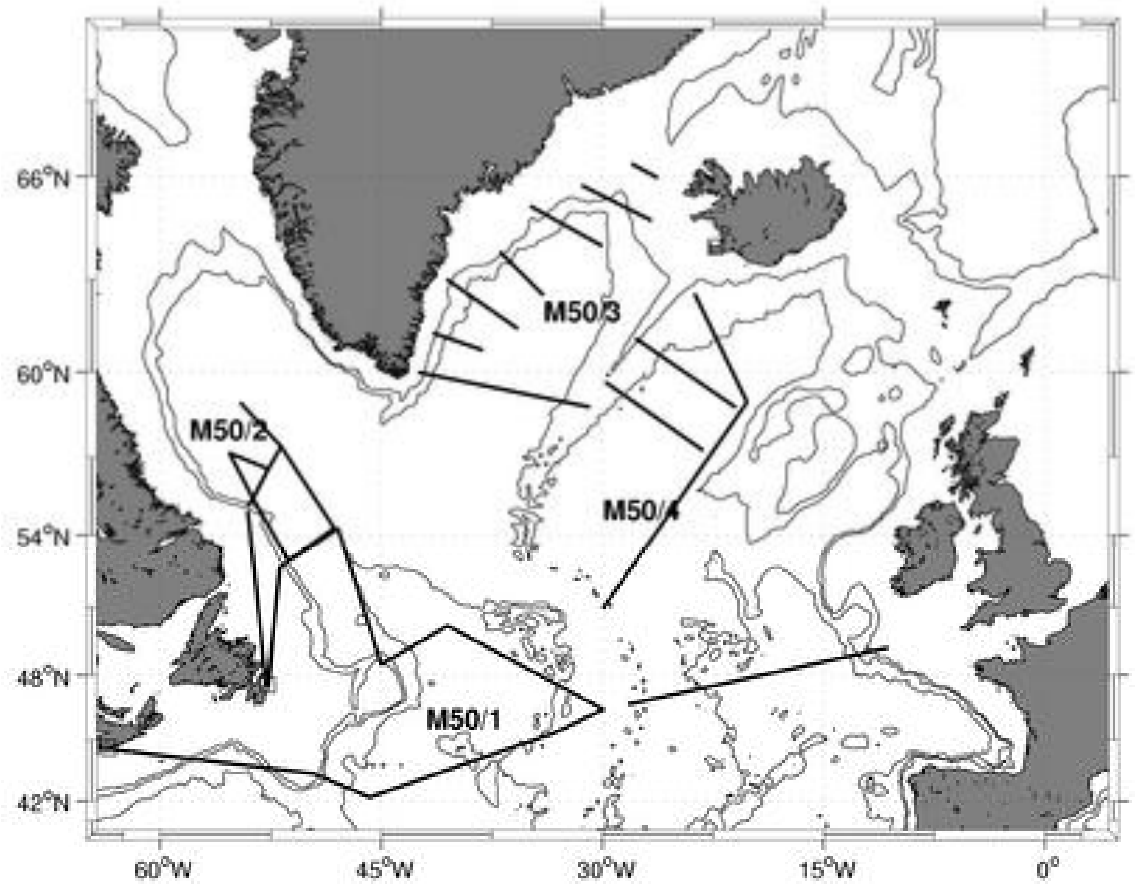

Fig. 1: Cruise track of METEOR cruise M 50.

Sonde mitgefierter ADCP (LADCP). Zur Charakterisierung der Wassermassen wurden CTD-Hydrographie und Tracermessungen (Freone) durchgeführt. Im tiefen westlichen Randstrom bei den Grand Banks wurde der seit 1997 installierte Tiefenwasserexport-Array ausgetauscht. Ebenfalls aufgenommen und wieder ausgelegt wurden Verankerungen bei 53°N sowie am Mittelatlantischen Rücken bei ca. 45°N.

Im zweiten Abschnitt (St. John's - St. John's) standen Verankerungsarbeiten ergänzt durch hydrographische Messungen in der Labradorsee und beim 53°N Verankerungsarray im Vordergrund. Diese Reise fand ebenfalls im Rahmen des Kieler SFB 460 statt. Die hydrographischen Messungen stellten eine Fortführung von jährlich seit 1996 stattfindenden Messungen dar, um die Variabilität der Wassermassentransformation und ihre Auswirkungen auf die Tiefenzirkulation zu untersuchen. Es wurden eine Reihe von Tomographie- und Konvektionsverankerungen geborgen und wieder neu ausgelegt.

Auf dem dritten Fahrtabschnitt (St. Johns – Reykjavik) wurden Verankerungsarbeiten und hydrographische Messungen entlang der Südostküste Grönlands von Kap Farvel bis zur Dänemarkstraße unter der Leitung des Instituts für Meereskunde der Universität Hamburg durchgeführt. Das wissenschaftliche Ziel hierbei ist die längerfristige Zustandsbeschreibung der Overflow-Komponenten im nordwestlichen Atlantik und die Erfassung ihrer zeitlichen Variabilität und schließt dabei an das EU-Projekt VEINS (Variability of Exchanges in the Northern Seas) an.

Während des letzten Fahrtabschnittes (Reykjavik - Deutschland) bestand das Ziel darin, die Ausbreitung und Vermischung von Wassermassen in den Overflow-Gebieten um Island und speziell im östlichen Becken des subpolaren Nordatlantiks zu untersuchen. Die Arbeiten

gehörten zu den wiederholt durchgeführten Feldprogrammen des Kieler SFB 460 und des Hamburger Bundesamtes für Seeschiffahrt und Hydrographie (WOCE-Schnitt A2). Die Beobachtungen zur Tiefenzirkulation und zu Massenverteilung mit zugehörigen Strömungsmessungen umfassten auch Nährstoff-, CO_2- und Tracermessungen. Ferner wurde den früher entdeckten Spuren von Methanausscheidungen am Mittelatlantischen Rücken von einer GEOMAR-Forschergruppe aus Kiel nachgegangen.

Reseach Objectives

The research of METEOR cruise M 50 was mainly in the context of the Kiel Sonderforschungsbereich 460 as well as on the VEINS/ASOF projects.

Sonderforschungsbereich SFB 460

The Sonderforschungsbereich SFB 460 „Dynamics of thermohaline circulation variability" started in 1996 at Kiel University. Main objective of the SFB 460 is to investigate the variability of the watermass formation and transport processes in the subpolar North Atlantic and to gain an understanding of its role in the dynamics of the thermohaline circulation and the ocean uptake of anthropogenic CO_2. The variability of circulation and water mass distribution are closely related with climate changes in northern Europe through the North Atlantic Oscillation (NAO). These connections are a focus of the ongoing research.

The research program of the SFB is based on a combination of physical-oceanographic, marine chemistry and meteorological observation programs, which are operated in close interaction with a continuous series of numerical models with moderate (50 km), high (15 km) and very high resolution (5 km), allowing a simulation of current structures and variability over a wide range of space and time scales. The main interests are, first of all, the water mass formation processes and the circulation of deep water in the subpolar North Atlantic, their interaction and integral effects, especially with regard to the uptake of anthropogenic CO_2. Second, the variability of the ocean - atmosphere interaction is investigated, and modelling investigations of large-scale aspects and causes of this variability are supplemented by the analysis of fluxes from different meteorological standard models in comparison with observations.

The legs M50/1, M50/2 and M50/4 were carried out within the context of the SFB 460. Several cruises had been carried out during the last three years to improve the data basis with a wide range of hydrographic, tracer and current measurement techniques for investigating the variability of the circulation in the North Atlantic. During the three M50-legs the study of the pathways of the deep circulation and variability of water mass distribution were of prime interest. Besides the shipboard measurements, a large part of the work was mooring work and the deployment of floats.

The marine chemistry group took samples on legs 1 and 4 for the analysis of total dissolved inorganic carbon, alkalinity, nutrients and dissolved oxygen. All analyses were carried out on board. Nutrients will be used mainly as indicators for water mass properties, while the other parameters are needed to calculate the uptake of anthropogenic CO_2 into the water column. A significant signal can be expected even at greater water depths in the study area. Transport of anthropogenic CO_2 into the Deep Water is mainly through the thermohaline circulation. Hence,

the investigations carried out during this cruise will serve to detect variations in later studies within the SFB.

VEINS/ASOF

VEINS (Variability of Exchanges in the Northern Seas) was an EU-MAST Project focussing on the variability of oceanic fluxes between the Arctic Ocean and the Northern North Atlantic for a period of three years. It was aimed at developing a cost-efficient array for the long-term monitoring of the polar and subpolar contributions to the decadal climate variability.

VEINS achieves a synoptic coverage of fluxes through Fram Strait, the Western Barents Shelf, the Iceland-Scotland Ridge and the Denmark Strait, including the continental slope of SE-Greenland. The latter was the work area for cruise leg M50/3, where the fluctuations of the Denmark Strait Overflow Water (DSOW)-transports and the entrainment of Atlantic water are major controls of North Atlantic Deep Water formation.

At present a new program "Arctic Subarctic Ocean Fluxes" (ASOF) is being planned in cooperation between several European partners, the US and Canada. The ASOF objective is monitoring of the ice export from and water mass exchange between the Arctic Ocean and the Atlantic and Pacific for the foreseeable future

Acknowledgements

The 50th cruise of RV METEOR served a multi-disciplinary group of projects in the North Atlantic Ocean. All groups and institutions involved helped to support the coordination work. It is our particular pleasure to thank the captains M. Kull and N. Jakobi and crew of all cruise legs for the flexible, friendly and very helpful attitude and professional assistance during the deployments of the complex moored arrays and the various kinds of shipboard measurement programs.

Special thanks is expressed to *Deutsche Forschungsgemeinschaft* (DFG) for making available the shiptime and funding for cruise M50. Projects of the *Sonderforschungsbereich 460* during several cruise legs were also funded by the DFG.

METEOR-Berichte 02-2

North Atlantic 2001

Part 1

Cruise No. 50, Leg 1

7 May – 31 May 2001, Halifax – St. John's

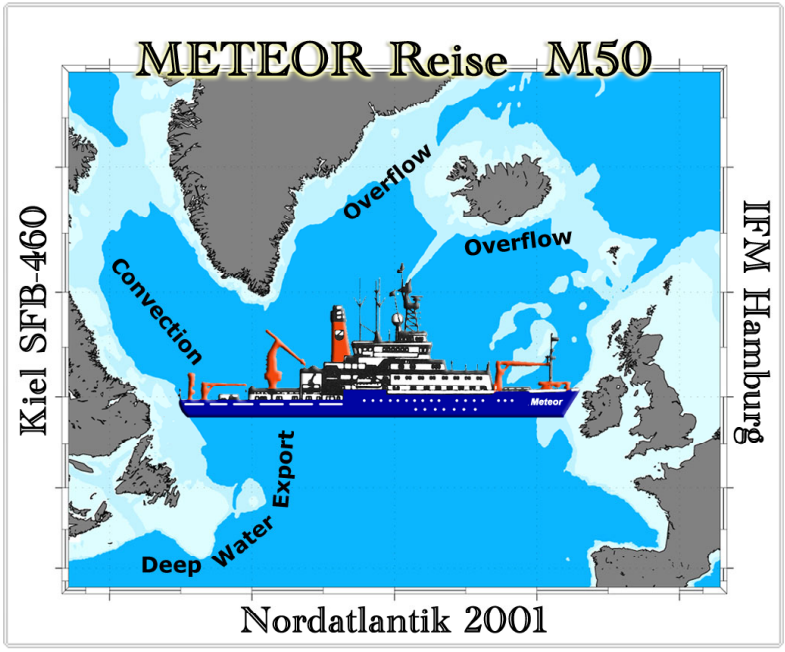

J. Fischer, Ch. Begler, P. Brandt, A. Coenen, U. Dombrowsky, K. Friis, K. Getzlaff, K. Jancke, H. Johannsen, G. Kahl, D. Kieke, H. Lübs, H. Lüger, M. Müller, W.-T. Ochsenhirt, U. Papenburg, H. Schmidt, M. Schütt, T. Steinhoff, L. Stramma, J. Stransky, P. Streu

Editorial Assistance:

Frank Schmieder
Fachbereich Geowissenschaften, Universität Bremen

Leitstelle METEOR
Institut für Meereskunde der Universität Hamburg

2002

Table of Contents (M 50/1)

1.1 Participants M 50/1

1	Fischer, Jürgen, Dr.	Chief Scientist	IfMK
2	Begler, Christian	Moorings	IfMK
3	Brandt, Peter, Dr.	CTD/ADCP-Watch	IfMK
4	Coenen, Andreas	CTD/ADCP-Watch	UBU
5	Dombrowsky, Uwe	CTD/ADCP-Watch	IfMK
6	Friis, Karsten, Dr.	CO_2-System	IfMK
7	Getzlaff, Klaus	CFC's, CCL_4	IfMK
8	Jancke, Kai	Moorings/ADCP	BSH
9	Johannsen, Hergen	Oxygen / Nutrients	IfMK
10	Kahl, Gerhard	Meteorology	DWD
11	Kieke, Dagmar	CFC's, CCL_4	UBU
12	Lübs, Holger	Moorings/CTD	BSH
13	Lüger, Heike	CO_2-System	IfMK
14	Müller, Mario	Moorings/ADCP	IfMK
15	Ochsenhirt, Wolf-Thilo	Meteorology	DWD
16	Papenburg, Uwe	Moorings/ADCP	IfMK
17	Schmidt, Hauke	CTD/ADCP-Watch	IfMK
18	Schütt, Martina	CFC's, CCL_4	IfMK
19	Steinhoff, Tobias	CO_2-System	IfMK
20	Stramma, Lothar, Dr.	Salinometry	IfMK
21	Stransky, Julia	CTD/ADCP-Watch	IfMK
22	Streu, Peter	CO_2-System	IfMK

Participating Institutions

IfMK Institut für Meereskunde an der Universität Kiel, Düsternbrooker Weg 20, 24105 Kiel - Germany, e-mail: jfischer@ifm.uni-kiel.de

DWD Deutscher Wetterdienst, Geschäftsfeld Seeschiffahrt, Bernhard-Nocht-Str. 76, 20359 Hamburg - Germany, e-mail: edmund.knuth@dwd.de

UBU Universität Bremen, Institut für Umweltphysik, Abt. Tracer-Oceanographie, Bibliotheksstraße, 28359 Bremen - Germany, e-mail: mrhein@physik.uni-bremen.de

1.2 Research Program

Leg M50/1 from Halifax to St. Johns, Canada, is embedded in the "Sonderforschungsbereich 460" (SFB-460) of the "Institut für Meereskunde, Kiel" (IFMK). The central research object of the SFB-460 is the thermohaline circulation and its variability in the northern North Atlantic. Central to the work performed during this leg are the SFB subprograms A4 and A5.

The aims of subprogram A4 are the quantification of the deep water circulation and its variability in response to the annually and longer term varying forcing fields in the western subpolar North Atlantic. Mass transports and water mass variability are at the focus of these investigations. A variety of observational methods are applied to reach these goals. Moored current meter stations at key locations of the deep circulation are installed for several years, and had to be serviced during this leg. The first current meter array is located at the Tail of the Grand Banks to measure the deep water export from the subpolar to the subtropical North Atlantic. The second array of moorings is located at the exit of the Labrador Sea to measure the deep water (especially the Labrador Sea Water) export out of the source region into the open subpolar North Atlantic. While the Grand Banks array has been recovered and redeployed the second array was only recovered and instruments are prepared to be redeployed during leg M50/2. The mooring work is summarized in Figure 1.1 and table 1.4 in chapter 1.6.

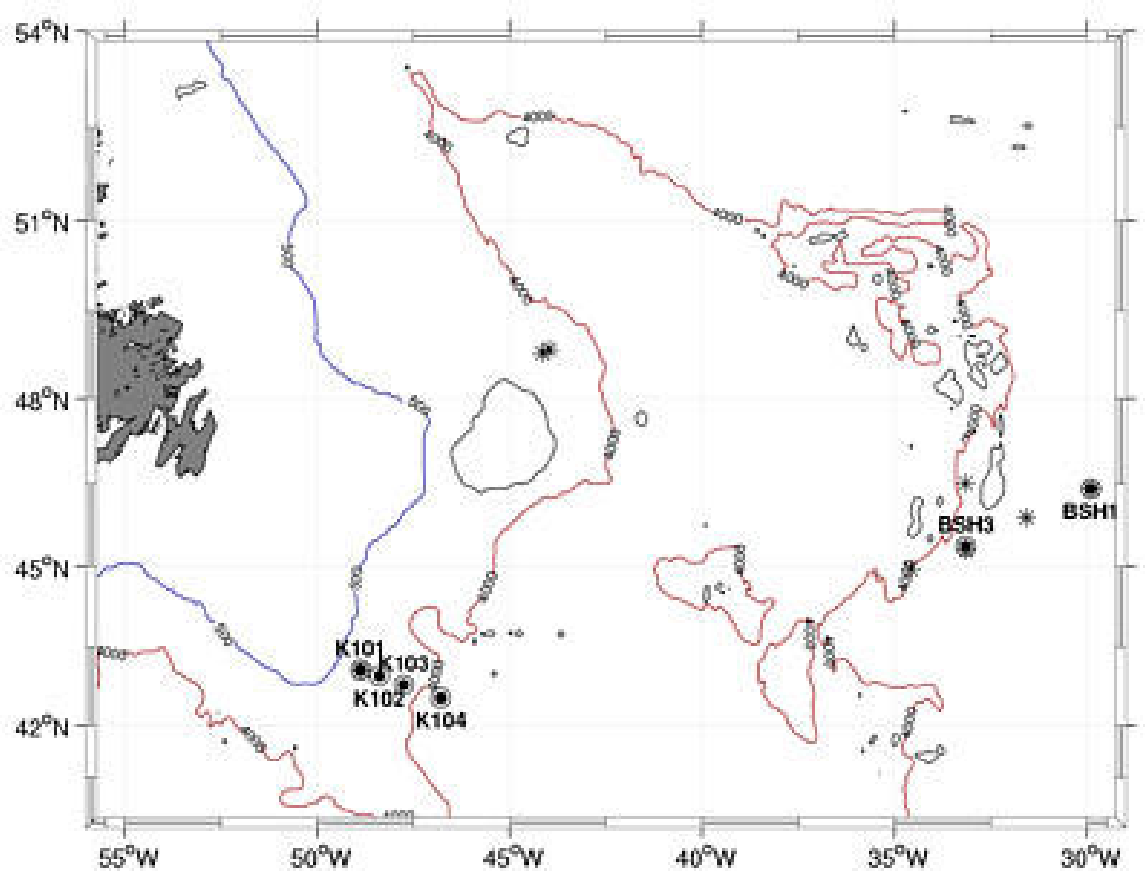

Fig. 1.1: Locations of deployed current meter moorings at the tail of the Grand Banks (IfM-Kiel) and at the Mid-Atlantic Ridge (BSH-Hamburg). Deployment positions of profiling floats (APEX) of IfM Kiel and BSH marked by *).

CTD/LADCP station work concentrated on three boundary current sections, see station map Figure 1.2, with one section replating the former WOCE section A2 from the Grand Banks extending to the Midatlantic Ridge, one section a repetition of the M45/3 – section north of Flemish Cap, and the third section at the exit of the Labrador Sea along the 53° N moored array.

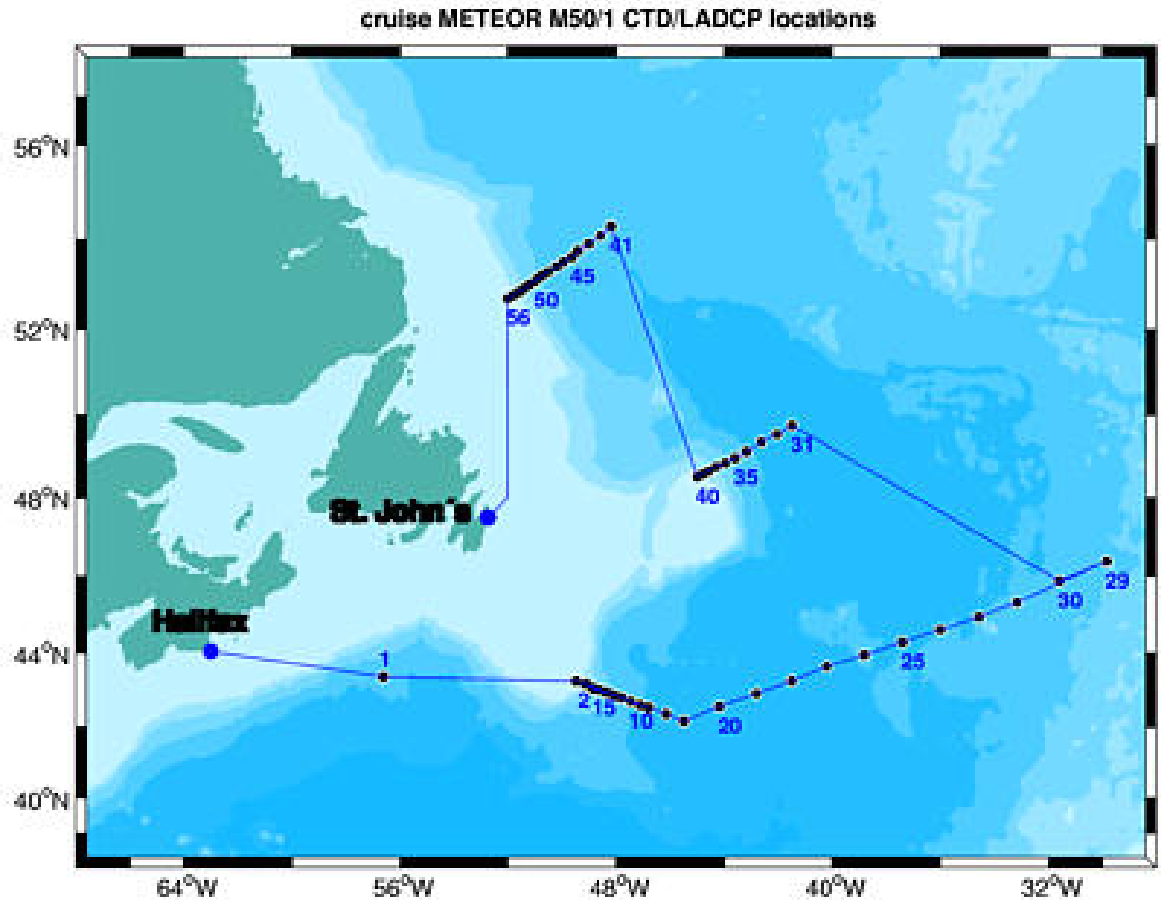

Fig. 1.2: Station list of CTD and LADCP locations of cruise M50/1.

An ADCP attached to the CTD rosette and lowered with it on each station enabled us to directly measure full ocean depth current profiles which are very important in a region of predominantly barotropic currents and in the absence of a reference level with no motion. Several additional parameters were measured from water samples taken at the CTD stations, the main focus being on CFC's (Freon 11 and Freon 12), CCL4 and nutrients taken at all stations. The third component consisted of underway measurements of currents by METEOR's new shipboard ADCP and sea surface parameters measured by the ship's thermosalinograph. These observations were supplemented by autonomous profiling floats (Figure 1.1), drifting with the deep currents and profiling the upper 1500 m of the water column; eight of these floats were launched during this leg (3 IFMK, 5 BSH).

The SFB subprogram A5 investigates the anthropogenic CO_2 increase of the subpolar North Atlantic. Four independent detection strategies were employed; (1) A backcalculation technique which is based on measurements of at least two of the four classical marine CO_2-parameters (total dissolved inorganic carbon, *p*H, total alkalinity, partial pressure of CO_2) together with

nutrients and oxygen in surface-to-deepwater profiles; (2) Determination of the carbon isotope ratio $^{12}C/^{13}C$ and phosphate in the water column; (3) Measurement of the ^{14}C-signal in the water column in context with historical data sets; (4) Continuous CO_2 fugacity measurements in the sea surface water and the overlying atmosphere. For the CO_2 working group the transatlantic WOCE A2 section has been repeated the fourth time since 1994 (M30). Therefore, an anthropogenic CO_2 increase should be detectable with respect to the sensitivity of the independent strategies (1)-(4). An additional aspect that can improve the sensitivity of all detection stategies is an improved understanding of the biological impact on the carbon cycle; therefore, samples for total organic carbon (TOC) and chlorophyll were taken.

The two moorings west of the Mid Atlantic Ridge are serviced by BSH since summer 1996. This mooring array covers the deep eastern boundary in the western basin. It was implemented as part of the WOCE activities along the A2/AR19 section. The velocity, temperature and salinity data will describe the long-term changes of this current system that appears to play an important role in the exchange of newly formed water masses such as the LSW within the ocean basin and across the ridge. The moorings have been redeployed for another year, to be recovered in summer 2002 by RV "GAUSS".

Floats have been increasingly used in the past decade to provide profiles of temperature and salinity of the top 1500 m of the ocean throughout the year and for using the Lagrangian displacement between ascents to estimate the current velocity at the parking level. Five APEX floats manufactured by Webb Corp., USA were reseeded at sites where in previous years similar floats had already been launched.

1.3 Narrative of the Cruise

Heavy loading activities took place on Monday, May 7, 2001, including the transport of tested instruments from Bedford Institude (BIO) to the METEOR. Departure from Halifax was as scheduled on Tuesday, May 8, a nice and sunny day. Winds were weak and METEOR sailed at 12 kn towards the edge of the Grand Banks. Most of the scientific party were still tying down their equipment.

In the afternoon of May 9, we had a boat manœuver where some of us had the opportunity to make some photographs from METEOR at sea during her 50ties cruise. This manœuver was followed by the first test station with the CTD/LADCP package lowered to 2000 m depth (table 1.3 in chapter 1.6). The ADCP used was inside the damaged container, but worked well during that first station. Most of the test-measurements were successful. Some of the scientific party and the staff of the electronics department worked hard to get METEOR's new ADCP, a 75kHz phased array called Ocean Surveyor, running.

By May 10, we were still steaming towards the edge of the Grand Banks, where we arrived at about 23:00. We now had two shipboard ADCP's running, a 150 kHz narrow band sytem built into the ship‘s hull and the new Ocean Surveyor in the sea chest. Both instruments showed surprisingly large ranges (400 m and 700 m). Overnight CTD stations in shallow water were carried out until the scheduled mooring recovery time at 6:00 (9:00 UTC) (Table 1.4 in chapter 1.6). Due to low visibility (foggy) the mooring work was shifted by 1.5h. At 7:35 we began to interrogate the releases of mooring K101 using first the shipboard transducer stem with no success. When lowering the hydrophon over the side of the ship both releases responded. At 8:15

the mooring was released and 10 min later the mooring radio indicated the surfacing of the mooring. The mooring top was found by using the radio bearings of the ships receiver and at 9:50 all components were safely recovered. Before the next mooring CTD stations were performed underway to mooring K102. This mooring was released at 14:20 (17:20 UTC); visibility was much better after crossing the NAC front a few miles west of the mooring position.

In between the mooring work, CTD stations were made towards mooring K103 which we recovered in the early morning of May 12. In the afternoon the last mooring off the Grand Banks (K104) was recovered.

On Sunday, May 13, we started to redeploy the moored array beginning with mooring K103 (2. deployment). On May 14, we deployed moorings K101 (2. depl.) and K102 (2. depl.). It was quite easy to launch K101 on the target position as winds and currents were low. As instruments had touched the deck during deployment (not severe) we decided to use a toggle release hook for the following deployments. As an additional activity the first IfM Kiel float was launched at 13:38 UTC.

Our arrival at the position of mooring K104_2 on 15.05.2001 was somewhat delayed due to head winds that slowed the ship down to 9 kn. Mooring work began with the first element launched at 11:58. At 13:32 UTC the stainless steel wire beneath the last Aanderaa broke on deck, but the instrument (and the rest of the mooring) was still save in the toggle release. Unfortunetely one of the seaman was hurt at his leg. This led to some unplanned maneuvers during which the mooring driftet northward, such that the target position could not be held. The water depth at this slightly different place was still ok: 4280m uncorrected (Correction about 8m), for final position see table 1.5 in chapter 1.6.

This was the last mooring activity at the Grand Banks and we headed towards the Midatlantic Ridge performing a CTD program along the former WOCE section A2. Station distance was only affordable at a little more than 60 nm in order to arrive at the western BSH mooring (3) during the morning of May 19. However, the weather became unfavourable with winds blowing at 6 to 7 Bft. from easterly directions.

At somewhat more rough weather we arrived at the BSH mooring in time. Southeasterly winds at 7-8 Bft., low visibility and rain showers made working on deck rather unpleasant. At 6:20 the mooring was released and it was sighted a little south of the expected position. The radio beacon worked but was difficult to hear. It took some time to recover the thermistor strings, but at 10:30 the releasers were savely recovered. Mooring recovery was followed by a CTD station and float (302) deployment. The weather became much better meanwhile and at 15:03 the deployment began at 45°26.87'N, 33°08.97'W. The thermistor strings went out much faster than expected. The anchor was dropped at 17:34 at 45°21.34'N, 33°09.28'W . Steaming to the top buoys we were able to observe the top element descending for final position of the mooring see table 1.5 in chapter 1.6.

Unfortunately some of us were not present during the M50 celebration (due to some delay in the mooring work), but had the nice dinner and some fresh beers thereafter. Kapt. Kull said a few words and thanked the Leitstelle and RF. T-shirts and Jubiläumsteller are a nice reminder for participating the 50th METEOR cruise.

On our way to the eastern BSH mooring (1) a BSH float was launched (table 1.6 in chapter 1.6) halfway between the moorings. The recovery of BSH-1 began at 08:04 (local). The

visibility was good and it was no problem to spot the ADCP buoy without the radio beacon operating on that mooring. At 11:15 the releasers were on deck.

As one of the immediate operations we tried to service the ADCP of that mooring, but were not able to establish good communication with the instrument. Therefore we decided not to redeploy that ADCP and altered the mooring top accordingly (replacing the Foam Float by 10 Benthos glass spheres). Deployment start was at 18:02 UTC and all instruments except the releasers were launched until 20:30 UTC, much faster than expected for the three thermistor strings. As we were 2 nm away from the target position the mooring was towed into position for about one hour. After the deployment the fourth BSH float was launched near the mooring position. Thereafter we steamed back to a position half way between the moorings for the last CTD station at that section (former WOCE A2 section).

After the last CTD station METEOR headed northwestward towards the Flemish Cap (FC) section. On our way to that section we dropped the last BSH Float about 75 nm from the beginning of the transit section. Wheather reports were unfavourable, prognosing a heavy storm lying between us and our destination. Winds and swell increased considerably during the day and the night to May 22. We had a stormy day and night with the ship heading into the wind at low (5-6 kn) speeds. A considerable delay had to be taken into account. On May 23, we reached the FC section and the first station began at 16:00 local (19 UTC). The station coverage had to be reduced from 12 to 10 stations in order to finish that section in time for the rest of the program. Station work went smooth and we were a little ahead of the schedule. Winds of May 24 are decreasing further. Two floats were released (Float 288 on CTD station 36, and Float 289 about midway between station 36 and 37 at 2000 m water depth).

Station work at the Flemish Cap section ended early morning of May 25, and we are heading northwestward to the 53°N - section where we expect some more CTD stations and the recovery of three moorings.

However, the transect to the 53°N section was faster than expected, as northerly winds were weaker than expected. Station work along that section went smoothly and we arrived at mooring K27 a little ahead of time. Recovery was scheduled for 12.30, after lunch. The recovery went very well and two hours later everything was on deck. Overnight station work kept us busy until the next morning. Two moorings should be recovered on May 28. The first, K28, was released after breakfast and was recovered safely at 10:45 (local). Then we steamed to the position of the last mooring, K29. We began to interrogate the two releases with both, the built-in hydrophone and one deployed over the side without success. During the next three hours we tried to release the mooring. Visibility was exellent, winds about 5 Bft from southerly directions. There were no signs of the mooring. We made a nearby CTD cast (about one mile away), which took about 2 hours. After that we surveyed the area with several observers on the bridge but without any success. As there was no immediate dredging possible, we decided to leave that operation for the second leg (M50/2). A little north of the mooring position we performed a Microcat calibration station with 6 Microcats mounted to the Rosette. The last stations along this section were performed during the moorning of May 29 at rather shallow water; somewhat shallower than in the sea charts, but approximately right in the TOPEX_TOPO bathymetry (2 nm resolution). After the last station we headed southward to St Johns and on the evening we had a nice little Glühwein Abschlussparty in the Geolab, and we reached St. John's as scheduled in the morning of May 31, 2001.

1.4 Preliminary Results

1.4.1 Mooring Activities

(J. Fischer)

Heavy mooring work dominated the working plans during the first week of the cruise. Four moorings located at the shelf edge at the southern tip of the Grand Banks had to be exchanged within 5 days. All mooring work had to be carried out during daylight hours, and between recovery and redeployment some time was needed to service the instruments as most of them were re-used in the new deployment. The mooring work is summarized in table 1.4 and 1.5 in chapter 1.6. Mooring recovery was done over the side using the Geological Boom without any problems. Deployments were carried out over the stern and using the A-frame for secure instrument deployment. Deployments went well and fast.

A first inspection of all instruments recovered showed that most of them had full, 22 months long records. One Aanderaa current meter lost the current speed record after about a year and one acoustic current meter had no data. Unfortunately the Aanderaa was redeployed before the detection of the problem with the speed sensor.

The 2 BSH moorings were exchanged on May 19 and 20, 2001; for final mooring positions see table 1.5 in chapter 1.6. In each of the recovered moorings one ring made of titanium was broken at the welding point, but due to the strength of the material it had opened only about a few mm. One shackle in an bouancy element was found without the bolt, but with signs of heavy corrosion at the position where the non-titanium splint must have been.

All Aanderaa current meter records stopped before the recovery date due to battery problems. The typical length of record is 4500 hrs, about six months. The Thermistor Chain Recorders showed no problems. The seacats and microcats manufactured by SBE showed no problems, except that 2 out of 4 microcats were giving read errors, when reading the data. A Broadband ADCP used in BSH 1 mooring could not be read and hence it was decided to take it back home for service and repair. The moorings head bouy had to be replaced by 10 Benthos elements. Further a pair of bouyancy elements was added at 2500 m depth, as calculation showed these elements being to small dimensioned. The deployment technique over the stern was new to BSH staff and it was noted that this technique is very safe and even faster than deployment over the side.

Preliminary Evaluation of the Mooring Data

Currents were rather weak, but at greater depths in the offshore moorings K103 and K104 the deep records show the deep western boundary current that is associated with the Denmark Strait Overflow Water. Currents in the Labrador Sea Water range were weak.

1.4.2 Direct Current Measurements with VMADCP/LADCP

(P. Brandt, J. Fischer, M. Dengler)

a) Technical Aspects

I) VMADCP

On the first leg of M 50, two vessel mounted acoustic Doppler current profiler (VMADCP), were used for data acquisition: a 153 kHz VMADCP mounted on METEOR'S bottom and a new 75 kHz phased array ADCP called Ocean Surveyor (OS) mounted in METEOR'S sea chest. Both ADCPs worked well throughout the cruise. While good data were obtained by the 153 kHz VMADCP to a depth of 400 m, the 75 kHz OS has a deeper measurement range. In most of the surveyed area, good data (50%-good criterion) were obtained by the OS to a depth of 600 m and even to a depth of 650 m during day time. The range especially of the OS decreased during heavy weather when METEOR headed against strong swell and wind waves. In particular, a heavy storm with wind speeds above 25 m/s led almost to a total loss of reliable data. Altogether, during 7% of the M50/1 cruise period, the depth down to which good data were acquired by the OS reduces to less than 300 m due to heavy weather.

The 75 kHz OS collected single ping data using a vertical resolution of 16 m with the first reliable depth cell located 24 m below the ship (8 m blanking range and first depth cell omitted). The first depth cell appeared to be contaminated in almost all profiles; it might be that the potential flow around the ships hull is responsible for this behavior. The ping interval was set to 2 s, which force the OS to ping as fast as possible leading to an effective time between pings of about 2.2 s. The processing mode was set to low resolution (long range). The chassis of the OS as well as the chassis of the VMADCP obtain heading information from the Fiber Optical Gyro (FOG) via an analog synchro interface. Ashtech headings, GPS data as well as digital Fiber Optical Gyro (FOG) headings were stored together with the velocity data by the RD-Instruments VmDas software package used with Windows NT.

The data of the 153 kHz VMADCP were collected using a bin length of 8 m, but sending 16m acoustic pulses for longer range. Further acquisition parameters were an ensemble interval of 5 min in which about 250 individual profiles are averaged, and a blank distance of 8 m. Together with the raw data, navigation information originating from the ships GPS receiver and the mean difference (for 5 min intervals) between the FOG- and Ashtech headings were stored by the user exit program ue4.exe in the ADCP raw data files. It is this mean heading difference that is used to correct individual 5 min ensembles for errors in the FOG synchro heading; thus basically Ashtech heading were used. The user exit program ue4.exe also aligned the PC clock to satellite time. For post-processing and calibration, the CODAS software package was used.

In the cruise report of our last cruise with METEOR, M47/1, we concluded that the new FOG should lead to an improvement of the acquired velocity data when using directly heading information from the FOG's digital interface. The electronic chassis of the VMADCP is only able to use a analog synchro signal to obtain heading information. It was shown that this analog heading signal shows an heading dependence, which is not present in the digital heading signal. However, the new OS has the capability to use also digital heading information. One aim of the calibration of the OS data was thus to investigate the data quality improvement due to METEOR'S new FOG compass when using directly its digital heading information.

By intercomparing heading values from the FOG, the Ashtech, and from the conventional Gyro, we found out that during M50/1 the FOG heading appears to fluctuate strongly with time (low frequency variability). While the differences between Ashtech and Gyro heading show the typical errors of the Gyro due to the ship's meridional velocity and acceleration (e.g., the Schuler oscillation), the differences between Ashtech- and FOG heading as well as between FOG- and Gyro heading show strong temporal fluctuation of up to 4 degrees on timescales of days. Such an behavior of the FOG was not observed on an earlier cruise, where the FOG heading was reliable. At the beginning of the next METEOR leg, M50/2, the FOG was rebooted and a speed correction was included in the setup. It turned out that the exclusion of the speed correction during M50/1 was responsible for the strong temporal fluctuations of the FOG heading signal. However, during M50/1 the Ashtech heading was, due to the implementation of a new firmware package, almost continuously available with only occasional short gaps. The FOG heading was therefore replaced by the Ashtech heading on a ping to ping basis for the OS and for five minute ensembles for the 150 kHz shipboard ADCP.

The shipboard ADCP data (OS and VMADCP) had to be calibrated for possible misalignments between the ADCP axis (usually the line between acoustic beams 3 and 4) and the ships axis (which of course is aligned with the ships compass). For calibration the usual acceleration / deceleration procedure for watertrack determination of misalignment angles was used. The assumption thereby is, that within a small region and a short time interval the currents are constant and any changes in absolute currents arise from nonperfect elimination of the ships speed over ground. This error is large at high ship speeds and small during station work. Thus, the aim of the calibration is to determine a misalignment angle for which the differences between on-station and underway measurements close to the station location are smallest in a least square sense for all calibration points. Basically this gives two independent calibration points per station, one when approaching the station and a second after the station has been finished. Approximately 100 independent estimates contributed to the calibration of the M50/1 data.

The standard deviation of the misalignment angle for the individual calibrations was obtained to be about 0.5° resulting in an error of the mean calibration angle of about 0.05° for M50/1. The error is calculated as the standard deviation divided by the square root of the number of independent contributions. No significant time dependence of the misalignment angle was found. For the VMADCP the standard deviation of the misalignment angle for the individual estimates was obtained to be about 0.5°, very similar to what was achieved for the OS data. At this point, we would like to acknowledge the support by the electronic engineers of the METEOR.

II) LADCP

On M50/1 all CTD-stations were accompanied by an ADCP attached to the CTD-rosette. The system in use was a narrow-band ADCP (NBADCP S/N 301). The NBADCP worked well throughout the whole cruise. Altogether 56 profiles were obtained. On all stations a ping rate of 12 pings/8s and a bin length of 16 m was used. While the data acquired above 2000 m water depth were of good quality, the data acquired at larger depths sometimes showed large spikes in the resulting currents which is possibly due to an interference with earlier pings.

b) Results

The near-surface current field of the western subpolar North Atlantic is characterized by the along-shore flowing Labrador Current carrying cold water from the north to the south and by the NAC carrying warm water from the south to the north. Figure 1.3 shows the current vectors averaged between 54 to 630 m as measured by the OS during M50/1. The current field is dominated by a pronounced eddy field that is superimposed to the main current system. the vertically averaged velocities within the Labrador Current reach maximum values around Flemish Cap of about 20 cm/s and slightly smaller values near the Grand Banks. The NAC flows near the Grand Banks in a narrow current branch east of the Labrador Current northward reaching the region northeast of Flemish Cap, where typically the Northwest Corner of the NAC can be found. In this region strong northeastward velocities of nearly 1 m/s were observed. A pronounced feature within this current map is the anticyclonic Mann Eddy, which is situated east of narrow current branch of the NAC near the Grand Banks. This eddy has an diameter of about 300 km and maximum velocities of more than 80 cm/s.

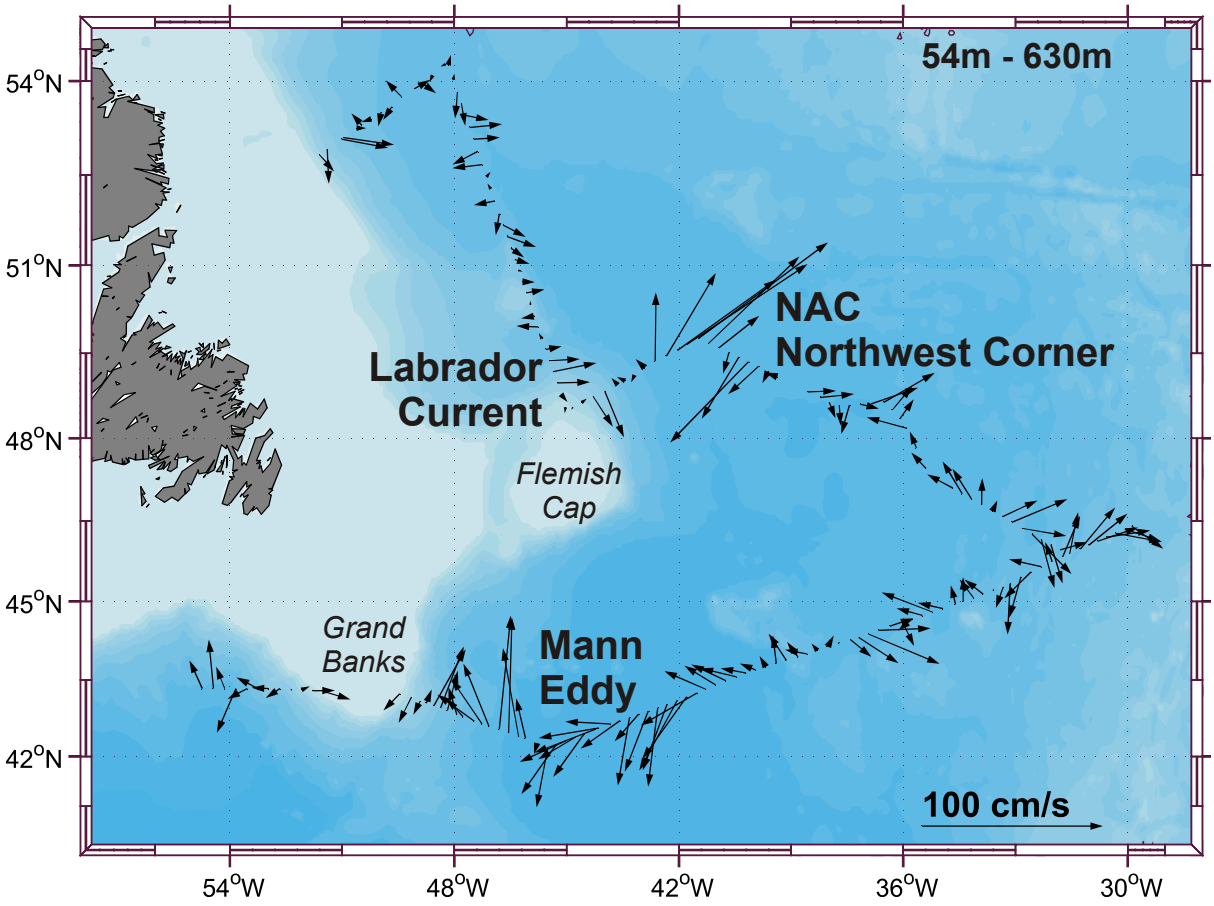

Fig. 1.3: Bottom topography of the western subpolar North Atlantic Ocean with current vectors from the OS. The arrows represent strength and direction of the velocity averaged between 54 and 630 m.

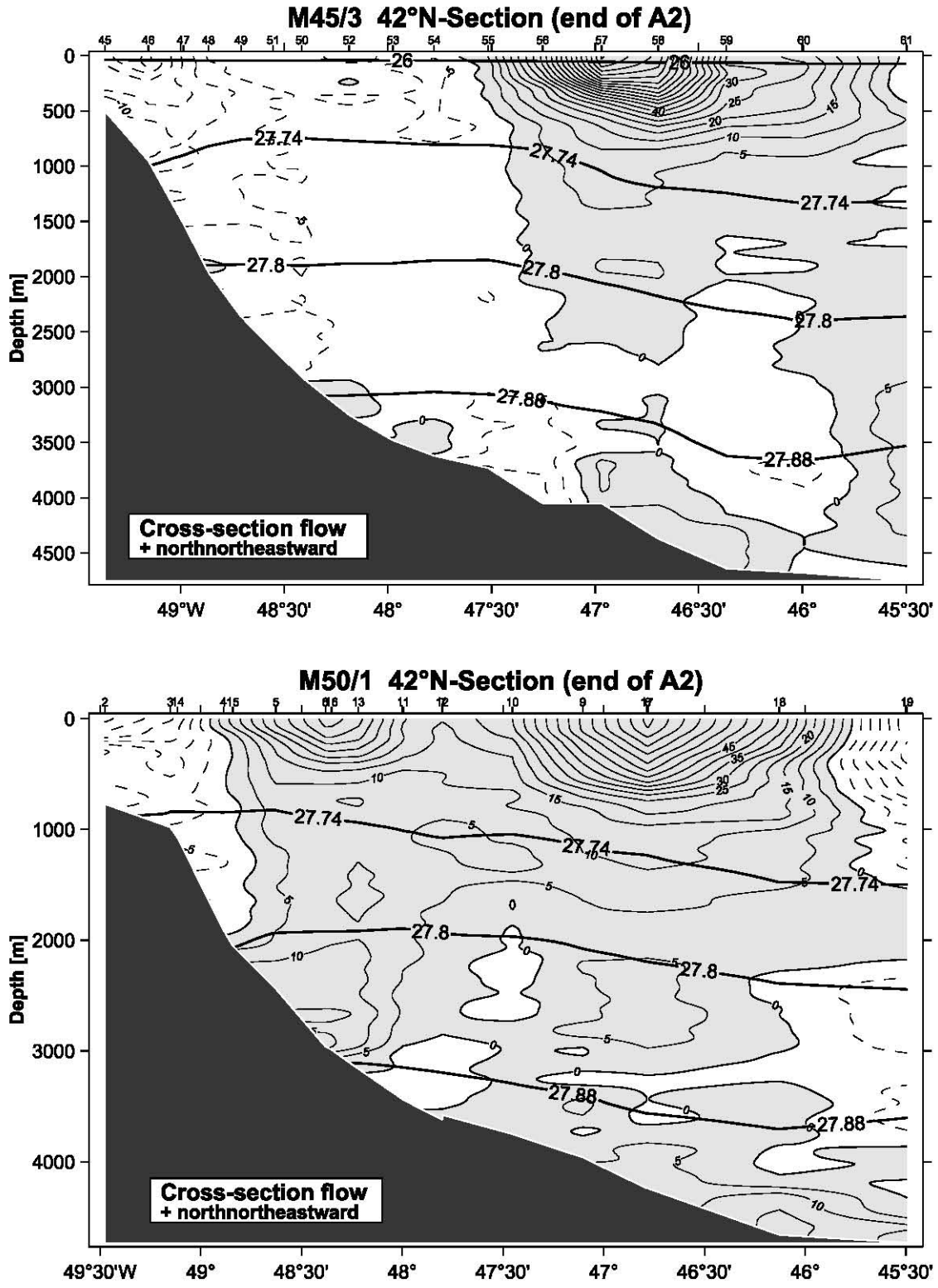

Fig. 1.4: LADCP section near 42°N (A2 section west of Grand Banks) for METEOR cruises M45/3 (July 1999) (upper panel) and M50/1 (lower panel) showing the cross-section current component in cm/s; positive flow is shaded. Also included are the isopycnals σ_θ=27.74, 27.8 and 27.88 (thick solid lines).

Figure 1.4 shows the cross-section current component for the 42°N sections for METEOR cruises M45/3 (July 1999) and M50/1 as measured by the NBADCP. While during July 1999 a large fraction of the flow confined to the shelf edge was in southward direction the northward flowing NAC (in May 2001) was found much closer to shelf. There was only a small gap through which Labrador Sea Water flows southward.

1.4.3 CTD - O_2 Station Work and Analysis

(L. Stramma)

a) Technical Aspects

The CTD-system used during the entire cruise M50/1 was a Seabird 9 plus. The CTD worked very well including the dissolved oxygen sensor. A Seabird bottle release unit was used with the rosette and except for some problems caused by too short bottle wires or wire problems with the thermometer frames, the release unit worked properly. In total 56 CTD stations were made during the leg M50/1. On all stations the LADCP was lowered with the CTD to the bottom.

For calibration purpose water samples were taken at 54 stations from the rosette bottles. Bottle salinities were determined with an Autosal salinometer (Kiel AS3). This salinometer showed drifts between measuring sessions as well as during the measurements, hence drift corrections had to be applied for all measurements. The salinometer used first, the Kiel AS7 showed heavy drift after a few bottles and then wide jumps during standby as well as measurements and could not be repaired and hence not be used. Oxygen from the bottle samples was determined by the Winkler titration method by hand. The CTD values for calibration were chosen from the downcast profiles to avoid hysteresis problems. Erroneous data were rejected when exceeding 2.8 times the standard deviation of the conductivity difference. Calibration of the SBE 9 CTD conductivity was done with on the basis of 173 sample pairs lying within the 2.8 times standard deviation criteria. After correcting the conductivity with respect to temperature, pressure, conductivity itself and time, the rms differences between the bottle and CTD conductivity samples were 0.0017 mS/cm corresponding to 0.00198 in salinity, despite the problems with the salinometer.

CTD pressure and temperature were compared to reversing electronic thermometers and barometers attached to some of the water bottles. The mean difference in pressure of 1 dbar was lower than the rms difference of 3.1 dbar and the mean difference in temperature 0.0019°C was lower than the rms difference of 0.0033°C, hence no corrections for pressure and temperature were done.

The calibration of dissolved oxygen with almost 900 water samples was quite accurate. After correction with respect to pressure, temperature and oxygen itself and temporal drift, the rms difference was 0.045 ml/l.

b) Water Mass Changes

The major aim of the hydrographic measurements is to investigate temporal changes of the water mass distribution, especially of the deep water masses, which are exported southward with the Deep Western Boundary Current. The upper range of the deep water is occupied by Labrador Sea Water (LSW), located in about 1500 m depth and revealing a salinity minimum and an

oxygen maximum. Below the LSW a salinity maximum occurs that is connected to an oxygen minimum. This water mass is called Charlie Gibbs Fracture Zone Water (CGFZW) or also named Iceland-Scotland Overflow Water (ISOW). Near the bottom, below about 2500 m in the Labrador Sea (at 52°N) and below about 3500 m in the New Foundland Basin (at 44°N) the water becomes less saline and colder then the CGFZW and is called Denmark Strait Overflow Water (DSOW).

LSW is formed in the Labrador Sea by winter convection, however, during the last years the LSW formation was weaker then normal and the LSW temperature and salinity increased. A first inspection of the M50/1-data showed that the LSW temperature and salinity further increased, hence no new LSW was formed, which reached the Deep Western Boundary Current. This increase in temperature and salinity compared to earlier cruises was observed at the western boundary in all three hydrographic sections. The strongest signal was observed at about 53°N shown in Figure 1.5. The thickness of the LSW-layer decreased compared to earlier observations in 1996, 1997, 1998 and 1999, while the temperature and salinity increased over the entire western boundary current region from 49°W to 51°30'W.

In contrast to the LSW the DSOW-signal was stronger at all three hydrographic sections. The increase of DSOW characteristics is presented as an example of the potential temperature distribution of the sections in May 2001 and July 1999 (Figure 1.6). Bottom temperatures in July 1999 had been about 1.5°C, but decreased to 1.2°C in May 2001. Related to the potential temperature changes the salinity at the bottom decreased from 34.885 in July 1999 to less than 34.870 in May 2001. This decrease in temperature and salinity shows the arrival of a strong pulse of DSOW, which can be traced at all three sections of M50.

The CGFZW located in-between the LSW and the DSOW shows no strong changes. A first glance at the data at 53°N indicates that the salinity maximum in May 2001 is weaker than that of July 1999 near the shelf break but of similar strength farther offshore. The same is true for the oxygen minimum. This might be an indication of a farther offshore location of the CGFZW, but a closer look into the data is necessary to investigate the changes in the CGFZW.

The results presented here are also confirmed by the tracer measurements presented in the next paragraph. It would be most useful to combine the observations from the CTD, the tracer measurements and the oxygen and nutrient measurement to present the combined view of the water masses. However, due to different calibration procedures the results are presented in separate paragraphs.

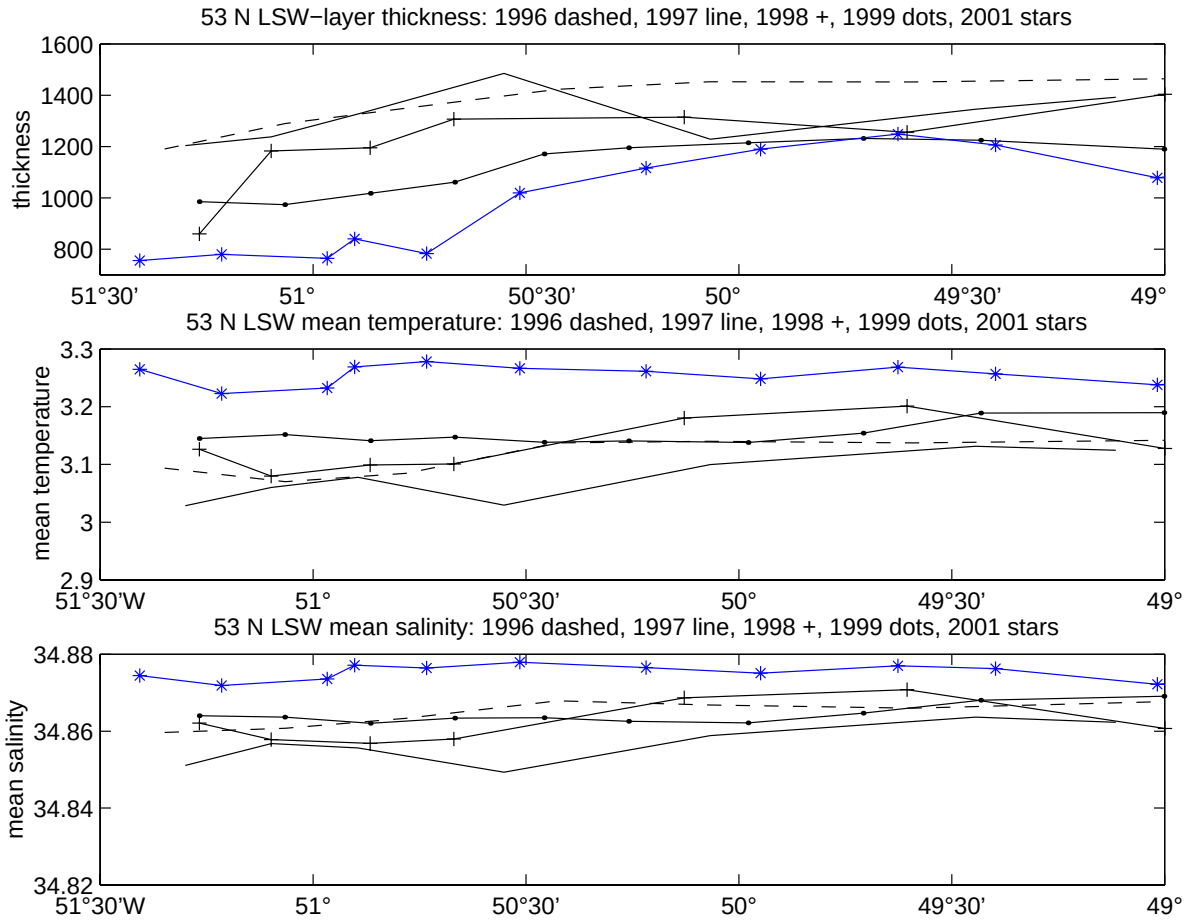

Fig.1.5: Layer thickness of the LSW at about 53°N (upper frame), mean temperature (middle frame) and salinity (lower frame) for cruises in 1996 (dashed line), 1997 (solid line), 1998 (+-line) 1999 (dot-line) and 2001 (star-line). The LSW is defined as the layer between the isopycnal sigma-theta 27.74 and 27.8.

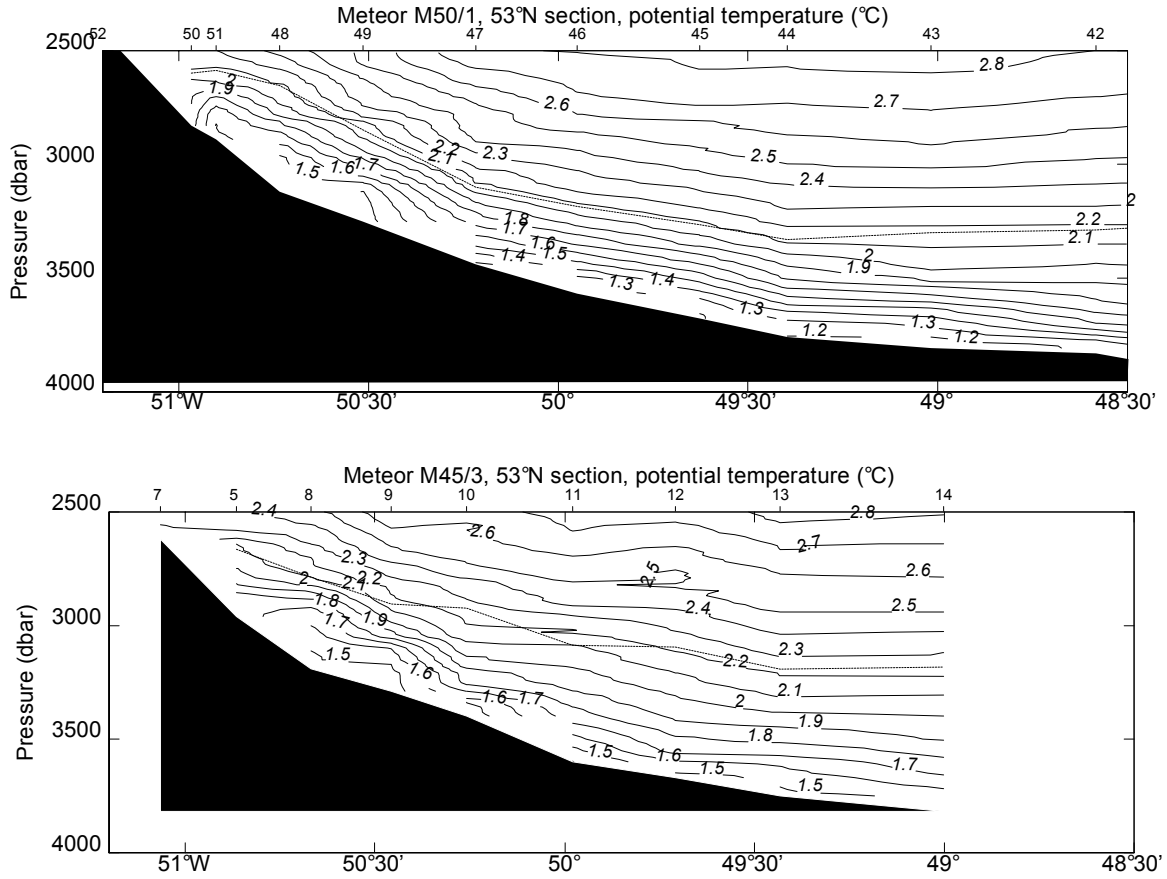

Fig.1.6: Potential temperature distribution near the shelf break at 53°N for a) May 2001 and b) July 1999. The broken line indicates the isopycnal sigma-theta = 27.88, indicating the upper boundary of the DSOW.

1.4.4 CFC's Station Work and Analysis

(D. Kieke, M. Schütt, K. Getzlaff)

a) Aims

Measurements of chlorofluorocarbon (CFC) and carbontetrachloride (CCl4) performed during cruise M50/1 serve to study the water mass characteristics and circulation of different deep water masses. A special focus is on investigating pathways and time scales of recently modes of Labrador Sea Water (LSW) as well as tracking the very cold and dense Denmark Strait Overflow Water (DSOW) upstream.

b) Technical Aspects

During M50/1, two gaseous chlorofluorocarbon (CFC) components, namely CFC-12 and CFC-11, have been analyzed. Water samples, sampled by precleaned 10 L Niskin bottles attached to a rosette/CTD system, are transferred in amounts of 20 ml to a purge and trap gas-chromatographic unit. Separation of the dissolved gases is performed using an gas-chromatoraphic packed column, detection is done using an Electron Capture Detector (ECD). ECD-signals are calibrated and converted into CFC concentration by means of standard gas.

Temporal variations of the ECD were about 6 % for both CFC components, thus being very stable in time. The temporal drift of the ECD is corrected by applying a calibration curve using six different gas volumes. These curves are taken before and after each station, assuming temporal changes between two calibrations being linear in time. All but one profiles were successfully analyzed, leading to 847 water samples in total. Reproducibility was checked by analyzing at least 10 % of the samples twice and standard deviation was found to be 0.8 % for CFC-12 and 0.6 % for CFC-11.

The analysis procedure of carbontetrachloride is similar to the one for CFCs. Both measurement units differ in using a capillary column instead of a packed one, as well as different carrier gas fluxes and purge and trap materials. At the beginning of the cruise, the CCl4 system suffered from a malfunctioned ventilator, which forced us to open the oven of the gas-chromatographic system and fix it. Afterwards, the system took more than a week to become fairly stable again. Thus, CCl4 measurements have only been performed from profile 29 onwards. In total, 318 water samples were analyzed. Reproducibility was found to be 1.4 %.

c) Pathways and Water Mass Characteristics

The program of cruise M50/1 aimed at repeating sections, performed in the framework of "SFB 460" during earlier years and, thus, investigating temporal variability of water mass properties and currents.

Labrador Sea Water (LSW) represents the upper layer of the Deep Western Boundary Current (DWBC). It is formed by winter time convection presumably in the central and southern Labrador Sea and carries low temperatures and salinities, but high oxygen and CFC concentrations. Bounding isopycnals used in this study are σ_θ=27.74 and σ_θ=27.80.

The first and southermost section from the Grand Banks to the Middle Atlantic Ridge (WOCE-A2-line) showed LSW focussing on the DWBC region with CFC-11 concentrations greater 2.6 pmol/kg, reaching down to a depth of 2400 m. Additionally, CFC- and oxygen rich LSW could be found at the western side of the Middle Atlantic Ridge (MAR) at about 43.5°W to 41.5°W. These increased concentrations (~3.2 pmol/kg) fall together with southward velocities measured by lADCP at this location, suggesting LSW being transported southward also far off-shore the continental shelf. Figure 1.7 shows LSW CFC concentrations for all sections performed during M50/1 in comparison to previous years.

The middle layer of the DWBC, bounded by the isopycnals σ_θ=27.80 and σ_θ=27.88 and namely Gibbs Fracture Zone Water (GFZW), is identified by low CFC-11 concentrations. Two cores show up west of 40°W. The first lies close to the shelf at 48°W at about 2400-2600m depth with CFC-11 concentrations less than 1.8 pmol/kg. The second covers the deep Newfoundland basin with concentrations less than 1.2 pmol/kg, but higher silicate concentrations (see figure 1.8, bottom). This core rather seems to be influenced by the presence of Antarctic Bottom Water (AABW).

The deepest and densest layer of the DWBC, the Denmark Strait Overflow Water (DSOW), showed the strongest signals during M50/1. Whereas previous Meteor cruises from 1997 and 1999 (M39/4, M45/3) revealed single DSOW cores in depths at about 3600m to 4200m, M50/1 showed a CFC- and oxygen enriched layer at the bottom of the section. Oxygen and CFC concentrations intensified from the southern to the northern sections. Antarctic Bottom Water (AABW) which spreads northward into the Newfoundland Basin and can be identified by its

high silicate content is displaced by DSOW during 2001. Comparisons with cruise data from 1994 and 1999 showed silicate concentrations being much smaller in 2001 than in previous years. 1994 and 1999 data showed bottom intensified silicate cores at around 30 micro mol/kg and more, whereas the silicate maximum during M50/1 only gave 26 micro mol/kg. The presence of a strongly developed DSOW seems to shift the AABW upwards in the water column by a few hundred meters.

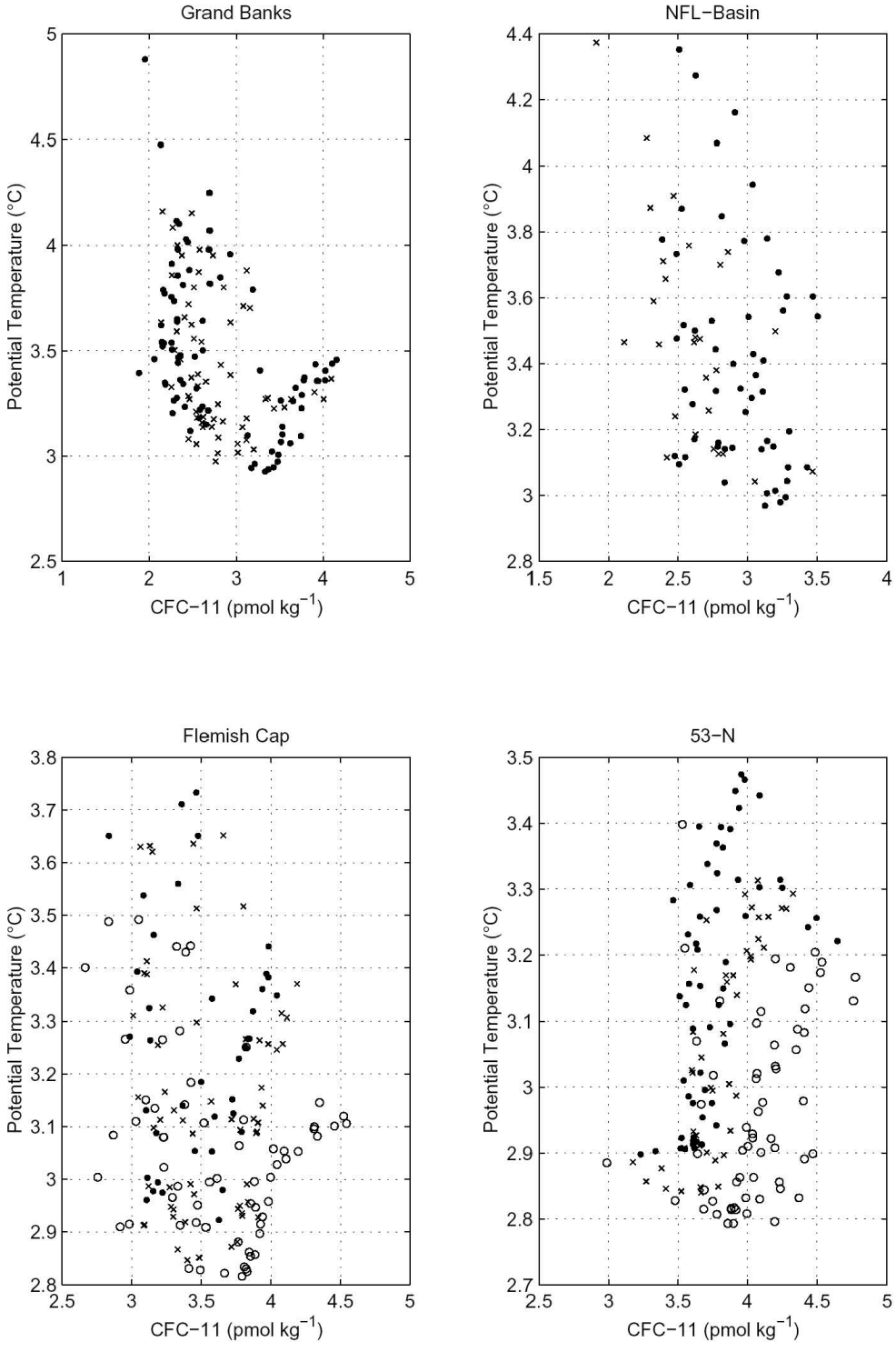

Fig. 1.7: CFC-11 concentration [pmol/kg] for LSW at all performed sections. Dots: M50/1, 2001; crosses: M45/3 1999; open circles M39/4, 1997.

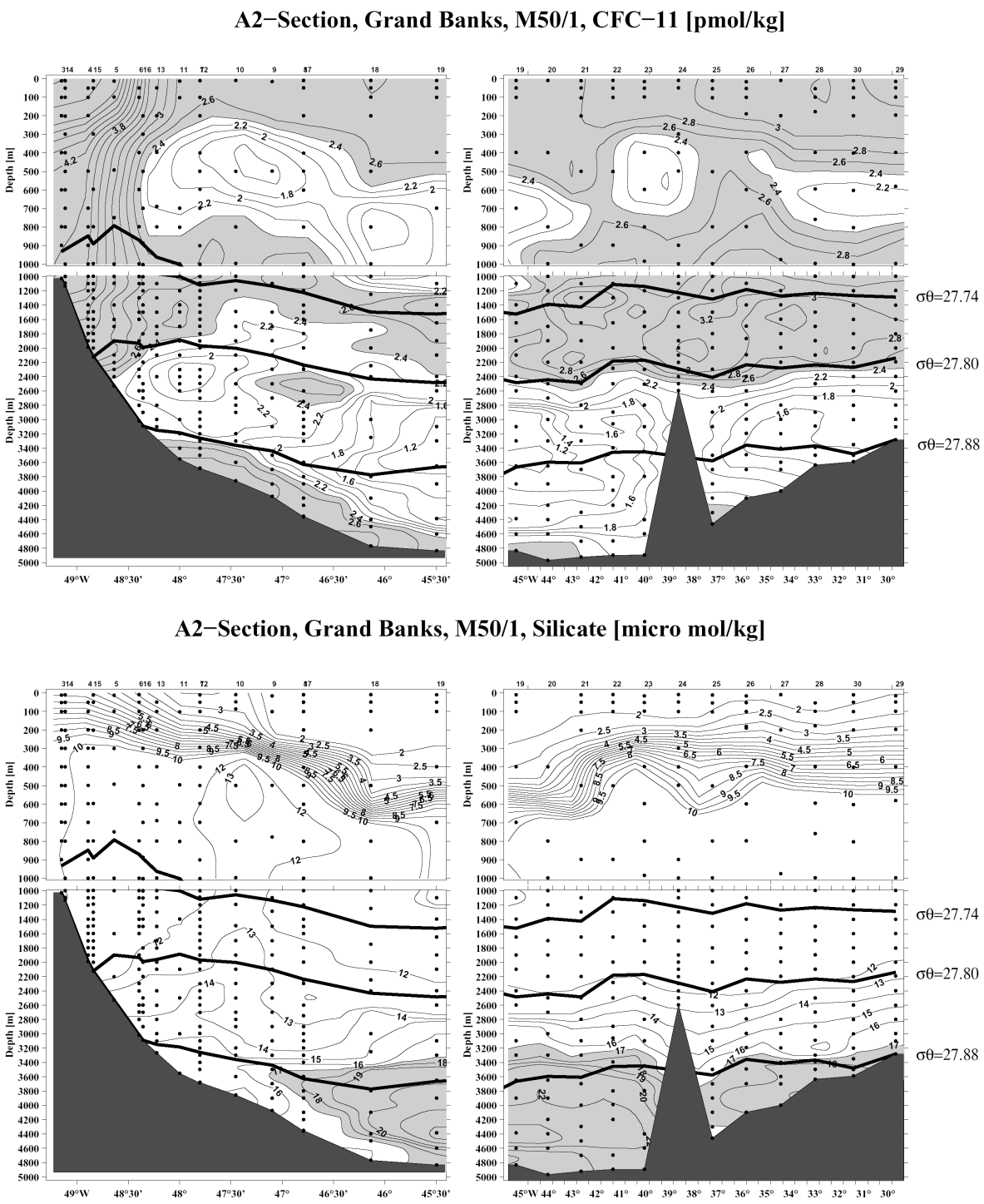

Fig. 1.8: CFC-11 [pmol/kg] (top) and silicate [μmol/kg] (bottom) along the A2 section. Thick lines denote isopycnals σ_θ=27.74, 27.80, and 27.88. CFC-11 concentrations greater 2.4 pmol/kg and silicate concentrations greater 17 micro mol/kg are shaded grey.

1.4.5 CO_2 Work and Preliminary Results

(K. Friis, H. Lüger, T. Steinhoff, P. Streu)

Methods

On the METEOR cruise M50/1 three of the possible four characteristic properties of the carbonate system were determined: total dissolved inorganic carbon (C_T, DIC), total alkalinity (A_T) and *p*H. The fourth parameter, partial pressure of carbon dioxide (pCO_2), was continuously measured in the sea surface (~5 m).

Sample Collection and Storage of CO_2 Samples

Two samples for each depth were collected in 500 ml glass bottles with ground glass stoppers. Using such large sample bottles enables two analyses to be performed on a single sample (*p*H first followed by A_T) and the second bottle was used to measure the C_T. A short drawing tube extending from the Niskin bottle to the bottom of the sample bottle was used to fill sample bottles. The stoppers were held down firmly with a large rubber band which secures to a clamp on the neck of the bottle. All samples were analyzed within 24 hours of being collected.

Sample Collection and Storage of ^{13}C and ^{14}C Samples

On leg M50/1, 444 samples for ^{13}C mass spectrometer analysis were collected. Each 100 mL bottle was carefully taken, poisoned with 50 µL $HgCl_2$ and afterwards crimp-sealed for storage and analysis onshore. Based on the ^{13}C data we will make a priority list for about 75 samples for ^{14}C mass spectrometer analysis, that can be done from the ^{13}C sample extract.

Sample Collection and Storage of TOC and Chlorophyll Samples

TOC samples were filled in glass tubes, that were combusted beforehand, frozen at –20°C and will be analysed onshore. This accounts for the chlorophyll samples, too, where one liter for each sample was collected, filtered and frozen at -20°C. 242 TOC samples and 69 chlorophyll samples were stored.

Total Dissolved Carbon Dioxide

The C_T analyses were made by a coulometric titration method using the SOMMA (single operator multi-parameter metabolic analyzer) system (Johnson et al., 1993). The SOMMA collects and dispenses an accurately known volume of seawater to a stripping chamber, acidifies it, sparges the CO_2 from the solution, dries the gas, and delivers it to a coulometer cell. The coulometer cell is filled with a partially aqueous solution containing monoethanolamine and a colorimetric indicator. A platinum cathode and a silver anode are positioned in the cell and the assembly is positioned between a light source and a photodetector in the coulometer. When the gas stream from the SOMMA stripping chamber passes through the solution, CO_2 is quantitatively absorbed, reacting with the ethanolamine to form a titratable acid. This acid causes the color indicator to fade. When the photodetector measures a color fade, the coulometer activates a titration current to neutralize the acid until the solution reaches its original color. The titration current is integrated over the time of the analysis, which provides a determination of CO_2 in the sample. Each sample is sparged and titrated until the amount of CO_2 coming from the stripping chamber is at blank level for four minutes - this is usually between 10 and 16 minutes

per sample. An integral part of the SOMMA is a gas calibration system that is used to calibrate the coulometer. In the gas calibration procedure, each of two gas sample loops is filled with pure CO_2 gas, the temperature of the loop and the atmospheric pressure are automatically measured so that the mass of CO_2 in the loop can be calculated. The contents of the loop are then injected into the SOMMA gas stream - following the same path through the stripping chamber and to the coulometer cell that is used by water sample sparge gas. The percent recovery of the CO_2 is calculated (typically about 99.96 - 99.98%) and a „calfactor" is entered into the software in order to determine the sample C_T following the equation:

$$C_T = \text{Calfactor} * \mu\text{mol} * (1000 / V_t * \rho)$$

Here, µmol is the result of the sample coulometric titration, V_t the sample volume at the sample temperature and salinity (T = 20°C), and ρ the density of sea water at the sample temperature and salinity.

After the instrument is calibrated, as additional reference, a bottle of certified reference material (CRM) and two duplicate samples per station are analyzed. The CRM bottles are prepared by Dr. Andrew Dickson's laboratory at the Scripps Institute of Oceanography. Normally the CO_2 content measured by the SOMMA should be within two micro moles/kg (about 0.1%) of the certified value.

Alkalinity Determination

Total Alkalinity (A_T) is determined by titration of seawater with a strong acid, following the electric motoric force with a proton sensitive electrode. The titration curve shows two inflection points, characterizing the protonation of carbonate and bicarbonate, respectively. The acid consumption up to the second point is equal to the titration alkalinity.

Alkalinity was determined by a semi-automatic analysator, the VINDTA instrument (Versatile Instrument for the Determination of Titration Alkalinity). It consists of two parts, the titration cell with its manifold for filling, draining and acid delivery and the data acquisition and system control unit (Mintrop et al., 2000).

Alkalinity is determined by titrating a seawater sample with hydrochloric acid (0.1 µM) and then measuring the *p*H using a reference and a glass electrode. The difference in *p*H potential is measured by a *p*H-Meter which delivers the data to the computer for calculation of the alkalinity. The program allows complete titration with preset volume increments of the acid.

A precisely known volume of the sample is filled into a glass pipette (volume 100 ml) and filled into the open cell. Then the sample is titrated with the acid. A stir bar inside the cell mixes acid and sample. The total volume of the acid added to the sample is 3.9 ml. The analysis is performed at 25 °C, which is maintained by a water bath.

The standardization is done the same way as the C_T samples, running a CRM (see above) in the beginning and two duplicats per station and finishing with a CRM. The alkalinity results should be within a range of 2-3 µmoles of the CRM values.

*p*H *determination*

The *p*H is determined by a spectrophotometric method that is based on the absorbance spectrum of a *p*H-indicator dye. All measurements are made with an automated system described in Friis (2001) and using meta-cresol purple as indicator dye. The indicator was calibrated for *p*H on the

total seawater scale (pH_T) by Clayton and Byrne (1993). For the *p*H calculation procedure we followed the description in Doe (1994).

Six samples can be analyzed per hour, which is one complete hydrocast within 4 to 5 hours. The indicator dye is dissolved in seawater and for analysis the mixing ratio (sample:indicator) is about 650:1. The analysis is performed at 21°C ± 1°C. During the spectrophotometric detection the exact temperature is measured by a calibrated Platinum resistence thermometer [± 0.05°C]. Afterwards all *p*H data are fitted to 21°C. This is done with the computer program ‚CO2SYS' by Lewis and Wallace (1998) using the dissociation constants after Mehrbach et al. (Millero and Dickson, 1987) constants and the corresponding A_T or C_T value. The standardization is done the same way as the C_T ans A_T samples, running a CRM in the beginning and two duplicats per station and finishing with a CRM. The pH results should be within a range of ± 0.005 pH units according to the accuracies in C_T and A_T of 2-3 µmoles of the CRM values.

CO_2 Partial Pressure Determination

The fourth analytical strategy involved the continous determination of the partial pressure of CO_2 (pCO_2) in surface water and in the overlying atmosphere. For this purpose an automated underway pCO_2 system (Körtzinger et al., 1996) with a non-dispersive infrared gas detector for CO_2 was continuously operated along the cruise track. A continous flow of seawater was drawn at 5 m depth from the ship's "moon pool" which was equipped with a CTD. Every 2 minutes a pCO_2 data point together with temperature and salinity from the CTD were logged along with the position data from an independent GPS system. Previous work (Körtzinger et al. 1996) has shown that the system is accurate and precise to ± 2 µatm. The instrument was calibrated using three standard gases with a known CO_2 concentration. These gases were measured approximately every 12 hours.

C_T, A_T and pH Quality Control

The quality control of the various parameters of the carbonate system was performed with the help of certified reference materials (CRM) and analysis of duplicates that were taken approximately every tenth sample. The CRMs were provided by Dr. Andrew Dickson and analyzed by Dr. D.C. Keeling by vacuum extraction with manometric detection at the SCRIPPS Institution of Oceanography in La Jolla, California. The CRMs are certified for C_T and A_T only, but have to have a constant *p*H. These standards are used to determine the accuracy and performance of the systems. The duplicates show the precision of the analytical instrument. For the *p*H quality control the CRM measurements allow assessment of the long term precision during the cruise, if a specific CRM batch is used fro the whole cruise. An overview of the quality controls is shown in Tab. 1.4.5.1. and in Fig. 1.9. The control samples show a very good agreement with the achievable accuracy and precision estimates according to Millero et al. (1993), that can be seen in Tab. 1.4.5.1 and Tab. 1.4.5.2.

Fig. 1.9 A and B show constant analytical C_T performance during the whole cruise. This is true for the A_T analyses, too (Fig. 1.9 C and D), with the exception of a significant underestimation of 0.89 µmol/kg from CRM measurements, that is obvious from the mean in Fig. 1.9 D. Based on the CRM quality control 0.9 µmol/kg were added on every sample A_T. Although the pH of the CRM measurements in Fig. 1.9 F show a significant deviation between the control of stations 54-84 and stations 87-126 this is within the accuracy range of Millero et

al. (1993) in Tab. 1.4.5.1 An uncertainty of ± 0.002 pH units corresponds with a C_T and A_T uncertainty of ± 1 µmol/kg and therefore seems to be acceptable. Nevertheless, the *p*H trend of the CRM measurements from Station 54 to 87 could be explained by aging of the Pt-100 temperature probe. This will be proved onshore, so that all *p*H data can be corrected, if it is neccessary. A temperature correction 0.1 °C leads to a *p*H correction of – 0.0015 pH units.

Tab. 1.1: Key data of the discrete C_T, A_T, pH analyses. The CRM measurements give an accuracy estimate, the duplicate measurements a precision estimate.

	C_T	**A_T**	***p*H$_T$ $^{21\,°C}$**
CRM: Analyzed bottles	26	52	40
Batches used	(52, 47, 41)	(52, 47, 41)	(52)
Mean deviation from certified CRM value	0.20 µmol/kg	- 0.89 µmol/kg	not certified for pH
(standard deviation)	(± 1.28 µmol/kg)	(± 1.58 µmol/kg)	(± 0.0017)
Duplicates: Analyzed pairs	38	58	66
Mean deviation from duplicate value	1.3 µmol/kg	2.1 µmol/kg	0.0016
(standard deviation)	(± 1.4 µmol/kg)	(± 1.45 µmol/kg)	(± 0.0016)

Tab. 1.2: State of the art of achievable accuracy and precision for C_T, A_T and pH measurements (Millero et al., 1993) in comparison to the M50/1 estimate.

Parameter	**Accuracy**	**M50/01 estimate**	**Precision**	**M50/01 estimate**
C_T	± 2 µmol/kg	± 1.28 µmol/kg	± 1 µmol/kg	± 1.4 µmol/kg
A_T	± 4 µmol/kg	± 1.58 µmol/kg	± 2 µmol/kg	± 1.45 µmol/kg
***p*H**	± 0.002	± 0.0017 µmol/kg	± 0.0004	± 0.0016 µmol/kg

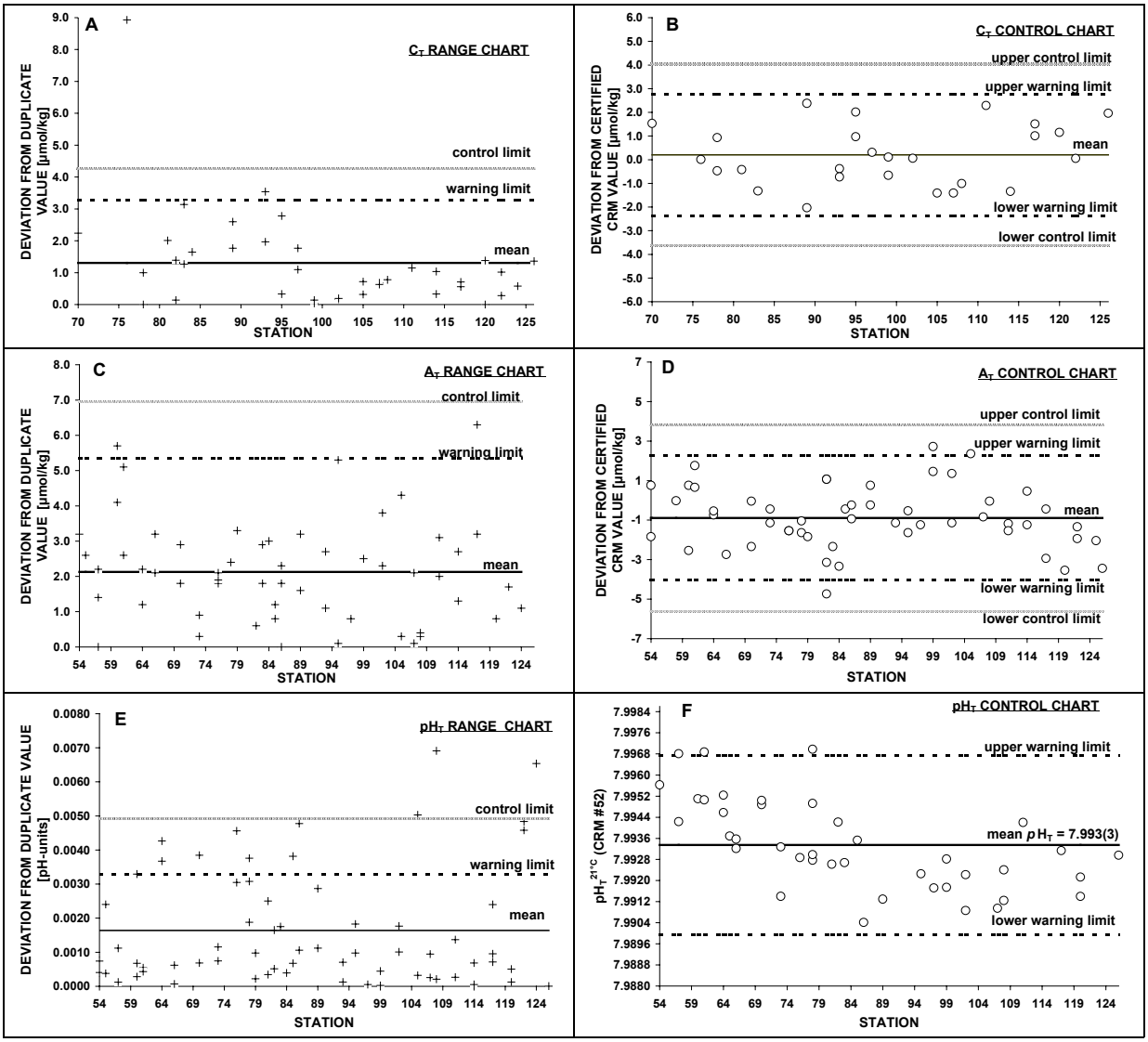

Fig. 1.9: Quality charts for C_T, A_T and pH_T analysis The range charts on the left-hand side are based on duplicate analysis of usually two niskin bottles per hydrocast. The control chart on the right-hand side are based on measurements of certified reference materials (CRM), that was at minimum one control measurement per hydrocast and parameter. Also shown are ‚warning' and ‚control limits', these are included according to a standard procedure for marine CO_2 parameter analysis in DOE (1994). The ‚warning limits' result in muliplying the standard deviation by two and the ‚control limits' by three. About 95 % of the plotted points should be within the warning limits.

Preliminary Results of the pCO_2

- The preliminary pCO_2 shipboard results (Fig. 1.10) illustrate typical aspects of pCO_2 in the central North Atlantic during the summer months:
- CO_2 sea surface conditions with pCO_2 undersaturation up to differences from 100 µatm are not rare.
- Plankton blooms and high photosynthesis activity are clearly seen in a decrease of sea surface pCO_2.

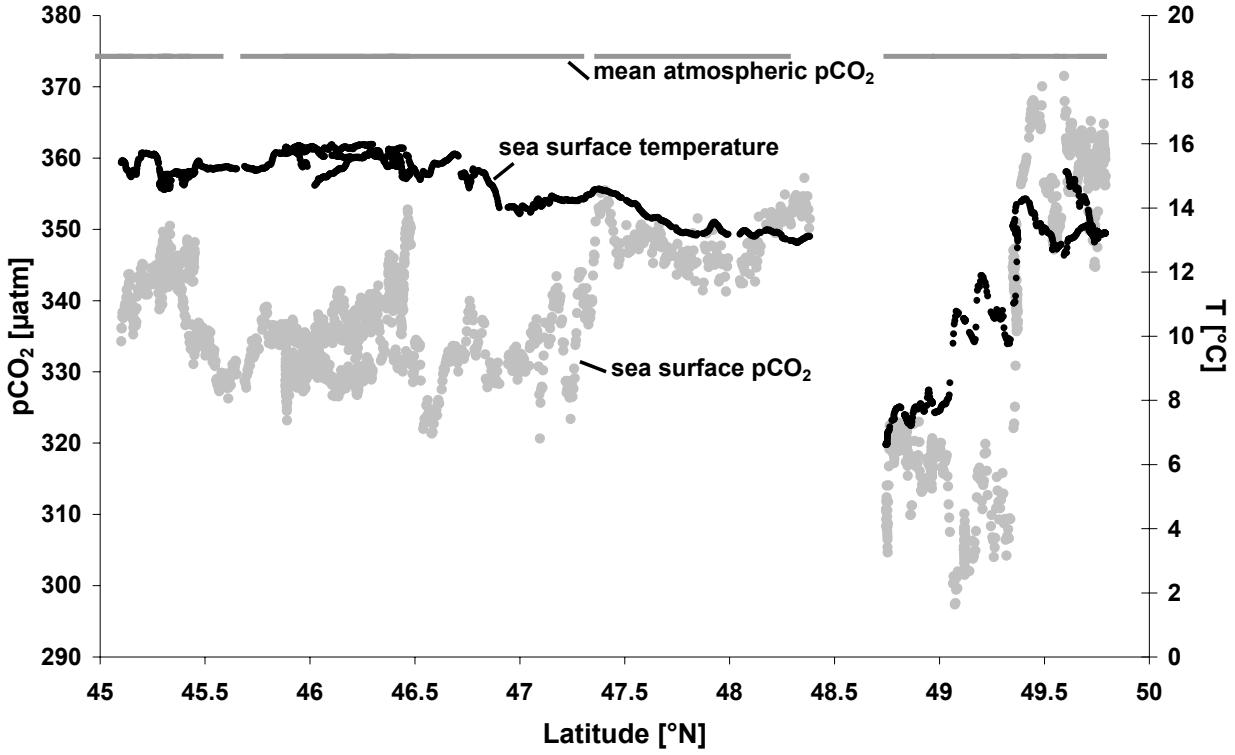

Fig. 1.10: Preliminary results of the pCO_2 measurements along the cruise track from 19 to 24 May, 2001.

- Sea surface temperature increase should lead to (from the thermodynamic point of view) an increase in pCO_2, but this effect can be masked by the biological processes.
- Sea surface temperature decrease should lead to a pCO_2 decrease through increased gas solubility, but this maybe compensated by a net CO_2 flux from the atmosphere into the ocean.
- Mixing of cold and warm water surface regimes can produce pCO_2 distribution patterns that can not easily interpreted with thermodynamic considerations.

Preliminary Results of the C_T, A_T and pH Analysis

A total number of 459 (416 individual samples) C_T samples, 663 (601 individual samples) A_T samples, and 688 (622 individual samples) pH samples were anlayzed. An overview of all data is given in Fig. 1.11 as surface-to-deepwater profiles. The carbonate parameters range from 2050 to 2185 µmol/kg for C_T, 2205 to 2440 µmol/kg for A_T and 7.76 to 8.13 for pH_T at 21 °C. All three parameters show highest variabilities from the surface to about 1000 m depth, which is mainly caused by biological activity from photosynthesis, calcification and respiration. Between the surface and 500 m one can also see two C_T and A_T branches, which matches the higher salinity and temperature data for higher values, and vice versa for lower values. The slight separation of two pH branches below 2500 m in Fig. 1.11 C indicates different source regions for the deeper water masses. Property-property-plots of pH_T vs. C_T and A_T vs. C_T (Fig. 1.12 A and B) show three different CO_2 patterns for the near surface waters, with high pH and variable A_T values. These CO_2 patterns come together with increasing C_T values, i.e. with less varaible C_T values in intermediate and deep water masses.

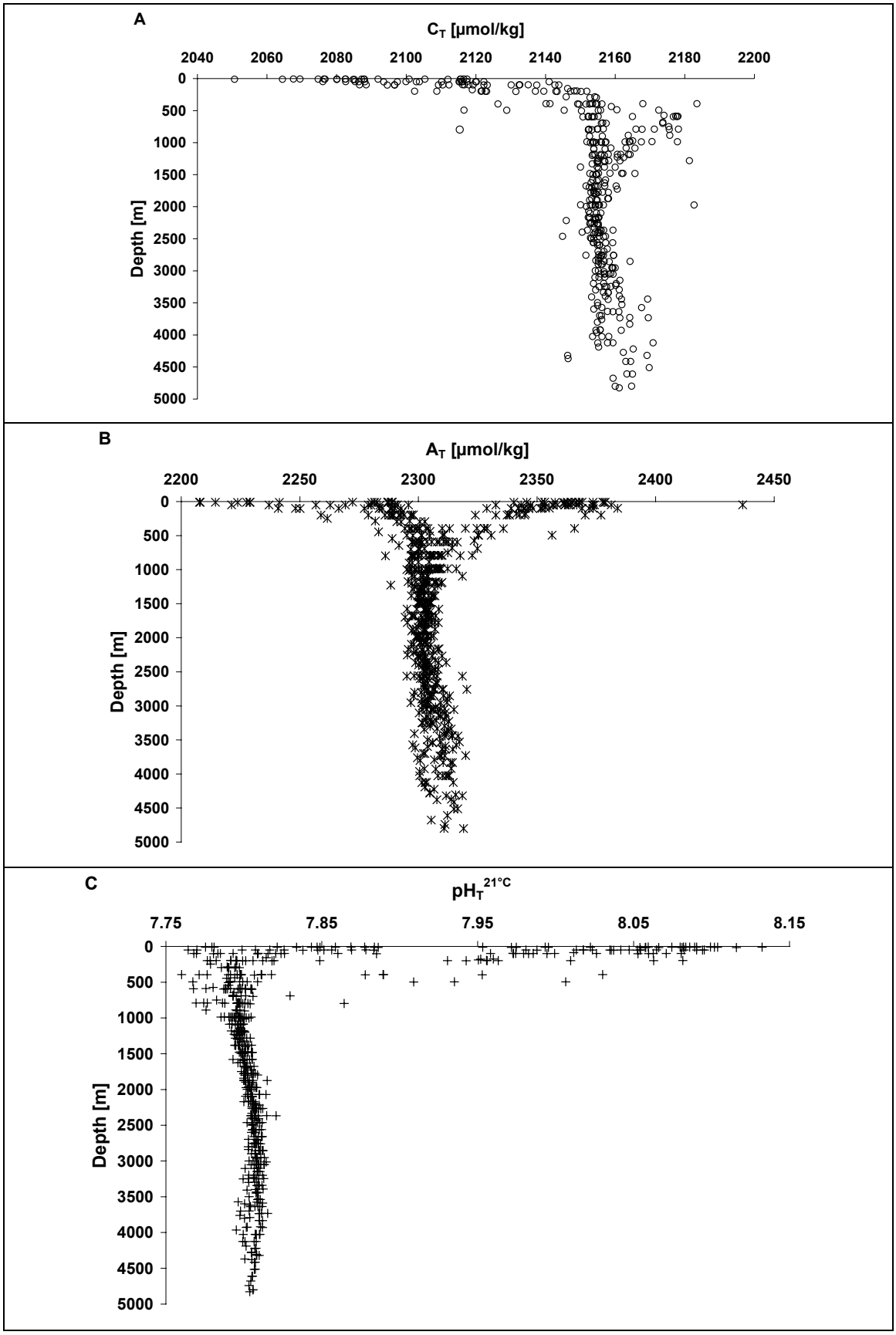

Fig. 1.11: Surface-to-deep water profiles of all C_T, A_T and pH_T measurements.

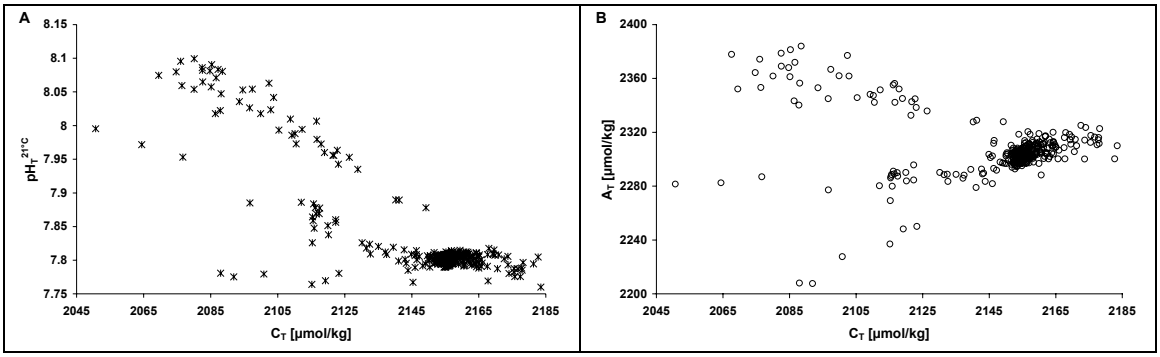

Fig. 1.12: Property-property-plots for C_T, A_T, pH_T. Both plots indicate three different CO_2 patterns near surface waters, with high pH and variable A_T values. These patterns come together with increasing C_T values, i.e. with less variable C_T values in intermediate and deep water masses.

1.4.6 Underway Measurements of Sea Surface Parameters

(H. Schmidt)

During METEOR cruise M50/1 the ships on-track observational system DVS was used to collect quasicontinuous near surface temperature and salinity (conductivity) from the ships thermo-salinograph, depth data by the PARASOUND and HYDROSWEEP echosounders as well as wind speed and wind direction data.

a) Thermosalinograph

After despiking (mainly salinity data) the thermosaliniogrph data was calibrated versus CTD data from 5 meter depth.

While the temperatures were in close agreement with those from the CTD, only a least square linear fit was necessary to consider the temperatur dependency of the devitations. We found the following calibration equation:

$$T_{corr} = A \times T_{thermosal} + B \qquad (1)$$

$$\text{with } A = -0.021 \text{ and } B = 0.2817.$$

The salinity measurements showed larged differences initially. After calibration thermosalinograph- and CTD salinity agreed within a standard deviation of 0.145 and a mean offset of 0.169. Salinity- and SST- maps have been constructed with the calibrated data.

b) Wind speed and direction

Wind speed and wind direction were measured on port and on starboard of the ship. For the graphic only luv data were used. Figure 1.13 shows the recorded wind vectors during M50/1.

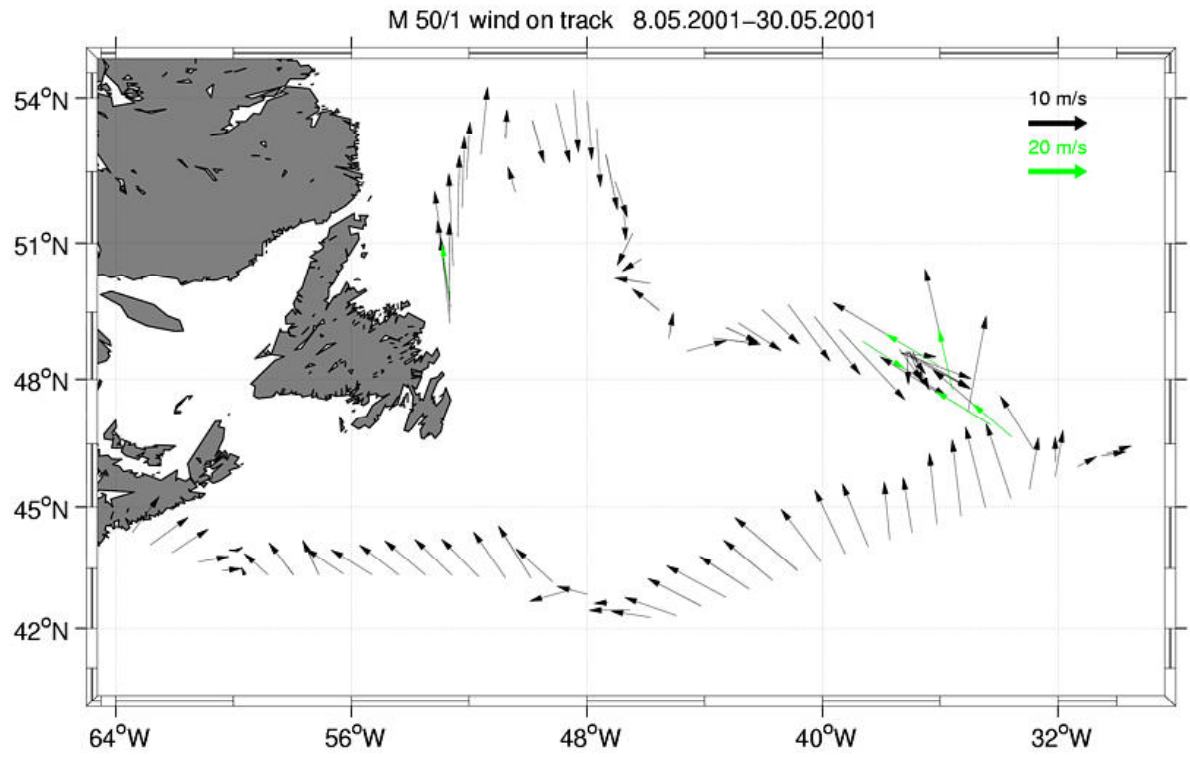

Fig. 1.13: Wind speed and direction on M50/1.The black arrows are scaled with 10 m/s and gray arrows are scaled with 20 m/s.

1.4.7 Deployment of Profiling Floats

Three profiling floats of type APEX were deployed in the Deep Western Boundary Current regime; one off the Grand Banks and two off Flemish Cap. For positions and launch times see table 1.6 in chapter 1.6. These three were IFMK floats, and were programmed to drift at 1500 m and rising to the surface every ten days. The other bunch of 5 floats were from the BSH and were deployed near the Midatlantic Ridge in the vicinity of the BSH moorings. These floats also drift at 1500 m depth at a 14-day schedule. All floats were started several hours before launch, such that the initial surface time remained short (a few hours only).

1.5 Weather Conditions during M50/1

When the METEOR left Halifax, NS, on May 08, 2001, she had a sunny day with light westerly winds under the influence of an elongated high that extended south of Newfoundland to south of New York. However, a gale center of 1005 was situated south of Bermuda, moving northeast so that winds backed southeast on May 09. The gale center intensified to 1000 on May 11, lying south of Cape Breton Island, and winds were up to 6 Bft on our position. Then, the gale center changed ist course to move southeast, passing south of the research vessel on May 14 when we observed northeasterly winds 6 Bft abating to 5 Bft 5 but slowly. However, a low is never alone in creating winds. The high over Greenland had been strengthened to 1040 by a low that had moved from New England to the eastern entrance of Hudson Strait, and it had developed a wedge of 1030 south of Greenland. The gale center reached the Azores on May 15 and moved further east during the next days, thereby filling. Meanwhile, another gale center 1000 had

developed near 40 North 57 West, intensifying to 995 the next day at 55 West. Prior to passage of a cold front on May 18, southeasterly gales of 7 Bft were observed at the METEOR, and during passage of the front, there were southerly gales force 8 Bft. The high south of Greenland had meanwhile migrated east to the Bay of Biscay. The gale center turned northeast, moving quicker than before and intensifying to 990 on May 19 at 48 North 40 West while winds at our position veered southwest and abated somewhat. During the next days, this gale center moved northwest, then turned southwest, filling thereby until its vestiges merged with the next storm center. A secondary low went up past Iceland to the Norwegian Sea where it found favourable conditions for development into a gale center. When METEOR reached her easternmost position on May 20, winds had veered further to the northwest, force being 5 Bft.

On May 19, south of Cape Hatteras a new low 1010 had formed, central presure being down to 1005 during May 20 when the low passed far south of Newfoundland. Conditions being favourable for further development into a storm center, it followed its predecessor as far as its path was concerned. A central pressure of 995 was reached at 06 UTC on May 21 at 42 North 42 West and 980 by 18 UTC at 46 North 38 West. Our research ship, in the meantime, was under way on a northwesterly course to 49'45 North 41'30 West, the starting point for another series of probing positions. Winds were already up to southeast 9 Bft, and at 06 UTC on May 22, even a storm of southeast 10 Bft was recorded for a few hours. Central pressure of the storm center was 965, and at the ship lowest recorded pressure was 968,6. It can be concluded that the storm center was passed within a few miles. Thereafter, the storm center began to fill, central pressure reaching 970 by 18 UTC on May 22 and 980 by 06 UTC on May 23 while we experienced westerly to northwesterly gales of 8 Bft. By 18 UTC on that day, central presure was further up to 985 at 52 North 36 West, and the northwesterly winds had abated to 6 Bft.

During the next few days, filling went on up to a central pressure of 1000, and the low moved up to 52 Nord 38 West, then turned southwest to south, passing again within a short distance of the ship, its passage being nearly unnoticed (that is, except on the weather map) and then swinging southeast to east.

Meanwhile, a high of up to 1035 had established itself over the northern part of Hudson Bay on May 25, and this migrated southeast to Labrador during May 26, weakening to 1025. Still, it was responsible for northerly winds of 6 Bft on METEOR's probing position by then.

Movement of the high did not stop there, the high reaching 40 North 50 west by May 28. By that time it became stationary, but ist central pressure did not stop strengthening. When it had passed Newfoundland, it had created favourable conditions for the development of a low over northern Quebec in its wake. This low formed in due course on May 27 and intensified to 995 until May 29. At the same time, a low of 1007 developed near Cape Cod, moving northeast. On the eastern flank of both these lows, strong southerly winds developed. Dealing with those, the METEOR headed for St. John's and called there on May 31, 2001.

The meteorological instruments proved to be of no concern during this cruise. The same can be said, fortunately, of the METCO computer processing and storing the data.

As far as the global radiation data measured during the cruise are concerned, there is an additional clue to the data being reliable: they are sent for immediate inspection weekly to the German Weather Service's facilities in Hamburg, and they have not been declared faulty there. So, it can be concluded that all data made available to the scientific crew by the ship's weather station are reliable.

1.6 Station List M 50/1

Table 1.3: CTD/ADCP List

Meteor M50/1 CTD Stations

Profile	Station	Date	Time	Latitude	Longitude	Water Depth	Profile Depth	Comment
1	53	09.05.01	19:56	43° 21.41' N	56° 36.45' W	3458	2008	
2	54	11.05.01	01:37	43° 14.63' N	49° 28.53' W	903	807	
3	55	11.05.01	04:15	43° 10.00' N	49° 9.01' W	1062	1028	
4	56	11.05.01	08:50	43° 4.58' N	48° 53.43' W	2015	1989	
5	58	11.05.01	14:05	43° 0.81' N	48° 38.22' W	2548	2530	
6	60	11.05.01	20:14	42° 57.20' N	48° 23.61' W	3030	3018	
7	61	12.05.01	06:09	42° 47.53' N	47° 48.00' W	3662	3682	
8	64	12.05.01	19:21	42° 31.16' N	46° 47.49' W	4326	4360	
9	65	13.05.01	01:07	42° 35.26' N	47° 5.79' W	4044	4074	
10	66	13.05.01	05:33	42° 41.05' N	47° 27.07' W	3833	3857	
11	67	13.05.01	10:28	42° 50.53' N	47° 59.86' W	3535	3553	
12	69	13.05.01	19:25	42° 47.67' N	47° 48.10' W	3667	3687	
13	70	13.05.01	23:33	42° 54.19' N	48° 13.27' W	3258	3267	
14	71	14.05.01	06:38	43° 10.64' N	49° 6.83' W	1170	1135	
15	73	14.05.01	11:45	43° 2.31' N	48° 50.41' W	2153	2124	
16	75	14.05.01	20:15	42° 55.48' N	48° 21.34' W	3069	3090	
17	76	15.05.01	07:28	42° 31.17' N	46° 47.44' W	4303	4353	
18	78	15.05.01	18:07	42° 21.06' N	46° 8.12' W	4679	4769	
19	79	16.05.01	00:14	42° 9.73' N	45° 29.61' W	4750	4834	
20	80	16.05.01	09:35	42° 32.99' N	44° 11.10' W	4877	4969	
21	81	16.05.01	19:17	42° 54.25' N	42° 48.66' W	4841	4923	
22	82	17.05.01	04:33	43° 14.95' N	41° 30.00' W	4825	4896	
23	83	17.05.01	13:43	43° 37.98' N	40° 12.15' W	4816	4895	
24	84	17.05.01	22:41	43° 57.04' N	38° 47.95' W	2615	2597	
25	85	18.05.01	06:26	44° 17.11' N	37° 23.87' W	4408	4461	
26	86	18.05.01	14:28	44° 36.98' N	36° 0.00' W	4052	4097	
27	87	18.05.01	22:51	44° 57.06' N	34° 35.01' W	3958	3998	
28	89	19.05.01	14:15	45° 20.10' N	33° 9.53' W	3615	3635	
29	93	20.05.01	14:22	46° 23.52' N	29° 50.56' W	3240	3283	
30	95	21.05.01	06:10	45° 53.07' N	31° 34.98' W	3590	3591	
31	97	23.05.01	18:56	49° 45.30' N	41° 29.31' W	4403	4456	
32	98	24.05.01	01:00	49° 32.40' N	42° 2.75' W	4448	4472	
33	99	24.05.01	06:43	49° 21.15' N	42° 37.61' W	4228	4270	
34	100	24.05.01	11:43	49° 7.36' N	43° 10.69' W	3941	3957	
35	101	24.05.01	15:58	48° 57.95' N	43° 35.54' W	3467	3469	
36	102	24.05.01	19:56	48° 50.93' N	43° 57.89' W	2418	2367	
37	104	24.05.01	23:26	48° 45.12' N	44° 18.47' W	1809	1788	
38	105	25.05.01	02:05	48° 38.43' N	44° 35.07' W	1395	1368	
39	106	25.05.01	04:33	48° 33.98' N	44° 47.86' W	1036	1003	
40	107	25.05.01	06:45	48° 30.02' N	45° 0.04' W	815	785	
41	108	26.05.01	18:22	54° 16.97' N	48° 10.97' W	3949	3965	
42	109	26.05.01	22:41	54° 4.94' N	48° 35.06' W	3818	3837	
43	110	27.05.01	03:20	53° 53.90' N	49° 1.04' W	3793	3810	
44	111	27.05.01	07:46	53° 44.96' N	49° 23.83' W	3747	3763	
45	112	27.05.01	11:35	53° 36.78' N	49° 37.58' W	3676	3688	
46	114	27.05.01	18:56	53° 30.96' N	49° 56.96' W	3570	3574	
47	115	27.05.01	22:44	53° 23.99' N	50° 13.08' W	3450	3449	
48	116	28.05.01	03:08	53° 12.45' N	50° 44.01' W	3126	3127	
49	117	28.05.01	06:16	53° 17.53' N	50° 30.88' W	3255	3251	
50	120	28.05.01	19:56	53° 5.30' N	50° 58.02' W	2857	2839	
51	121	28.05.01	23:32	53° 8.07' N	50° 54.15' W	2904	2895	
52	122	29.05.01	03:45	53° 0.52' N	51° 12.88' W	2410	2410	
53	123	29.05.01	06:35	52° 55.47' N	51° 24.43' W	2069	2041	
54	124	29.05.01	09:13	52° 50.96' N	51° 34.84' W	1364	1323	
55	125	29.05.01	11:31	52° 46.56' N	51° 47.15' W	446	450	
56	126	29.05.01	13:41	52° 41.62' N	52° 0.60' W	310	288	

Table 1.4: M50/1 Mooring recovery

MOORING	DATE OF RECOVERY	START (UTC)	END (UTC)	COMMENTS
K101_1	May 11. 2001	11:46	12:46	low visibility
K102_1	May 11. 2001	17:20	19:24	
K103_1	May 12. 2001	10:09	11:53	
K104_1	May 12. 2001	16:45	18:41	
BSH K3	May 19. 2001	09:20	13:30	
BSH K1	May 20. 2001	11:04	14:15	radio defect
K27	May 27. 2001	15:39	17:50	
K28	May 28. 2001	08:46	10:36	radio defect
K29				not found

Table 1.5: M50/1 Mooring deployments

MOORING	DEPLOYMENT	UTC	LATITUDE	LONGITUDE	WATER DEPTH
K101_2	May 14. 2001	11:05	43° 04.0' N	48° 52.5' W	2016 m (corr.)
K102_2	May 14. 2001	19:21	42° 57.0' N	48° 23.5' W	3001 m (corr.)
K103_2	May 13. 2001	18:51	42° 46.8' N	47° 45.2' W	3600 m (corr.)
K104_2	May 15. 2001	14:20	42° 31.8' N	46° 47.35' W	4310 m (corr.)
BSH 3 2001	May 19. 2001	20:34	45° 21.67' N	33° 09.40' W	3640 m (uncorr.)
BSH 1 2001	May 20. 2001	21:32	46° 24.26' N	29° 54.60' W	3220 m (corr.)

Table 1.6: Float Deployments

S/N	Dec-Argos-ID	Hex-Argos-ID	Start time UTC	Launched UTC	Position	Remarks
IFM						
283	03836	3BF23	14.05.01 / 12:07	14.05.01 / 13:38	43°N3,44 / 48°W50,63	touched the ship during launch
288	13811	D7CD1	24.05.01 / 17:16	24.05.01 / 21:45	48°N49,85 / 43°W58,16	WD 2300m
289	13812	D7D3B	24.05.01 / 19:10	24.05.01 / 22:40	48°N47,06 / 44°W08,92	WD 2000 m
BSH						
298	21612	51B29	18.05.01 / 22:15	19.05.01 / 01:15	44°N56,92 / 34°W34,51	
299	22005	57D64	20.05.01 / 02:16	20.05.01 / 03:38	45°N53,09 / 31°W34,95	

300	22335	5CFF7	20.05.01 / 17:55	20.05.01 / 22:00	46°N24,28 / 29°W53,62	
301	15396	F0933	21.05.01 / 10:02	21.05.01 / 15:21	46°N30,19 / 33°W09,90	
302	15398	F0995	19.05.01 / 13:40	19.05.01 / 16:30	45°N18,78 / 33°W09,00	

Tabel 1.7: Marine chemistry measurements

Station/Profil	**C_T/Dup.**	**PH/Dup.**	**A_T/Dup.**	**^{13}C**	**TOC**	**Chlorophyll**
53/01	-	-	-	-	-	-
54/02	-	12/2	12/2	10	-	-
55/03	-	14/2	14/2	12	12	4
57/04	-	22/2	22/2	20	-	2
58/05	-	1	1	-	1	-
60/06	-	22/2	22/2	20	6	3
61/07	-	21/2	21/2	19	7	4
64/08	-	22/2	22/2	20	6	3
65/09	-	1	1	-	-	1
66/10	-	22/2	22/2	20	13	3
67/11	-	1	1	-	-	1
69/12	-	-	-	-	-	-
70/13	22/2	23/2	23/2	21	8	2
71/14	-	1	1	-	-	1
73/15	-	21/2	21/2	-	-	-
76/17	24/2	24/2	24/2	22	-	-
78/18	22/2	22/2	22/2	20	7	3
79/19	-	22/2	22/2	20	5	3
80/20	1	1	1	-	-	1
81/21	23/2	23/2	-	21	6	3
82/22	23/2	23/2	23/3	21	6	3
83/23	22/2	22/2	22	20	7	3
84/24	9/1	9/2	9/3	-	-	1
85/25	-	22/2	22/2	20	20	3
86/26	-	23/2	23/2	21	21	3
87/27	1	1	1	-	-	1
89/28	22/2	22/2	22/2	20	20	2
93/29	23/2	23/2	23/2	21	21	4
95/30	24/2	24/2	24/2	22	22	3
97/31	24/2	24/2	24/2	22	22	3
99/33	24/2	24/2	24/2	22	7	3
102/36	19/2	19/2	19/4	-	-	3

Station/Profil	C_T/Dup.	PH/Dup.	A_T/Dup.	^{13}C	TOC	Chlorophyll
105/38	12/2	12/2	10	8	8	2
107/40	11/2	11/2	11/2	-	-	-
108/41	24/2	24/2	24/2	22	22	3
111/44	24/2	24/2	24/2	22	-	-
114/46	23/2	23/2	23/2	-	-	-
117/49	24/2	24/2	24/2	-	-	-
120/50	23/2	23/2	23/2	-	-	-
122/52	13/1	13/1	13/1	-	-	-
124/54	12/1	12/1	12/1	-	-	-
125/55	5	5	5	-	-	-
126/56	4/1	4/1	4/1	-	-	-
Total:	459/43	688/66	663/62	444	242	69

1.7 Concluding Remarks

It is our particular pleasure to thank captain M. Kull and his crew for the friendly, professional and helpful attitude, that made this cruise pleasant and very successful. We also thank our colleagues at the Bedford Institute of Oceanography, Allyn Clarke and Murray Scotney, for their generous help when we were faced by the problem with our damaged container and all the instruments inside.

Funding for the work at M50/1 was granted by the Deutsche Forschungsgemeinschaft (DFG) through the SFB-460 and by making the ship time available. This is greatly appreciated.

1.8 References

Clayton, T.D. and Byrne, R.H., 1993. Spectrophotometric seawater pH measurements: Total hydrogen ion concentration scale calibration of m-cresol purple and at-sea results. Deep Sea Res., 40(1): 2115-2129.

Doe, 1994. Handbook of methods for the analysis of various parameters of the carbon dioxide system in sea water. ORNL/CDIAC-74, U. S. Dep. of Energy, Oak Ridge Natl. Lab., Oak Ridge, Tenn., USA.

Friis, K., 2001. Separation von anthropogenem CO_2 im Nordatlantik – Methodische Entwicklungen und Messungen. Dissertation. Christian-Albrechts-Universität zu Kiel, Kiel, 137 pp.

Johnson, K.M., Wills, K.D., Butler, D.B., Johnson, W.K. und Wong, C.S., 1993. Coulometric total carbon dioxide analysis for marine studies: Maximizing the performance of an automated gas extraction system and coulometric detector. Mar. Chem., 44(2-4): 167-188.

Körtzinger, A., Thomas, H., Schneider, B., Gronau, N., Mintrop, L. und Duinker, J.C., 1996. At-sea intercomparison of two newly designed underway pCO2 systems - encouraging results. Mar. Chem., 52(2): 133-145.

Lewis, E. und Wallace, D.W.R., 1998. CO2SYS - Program developed for the CO2 system calculations. Carbon Dioxide Inf. Anal. Center; Report ORNL/CDIAC-105, Oak Ridge, Tenn., U.S.A.

Millero, F.J. and Dickson, A.G., 1987. A comparison of the equilibrium constants for the dissociation of carbonic acid in seawater media. Deep Sea Res., 34A(10): 1733-1743.

Millero, F.J., Byrne, R.H., Wanninkhof, R., Feely, R., Clayton, T., Murphy, P. und Lamb, M.F., 1993. The internal consistency of CO2 measurements in the Equatorial Pacific. Mar. Chem., 44(2-4): 269-280.

Mintrop, L., Perez, F.F., Gonzalez-Davila, M., Santana-Casiano, J.M. und Körtzinger, A., 2000. Alkalinity determination by potentiometry: intercalibration using three different methods. Ciencias Marinas, 26(1): 23-37.

METEOR-Berichte 02-2

North Atlantic 2001

Part 2

Cruise No. 50, Leg 2

1 June – 19 June 2001, St. John's – St. John's

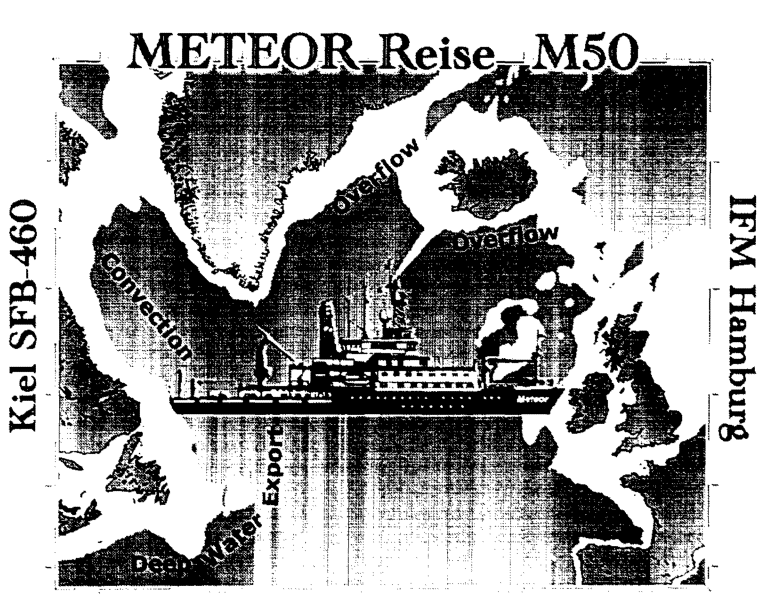

F. Schott, K. Affler, Ch. Begler, M. Busack, J. Dengg, M. Dengler, G. Fraas, G. Kahl, D. Kieke, D. Kindler, R. Link, B. Manzke, Ch. Mertens, M. Müller, G. Niehus, W.-T. Ochsenhirt, U. Papenburg, A. Pinck, R. Schoenefeldt, M. Schütt, Th. Truscheit

Editorial Assistance:

Frank Schmieder
Fachbereich Geowissenschaften, Universität Bremen

Leitstelle METEOR
Institut für Meereskunde der Universität Hamburg

2002

Table of Contents (M 50/2)

2.1 Participants M 50/2

1	Schott, Friedrich, Prof., Dr.	Chief Scientist	IfMK
2	Affler, Karina	Salinometry	IfMK
3	Begler, Christian	Moorings	IfMK
4	Busack, Michael	Technical support	IfMK
5	Dengg, Joachim, Dr.	CTD/ADCP-Watch	IfMK
6	Dengler, Marcus, Dr.	CTD/ADCP-Watch	IfMK
7	Fraas, Gerd	CTD/Moorings	UBU
8	Kahl, Gerhard	Meteorology	DWD
9	Kieke, Dagmar	CFC's, CCL_4	UBU
10	Kindler, Detlef	Tomography	IfMK
11	Link, Rudolf	Tomography	IfMK
12	Manzke, Bert	Oxygen	IfMK
13	Mertens, Christian, Dr.	Data processing	UBU
14	Müller, Mario	Moorings/ADCP	IfMK
15	Niehus, Gerd	CTD/ADCP-Watch	IfMK
16	Ochsenhirt, Wolf-Thilo	Meteorology	DWD
17	Papenburg, Uwe	Moorings	IfMK
18	Pinck, Andreas	Telemetry, CTD	IfMK
19	Schoenefeldt, Rena	CTD/ADCP-Watch	IfMK
20	Schütt, Martina	CFC's, CCL_4	IfMK
21	Truscheit, Thorsten	Meteorology	DWD

Participating Institutions

IfMK Institut für Meereskunde an der Universität Kiel, Düsternbrooker Weg 20, 24105 Kiel - Germany, e-mail: fschott@ifm.uni-kiel.de

DWD Deutscher Wetterdienst, Geschäftsfeld Seeschiffahrt, Bernhard-Nocht-Str. 76, 20359 Hamburg - Germany, e-mail: edmund.knuth@dwd.de

UBU Universität Bremen, Institut für Umweltphysik, Abt. Tracer-Oceanographie, Bibliotheksstraße, 28359 Bremen - Germany, e-mail: mrhein@physik.uni-bremen.de

2.2 Research Program

The deep reaching convection in the Labrador Sea forms the upper component of the North Atlantic Deep Water and hence the southward flowing branch of the thermohaline circulation. From time series of ocean weather ship "BRAVO" significant interannual variation of the convection activity is known. Hence the Labrador Sea is an ideal region to investigate convection processes, its variability and its impact on the water masses and the circulation of the deep water. During the years of the SFB 460 the convection activity continously decreased. In the year 2000 the layer of homogenously mixed Labrador Sea Water was thinner than in the 20 years before.

The work in the Labrador Sea within the context of the SFB 460 focusses on the investigation of convection activity in the subpolar gyre, on large-scale water mass distributions, spreading and transformation processes as well as their relation to the thermohaline circulation. This is expected to lead to a better understanding of the forcing of convection and its variability e.g. in the context of the NAO, as well as of the impact of convection variability on the water masses and the overturning circulation of the Atlantic. Convection observations with moored stratification-, current- and tomography measurements, which started several years ago, was continued on M50/2.

Previous work with moorings as well as the analysis of satellite altimetry have shown that the Labrador Sea is governed by an energetic eddy field. Formation mechanisms are instabilities of the boundary currents, wind field variations and the delay of the convection regime. These eddy fields and its interaction with the mean circulation shall be further investigated during M50/2.

Model evidence further shows that the so called "preconditioning", the prefered weakening of the stratification by uprise of the isopycnals, can be enhanced locally by cold, cyclonic eddies. In consequence, the location of deepest convection can move with such eddies and influence also the restratification.

It was planned to trace such eddies by RAFOS-floats. To really be useful during the convection period, RAFOS floats were moored in a float park in the convection region to be released next winter. Further hydrographic measurements with CTD-, ADCP- and Freon-measurements were carried out to describe the water mass distribution in the Labrador Sea.

2.3. Narrative of the Cruise

RV METEOR cruise M/50 left St. John's in the morning of 2 June 2001. During the two-day transit to the tomography array north of Hamilton Bank it was mostly foggy and some ice was encountered, without causing delays. The first mooring position, K42 (Fig. 2.1), was reached in the early morning of 4 June. The weather was perfect with calm seas and mostly good visibility. The mooring and its three transponders were retrieved in good time and the first CTD/LADCP cast was taken (see table 2.1 in chapter 2.6), with instructions for those CTD watch members that were unfamiliar with the system. After some CTDs along the AR7W line during the subsequent night, the retrieval of mooring K41 (see table 2.2 in chapter 2.6) and its transponders was accomplished on 5 June. On 6 June followed the retrieval of the third tomography station, K43, with its transponders. METEOR then had to hurry on to the cycling CTD mooring, position K40, located some 43 nm away. This station was retrieved in the evening of 6 June under quickly

deteriorating visibility. Although close by the top float could only be located in on by use of the 27 MHz buoy transmitter and METEOR's direction finder.

The cruise then moved southward along the shelf edge toward the 53°N moored array (Fig. 2.1) with CTD casts taken along the way for calibration of the acoustic tomography ray paths. Further east, an extended ice field was encountered at the shelf edge, combined with poor visibility, forcing us to make a seaward detour. This resulted in a delayed arrival at 53°N where the intent was to drag for that boundary array mooring K29 which had not been acoustically located on the preceding cruise leg M50/1 and to redeploy three new moorings.

Due to the delay and rougher weather on 8 June it was decided to spend the rest of that day deploying the moorings K38 and K39, which was successfully accomplished on the evening of 8 June. Early in the morning of 9 June the dragging operation was prepared by deploying nearly 10 km of tow wire around the mooring and then dragging around it on various courses. Since the mooring location is known fairly precisely and it was held up by a lot of net buoyancy in the water, such dragging should cut the thin mooring wire and let the mooring float up to the surface. The operation was carried out a number of times but with no success, and the conlusion was that the mooring was no longer in its place.

After CTD/ADCP work along the 53°N array line during the following night, the third array mooring, K37, was deployed on 9 June in the early morning. Then a northwesterly CTD line parallel to the Labrador Sea axis was started, running about normal to the WOCE AR7W line. In the course of the work, evaluation of the „Ocean Surveyor" Phased Array was continued that had been started by the previous group on M50/1. The range and data quality of the instrument are superb, while the problems in feeding heading directions into the system continued. This problem can, however, be avoided by merging heading data with the raw ADCP data in the computer outside the RDI processing system.

On 13 June the northernmost tomography station, K53, was deployed smoothly. The transponders were deployed and tracks for determining their positions acoustically were run normal to the transponder triangle sides. Along the way westward toward position K51, a CTD cast on the connection line K51-K53 as well on the WOCE line north of K51 were taken. In the morning of 14 June deployment of mooring K51 started. This mooring is equipped with a flexible surface link, allowing satellite transfer of records from near-surface Microcat temperature and salinity recorders. After K51 and associated transponders were deployed, the Pegasus profiler was launched in order to obtain comparison profiles with the LADCP. In particular, we were interested in the near-bottom shear layer where bottom reflections reduce LADCP data quality. However, the instrument stopped transmitting right after launch. Most likely it was damaged in the crash of the container when it was unloaded in Halifax before the leg M50/1. Fortunately, the Pegasus returned to the surface at about the expected time and could be recovered.

Continuing the WOCE line with CTD/LADCP stations toward the position of the last mooring to be deployed, station K52 was reached in the morning of 15 June. Mooring K52 and transponders were deployed, and simultaneously with the subsequent CTD/LADCP cast a Pegasus comparison profile was taken with the backup Pegasus instrument. In the evening of 15 June, station work around K52 was accomplished and the WOCE line was completed with two more stations toward the shelf edge off Hamilton Bank, where station work was terminated. In

addition to the hydrographic and mooring work 4 profiling ALACE floats were launched during this leg (see table 2.3 in chapter 2.6).

Altogether, 4 moorings were retrieved and 7 redeployed on this cruise leg, and 3 transponder sets had to be retrieved and redeployed, as well. 33 CTD/LADCP casts were taken with emphasis on our two repeat lines normal to the boundary current and a wealth of deep-eaching shipboard ADCP and rosette-mounted LADCP profiles were obtained. Most of the calibration and first processing could already be accomplished during the cruise and on the return voyage to St. John's. The port was reached in the morning of 18 June, 2001.

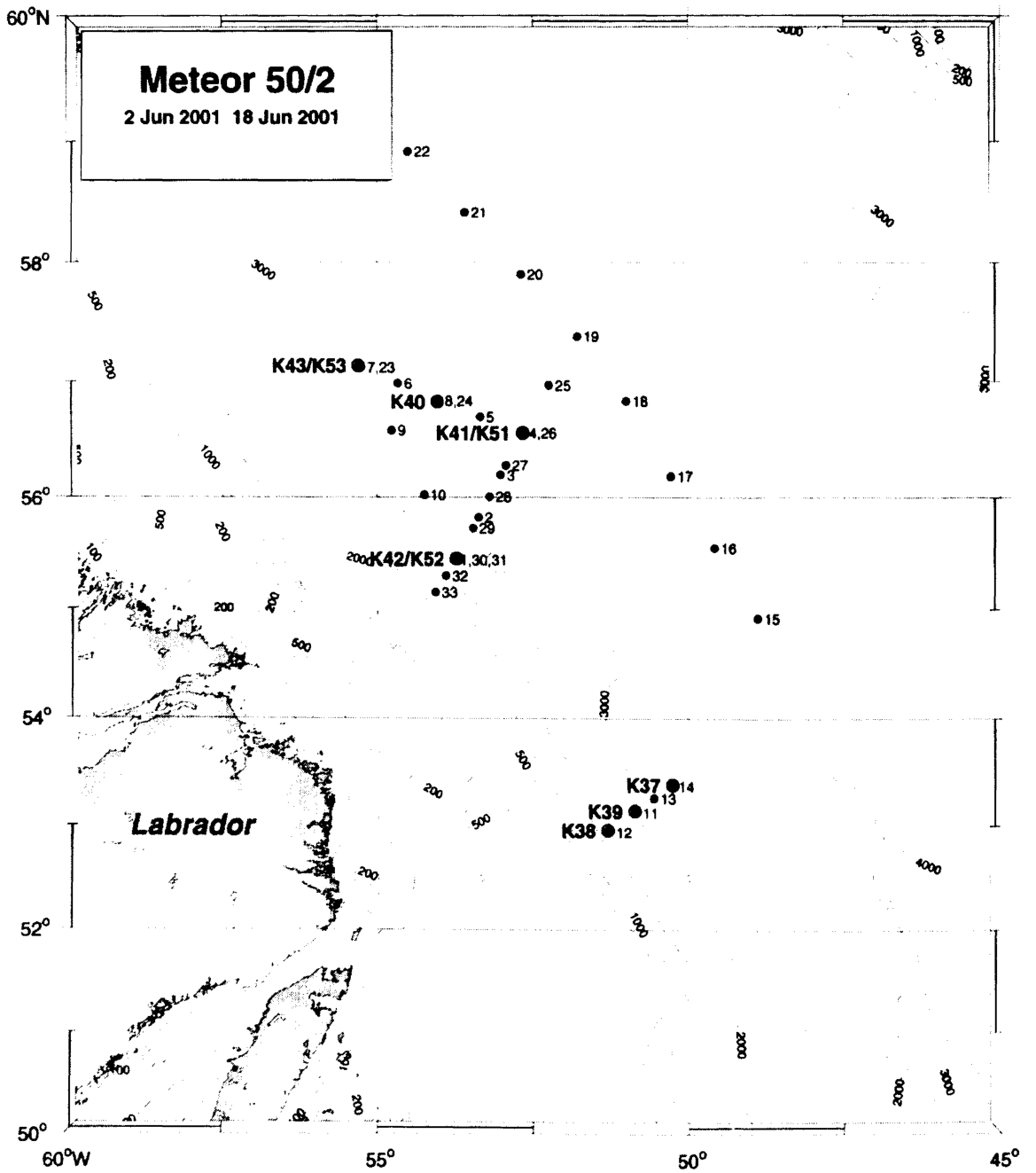

Fig. 2.1: Cruise map of METEOR cruise M50/2 with CTD-stations and mooring locations.

2.4 Preliminary Results

2.4.1 Convection Activity 2000/1 from Moored ADCPs, T/S Records

(C. Mertens, F. Schott)

a) Mooring Activities, Data Retrieval, Calibrations

Observations of deep convection were carried out at the moored stations K40 and K41, both deployed during Hudson cruise 9 in summer 2000. Mooring K41 was equipped with a upward looking ADCP at 300 m depth, one additional current meter near the bottom, and a number of temperature/conductivity (MicroCAT) and temperature/pressure (miniTD build at the IfM Kiel) recorders in the upper 1500 m. Most instruments were successfully recovered and had full records, except for the topmost MicroCAT that was torn off on 12 July, 2000 and one miniTD that returned no data. Thus the time series of convection observations in the central Labrador Sea, beginning in summer 1996, is now extended to five years. After their recovery, the MicroCAT recorders were lowered with the rosette and compared with the CTD measurements to check their long-term stability.

At mooring K40, located northwestward of K41, a moored CTD-profiler was installed. The profiler is designed to climb up and down the mooring wire while aquiring CTD data. Additionally mooring K40 was equipped with a downward looking ADCP and a miniTD as the top elements. The profiler data cannot be read out during the cruise, and the instrument has first to be returned to the manufacturer for data retrieval. The ADCP had a full record, and the miniTD contained atemperature time series, but no pressure data.

Mooring K42 was located in the boundary current region of the Labrador Sea and carried similar instruments as K41, that were an upward looking ADCP at 350 m, two current meters at deeper levels, and a number of MicroCATs and miniTDs in the upper 1500 m. Again most of the instruments returned full data records, except for the ADCP that showed some corrosion near the transducers from a minor flooding. One of the miniTDs lacked the pressure measurements, but had temperature data.

The northernmost mooring K43 formed a tomography array with the moorings K41 and K42 (see Section 2.4.2), and was additionally equipped with two MicroCATs, one miniTD (that returned no data), and one current meter. Further, two 400 m thermistor strings were deployed, but both were malfunctioning.

Most of the intruments were refurbished during the M50/2 cruise, and redeployed into the moorings K51, K52, and K53, as well as into the so called 53°N-Array (K37, K38, and K39), where the moorings K27 and K28 had already been recovered during M50/1. The attempt was made to dredge for the missing mooring K29, but without success (see Section 2.3).

b) Results

The by now five year time series of observations in the central Labrador Sea revealed considerable variability of convection activity in this area. During the winter of 1996/97 deep convection reaching to depths of about 1300 m and a temperature of about 2.7 °C of the deepest mixed layer were observed (Figure 2.2). The following two winters (1997/98 and 1998/99) showed rather shallow convection to about 550 m depth at the central convection moorings, and higher temperatures of the final winter mixed layer of 2.8°C and 2.95°C, respectively. Deeper

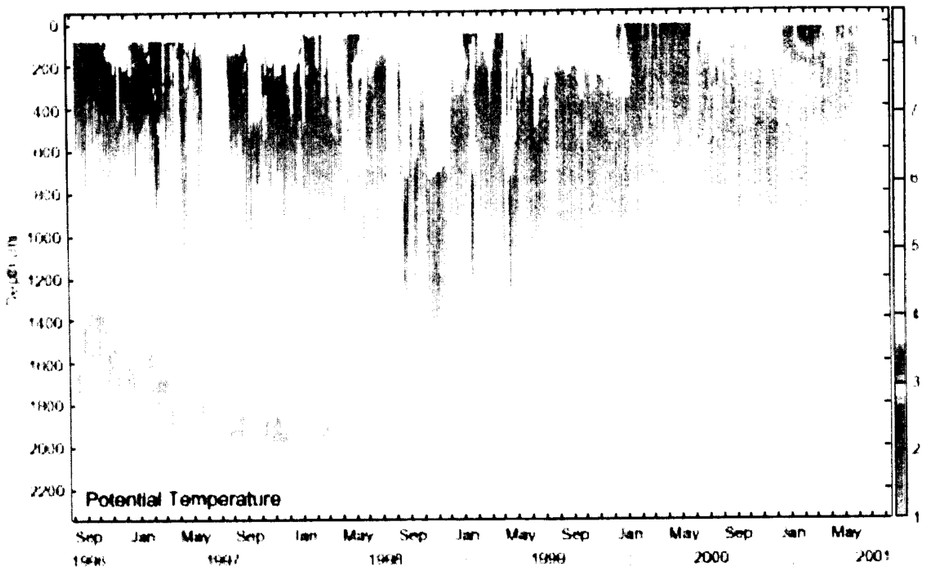

Fig. 2.2: Mean daily potential temperature at the convection moorings (K1, K11, K21, K31, and K41) in the central Labrador Sea from 1996 to 2001. The contour interval is 0.1 °C.

convection to about 1000 m was observed in 1999/2000, again with a relatively warm winter mixed layer of about 3°C. The temperature time series from the last winter at mooring K41 show the shallowest winter mixed layer of the observational period. Mixed layer deepening to only about 300 m was observed. However, increased temperature fluctuations down to about 800 m during April and May 2001 indicate, that deeper convection might have occurred in the vicinity of the mooring.

That ADCP vertical velocity records obtained at mooring K41 confirm that no deep convection took place at the mooring location as no burst of downward motion corresponding to convection cells (plumes) were observed. Northwestward at mooring K40, a number of events of downward motion exceeding 5 cm/s occurred during mid February, indicating that the convection activity might have been more intense towards the northern Labrador Sea.

The temperature time series at the convection moorings show a general warming of the upper 1500 m of the water column over the first three years of observations. The largest warming occurred in the upper 500 m with the annual cycle superimposed. Linear trends fitted to the temperature time series show that the warming decreases towards the lower layers. The annual warming rate resulting from the linear fits ranges from 0.16°C/yr in the upper 500 m to 0.12°C/yr for the 1000 - 1500 m layer. The heat fluxes equivalent to the increasing temperature range from 10.3 W/m^2 in the upper layer to 8.1 W/m^2 in the lowest layer. The mean annual warming rate over the 1500 m water column results in 0.15 °C/yr corresponding to a net heat flux of 28.3 W/m^2. The temperature development observed during the last two years shows that this warming trend has stopped and that despite the moderate convection activity the average temperature stayed relatively constant.

2.4.2 Tomography, Recovery and Re-deployment of Ocean Acoustic Tomography Moorings

a) Technical Aspects

Recovery of the 2000/2001 array

During METEOR-cruise M50/2 two WEBB-type ocean acoustic tomography transceivers (center frequency of transmission 400 Hz) and one HLF5-type transceiver (250 Hz) were recovered safely, together with their three bottom mounted acoustic transponders which were arranged in a triangular shaped array (side length of 5000 m) around the base of each tomography mooring in order to navigate the tomographic devices for horizontal and vertical motions.

The tomography instruments were part of the moorings K41, K42 and K43, respectively, which had been deployed in June 2000 during a joint Canadian/German Labrador Sea cruise on the Canadian Coast Guard Ship HUDSON (see fig. 2.1). The deployment period lasted from 29 May 2000 (deployment of first transceiver) until 6 June 2001 (recovery last of instrument), and the transceivers worked in concert from 13 June 2000 until 1 June 2001, i. e. for 353 days.

All instruments finished their tasks as scheduled. However, after about 120 days the HLF5-type instrument in mooring K43 stopped transmitting, most probably because of a failiure of the Lithium-battery package driving the 250-Hz-transmitter. The reason for that might have been some blown fuses, due to an unusually high current drainage of the sound source. This has to be analyzed in detail after the cruise. Nevertheless, the receiving activities - and all other functions being supplied by an indepedent alkaline battery package - were not affected by this failiure. Hence, high quality receptions from both the other instruments K41 and K42 (see cruise map), which worked on schedule and without technical problems, could be recorded over the whole deployment duration.

The insonified section between K41 and K42 was covered by two-way transmissions all the time, since both instruments transmitted and received quasi simultaneously. This allows for reciprocal reception processing, which will increase the travel-time accuary remarkably. On the other two legs (K41-K43 and K42-K43), reciprocal reception could be recorded until the HLF5 had stopped transmitting. For the remaining time only one-way receptions are available.

Re-deployment

The new ocean acoustic tomography array for the period June 2001 until June 2002 (as scheduled) consists of three moorings K51, K52 and K53, which were to be deployed in a triangle with side lengths of 140 km (K51-K52), 210 km (K52-K53), and 172 km (K53-K51) (see figure 2.1), together with their bottom mounted transponders. It follows the same geometry of the previous year by replacing K41 through K51 and K42 through K52, again using WEBB-type transceivers and replacing the HLF5 type transceiver K43 by a third Webb-type instrument, now called K53.

This one has been repaired and refurbished prior to the M50/2 cruise at the manufacturer. A closer look at the recorded engineering data from the two recovered WEBB instruments showed that they could be re-deployed for the next annual period with no doubts. They were refurbished on board R/V METEOR during calm weather conditions, by replacing their heavy battery packages, and extensive tests were performed. After deployment all moorings were supplied with three releasable bottom transponders each. Their absolute positions were surveyed by

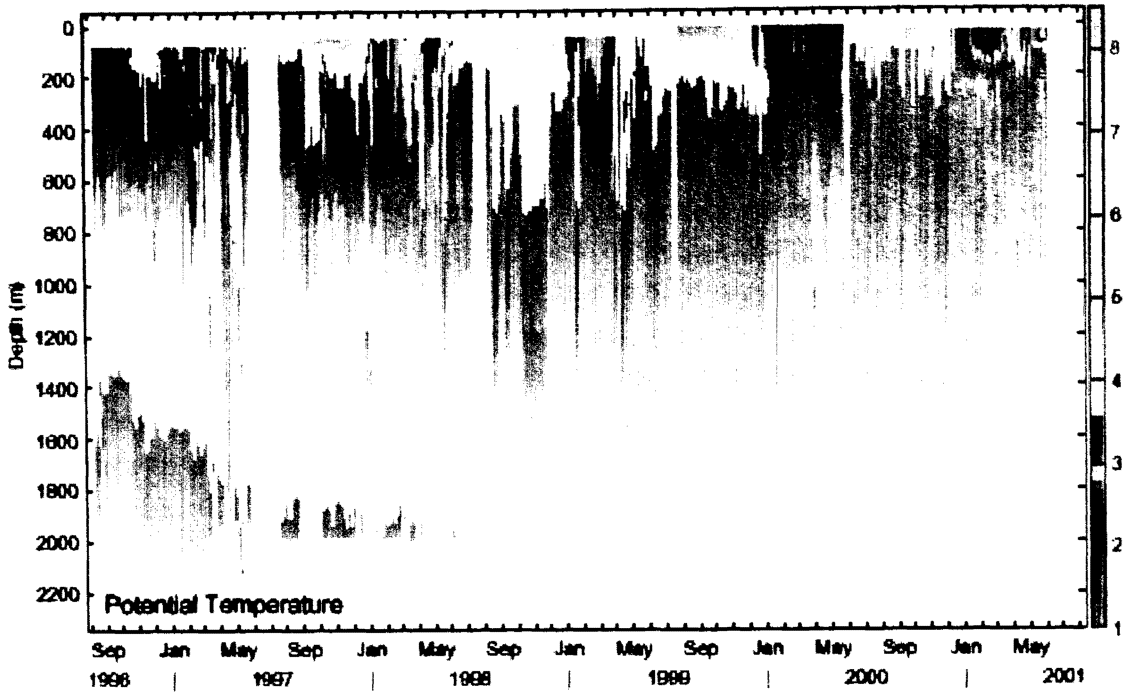

Fig. 2.2: Mean daily potential temperature at the convection moorings (K1, K11, K21, K31, and K41) in the central Labrador Sea from 1996 to 2001. The contour interval is 0.1 °C.

convection to about 1000 m was observed in 1999/2000, again with a relatively warm winter mixed layer of about 3°C. The temperature time series from the last winter at mooring K41 show the shallowest winter mixed layer of the observational period. Mixed layer deepening to only about 300 m was observed. However, increased temperature fluctuations down to about 800 m during April and May 2001 indicate, that deeper convection might have occurred in the vicinity of the mooring.

That ADCP vertical velocity records obtained at mooring K41 confirm that no deep convection took place at the mooring location as no burst of downward motion corresponding to convection cells (plumes) were observed. Northwestward at mooring K40, a number of events of downward motion exceeding 5 cm/s occurred during mid February, indicating that the convection activity might have been more intense towards the northern Labrador Sea.

The temperature time series at the convection moorings show a general warming of the upper 1500 m of the water column over the first three years of observations. The largest warming occurred in the upper 500 m with the annual cycle superimposed. Linear trends fitted to the temperature time series show that the warming decreases towards the lower layers. The annual warming rate resulting from the linear fits ranges from 0.16°C/yr in the upper 500 m to 0.12°C/yr for the 1000 - 1500 m layer. The heat fluxes equivalent to the increasing temperature range from 10.3 W/m^2 in the upper layer to 8.1 W/m^2 in the lowest layer. The mean annual warming rate over the 1500 m water column results in 0.15 °C/yr corresponding to a net heat flux of 28.3 W/m^2. The temperature development observed during the last two years shows that this warming trend has stopped and that despite the moderate convection activity the average temperature stayed relatively constant.

2.4.2 Tomography, Recovery and Re-deployment of Ocean Acoustic Tomography Moorings

a) Technical Aspects

Recovery of the 2000/2001 array

During METEOR-cruise M50/2 two WEBB-type ocean acoustic tomography transceivers (center frequency of transmission 400 Hz) and one HLF5-type transceiver (250 Hz) were recovered safely, together with their three bottom mounted acoustic transponders which were arranged in a triangular shaped array (side length of 5000 m) around the base of each tomography mooring in order to navigate the tomographic devices for horizontal and vertical motions.

The tomography instruments were part of the moorings K41, K42 and K43, respectively, which had been deployed in June 2000 during a joint Canadian/German Labrador Sea cruise on the Canadian Coast Guard Ship HUDSON (see fig. 2.1). The deployment period lasted from 29 May 2000 (deployment of first transceiver) until 6 June 2001 (recovery last of instrument), and the transceivers worked in concert from 13 June 2000 until 1 June 2001, i. e. for 353 days.

All instruments finished their tasks as scheduled. However, after about 120 days the HLF5-type instrument in mooring K43 stopped transmitting, most probably because of a failiure of the Lithium-battery package driving the 250-Hz-transmitter. The reason for that might have been some blown fuses, due to an unusually high current drainage of the sound source. This has to be analyzed in detail after the cruise. Nevertheless, the receiving activities - and all other functions being supplied by an indepedent alkaline battery package - were not affected by this failiure. Hence, high quality receptions from both the other instruments K41 and K42 (see cruise map), which worked on schedule and without technical problems, could be recorded over the whole deployment duration.

The insonified section between K41 and K42 was covered by two-way transmissions all the time, since both instruments transmitted and received quasi simultaneously. This allows for reciprocal reception processing, which will increase the travel-time accuary remarkably. On the other two legs (K41-K43 and K42-K43), reciprocal reception could be recorded until the HLF5 had stopped transmitting. For the remaining time only one-way receptions are available.

Re-deployment

The new ocean acoustic tomography array for the period June 2001 until June 2002 (as scheduled) consists of three moorings K51, K52 and K53, which were to be deployed in a triangle with side lengths of 140 km (K51-K52), 210 km (K52-K53), and 172 km (K53-K51) (see figure 2.1), together with their bottom mounted transponders. It follows the same geometry of the previous year by replacing K41 through K51 and K42 through K52, again using WEBB-type transceivers and replacing the HLF5 type transceiver K43 by a third Webb-type instrument, now called K53.

This one has been repaired and refurbished prior to the M50/2 cruise at the manufacturer. A closer look at the recorded engineering data from the two recovered WEBB instruments showed that they could be re-deployed for the next annual period with no doubts. They were refurbished on board R/V METEOR during calm weather conditions, by replacing their heavy battery packages, and extensive tests were performed. After deployment all moorings were supplied with three releasable bottom transponders each. Their absolute positions were surveyed by

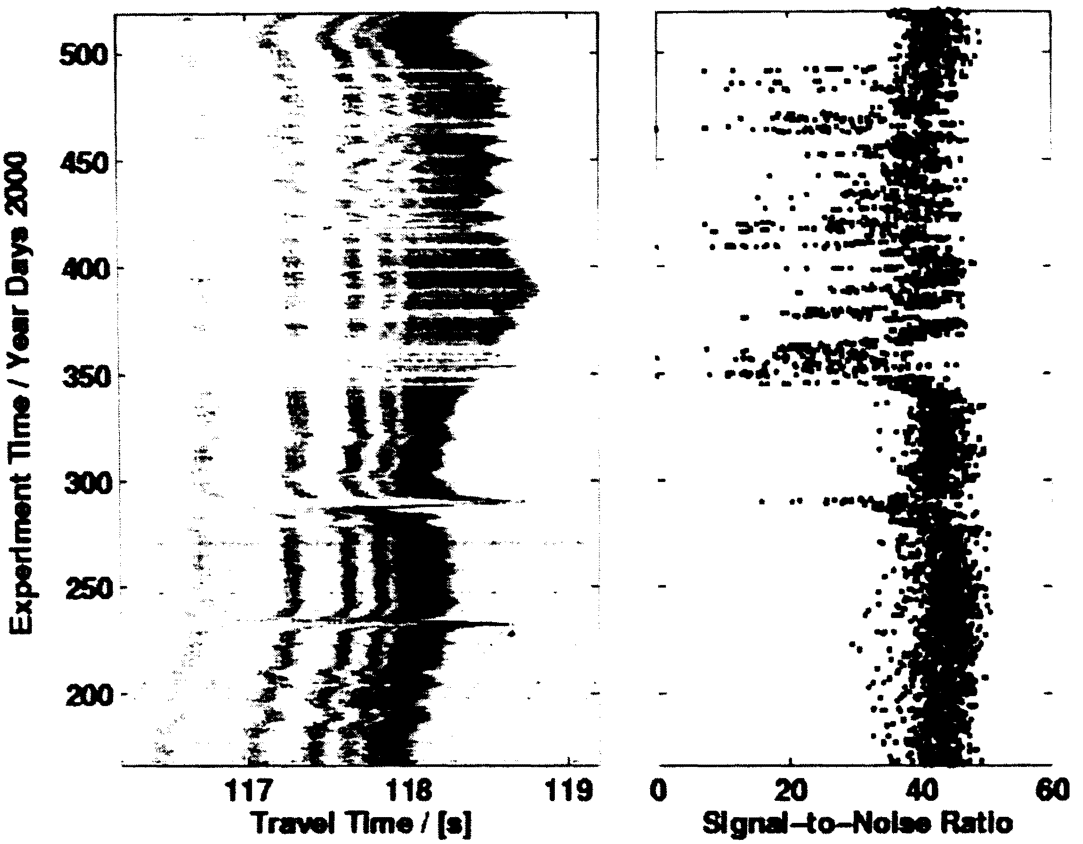

Fig. 2.3: (left) Time series of observed acoustic arrival patterns for the transceiver pair K43-K41 received by K43. The gray scale is a measure for the intensity of the received acoustic signal. Receptions are not corrected for clock drift or mooring motion. (right) Corresponding signal-to-noise ratio.

measuring their distances (acoustically) to the ship's transducer on different courses and using highly acurate GPS navigation for the positioning of the vessel.

b) Preliminary results

Some preliminary results of the deployment period 2000/2001 in terms of acoustic travel time patterns and signal-to-noise ratio for receptions at K43 from K41 are shown in Fig. 2.3.

The left panel represents the intensity of acoustic arrivals along travel time on a gray scale, drawn against experiment time on the y-axis. They are not yet corrected for mooring motion and clock drift, being necessary for further analysis and inversion of the data. Compared to previous deployment periods the vertical displacement of the devices due to mooring motion was moderate, reaching values above 200 m during a few events, only.

In the earlier and middle travel time part of the receptions 4 to 5 arrival groups (each consisting of a peak triplet) can clearly be distinguished for most of the experiment duration. Those groups will mainly be used for inverting travel times into sound speed and hence into temperature. They can be associated with triplets of particular sound propagation rays (so-called eigen rays, according to a raytrace model) sampling different portions of the water column, from the surface down to depths between 600 m (latest group) and 2500 m (first group).

In the right panel the corresponding signal-to-noise ratio for each reception is plotted. Since successful inversions can be done using receptions of a SNR higher than 25, a fairly continous

temperature time series will result from this example, showing values well above 40 over most of the time. Some periods of lower SNR values can clearly be associated with strong mooring motion events, indicated by pronounced travel time disturbances, e. g. arround year day 290.

The SNRs for the other sections are a little weaker, but still in a useable range for most of the receptions and allowing for successful inversions. In general it can be said, that the tomography deployment period 2000/2001 had yielded a data set of promising quality, which will be processed in order to extent the already existing 3-year long timeseries (on some legs) by another year.

2.4.3 Telemetry

During the recovery of mooring K41 only the lower part of the last year's surface telemetery array (consisting of a CO2 sensor, a MicroCat and a PT-logger) could be retrieved. The surface buoy and one MicroCat were lost from the mooring in July 2000, i. e. 7 weeks after deployment. From ARGOS satellite receptions it is known that it still drifts on an eastward course towards Scotland.

The mechanically re-designed telemetry system was successfully deployed on the top of mooring K51. The small 17'' surface buoy contains an inductive modem, a small size PC and an ARGOS transmitter operated by a micro controller. Every 2 hours the surface buoy receives temperature, conductivity and pressure data via the inductive link, delivered by the two MicroCats which are placed at 10 m and 40 m depth. The collected data are than transmitted to the ARGOS satellite system using a repetition rate of 20 seconds lasting for 110 minutes. This procedure happens every 4 hours.

2.4.4 Water Mass Variability of the Labrador Sea 2000/01 vs. Previous Years

Calibration CTD, Oxygen

During the M50/2 cruise a total of 33 CTD casts were obtained using a Sea-Bird Electronics SBE 9/11 system (IfM Kiel SBE1) that was additionally equipped with a Beckman dissolved oxygen sensor. The probe was attached to a 24 bottle 10 l General Oceanic rosette water sampler with a Sea-Bird bottle release unit. Two bottles were left out for a lowered ADCP system, hence a maximum of 22 bottles was used. The complete system worked properly throughout the entire cruise.

Four bottles were equipped with electronic reversing pressure and temperature sensors, used to check the stability of the laboratory calibration. Within the accuracy of the reversing thermometers no deviations were found and no further correction to the laboratory calibration was applied.

Salinity samples, typically six per profile, were analysed onboard using a Guildline Autosal 7 salinometer. The problems that occurred during M50/1 with the instrument were solved at the beginning of M50/2, and most of the time the salinometer worked fine with a drift of less than 0.002 in salinity during a measurement session. One session had to be interrupted due to a larger drift. After correcting the CTD measurements for a pressure, conductivity, and time dependence, the rms difference of 150 of the 184 samples was 0.0014 mS/cm for conductivity, corresponding to 0.0017 in salinity.

Oxygen samples were analyzed with traditional Winkler titration. Again typically six samples were taken per profile plus double samples on some stations. The coefficients for computing oxygen concentration from the CTD oxygen sensor were refitted, and a temporal drift was corrected afterwards. The resulting rms difference was 0.025 ml/l, using 197 of the 215 samples that were taken.

Hydrography

The major CTD sections occupied during M50/2 were the western part of the WOCE AR7W line and a section running from the southeast to the northwest through the inner Labrador Sea. Additionally CTD stations were carried out at the mooring locations and along the lines connecting the tomography stations.

The major aim of the hydrographic measurements along the AR7W line is to investigate the temporal changes of water mass properties in the formation region of Labrador Sea Water (LSW). Figure 2.4 shows salinity sections along the western part of the AR7W line from each summer between 1996 and 2001 together with the isopycnals separating the deep water masses. LSW is found at densities between σ_θ = 27.74-27.8. The salinity maximum between σ_θ = 27.80-27.88 belongs to Iceland-Scotland Overflow Water (ISOW) that enters the western North Atlantic through the Charlie Gibbs Fracture Zone. The deepest water mass is the Denmark Strait Overflow Water (DSOW) below a density of σ_θ = 27.88.

In summer 1996 the upper boundary of the LSW layer (σ_θ = 27.74) was found at a depth of about 500 m. Over the following years the 27.74 isopycnal deepened to about 1000 m in summer 1999, due to relatively weak convection activity. The decreasing thickness of the LSW layer was accompanied by increasing salinity and temperature. More intense convection took place in the central Labrador Sea during the winter of 1999/2000 as indicated by the low salinity in the upper 1000 m observed during the Hudson cruise in summer 2000, but the convection did not mix the water column below the density of 27.74.

Temperature and salinity obtained along the section from the southeast to the northwest of the central Labrador Sea are shown in Figure 2.5 together with the density surfaces separating the deep water masses and the density surface σ_θ = 27.70 that approximately marks the lower boundary of the surface salinity minimum. The layer between σ_θ = 27.7-27.74 shows low salinity generated by convective mixing and an increasing thickness towards the northwest that indicates possibly more intense convection northward of the AR7W line. CTD profile 17 shows the same low salinity of about 34.82 and low temperature of about 3°C around a depth of 1000 m as the northernmost stations, together with strong sloping isopycnals. This structure indicates convectively generated water southward of the AR7W line, that is possibly trapped in a mesoscale eddy.

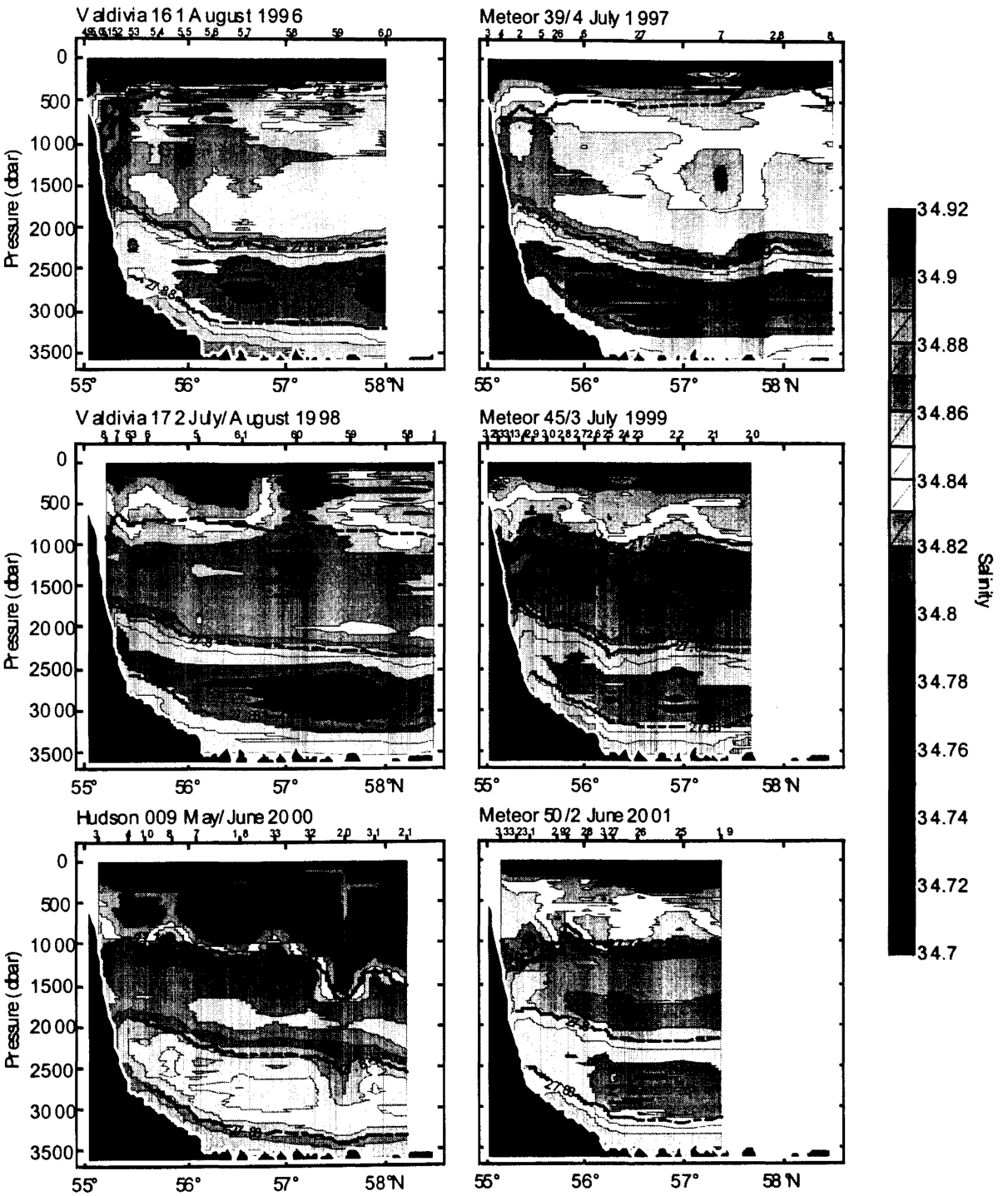

Fig. 2.4: Salinity sections along the western part of the WOCE AR7W line obtained during consecutive summer cruises between 1996 and 2001. The contour interval is 0.01. Isopycnals denoting water mass boundaries are shown as solid lines. Please note, that the Hudson data of 2000 are only preliminary data.

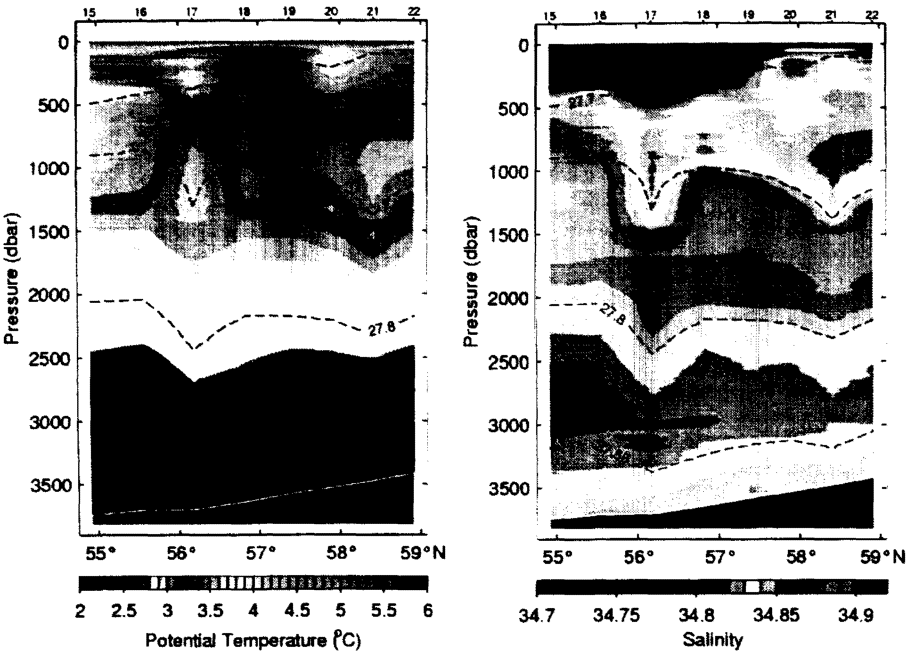

Fig. 2.5: Temperature (left) and salinity (right) distribution along a section from the southwest to the northeast of the central Labrador Sea obtained during M50/2. The contour intervals are 0.1°C for temperature and 0.01 for salinity. Selected isopycnals are shown as solid lines.

c) Tracer Measurements (CFC-11, CFC-11, and CCl_4) (D. Kieke and M. Schütt)

Technical Aspects

During cruise M50/2, tracer measurements including chlorofluorocarbons (CFC) and carbontetrachloride (CCl_4) have been continously performed on all but two profiles. Profiles 23 and 24 have been left out, for these have been repeats of profiles 7 and 8 and have only been performed down to 1500 dbar. Details of the measuring techniques during cruises M50/1 and M50/2 are described in chapter 1.4.4. Reported CFC concentrations are based on SIO93 scale (R. Weiss, Scripps Institution of Oceanography, La Jolla, USA).

During M50/1, the stability of CCl_4-system suffered from a larger repair of the gas-chromatographic oven. Measurements during M50/2 showed improved stability in the calibration curves in comparison to M50/1, but final checks are still needed to estimate the quality of the gained CCl_4 data. The CFC-system, however, worked continously well.

Altogether, 548 CFC-11 and CFC-12 samples as well as 441 CCl_4 samples have been investigated. About 10-11% of the water samples have been analysed twice to check reproducibility. Standard deviation was found to be +/-0.54% and +/-0.52% for CFC-12 and CFC-11, as well as +/-0.62% for CCl_4. The F11/F12 ratios ranged from about 2 to 2.2, surface saturations varied from 99%-111% for CFC-11 and 104%-111% for CFC-12 at temperatures ranging from 3.3°C-6°C.

Preliminary Results

Besides the extensive mooring programme, two major hydrographic sections have been investigated during M50/2, the first one crossing the central Labrador Sea from the Canadian

shelf towards Greenland (WOCE line AR7W), the other one following the axis of the Labrador Sea in south-northward direction.

Strong emphasis of the research programme lies on the investigation of interannual variability of Labrador Sea Water (LSW). As could be found during cruise M50/1 (chapter 1.4.3), LSW warmed in 2001 and became saltier on the more southern sections. Figure 2.6 shows the CFC/temperature correlation of the 2001-LSW-mode in comparison to 1997- and 1999-modes (density range σ_θ=27.74-27.80) in the formation area of LSW along WOCE-line AR7W. Interannual differences in the CFC-concentration can be seen more clearly in the CFC-12 concentration, showing, that the 2001-LSW-mode has lower CFC-12 concentrations in comparison to 1997 and 1999. CFC-11 concentrations from 1999 and 2001 are about comparable with a tendency to lower values during 2001. LSW temperatures increased from 1997 to 1999, but remained comparable to 1999 during M50/2. First results from moorings recovered during M50/2 show that convection activity during winter 2000/2001 was quite weak, resulting in convection depths of only 300 m. Thus, the renewal of LSW defined as water in the density range σ_θ =27.74-27.80 did not take place during winter 2000/2001.

The horizontal distribution of CFC-11 in the LSW layer during cruises M50/1 and M50/2 (Fig. 2.7, top) shows a decrease of concentration from the Labrador Sea southward to the Grand Banks/Newfoundland basin region. High CFC-11 concentrations (> 3.7 pmol kg^{-1}) are found in the Labrador Sea basin as well as in the Deep Western Boundary Current (DWBC) area, indicating LSW being transported southward within the DWBC. Nevertheless, CFC-rich regions, with concentrations similar to the area off-shore Flemish Cap outside the DWBC region, are also found in the middle of the Newfoundland basin and at the western flank of the Mid Atlantic Ridge. This gives some hint that there might be different routes of LSW being exported to the south. High CFC-11 concentrations at about 3.7 pmol kg^{-1} can also be found in the Denmark Strait Overflow Water (DSOW) layer in the central Labrador Sea (Fig. 2.7, bottom). Similar to LSW, concentrations decrease on the way south. In the central Newfoundland Basin, water denser than σ_θ=27.88 is a mixture of DSOW and CFC-poor Antarctic Bottom Water (AABW). DSOW is constrained to the DWBC region, but small portions also seem to be exported southward near the Mid Atlantic Ridge.

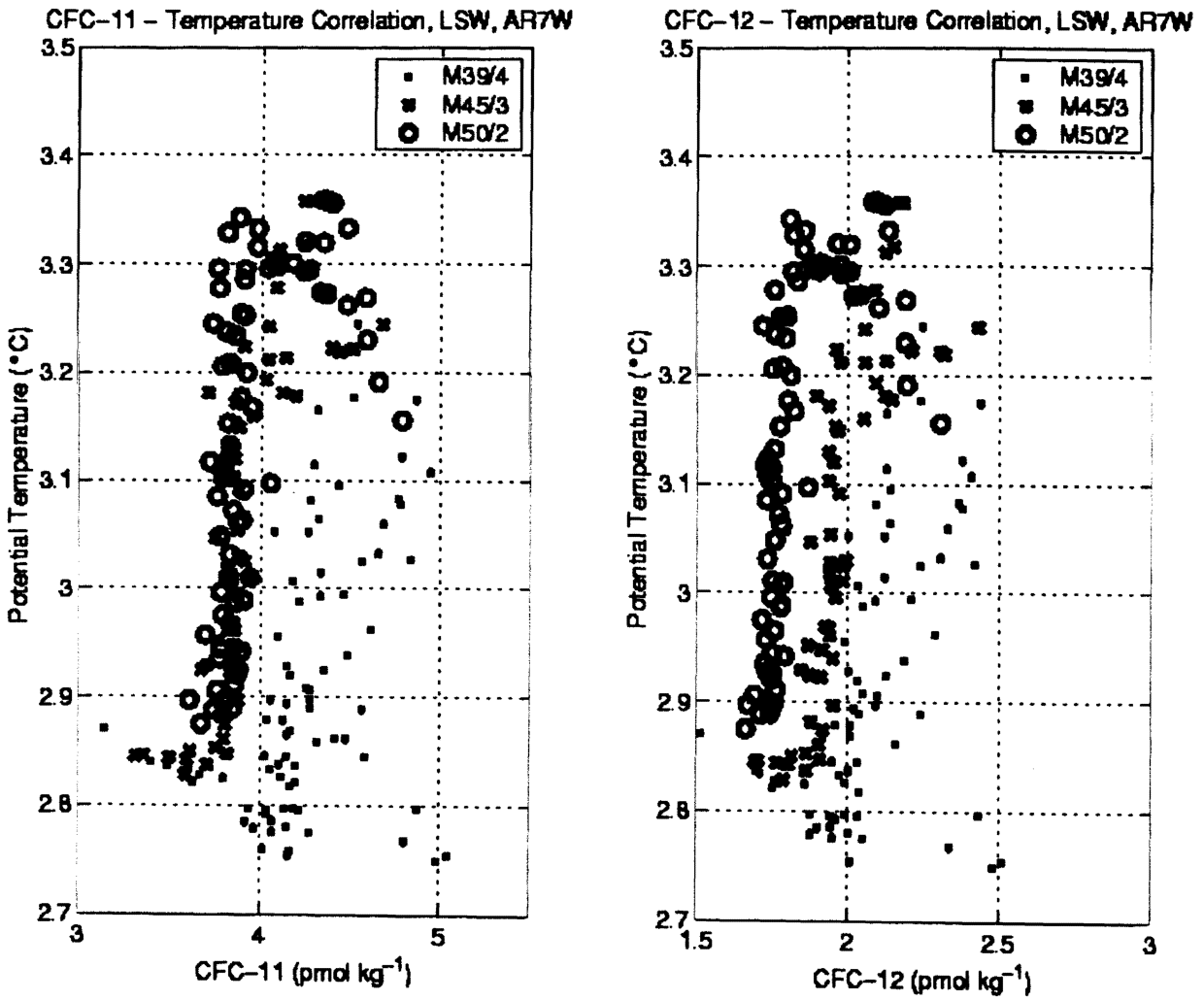

Fig. 2.6: CFC-concentration versus potential temperature in the LSW layer, AR7W section.

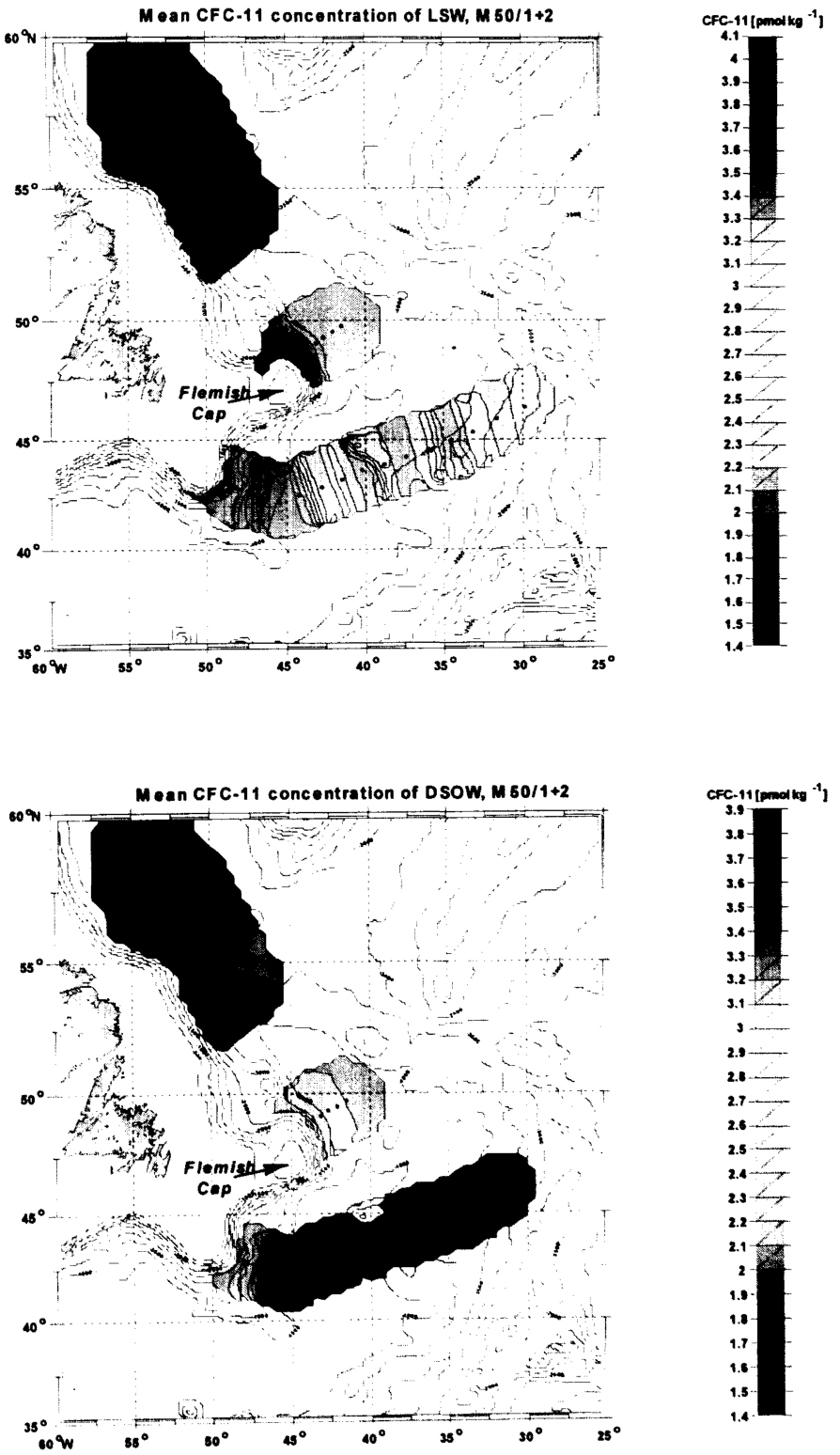

Fig. 2.7: Horizontal distribution of CFC-11 [pmol kg $^{-1}$] in the LSW layer (top) (σ_θ=27.74-27.80) and in the DSOW layer (bottom) (σ_θ>=27.88). Data are from cruises M 50/1 and M 50/2.

2.4.5 Direct Current Observations with VMADCP/LADCP

(M. Dengler, F. Schott, J. Dengg)

a) Technical Aspects

I) VMADCP

During M50/2, two vessel mounted ADCPs were continuously sampling the upper water column. As on leg M50/1, METEOR 's new 75 kHz phased array ADCP, the Ocean Surveyor, was installed in the sea chest, while the 153 kHz ADCP was installed in the ship's hull. Both instruments worked well throughout the cruise. During rough seas, the depth range of the Ocean Surveyor, which is capable of sampling to depths near 700 m, was sometimes reduced to 200-300 m over periods of 5 to 10 minutes. This was probably due to air bubbles directly below the transducers of the ADCP. Furthermore, the data of the first bin showed unrealistically high velocities in both current components, which could not be corrected in post-processing. Therefore the Ocean Surveyor sampled the water column below 50 m only. The 153 kHz ADCP did not show severe interferences during rough seas and reliably sampled the water column between 25 m and 300 m depths.

The configurations of the instruments were identical to those used during M50/1 (section 1.4.2). The Ocean Surveyor was sampling at the fastest rate of about 2.2 s, a vertical resolution of 16 m and a blank of 8 m. Navigation and heading information (GPS, Ashtech) were stored along with the velocities through two serial interfaces of the data acquisition PC. The 153 kHz ADCP was recording 300 s ensembles and the bin length was set to 8 m. The blanking interval was 8 m and a pulse length of 16 m was chosen to obtain a more energetic transducer signal.

At the beginning of the leg, the chief electronic rebooted the Fiber Optic Compass (FOG) and included a speed correction in the setup. This eliminated the erroneous strong temporal fluctuations of the FOG heading observed during the first leg of M50 (section 1.4.2). Both ADCPs use the syncro version of the FOG heading connected directly to the chassis of the ADCP to transform the measured velocities into an earth coordinate system. On an earlier cruise (M47/1), a heading dependent error of this signal was found, having a sinusoidal shape with a minimum deviation of -0.2° at 150° heading and a maximum deviation of +0.2° at a heading of 270°. As suggested by the manufacturer, METEOR's system operators altered the delay time interval of the syncro converter of the FOG from 50 ms to 100 ms, but this did not reduce the error.

If not accounted for, the heading dependent error of the syncro FOG heading greatly reduces the quality of the velocity data, especially during transit. An error of 0.3° leads to a systematic error of 3 cm s^{-1} in the velocities at a cruising speed of 12 knots. In post-processing of the Ocean Surveyor data, we therefore substituted the syncro-FOG heading values of each single ping with the heading values from the digital FOG and from the Ashtech system. Along with the velocity data, the FOG headings from the digital interface as well as the headings from the Ashtech 3-D GPS receiver were recorded simultaneously during data acquisition. The digital FOG signal does not have a heading dependent error. The Ashtech receiver, which is known to have occasional dropouts, worked well throughout the cruise. The largest data gap was 10 s and for more than 99.5% of each 2.2 s ping an Ashtech heading was available.

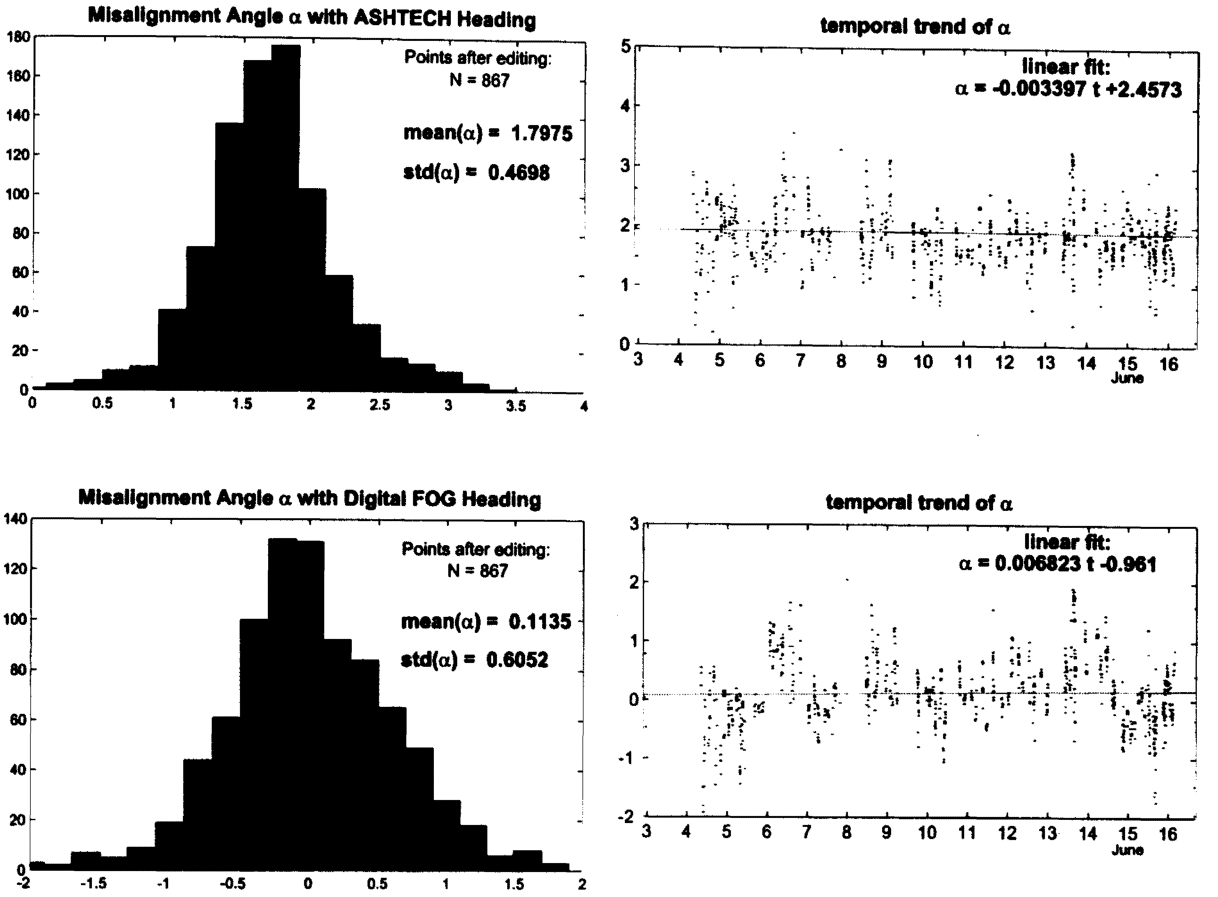

Fig. 2.8: Distribution of the misalignment angle calibrated using velocity data corrected with heading values from the Ashtech system (upper left) and heading data from the digital FOG (upper right). Lower plots show misalignment angle against time again calculated with an Ashtech heading correction (left) and a FOG heading correction (right).

The heading values of two independent systems, the digital FOG and Ashtech enabled us to evaluate the quality of the heading data in conjunction with the ADCP velocities. A measure of the accuracy of the ADCP velocities is the scatter of the transducer misalignment angle around its mean. Correcting the erroneous syncro FOG heading with the digital FOG heading lead to a standard deviation of the alignment angle of 0.61°, while the standard deviation was reduced to 0.47° for the GPS-based headings (Figure 2.8). Furthermore, the unrealistic temporal drift of the misalignment angle was lower when the Ashtech heading was used.

Although the heading values of the Fiber Optic Compass is of higher quality than the vessels gyro compass, it is concluded that the FOG heading values are of less quality than the heading values of the Ashtech 3-D GPS receiver. We therefore suggest the use of the Ashtech heading to correct the erroneous syncro-FOG heading in post-processing of the velocity data of both vessel mounted ADCPs in the future. The calibration of the misalignment angle had a value of 1.80° against the Ashtech heading (Figure 2.8) during M50/1 and M50/2.

II) LADCP

During the entire cruise a narrow-band ADCP (S/N 301) was attached to the CTD-rosette to obtain a profile of horizontal velocity on each hydrographic station. The set up of the lowered ADCP was identical to the one during M50/1 (section 1.4.2). Although the ADCP worked well throughout the cruise, the data from station 141, profile 13, were lost due to digital storage problems. On all other CTD-stations, velocity profiles were obtained. Due to improvements of the post-processing software, the calibrated velocity profiles were of high quality compared to LADCP profiles collected on previous cruises.

b) Results

During M50/2, two realizations of the WOCE-line AR7W were sampled from the western continental shelf well into the central Labrador Basin. The sections were completed about 10 days apart. The cross section velocities measured by the Ocean Surveyor (Figure 2.9) show large differences between the two realizations. While elevated southeastward velocities were found close to the continental shelf during June 1st to 3rd only, southeastward velocities were found over most of the section 10 days later. Velocity time series from moorings also show strong temporal variability with periods between 5 to 30 days. Possible causes of these intraseasonal fluctuations are instabilities of the western boundary current or eddies. Barotropic tidal velocities are also present in this area and may also contribute to current variability.

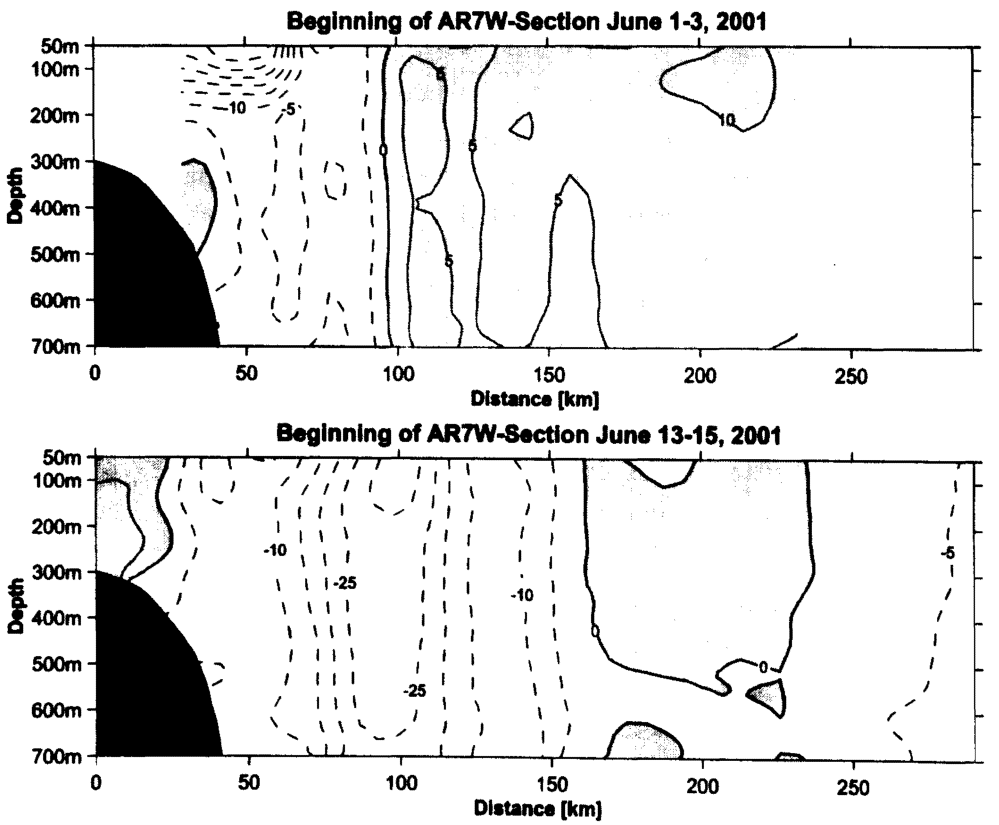

Fig. 2.9: Cross section velocities in cm s^{-1} from the Ocean Surveyor collected on the WOCE AR7 Section during June 1st to June 3rd (upper panel) and between June 13-15 (lower panel). Positive (filled) velocities are northeastward.

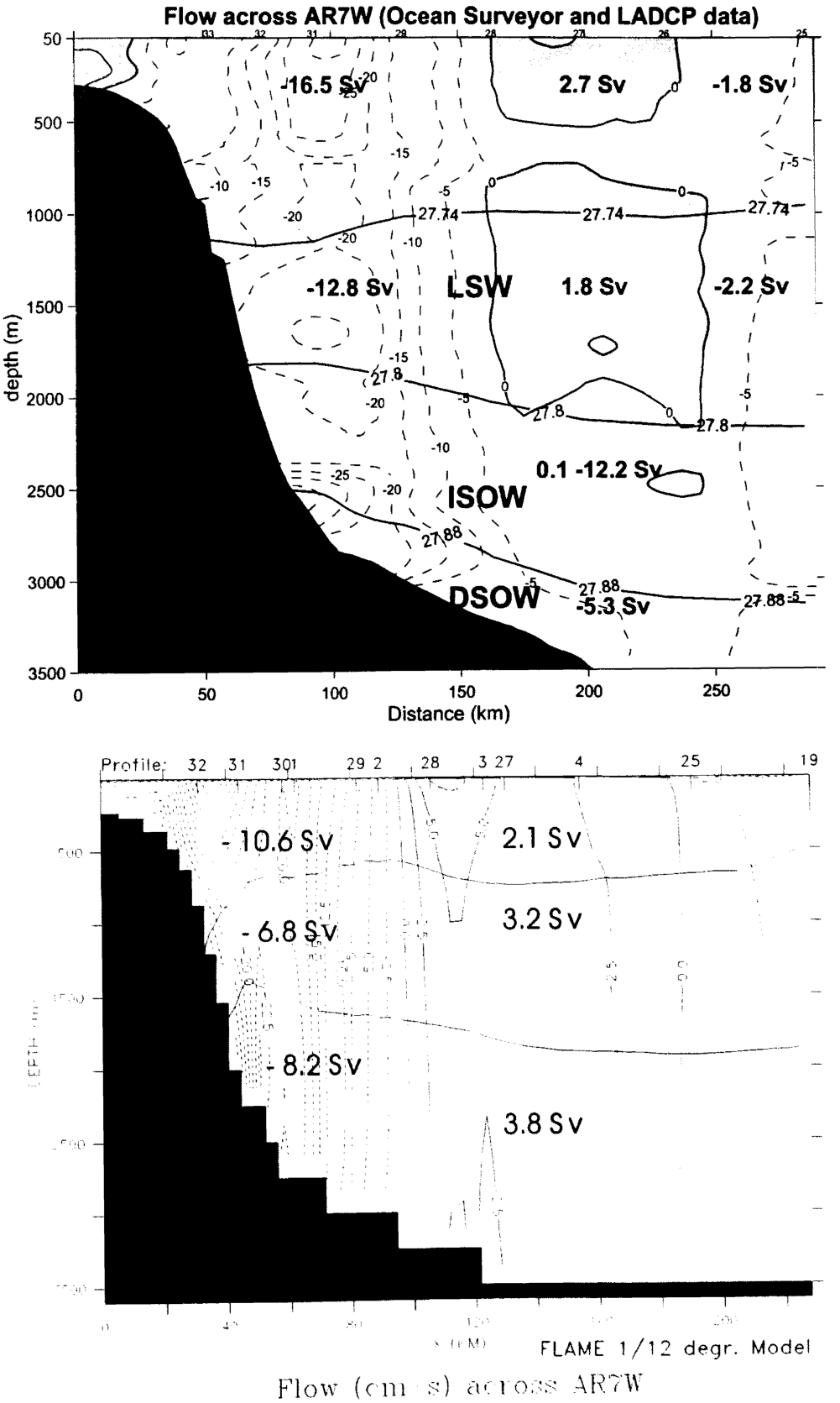

Fig. 2.10: A composite of Ocean Surveyor and LADCP velocities (in cm s^{-1}) and transports across the AR7W section (upper panel). The lower panel show velocity and transport from the 1/12° FLAME model for the same section.

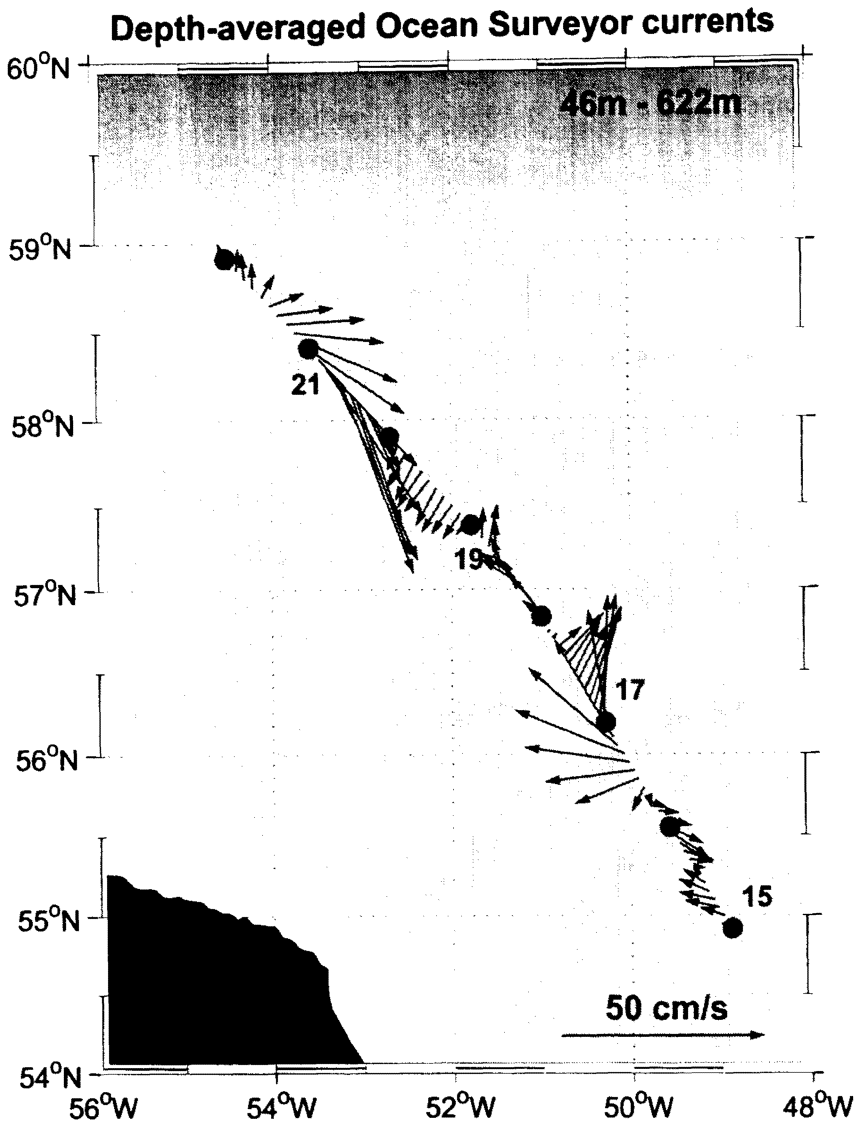

Fig. 2.11: Depth-averaged Ovcean Surveyor velocities from a northwestern section in the central Labrador Sea.

Due to the dense station spacing during the second section, the LADCP profiles and ocean surveyor velocities could be combined to estimate transports in different density classes throughout the water column. The potential densitiy interval between 27.74 and 27.8 represents the Labrador Sea Water (LSW), potential density between 27.8 and 27.88 the Iceland-Scotland Overflow Water (ISOW) and densities larger than 27.88 the Denmark Strait Overflow Water (DSOW). The results are shown in Figure 2.10.

The LSW-layer was found at depths between about 1000 m and 2000 m. Close to the western boundary, 12.8 Sv of LSW were transported southeastward while at about 100 km away from the continental slope, northwestward flow was present having a transport of 1.8 Sv. The depths of the LSW layer and its transports compare well with the results from the monthly average 1/12° FLAME model shown in the lower panel of Figure 2.10. Furthermore, the model realizations indicate that the northwestward flow at this latitude is part of a weak current which exists eastward of the Labrador Current. In the ISOW layer, a southwestward transport of 12.2 Sv was determined which again is in reasonable agreement with the results from the FLAME model. Finally, in the DSOW layer, a southeastward transport of 5.3 Sv was determined. No equivalently high densities are present in the model realization.

Depth-average velocities collected on a section running from the southeast to the northwest of the central Labrador Sea (Figure 2.11) show two pronounced anti-cyclonic eddies. As suggested in Figure 2.5, the watermass trapped inside the eddies is colder and less saline than the surrounding waters, suggesting that convectively generated water is trapped inside these features.

2.4.6 Float work

a) Profiling floats (APEX) (F. Schott)
Four APEX floats were deployed in teh Labrador Current near the 53°N array (Table 2.6.3) to follow pathways of the Labrador Sea Water. The floats complement the deployment during leg M50/1 (section 1.4.7). They drift at 1500 m and surface at 10 day time intervals, taking CTD profiles.

b) RAFOS float park
As in the previous year four DLD-II-type RAFOS floats were parked at the sea floor close to mooring K51 at the position 56°33.20'N, 52°41.21'W. They are programmed to be released by dropping their anchors and ascending to their targeted depth of 700 m in March 2002, i. e. during the expected deep convection phase of the next winter.

The following drifting period will last for 390 days. The anticipated surfacing time is April 2003. For the whole period they are receiving acoustic signals from one standard RAFOS sound source deployed in the boundary current array near 53N at a frequency of 260 Hz and from the three modified tomography sources at a frequency of 400 Hz in order to determine their horizontal positions. The intention of this experiment is to get the floats trapped in so-called instability eddies (which are believed to develop during and after deep convection) and to follow them.

2.4.7 Underway Measurements of Sea-Surface Parameters (DVS)

During cruise METEOR M50/2 a dataset of navigational, meteorological and oceanographical parameters was recorded from the ships data distribution system (DVS).

The extracted near surface parameter (temperature, salinity) were calibrated versus CTD measurement in 5 m depth. The comparison of mainly the salinity data shows large differences between the measurements of thermosalinograph and CTD, especially at the beginning and at the end of the cruise. After despiking and calibration the agreement is improved, with a mean difference of 0.31 and a standard deviation of 0.11.

The temperature between thermosalinograph and CTD agree quite good, with a mean difference of 0.19 and a standard deviation of 0.03. The calibration equation:

$$T_{corr} = A \times T_{thermosal} + B, \qquad \text{with } A = -0.025,\ B = 0.265$$

Salinity- and SST-maps have been constructed with the calibrated data.

2.5 Weather and Ice conditions during M50/2

When the METEOR left St. John's, NF, on June 02, 2001, a high of 1036 situated halfway between Iceland and the Azores was extending a wedge of 1020 to Belle Isle Strait and into the Gulf of St. Lawrence. A gale center of 1007 had moved to a position southeast of Cape Race so that the ship met with northeasterly winds about 5 Bft when leaving port.

The wedge of high pressure strengthened and was swinging northward to include the Labrador Sea, Hudson Strait and northern part of Hudson Bay on June 3. For METEOR this meant light southerly winds and thick fog while still in the Labrador Current. Meanwhile a low 1000 that had moved to the Great Lakes while the ship had been in port had been slowly moving east

and had reached the St. Lawrence Seaway by June 4, a secondary low moving along the coast having reached Halifax. Advection of warm air masses was thus strengthened over METEOR's working area, and fog persisted though surface water temperatures were rising and light southerly winds were still being recorded on June 5.

During the cruise M50/2, the weather and its developments was not the only thing keeping the weathermen busy. Monitoring of ice conditions was vital because of the possibility that drifting ice might impeed access to a mooring position for some time. When the METEOR put out to sea, the fast ice extended south from Davis Strait, adhering to the Labrador coast as far south as the entrance to Hamilton Inlet. During the first days of June, the Labrador Current and moderate northwesterly winds over that region had combined to initiate a southeasterly ice drift, a tongue of ice extending from the fast ice rim at about 55 Nord 57 West to 55 North 54 West by June 2. By June 5, southerly winds had reached the region, the ice tongue consequently swinging north some miles. On June 6, the ice tongue parted with the fast ice rim, the free floating ice melting, but posing a threat until June 11 when it was reported having vanished. Some floes of ice had followed the ice tongue, but they had fared no better, and in that way – splitting into tongues and floes that drift and melt individually – the fast ice rim had thinned considerably at the Labrador coast by that day.

The whole cruise was conducted in the region where icebergs may be encountered, especially during this time of the year.

During June 6, there were southeasterlies of 6 to 7 Bft under the influence of a low 1005 that had developed over the southern part of Baffin Island and headed east for Western Greenland. On June 7, it moved away northward, and the southerly winds were back to light again on METEOR. The persisting fog was thick as the ship moved past the area where the ice tongue was drifting freely, and in order to minimize the threat our vessel moved but slowly.

Meanwhile, the low over the S. Lawrence Seaway had intensified to 1000 and had reached Newfoundland. The southeasterlies were up to 5 to 6 Bft as the low intensified to 995 over Newfoundland's Funk Island Bank on June 8 and stalled on June 9 while lying just east of Belle Isle Strait. On the next day another trough approached the lower St. Lawrence region, and the low moved on northward, thereby filling.

June 11 saw the next low 1008 having already arrived over Newfoundland, turning north there just like its predecessor. At the same time, a low moving southeast from the Great Lakes had reached 1000 at Southampton Island in the northern part of Hudson Bay. There, it stalled and eventually filled. However, a secondary low intensified to 1000 just southwest of Ungava Bay on June 12, a trough trailing behind. The next day, the low intensified to a gale center 995 over Ungava Bay for some time, and the trough developed into a low 1000 of its own as it moved over Northern Quebec. Winds were up to Southeast 7 Bft where METEOR was working then. Both lows filled and finally dissipated by June 15. A secondary low had developed east of Newfoundland during June 14, and as this new low intensified into a gale center 995 by June 16 further east on the Atlantic, moderate northeasterly winds accompanied our research vessel towards St. John's, NF, where she called on June 18, 2001.

The recording of meteorological data went on smoothly and uninterrupted during the cruise so that there is no reason to doubt their accuracy within the construction limits of the instruments deployed. There was one exception, though – the amount of rainfall was not measured during the cruise.

2.6 Station List

Table 2.1: CTD List

METEOR M50/2 CTD/LADCP Stations

Profile	Station	Date	Time	Latitude	Longitude	Water Depth	Profile Depth	Comment
1	127	04.06.01	13:50	55° 26.48' N	53° 46.25' W	2724	2723	K42
2	128	04.06.01	20:23	55° 49.35' N	53° 21.90' W	3117	3101	
3	129	05.06.01	00:50	56° 11.71' N	53° 0.56' W	3399	3381	
4	130	05.06.01	14:20	56° 33.41' N	52° 39.31' W	3489	3472	K41
5	131	05.06.01	19:07	56° 41.73' N	53° 20.17' W	3378	3361	
6	132	06.06.01	01:41	56° 58.98' N	54° 39.79' W	3207	3193	
7	133	06.06.01	06:04	57° 7.14' N	55° 15.12' W	3070	3067	K43
8	134	06.06.01	22:59	56° 50.06' N	54° 0.13' W	3328	3311	K40
9	135	07.06.01	04:30	56° 34.84' N	54° 45.89' W	3153	3145	
10	136	07.06.01	10:37	56° 1.18' N	54° 14.88' W	3190	3177	
11	138	08.06.01	21:17	53° 7.53' N	50° 50.53' W	2944	2937	K39
12	139	09.06.01	03:29	52° 56.51' N	51° 16.58' W	2293	2265	K38
13	141	10.06.01	01:23	53° 15.82' N	50° 33.37' W	3164	3145	
14	142	10.06.01	05:00	53° 22.82' N	50° 15.80' W	3358	3346	K37, no LADCP
15	143	10.06.01	19:45	54° 55.06' N	48° 52.94' W	3697	3681	
16	144	11.06.01	02:45	55° 33.02' N	49° 34.79' W	3663	3646	
17	145	11.06.01	09:24	56° 11.04' N	50° 16.97' W	3655	3640	
18	146	11.06.01	15:43	56° 49.93' N	50° 59.94' W	3596	3579	
19	147	12.06.01	00:52	57° 22.88' N	51° 47.07' W	3533	3517	
20	148	12.06.01	07:08	57° 53.93' N	52° 40.91' W	3482	3468	
21	149	12.06.01	13:26	58° 24.93' N	53° 34.90' W	3430	3415	
22	150	12.06.01	21:32	58° 55.00' N	54° 30.09' W	3371	3355	
23	151	13.06.01	14:48	57° 7.32' N	55° 14.68' W	3103	1493	K53
24	152	13.06.01	22:26	56° 50.04' N	54° 2.01' W	3342	1484	
25	153	14.06.01	05:46	56° 58.03' N	52° 14.22' W	3513	3497	
26	154	14.06.01	17:30	56° 32.98' N	52° 40.69' W	3488	3471	K51
27	155	14.06.01	23:52	56° 16.81' N	52° 55.54' W	3499	3482	
28	156	15.06.01	04:13	56° 0.30' N	53° 11.21' W	3235	3221	
29	157	15.06.01	08:22	55° 43.52' N	53° 27.49' W	3024	3013	
30	158	15.06.01	17:30	55° 26.56' N	53° 41.83' W	2744	605	K52
31	158	15.06.01	18:34	55° 26.26' N	53° 40.85' W	2753	2741	Pegasus
32	159	15.06.01	23:57	55° 17.94' N	53° 53.69' W	2299	2307	
33	160	16.06.01	02:44	55° 8.89' N	54° 4.12' W	1227	1208	

Table 2.2: Mooring List

Mooring ID	Position	Date / time	Water depth	Deployed/retrieved	Mooring type
K38	52°N57,50 / 51°W18,10	08.06.2001 / 14:59 UTC	2464 m	Deployed	Boundary-Current-Mooring
K39	53°N08,50 / 50°W52,10	08.06.2001 / 20:46 UTC	2885 m	Deployed	Boundary-Current-Mooring
K37	53°N23,50 / 50°W15,40	10.06.2001 / 10:48 UTC	3380 m	Deployed	Boundary-Current-Mooring
K51	56°N33,50 / 52°W39,50	14.06.2001 / 15:13 UTC	3510 m	Deployed	Tomography/Convection-Mooring
K52	55°N27,20 / 53°W43,60	15.06.2001 / 15:49 UTC	2791 m	Deployed	Tomography/Convection-Mooring
K53	57°N08,00 / 55°W17,50	13.06.2001 / 14:00 UTC	3098 m	Deployed	Tomography/Convection-Mooring
K40	56°N49,68 / 54°W01,65	06.06.2001 / 21:49 UTC	3325 m	Retrieved	Boundary-Current-Mooring
K41	56°N33,60 / 52°W39,50	05.06.2001 / 11:15 UTC	3495 m	Retrieved	Tomography-Convection-Mooring
K42	55°N27,18 / 53°W43,55	04.06.2001 / 11:24 UTC	2775 m	Retrieved	Tomography/Convection-Mooring
K43	57°N08,08 / 55°W17,57	06.06.2001 / 11:05 UTC	~ 3075 m	Retrieved	Tomography/Convection-Mooring

Table 2.3: Floats

S/N	Dez-Argos-ID	Hex-Argos-ID	Startzeit	Aussetzzeit	Aussetzposition
IFM					
284	03837	3BF70	09.06.01 / 11:12	09.06.01 / 12:02	53°N04,95 / 50°W58,64
285	02194	2248F	09.06.01 / 20:38	09.06.01 / 23:33	53°N01,63 / 50°W55,53
286	02195	224DC	08.06.01 / 13:52	08.06.01 / 15:09	52°N57,63 / 51°W17,94
287	02196	22536	08.06.01 / 18:58	08.06.01 / 23:43	53°N06,99 / 50°W50,45

METEOR-Berichte 02-2

North Atlantic 2001

Part 3

Cruise No. 50, Leg 3

20 June – 15 July 2001, St. John's – Reykjavik

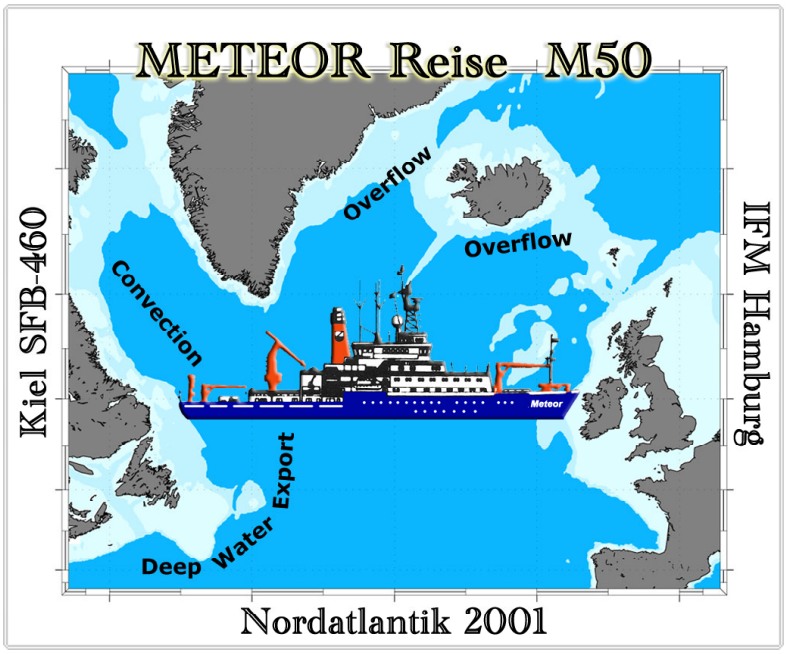

J. Holfort, K. Bulsiewicz, G. Hargreaves, S. Hüttemann, G. Kahl, A. Kirch, K. Kirchner, A. Moll, G. Quast, J. Read, F. Rellensmann, B. Rudels, K. Schulze, V. Sommer, Th. Truscheit, N. Verch, A. Welsch

Editorial Assistance:

Frank Schmieder
Fachbereich Geowissenschaften, Universität Bremen

Leitstelle METEOR
Institut für Meereskunde der Universität Hamburg

2002

Table of Contents

3.1 Participants M 50/3

Name	Speciality	Institute
Holfort, Jürgen	Chief scientist	IfMH
Bulsiewicz, Klaus	Tracer	UBU
Hargreaves, Geoffrey	Moorings	POL
Hüttemann, Sören	Student, Oceanography	IfMH
Kahl, Gerhard	Meteorology	DWD
Kirch,Anja	Alkenons	IfMK
Kirchner, Kerstin	Student, Oceanography	IfMH
Moll, Alexander	Student, Tracer	UBU
Quast, Gerlinde	Student, Oceanography	IfMH
Read, John	Moorings	CEFAS
Rellensmann, Falk	Student, Oceanography	IfMH
Rudels, Bert	Oceanography	FIMR
Schulze, Klaus	Oceanography	IfMH
Sommer, Volker	Student, Tracer	UBU
Truscheit, Thorsten	Meteorology	DWD
Verch, Norbert	Oceanography	IfMH
Welsch, Andreas	Moorings	IfMH

Participating Institutions

CEFAS Centre for Environment, Fisheries & Aquaculture Science, Lowestoft Laboratory, Lowestoft, Suffolk NR33 0HT, U.K.

DWD Deutscher Wetterdienst, Geschäftsfeld Seeschiffahrt, Bernhard-Nocht-Str. 76, 20359 Hamburg - Germany, e-mail: edmund.knuth@dwd.de

FIMR Finnish Institute for Marine Research, P.O. Box 33, Lyypekinkuja 3a, 00931 Helsinki, Finland

IfMH Institut für Meerskunde an der Universität Hamburg, Tropolowitzstr. 7, 22529 Hamburg - Germany, e-mail: holfort@ifm.uni-hamburg.de

IfMK Institut für Meereskunde an der Universität Kiel, Düsternbrooker Weg 20, 24105 Kiel - Germany, e-mail: jfischer@ifm.uni-kiel.de

POL Proudman Oceanographic Laboratory, Bidston Observatory, Birkenhead, Merseyside L43 7RA - U.K.

UBU Universität Bremen, Institut für Umweltphysik, Abt. Tracer-Oceanographie, Bibliotheksstraße, 28359 Bremen - Germany, e-mail: mrhein@physik.uni-bremen.de

3.2 Research Program

The cruise leg M50/3 was a continuation of the work done in the EC- project VEINS (Variability of exchanges in the Northern Seas), where eighteen countries contributed to field work and modeling of the transport fluctuations through the major ocean passages between the Arctic Ocean and the Northern North Atlantic. This cruise focussed on the fluxes and the changes in the properties of water masses in the area from the Denmark Strait to the southern tip of Greenland. It is a repeat of the METEOR cruise M39/5 in 1997, the VALDIVIA cruise 173 in 1998, the METEOR cruise M45/4 in 1999 and the Poseidon cruise 263 in 2000.

The ideas about the composition of the Denmark Strait Overflow Water (DSOW) have changed considerably within the last couple of years. This changing view did also arise due to the long term measurements within the VEINS program. Some of these measurements were also done on previous cruises with FS METEOR. Actually the overflow is related to the waters of the western boundary currents of the Nordic Seas. This results in Arctic, Polar and Atlantic contributions to the Denmark Strait Overflow. The present concept consists of equal contributions of Arctic Intermediate Waters, Arctic Ocean Deep Waters and recirculated Atlantic Water in the composition of overflow waters.

Of course this composition can change with time. On longer temporal scales the atmospheric forcing changes, and the formation of water masses depends also on this forcing. The predominant signal of this changes is the North Atlantic Oscillation. The exact nature of the relations between changes in atmospheric forcing and changes in the composition and strength of the overflow is still unclear and a subject of our investigations. But recently a coherence was found between inter-annual temperature changes of the DSOW at 64°N, changes in the temperature in the Greenland Sea and also with changes in the Atlantic Waters in the Westspitsbergen Current.

For several years now hydrographic sections were taken regularly along the East Greenland continental slope south of Denmark Strait. Several moorings are deployed along one of this sections at about 64°N. This mooring line consists of 6 moorings with current meters, two inverted echo sounders and one bottom mounted ADCP. This field word is a cooperative effort of institutions from Germany, Iceland, Finland and Great Britain.

The METEOR cruise 50/3 aims at repeating those six standard sections, with the difference that the southernmost section will be extended till the Mid-Atlantic Ridge (Fig. 3.1). For a better characterization of water masses, CFC's and SF6 measurements will be taken on these sections. The moorings will be re-covered and then deployed again. A new kind of mooring was deployed on the shelf last year with FS POSEIDON. This mooring consists of a tube, about 50m long, with 2 integrated temperature and salinity sensors (microcats). The goal of the tube itself is to protect the sensor from being destroyed by ice. This mooring will also be recovered and two such moorings will be deployed.

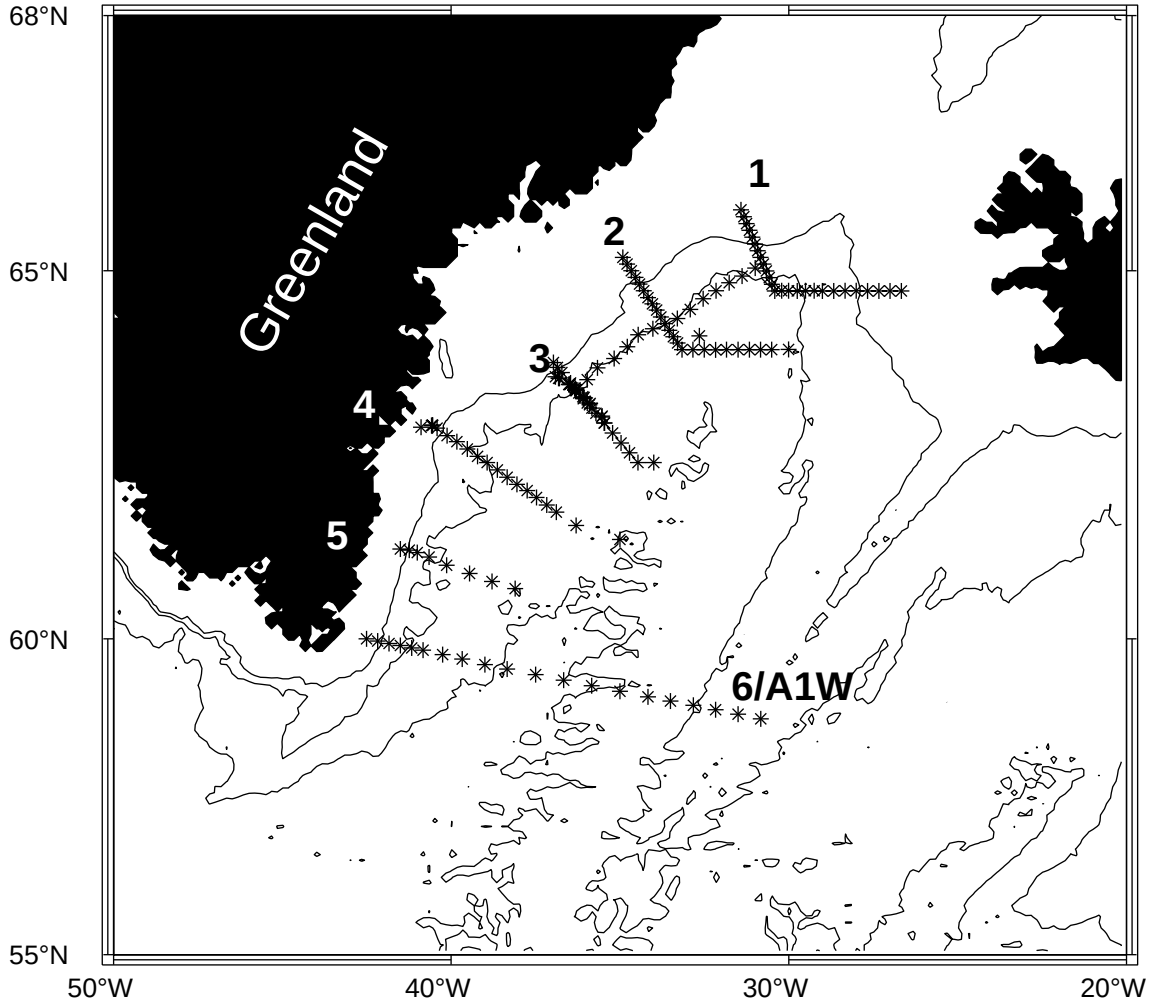

Fig. 3.1: Positions of the stations made during M50/3 and numbers of the VEINS hydrographic sections. The mooring array is located along section 3, the tube moorings are located on the shelf at the western end of section 4. The spacing of depth isolines is 1000 m.

3.3 Narrative of the Cruise

The RV METEOR left St. John's on June 21, 2001 and headed to 58°47,8' N 030°49,8' W, a point above the Mid-Atlantic-Ridge, arriving on June 25. From there a hydrographic section was taken towards the southern tip of Greenland. This section was a repeat of the western part of WOCE section A1E, the eastern part was occupied at the same time by RV COMMANDER JACK. Regretfully, due to problems with the CTD cable on RV COMMANDER JACK, the ships didn't meet and there is a time gap of 5 days between both parts.

This first section, the westernmost stations compromising also VEINS section 6, was finished on June 28. The hydrographic work continued with VEINS section 5, a section perpendicular to the continental shelf north of the first section. The CTD system worked very well and also showed no problems during the rest of the cruise. Station positions and section numbering are given in table 1 in chapter 3.6 and shown in figure 3.1.

The survey of the next two sections was interrupted by mooring work. While CTD work can also be done during night and not so good weather, we needed daylight and fine weather for the mooring work. We recovered one and deployed two tube moorings at the western end of section

4. The tube could only be recovered in two pieces, but no instrument was lost. The deployment of the tubes, with a length of about 45 m quite bulky, was much easier as expected. The weather was also very fine during deployment and we had a fantastic view of the Greenland coast. Along section 3 a total of eight moorings were successfully recovered and deployed.

After the mooring work we continued the hydrographic work with 3 sections perpendicular to the continental rise, connected with stations along a water depth of about 2000 m. As the weather had been quite reasonable during the whole cruise, we had enough time to increase the spatial resolution of this last sections up to about 5 nautical miles between stations. Due to ice section 1 could not started as far north on the shelf as planned.

Along the CTD sections, although not at every station, water was sampled at 10 to 20 levels for analysis of CFC's. At some selected stations water samples were taken for the analysis of SF6 in the overflow water, at other stations some samples were taken for the analysis of alkenones.

Continuos measurements were taken with up to two vessel mounted ADCP's. The pCO_2 in air and surface waters were analyzed, surface waters were filtered for the determination of alkenons and meteorological measurements were done on a routinely basis. The acquisition computer (an old 286) of the 150 Hz ADCP broke done on July 8 and could not be repaired. Also many of the data was also lost, because the hard disk couldn't be read from another computer. But the second ADCP with 75 Hz showed no problems during the whole cruise.

RV METEOR arrived in the port of Reykjavik on July 15, 2001.

3.4 Preliminary Results

3.4.1 Hydrography

The hydrographic measurements were done with a Seabird CTD, the same instrument as the legs before. The pressure offset in air of 0.0 to 0.2 dbar and was neglected, a comparison with the reversing thermometers showed that no in situ calibration of temperature and pressure were necessary. Bottle salinities were determined with an AUTOSAL salinometer, which was calibrated using standard seawater. The conductivity showed a constant offset of 0.0018 mS/cm, after calibration the accuracy for conductivity (respective salinity) is better then 0.003 (see Figure 3.2). Samples for oxygen were taken and analyzed regularly. This values were used to calibrate the oxygen sensor on the CTD.

At section 1 (see Figure 3.3) the Denmark Strait Overflow water can be clearly seen as a layer of low salinity and temperature sitting on the Greenland slope. This layer can be traced till the southernmost section 6, although with increasing temperature and salinity due to mixing with ambient water. The core of the overflow, located at about 1500 m to 2000 m depth, is connected with the also dense, cold, low salinity waters on the shelf. The water on the shelf is only slightly less dense (σ_2~37.10 kg/m^3) then the overflow (σ_2~37.20 kg/m^3). So there is the possibility that part of the waters denominated overflow does not originate from the Denmark Strait sill but comes from the shelf.

In comparison with previous cruises and historic data (see Figure 3.4) it can be noted: Compared to last year (2000) the salinity (and temperature) of the overflow increased slightly, but did not reach the high salinity values of 1996 and are comparable to the values in the years 1994 and 1995.

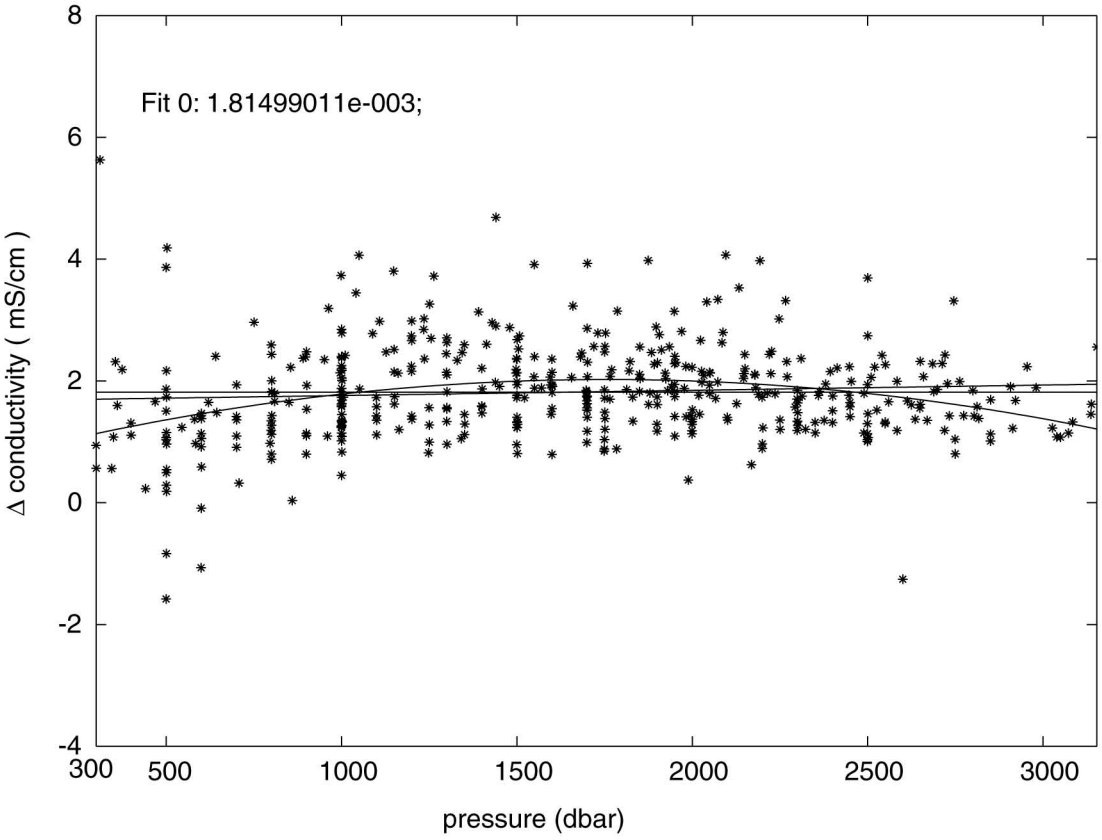

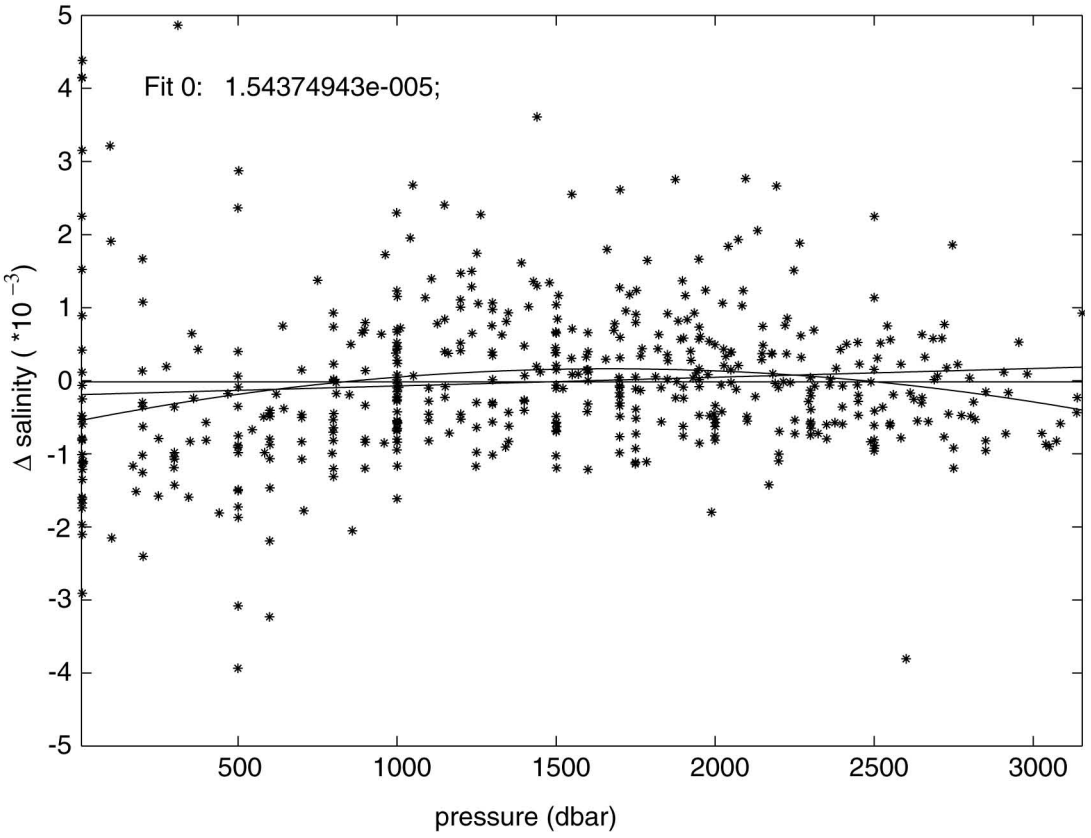

Fig. 3.2: Difference between CTD and bottle data in conductivity before calibration (a) and in salinity after calibration (b).

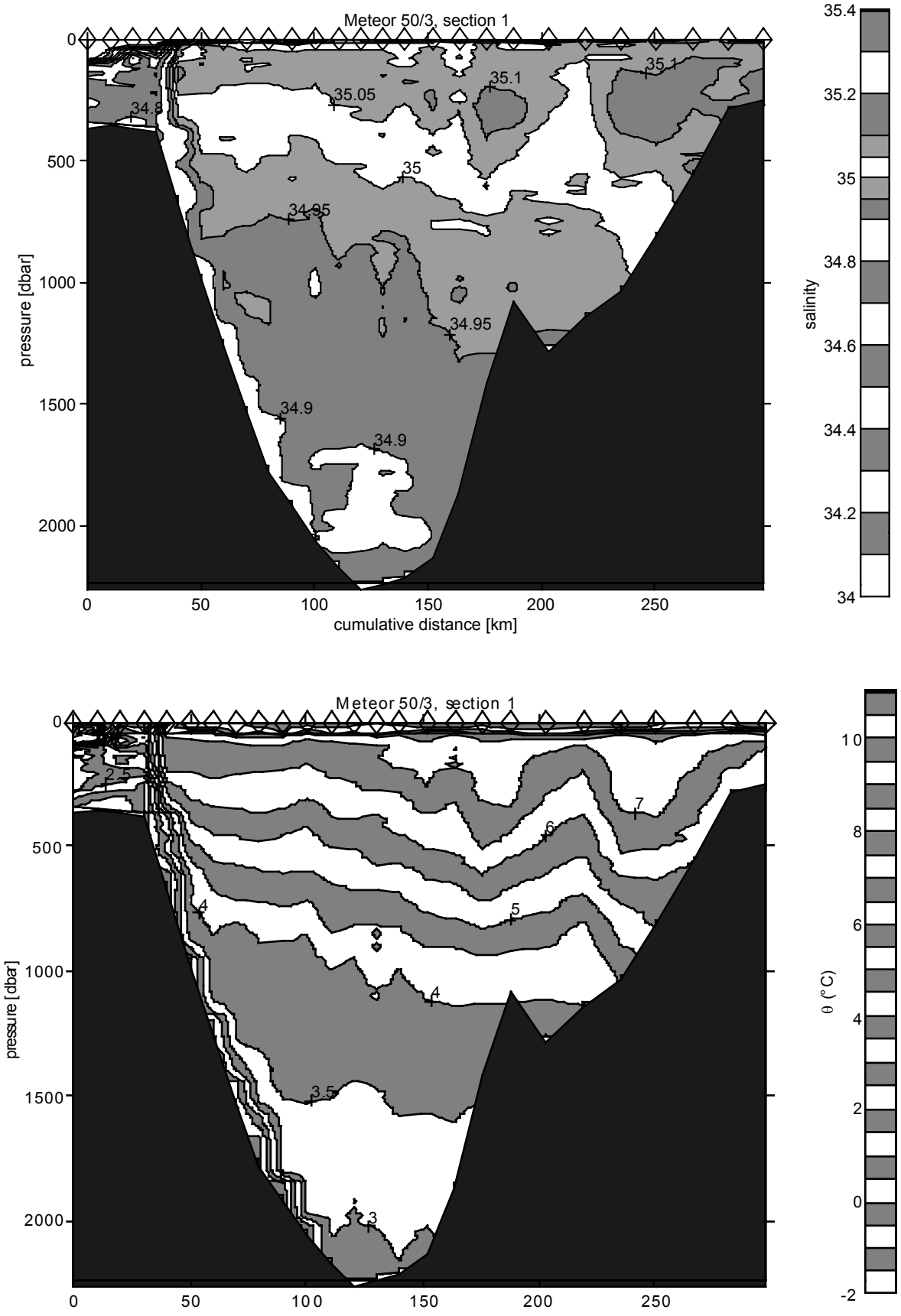

Fig. 3.3: Salinity (a) and potential temperature (b) along section 1.

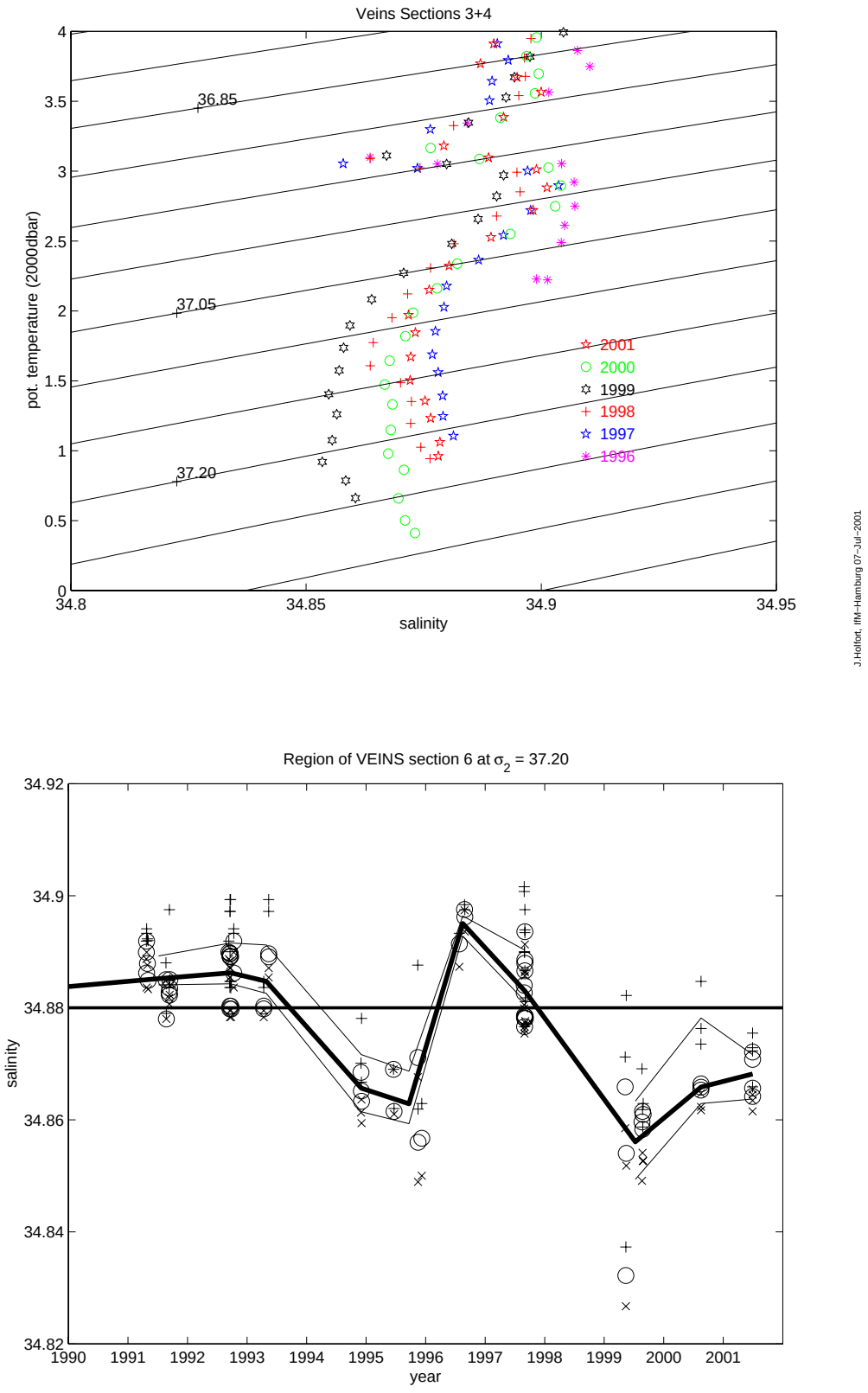

Fig. 3.4: a) Mean θ/S (averaged along isopycnals) diagrams for sections 3 and 4 of cruise M50/3 compared to previous cruises. b) Salinities of stations in the region of VEINS section 6 for a density layer around σ_2=37.20 kg/m^3. Circles are the median values of each profile in the density range +- 0.07, crosses and stars the minimum, respective maximum salinities in the density range +- 0.10. The median values of each year are connected with lines, the heavy line being the median values.

3.4.2 Moorings

The current and temperature data from the recovered Aandera current meters was available shortly after recovery. Data from the inverted echo sounders needs more processing and is still not available.

The recovered tube moorings had fallen apart in two pieces. It did not break, but split into two pieces because of loosened screws. From the pressure record (see Figure 3.5) it can be deduced that it happened in the end of January 2001. After this the two parts were connected just with an rope of 45 m length. The new tubes that were deployed have another connection between the individual elements, that should be more durable. The whole mooring tilted quite strongly, resulting in depth excursion of more than 100 m. Because it also happened after the tube went apart it is not ice but most probably the effect of strong currents. The drag on the tube is too strong compared to its buoyancy, the new tubes have a smaller diameter and should therefore have a better drag/buoyancy relation. The dominant signals in the pressure signal (and therefore also in the velocity, although no current meter was attached to the mooring) are the tides. There is no peak at the inertial frequency.

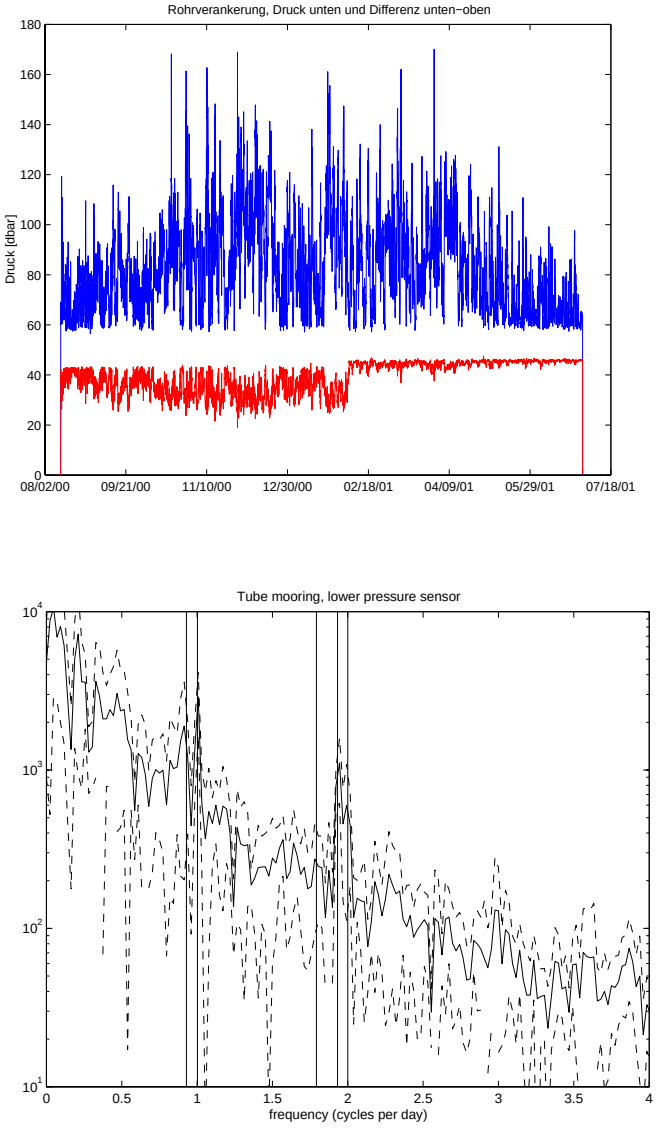

Fig. 3.5: a) Time series of pressure at the lower instrument of the tube mooring and difference of pressures between the upper and lower instrument. b) Power spectrum of the pressure at the lower instrument. Vertical lines gives the frequencies of the M2, S2, K1 O1 tides and of the inertia frequency.

3.4.3 Tracer Measurements (CFC-11 and CFC-12)

The discussion of the measurements of this leg are given in the chapter for leg M50/4.

3.4.4 Alkenones

(A. Kirch)

Alkenones are methyl and ethyl ketones consisting of chains of 37-40 carbon atoms with two double bonds up to four. These compounds are produced, probably as membrane lipids, by various Haptophyceae algae. In marine environments the coccolithophorid species *Emiliania huxleyi* is dominant and is well-known for its large blooms in the euphotic zone of the oceans.

The biosynthesis of alkenones in marine systems depends on the ambient water temperature. For example, in low temperature regimes, the amount of higher unsaturated ketones is increasing with temperature. The degree of unsaturation of C_{37} alkenones (only methyl ketones) is usually expressed in terms of U^{K}_{37} and $U^{K'}_{37}$ indices. Since the U^{K}_{37} and $U^{K'}_{37}$ indexes (the compositions of the alkenones) remain unchanged when released after the end of coccolithophorid blooms, they can be traced from the the euphotic zone down to the sediment. Successful temperature calibrations in field and laboratory experiments allows the use of U^{K}_{37} and $U^{K'}_{37}$ indices for the reconstruction of sea surface paleotemperatures.

The estimate of paleo-pCO_2 by measuring the $\delta^{13}C$ values of the alkenones, might add a valuable new aspect to the application of alkenones as biomarkers. Atmospheric CO_2 exchanges across the atmosphere-ocean interface. Dissolved CO_2 is transformed into organic carbon, for example during the biosynthesis of the alkenones, resulting in a characteristic isotopic signature. However, the isotopic signature may also influenced by environmental and growth conditions, such as the availability of light and nutrients, which makes the reconstruction of the pCO_2 doubtful.

The aim of our study is the determination of the ^{13}C isotopic signature of long-chain unsaturated methyl ketones (C_{37} alkenones) during coccolithophorid blooms in the North Atlantic Ocean. The ^{13}C signal will be observed from the formation of alkenones during the bloom until the burial in the sediment.

During the cruise METEOR M50/3 samples were taken for the analysis of the alkenones in the euphotic zone (from the surface down to the chlorophyll maximum). Additionally, complementary samples for the determination of particulate organic carbon (POC), suspended particulate material (SPM), chlorophyll and nutrients were taken. pCO_2 was measured almost continuously as described for M50/1 (see leg 1, 1.4.5).

A comprehensive list of the samples taken during the cruise is given in table 2 in chapter 3.6.

3.5 Weather and Ice Conditions during M50/3

When the METEOR left St. John's, NF, Canada, on June 21, 2001, a gale center of 990 hPa had just entered the Labrador Sea, moving east and filling slowly. Northwesterly winds of 6 to 7 Bft were felt on the ship's position while she headed northeast for the starting position of the first of

several hydrographic sections in waters off Southeastern Greenland. On June 23, a trough encircling the slowly filling gale center caused a temporary intensification from 1000 hPa to 995 hPa at 53 North 25 West. At the same time, a flat low just east of Southeastern Greenland had intensified to 1000 hPa, and between those two lows the METEOR experienced southwesterly winds of 5 Bft on June 25 when hydrographic work was about to begin. Filling of the low over the Irminger Sea reduced wind velocity to 4 Bft and direction to back east so that work was unhampered. When the research vessel reached Walloe, southeastern Greenland, on June 28, northeasterly winds were up to 6 Bft just because of the coast's proximity. This was shown when the ship went out into the Irminger Sea, heading for the starting position for the next hydrographic section on June 29 when wind force was down to 4 Bft again. Meanwhile the wedge of high pressure that extended from central to southern Greenland over the Inland Ice had weakened so that winds remained northerly 4 Bft on June 30 when the ship reached mooring arrays at 63°North so close to the coast that it showed clearly and in bright sunshine. The air masses originated from over the Inland Ice indeed because an air temperature of 2°C was the chilliest one recorded during the cruise.

At the same time a low migrating east from Newfoundland had reached the area southeast of Greenland, central pressure being 992 hPa. As it turned northeast during July 1, northeasterly winds increased to 7 Bft on the METEOR's probing position. As the low started to fill winds were slow to abate to North 5 Bft on July 2, but by July 3 conditions were light and variable, and the opportunity was being taken to recover and deploy again a new type of mooring consisting of a tube 50 m long with built-in CTD instruments.

However, a gale center that had been tracked from southwest of the Great Lakes to the northern rim of Hudson Bay, then swinging east, had reached the Labrador Sea by July 3, filling there but inducing a new low on the east coast of southern Greenland that quickly intensified into a gale center 1003 hPa by July 4 when the METEOR experienced North to Northwest 7 Bft. These gales were short-lived because the gale center quickly moved away to Iceland. During the next two days winds were light and variable. However, meanwhile the gale center from the Labrador Sea was following the track taken by the low it had induced, central pressure in the Irminger Sea being 1000 hPa by July 7 when the METEOR observed strong northwesterly to northerly winds of 6 Bft. The low then filled further swinging southeast and eventually merging with the next of it's kind.

In June, a prominent feature of the average North Atlantic weather chart had been absent: the Azores High. If it was there, it had been weaker than normal, or the subtropical high could be found near to its winter position at Bermuda. Now it established itself just west of the Azores with a central pressure of over 1030 hPa. Opposing a low, albeit a weak one, in the vicinity of Iceland, the scene is set for quick developments starting in the greater Newfoundland area. There was no long wait: during July 8, a low of 1003 hPa passed Goose Bay, Labrador, Canada, heading east and developing into a gale center by noon of the same day at 55 North 43 West. By July 9, central pressure was 993 hPa at 57 North 20 West, and by July 11, central pressure was 997 hPa at the Scottish eastern coast. The storm center then turned northeast to lie to the south of the Lofot islands, Norway, in the evening of July 12, central pressure being 991 hPa. During July 9, a vital part of the cold air masses involved in the circulation of the gale center passed Denmark Strait, and METEOR, working to the west of that passage, observed northeasterly gales of 7 to 8 Bft. So she was not being hard hit.

When the ship reached the area south of Ammassalik, eastern Greenland, winds were down to light and variable, and as a low to the leeward side of the high mountains in that area was forming there was an exceptional view from afar including a fantastic Fata Morgana that emphasized the rim of the ice that barred access to the coast, not to mention hills being shown upside down in a considerable height above the ground.

During the last few days of the voyage there were light to moderate westerly winds that backed to moderate easterlies when our research vessel headed for Reykjavik, Iceland, calling there on July 15.

Ice charts were closely monitored as they were issued by the Danish Meteorological Institute, being sent to the ship by the Institut für Meereskunde, University of Kiel, or by the Bundesamt für Seeschifffahrt und Hydrographie, Hamburg. When the ship was still on her way to Greenland, accessibility of mooring positions near the coast was in question, but when this question became vital, new ice charts reassured free access to the positions. Icebergs were seen but a few.

3.6 List of Stations

Table 1: CTD-Station List

EXPO-CODE	Section Name	Stat. No.	Cast No.	Cast Type	Date mmddyy	Time UTC	Code	Position Latitude	Position Longitude	Code	Bottom depth	Meter Wheel	Max Press.	Bottom Dist.	Comments
06ME50/3		161	01	ROS/CTD	062101	1220	BE	50 18.67 N	47 48.99 W	GPS	2710				
06ME50/3		161	01	ROS/CTD	062101	1318	BO	50 18.62 N	47 49.23 W	GPS	2714	2682	1500		Test Station
06ME50/3		161	01	ROS/CTD	062101	1411	EN	50 18.29 N	47 49.48 W	GPS	2715				
06ME50/3	VEINS-6	162	01	ROS/CTD	062501	1442	BE	58 47.79 N	30 49.68 W	GPS	1264				
06ME50/3	VEINS-6	162	01	ROS/CTD	062501	1507	BO	58 47.75 N	30 49.34 W	GPS	1225		1237	14	
06ME50/3	VEINS-6	162	01	ROS/CTD	062501	1545	EN	58 47.63 N	30 48.92 W	GPS	1259				
06ME50/3	VEINS-6	163	01	ROS/CTD	062501	1733	BE	58 52.02 N	31 30.00 W	GPS	1518				
06ME50/3	VEINS-6	163	01	ROS/CTD	062501	1827	BO	58 52.03 N	31 29.88 W	GPS	1513	1487	1505	14	
06ME50/3	VEINS-6	163	01	ROS/CTD	062501	1913	EN	58 52.02 N	31 29.91 W	GPS	1516				
06ME50/3	VEINS-6	164	01	ROS/CTD	062501	2145	BE	58 56.18 N	32 10.18 W	GPS	1770				
06ME50/3	VEINS-6	164	01	ROS/CTD	062501	2221	BO	58 56.04 N	32 09.56 W	GPS	1778	1751	1770	14	
06ME50/3	VEINS-6	164	01	ROS/CTD	062501	2326	EN	58 56.09 N	32 09.07 W	GPS	1627				
06ME50/3	VEINS-6	165	01	ROS/CTD	062601	0141	BE	59 00.28 N	32 49.54 W	GPS	2157				
06ME50/3	VEINS-6	165	01	ROS/CTD	062601	0223	BO	59 00.53 N	32 48.44 W	GPS	2136		2126	15	
06ME50/3	VEINS-6	165	01	ROS/CTD	062601	0312	EN	59 00.72 N	32 47.31 W	GPS	2141				
06ME50/3	VEINS-6	166	01	ROS/CTD	062601	0543	BE	59 04.04 N	33 30.06 W	GPS	2315				
06ME50/3	VEINS-6	166	01	ROS/CTD	062601	0621	BO	59 04.10 N	33 29.68 W	GPS	2329	2295	2322	14	
06ME50/3	VEINS-6	166	01	ROS/CTD	062601	0721	EN	59 04.18 N	33 29.44 W	GPS	2325				
06ME50/3	VEINS-6	167	01	ROS/CTD	062601	0926	BE	59 07.91 N	34 10.38 W	GPS	2302				
06ME50/3	VEINS-6	167	01	ROS/CTD	062601	1014	BO	59 07.82 N	34 10.38 W	GPS	2298	2268	2293	14	
06ME50/3	VEINS-6	167	01	ROS/CTD	062601	1117	EN	59 07.87 N	34 10.11 W	GPS	2281				
06ME50/3	VEINS-6	168	01	ROS/CTD	062601	1529	BE	59 13.05 N	34 59.88 W	GPS	2726				
06ME50/3	VEINS-6	168	01	ROS/CTD	062601	1621	BO	59 13.06 N	34 59.77 W	GPS	2709		2733	15	
06ME50/3	VEINS-6	168	01	ROS/CTD	062601	1724	EN	59 13.01 N	34 59.86 W	GPS	2281				
06ME50/3	VEINS-6	169	01	ROS/CTD	062601	1946	BE	59 18.01 N	35 50.08 W	GPS	3119				
06ME50/3	VEINS-6	169	01	ROS/CTD	062601	2048	BO	59 17.91 N	35 50.12 W	GPS	3120	3097	3137	14	
06ME50/3	VEINS-6	169	01	ROS/CTD	062601	2200	EN	59 17.82 N	35 50.24 W	GPS	3120				
06ME50/3	VEINS-6	170	01	ROS/CTD	062701	0025	BE	59 22.98 N	36 40.11 W	GPS	3121				
06ME50/3	VEINS-6	170	01	ROS/CTD	062701	0124	BO	59 23.04 N	36 39.86 W	GPS	3100	3101	3139	15	
06ME50/3	VEINS-6	170	01	ROS/CTD	062701	0231	EN	59 23.15 N	36 39.58 W	GPS	3120				
06ME50/3	VEINS-6	171	01	ROS/CTD	062701	0501	BE	59 27.99 N	37 29.99 W	GPS	3139				
06ME50/3	VEINS-6	171	01	ROS/CTD	062701	0608	BO	59 28.02 N	37 30.02 W	GPS	3139	3111	3154	14	
06ME50/3	VEINS-6	171	01	ROS/CTD	062701	0723	EN	59 28.11 N	37 29.93 W	GPS	3140				
06ME50/3	VEINS-6	172	01	ROS/CTD	062701	0951	BE	59 33.04 N	38 20.34 W	GPS	3060				
06ME50/3	VEINS-6	172	01	ROS/CTD	062701	1051	BO	59 33.10 N	38 20.32 W	GPS	3061	3040	3072	14	
06ME50/3	VEINS-6	172	01	ROS/CTD	062701	1204	EN	59 33.11 N	38 20.15 W	GPS	3061				
06ME50/3	VEINS-6	173	01	ROS/CTD	062701	1358	BE	59 36.98 N	38 59.98 W	GPS	2946				
06ME50/3	VEINS-6	173	01	ROS/CTD	062701	1455	BO	59 36.96 N	39 00.04 W	GPS	2944		2954	12	
06ME50/3	VEINS-6	173	01	ROS/CTD	062701	1600	EN	59 37.01 N	38 59.85 W	GPS	2947				
06ME50/3	VEINS-6	174	01	ROS/CTD	062701	1804	BE	59 42.06 N	39 40.11 W	GPS	2795				
06ME50/3	VEINS-6	174	01	ROS/CTD	062701	1900	BO	59 42.08 N	39 40.00 W	GPS	2796	2764	2800	14	
06ME50/3	VEINS-6	174	01	ROS/CTD	062701	2005	EN	59 42.03 N	39 40.10 W	GPS	2798				
06ME50/3	VEINS-6	175	01	ROS/CTD	062701	2157	BE	59 45.97 N	40 15.17 W	GPS	2638				
06ME50/3	VEINS-6	175	01	ROS/CTD	062701	2246	BO	59 45.87 N	40 15.34 W	GPS	2636	2611	2636	14	
06ME50/3	VEINS-6	175	01	ROS/CTD	062701	2345	EN	59 45.94 N	40 15.43 W	GPS	2638				
06ME50/3	VEINS-6	176	01	ROS/CTD	062801	0130	BE	59 49.97 N	40 50.04 W	GPS	2383				
06ME50/3	VEINS-6	176	01	ROS/CTD	062801	0215	BO	59 50.03 N	40 50.08 W	GPS	2381	2354	2376	15	
06ME50/3	VEINS-6	176	01	ROS/CTD	062801	0303	EN	59 50.11 N	40 50.35 W	GPS	2375				
06ME50/3	VEINS-6	177	01	ROS/CTD	062801	0409	BE	59 51.95 N	41 09.93 W	GPS	2061				
06ME50/3	VEINS-6	177	01	ROS/CTD	062801	0449	BO	59 52.00 N	41 10.04 W	GPS	2036	2036	2049	14	
06ME50/3	VEINS-6	177	01	ROS/CTD	062801	0537	EN	59 52.00 N	41 10.11 W	GPS	2059				

06ME50/3	VEINS-6	178	01	ROS/CTD	062801	0642	BE	59 53.98 N	41 30.14 W	GPS	1905				
06ME50/3	VEINS-6	178	01	ROS/CTD	062801	0723	BO	59 53.96 N	41 30.15 W	GPS	1905	1872	1892	14	
06ME50/3	VEINS-6	178	01	ROS/CTD	062801	0808	EN	59 53.98 N	41 30.07 W	GPS	1906				
06ME50/3	VEINS-6	179	01	ROS/CTD	062801	0912	BE	59 55.86 N	41 50.36 W	GPS	1828				
06ME50/3	VEINS-6	179	01	ROS/CTD	062801	0949	BO	59 55.68 N	41 50.80 W	GPS	1828	1797	1812	14	
06ME50/3	VEINS-6	179	01	ROS/CTD	062801	1041	EN	59 55.53 N	41 51.58 W	GPS	1827				
06ME50/3	VEINS-6	180	01	ROS/CTD	062801	1140	BE	59 58.04 N	42 10.42 W	GPS	516				
06ME50/3	VEINS-6	180	01	ROS/CTD	062801	1154	BO	59 57.98 N	42 10.72 W	GPS	485		468	14	
06ME50/3	VEINS-6	180	01	ROS/CTD	062801	1211	EN	59 57.90 N	42 10.96 W	GPS	479				
06ME50/3	VEINS-6	181	01	ROS/CTD	062801	1316	BE	59 59.90 N	42 30.16 W	GPS	190				
06ME50/3	VEINS-6	181	01	ROS/CTD	062801	1323	BO	59 59.89 N	42 30.35 W	GPS	188		172	14	
06ME50/3	VEINS-6	181	01	ROS/CTD	062801	1335	EN	59 59.85 N	42 30.49 W	GPS	186				
06ME50/3	VEINS-5	182	01	ROS/CTD	062901	0325	BE	60 44.00 N	38 06.20 W	GPS	2905				
06ME50/3	VEINS-5	182	01	ROS/CTD	062901	0425	BO	60 44.00 N	38 05.98 W	GPS	2903	2880	2913	14	
06ME50/3	VEINS-5	182	01	ROS/CTD	062901	0527	EN	60 44.01 N	38 05.99 W	GPS	2902				
06ME50/3	VEINS-5	183	01	ROS/CTD	062901	0728	BE	60 50.01 N	38 47.28 W	GPS	2813				
06ME50/3	VEINS-5	183	01	ROS/CTD	062901	0824	BO	60 50.06 N	38 47.17 W	GPS	2813	2781	2817	14	
06ME50/3	VEINS-5	183	01	ROS/CTD	062901	0927	EN	60 50.16 N	38 46.98 W	GPS	2814				
06ME50/3	VEINS-5	184	01	ROS/CTD	062901	1122	BE	60 56.92 N	39 27.07 W	GPS	2580				
06ME50/3	VEINS-5	184	01	ROS/CTD	062901	1213	BO	60 57.11 N	39 26.68 W	GPS	2584	2551	2584	14	
06ME50/3	VEINS-5	184	01	ROS/CTD	062901	1312	EN	60 57.15 N	39 26.44 W	GPS	2586				
06ME50/3	VEINS-5	185	01	ROS/CTD	062901	1511	BE	61 03.98 N	40 08.06 W	GPS	2192				
06ME50/3	VEINS-5	185	01	ROS/CTD	062901	1553	BO	61 04.02 N	40 08.08 W	GPS	2188	2145	2181	14	
06ME50/3	VEINS-5	185	01	ROS/CTD	062901	1643	EN	61 04.05 N	40 08.04 W	GPS	2189				
06ME50/3	VEINS-5	186	01	ROS/CTD	062901	1820	BE	61 10.99 N	40 39.29 W	GPS	1895				
06ME50/3	VEINS-5	186	01	ROS/CTD	062901	1900	BO	61 10.98 N	40 39.14 W	GPS	1896	1868	1884	14	
06ME50/3	VEINS-5	186	01	ROS/CTD	062901	1939	EN	61 11.05 N	40 39.12 W	GPS	1894				
06ME50/3	VEINS-5	187	01	ROS/CTD	062901	2051	BE	61 14.94 N	41 00.03 W	GPS	1798				
06ME50/3	VEINS-5	187	01	ROS/CTD	062901	2130	BO	61 14.68 N	41 00.31 W	GPS	1803	1796	1790	14	
06ME50/3	VEINS-5	187	01	ROS/CTD	062901	2214	EN	61 14.35 N	41 00.73 W	GPS	1817				
06ME50/3	VEINS-5	188	01	ROS/CTD	062901	2303	BE	61 16.87 N	41 14.58 W	GPS	1423				
06ME50/3	VEINS-5	188	01	ROS/CTD	062901	2334	BO	61 16.64 N	41 14.80 W	GPS	1451	1429	1440	14	
06ME50/3	VEINS-5	188	01	ROS/CTD	063001	0006	EN	61 16.34 N	41 15.00 W	GPS	1477				
06ME50/3	VEINS-5	189	01	ROS/CTD	063001	0100	BE	61 17.97 N	41 30.30 W	GPS	236				
06ME50/3	VEINS-5	189	01	ROS/CTD	063001	0109	BO	61 17.98 N	41 30.40 W	GPS	240	219	223	14	
06ME50/3	VEINS-5	189	01	ROS/CTD	063001	0121	EN	61 17.97 N	41 30.41 W	GPS	240				
06ME50/3	VEINS-4	190	01	MOR	063001	1106	BE	63 00.00 N	40 33.10 W	GPS	300				Recovery of mooring tube
06ME50/3	VEINS-4	190	01	MOR	063001	1208	EN	63 00.60 N	40 35.30 W	GPS	300				
06ME50/3	VEINS-3	191	01	ROS/CTD	070101	0104	BE	63 02.00 N	35 27.15 W	GPS	2656				
06ME50/3	VEINS-3	191	01	ROS/CTD	070101	0149	BO	63 02.01 N	35 27.18 W	GPS			2658	14	
06ME50/3	VEINS-3	191	04	ROS/CTD	070101	0527	EN	63 01.97 N	35 27.14 W	GPS					4 JOJO Profiles
06ME50/3	VEINS-3	192	01	MOR	070101	0658	BE	63 06.90 N	35 32.60 W	GPS	2590				
06ME50/3	VEINS-3	192	01	MOR	070101	0817	EN	63 07.10 N	35 32.40 W	GPS					Recovery of mooring G2
06ME50/3	VEINS-3	193	01	MOR	070101	0940	BE	63 16.70 N	35 54.00 W	GPS	2536				
06ME50/3	VEINS-3	193	01	MOR	070101	1120	EN	63 17.00 N	35 52.60 W	GPS					Recovery of mooring UK2
06ME50/3	VEINS-3	194	01	MOR	070101	1207	BE	63 21.40 N	36 05.30 W	GPS	2200				
06ME50/3	VEINS-3	194	01	MOR	070101	1322	EN	63 21.60 N	36 06.20 W	GPS					Recovery of mooring G1(FI)
06ME50/3	VEINS-3	195	01	MOR	070101	1415	BE	63 27.90 N	36 18.00 W	GPS	1998				
06ME50/3	VEINS-3	195	01	MOR	070101	1533	EN	63 28.00 N	36 19.50 W	GPS					Recovery of mooring UK1/IES
06ME50/3	VEINS-3	196	01	MOR	070101	1533	BE	63 28.00 N	36 19.50 W	GPS	1987				
06ME50/3	VEINS-3	196	01	MOR	070101	1630	EN	63 28.50 N	36 20.20 W	GPS					Recovery of mooring UK1
06ME50/3	VEINS-3	197	01	MOR	070101	1715	BE	63 32.70 N	36 31.00 W	GPS	1780				
06ME50/3	VEINS-3	197	01	MOR	070101	1816	EN	63 33.20 N	36 33.00 W	GPS					Recovery of mooring F2
06ME50/3	VEINS-3	198	01	MOR	070101	1912	BE	63 37.60 N	36 49.30 W	GPS	1598				
06ME50/3	VEINS-3	198	01	MOR	070101	2010	EN	63 38.20 N	36 49.60 W	GPS					Recovery of mooring F1(G)
06ME50/3	VEINS-4	199	01	ROS/CTD	070201	0900	BE	61 25.99 N	35 00.00 W	GPS	2911				
06ME50/3	VEINS-4	199	01	ROS/CTD	070201	0955	BO	61 26.17 N	35 44.57 W	GPS	2911	2900	2921	14	
06ME50/3	VEINS-4	199	01	ROS/CTD	070201	1109	EN	61 26.37 N	35 44.56 W	GPS	2912				
06ME50/3	VEINS-4	200	01	ROS/CTD	070201	1311	BE	61 37.91 N	36 18.01 W	GPS	2800				
06ME50/3	VEINS-4	200	01	ROS/CTD	070201	1405	BO	61 38.17 N	36 18.45 W	GPS	2797	2768	2804	14	
06ME50/3	VEINS-4	200	01	ROS/CTD	070201	1508	EN	61 38.43 N	36 18.27 W	GPS	2797				
06ME50/3	VEINS-4	201	01	ROS/CTD	070201	1712	BE	61 49.06 N	36 53.16 W	GPS	2684				
06ME50/3	VEINS-4	201	01	ROS/CTD	070201	1806	BO	61 49.09 N	36 53.15 W	GPS	2687	2640	2688	15	
06ME50/3	VEINS-4	201	01	ROS/CTD	070201	1910	EN	61 49.04 N	36 52.95 W	GPS	2687				
06ME50/3	VEINS-4	202	01	ROS/CTD	070201	2022	BE	61 54.97 N	37 09.97 W	GPS	2625				
06ME50/3	VEINS-4	202	01	ROS/CTD	070201	2113	BO	61 55.10 N	37 10.11 W	GPS	2623	2590	2624	14	
06ME50/3	VEINS-4	202	01	ROS/CTD	070201	2207	EN	61 55.23 N	37 10.69 W	GPS	2621				
06ME50/3	VEINS-4	203	01	ROS/CTD	070201	2310	BE	62 01.30 N	37 28.38 W	GPS	2561				
06ME50/3	VEINS-4	203	01	ROS/CTD	070201	2358	BO	62 01.65 N	37 29.37 W	GPS	2559	2535	2560	14	
06ME50/3	VEINS-4	203	01	ROS/CTD	070301	0058	EN	62 02.07 N	37 30.50 W	GPS	2555				
06ME50/3	VEINS-4	204	01	ROS/CTD	070301	0156	BE	62 06.90 N	37 44.98 W	GPS	2526				
06ME50/3	VEINS-4	204	01	ROS/CTD	070301	0245	BO	62 06.69 N	37 45.06 W	GPS	2529	2496	2526	13	
06ME50/3	VEINS-4	204	01	ROS/CTD	070301	0332	EN	62 06.84 N	37 45.28 W	GPS	2530				
06ME50/3	VEINS-4	205	01	MOR	070301	1440	BE	63 00.20 N	40 32.70 W	GPS	303				Deployment Tube04
06ME50/3	VEINS-4	206	01	MOR	070301	1638	BE	62 58.60 N	40 53.30 W	GPS	300				Deployment Tube03
06ME50/3	VEINS-4	207	01	ROS/CTD	070301	1745	BE	63 00.00 N	40 35.01 W	GPS	403				
06ME50/3	VEINS-4	207	01	ROS/CTD	070301	1800	BO	62 59.99 N	40 35.17 W	GPS	409	387	392	14	

06ME50/3	VEINS-4	207	01	ROS/CTD	070301	1811	EN	63 00.01 N	40 35.33 W	GPS	414				
06ME50/3	VEINS-4	208	01	ROS/CTD	070301	1853	BE	62 57.92 N	40 24.84 W	GPS	220				
06ME50/3	VEINS-4	208	01	ROS/CTD	070301	1903	BO	62 57.93 N	40 24.97 W	GPS	218	205	208	14	
06ME50/3	VEINS-4	208	01	ROS/CTD	070301	1912	EN	62 57.96 N	40 25.06 W	GPS	218				
06ME50/3	VEINS-4	209	01	ROS/CTD	070301	2018	BE	62 51.93 N	40 07.04 W	GPS	1698				
06ME50/3	VEINS-4	209	01	ROS/CTD	070301	2054	BO	62 52.01 N	40 07.13 W	GPS	1694	1670	1684	14	
06ME50/3	VEINS-4	209	01	ROS/CTD	070301	2134	EN	62 51.96 N	40 07.05 W	GPS	1695				
06ME50/3	VEINS-4	210	01	ROS/CTD	070301	2236	BE	62 46.95 N	39 49.95 W	GPS	1931				
06ME50/3	VEINS-4	210	01	ROS/CTD	070301	2313	BO	62 46.91 N	39 49.14 W	GPS	1932	1906	1924	14	
06ME50/3	VEINS-4	210	01	ROS/CTD	070301	2351	EN	62 46.80 N	39 49.36 W	GPS	1935				
06ME50/3	VEINS-4	211	01	ROS/CTD	070401	0100	BE	62 40.98 N	39 31.11 W	GPS	1974				
06ME50/3	VEINS-4	211	01	ROS/CTD	070401	0136	BO	62 40.95 N	39 31.10 W	GPS	1974	1932	1953	14	
06ME50/3	VEINS-4	211	01	ROS/CTD	070401	0217	EN	62 40.96 N	39 31.05 W	GPS	1976				
06ME50/3	VEINS-4	212	01	ROS/CTD	070401	0330	BE	62 35.02 N	39 13.11 W	GPS	2029				
06ME50/3	VEINS-4	212	01	ROS/CTD	070401	0405	BO	62 35.07 N	39 13.02 W	GPS	2030	1999	2019	14	
06ME50/3	VEINS-4	212	01	ROS/CTD	070401	0444	EN	62 35.08 N	39 12.95 W	GPS	2032				
06ME50/3	VEINS-4	213	01	ROS/CTD	070401	0550	BE	62 30.00 N	38 56.12 W	GPS	2166				
06ME50/3	VEINS-4	213	01	ROS/CTD	070401	0635	BO	62 30.05 N	38 56.31 W	GPS	2160	2125	2150	14	
06ME50/3	VEINS-4	213	01	ROS/CTD	070401	0725	EN	62 30.19 N	38 56.77 W	GPS	2165				
06ME50/3	VEINS-4	214	01	ROS/CTD	070401	0845	BE	62 23.98 N	38 37.97 W	GPS	2280				
06ME50/3	VEINS-4	214	01	ROS/CTD	070401	0930	BO	62 24.20 N	38 38.68 W	GPS	2269	2250	2266	14	
06ME50/3	VEINS-4	214	01	ROS/CTD	070401	1013	EN	62 24.38 N	38 38.96 W	GPS					
06ME50/3	VEINS-4	215	01	ROS/CTD	070401	1143	BE	62 17.90 N	38 20.53 W	GPS	2368				
06ME50/3	VEINS-4	215	01	ROS/CTD	070401	1228	BO	62 17.88 N	38 20.61 W	GPS	2366	2334	2365	14	
06ME50/3	VEINS-4	215	01	ROS/CTD	070401	1320	EN	62 17.84 N	38 20.58 W	GPS	2369				
06ME50/3	VEINS-4	216	01	ROS/CTD	070401	1429	BE	62 12.08 N	38 03.04 W	GPS	2491				
06ME50/3	VEINS-4	216	01	ROS/CTD	070401	1518	BO	62 12.01 N	38 02.96 W	GPS	2490	2460	2488	14	
06ME50/3	VEINS-4	216	01	ROS/CTD	070401	1608	EN	62 12.02 N	38 03.02 W	GPS	2490				
06ME50/3	VEINS-3	217	01	ROS/CTD	070501	0205	BE	63 49.97 N	36 58.15 W	GPS	357				
06ME50/3	VEINS-3	217	01	ROS/CTD	070501	0215	BO	63 50.03 N	36 58.51 W	GPS	356	334	335	14	
06ME50/3	VEINS-3	217	01	ROS/CTD	070501	0224	EN	63 50.02 N	36 58.67 W	GPS	354				
06ME50/3	VEINS-3	218	01	ROS/CTD	070501	0311	BE	63 46.01 N	36 51.15 W	GPS	629				
06ME50/3	VEINS-3	218	01	ROS/CTD	070501	0328	BO	63 46.06 N	36 51.37 W	GPS	580	568	571	14	
06ME50/3	VEINS-3	218	01	ROS/CTD	070501	0340	EN	63 46.13 N	36 51.52 W	GPS	550				
06ME50/3	VEINS-3	219	01	ROS/CTD	070501	0425	BE	63 42.03 N	36 43.13 W	GPS	1715				
06ME50/3	VEINS-3	219	01	ROS/CTD	070501	0500	BO	63 42.08 N	36 43.22 W	GPS	1711	1691	1696	14	
06ME50/3	VEINS-3	219	01	ROS/CTD	070501	0541	EN	63 42.01 N	36 43.72 W	GPS	1675				
06ME50/3	VEINS-3	220	01	ROS/CTD	070501	0654	BE	63 33.89 N	36 27.91 W	GPS	1800				
06ME50/3	VEINS-3	220	01	ROS/CTD	070501	0733	BO	63 33.83 N	36 28.09 W	GPS	1796	1766	1785	14	
06ME50/3	VEINS-3	220	01	ROS/CTD	070501	0807	EN	63 33.77 N	36 28.25 W	GPS	1792				
06ME50/3	VEINS-3	221	01	MOR	070501	0829	BE	63 32.60 N	36 29.10 W	GPS					Recovery of mooring F2/ADCP
06ME50/3	VEINS-3	221	01	MOR	070501	0928	EN	63 31.90 N	36 28.60 W	GPS					
06ME50/3	VEINS-3	222	01	ROS/CTD	070501	1010	BE	63 29.98 N	36 20.00 W	GPS	1942				
06ME50/3	VEINS-3	222	01	ROS/CTD	070501	1049	BO	63 29.95 N	36 20.13 W	GPS	1942	1909	1930	14	
06ME50/3	VEINS-3	222	01	ROS/CTD	070501	1135	EN	63 29.96 N	36 19.79 W	GPS	1949				
06ME50/3	VEINS-3	223	01	MOR	070501	1157	BE	63 28.70 N	36 18.80 W	GPS					Deployment of mooring UK1/IES-2001
06ME50/3	VEINS-3	223	01	MOR	070501	1245	EN	63 28.69 N	36 18.81 W	GPS					
06ME50/3	VEINS-3	224	01	ROS/CTD	070501	1246	BE	63 28.69 N	36 18.76 W	GPS	1988			80	CO2
06ME50/3	VEINS-3	224	01	ROS/CTD	070501	1305	EN	63 28.74 N	36 18.97 W	GPS	1987				
06ME50/3	VEINS-3	225	01	MOR	070501	1414	BE	63 22.40 N	36 03.80 W	GPS					Deployment of mooring G1-2001
06ME50/3	VEINS-3	225	01	MOR	070501	1502	EN	63 21.80 N	36 04.30 W	GPS					
06ME50/3	VEINS-3	226	01	MOR	070501	1547	BE	63 17.60 N	35 52.90 W	GPS					Deployment of mooring UK2-2001
06ME50/3	VEINS-3	226	01	MOR	070501	1619	EN	63 17.00 N	35 53.10 W	GPS					
06ME50/3	VEINS-3	227	01	MOR	070501	1742	BE	63 07.50 N	35 31.50 W	GPS					Deployment of mooring G2-2001
06ME50/3	VEINS-3	227	01	MOR	070501	1805	EN	63 07.00 N	35 31.90 W	GPS					
06ME50/3	VEINS-3	228	01	ROS/CTD	070501	2034	BE	63 25.99 N	36 13.11 W	GPS	2097				
06ME50/3	VEINS-3	228	01	ROS/CTD	070501	2115	BO	63 25.96 N	36 13.10 W	GPS	2100	2075	2097	14	
06ME50/3	VEINS-3	228	01	ROS/CTD	070501	2202	EN	63 25.93 N	36 13.53 W	GPS	2096				
06ME50/3	VEINS-3	229	01	ROS/CTD	070501	2248	BE	63 23.02 N	36 06.00 W	GPS	2201				
06ME50/3	VEINS-3	229	01	ROS/CTD	070501	2331	BO	63 21.89 N	36 06.55 W	GPS	2198	2172	2194	14	
06ME50/3	VEINS-3	229	01	ROS/CTD	070601	0015	EN	63 21.94 N	36 07.00 W	GPS	2198				
06ME50/3	VEINS-3	230	01	ROS/CTD	070601	0108	BE	63 18.09 N	35 58.13 W	GPS	2306				
06ME50/3	VEINS-3	230	01	ROS/CTD	070601	0154	BO	63 17.98 N	35 58.35 W	GPS	2306		2298	14	
06ME50/3	VEINS-3	230	01	ROS/CTD	070601	0235	EN	63 17.89 N	35 58.21 W	GPS	2310				
06ME50/3	VEINS-3	231	01	ROS/CTD	070601	0329	BE	63 14.03 N	35 49.65 W	GPS	2415				
06ME50/3	VEINS-3	231	01	ROS/CTD	070601	0414	BO	63 14.01 N	35 49.95 W	GPS	2419	2384	2413	14	
06ME50/3	VEINS-3	231	01	ROS/CTD	070601	0515	EN	63 14.00 N	35 50.09 W	GPS	2417				
06ME50/3	VEINS-3	232	01	ROS/CTD	070601	0602	BE	63 09.97 N	35 42.89 W	GPS	2511				
06ME50/3	VEINS-3	232	01	ROS/CTD	070601	0653	BO	63 10.00 N	35 42.95 W	GPS	2511	2478	2510	14	
06ME50/3	VEINS-3	232	01	ROS/CTD	070601	0742	EN	63 10.02 N	35 42.95 W	GPS	2510				
06ME50/3	VEINS-3	233	01	ROS/CTD	070601	0850	BE	63 02.01 N	35 27.98 W	GPS	2655				
06ME50/3	VEINS-3	233	01	ROS/CTD	070601	0940	BO	63 02.04 N	35 27.84 W	GPS	2654	2636	2660	14	
06ME50/3	VEINS-3	233	01	ROS/CTD	070601	1036	EN	63 01.93 N	35 27.99 W	GPS	2654				
06ME50/3	VEINS-3	234	01	ROS/CTD	070601	1233	BE	62 54.09 N	35 13.00 W	GPS	2717				
06ME50/3	VEINS-3	234	01	ROS/CTD	070601	1312	BO	62 54.27 N	35 12.27 W	GPS	2718	2700	2720	13	
06ME50/3	VEINS-3	234	01	ROS/CTD	070601	1400	EN	62 54.10 N	35 11.57 W	GPS	2719				
06ME50/3	VEINS-3	235	01	ROS/CTD	070601	1506	BE	62 45.98 N	34 58.07 W	GPS	2764				
06ME50/3	VEINS-3	235	01	ROS/CTD	070601	1559	BO	62 46.16 N	34 57.58 W	GPS	2773	2745	2775	14	
06ME50/3	VEINS-3	235	01	ROS/CTD	070601	1700	EN	62 46.30 N	34 57.68 W	GPS	2773				
06ME50/3	VEINS-3	236	01	ROS/CTD	070601	1808	BE	62 37.93 N	34 42.95 W	GPS	2806				
06ME50/3	VEINS-3	236	01	ROS/CTD	070601	1906	BO	62 38.16 N	34 42.67 W	GPS	2806	2792	2813	14	
06ME50/3	VEINS-3	236	01	ROS/CTD	070601	2002	EN	62 38.33 N	34 42.53 W	GPS	2806				
06ME50/3	VEINS-3	237	01	ROS/CTD	070601	2111	BE	62 29.91 N	34 28.00 W	GPS	2842				
06ME50/3	VEINS-3	237	01	ROS/CTD	070601	2206	BO	62 29.97 N	34 28.10 W	GPS	2842	2812	2850	14	

06ME50/3	VEINS-3	237	01	ROS/CTD	070601	2311	EN	62 29.97 N	34 28.21 W	GPS	2841						
06ME50/3	VEINS-3	238	01	ROS/CTD	070701	0033	BE	62 30.03 N	33 59.95 W	GPS	2899						
06ME50/3	VEINS-3	238	01	ROS/CTD	070701	0125	BO	62 30.07 N	34 00.15 W	GPS	2920	2848	2907	16			
06ME50/3	VEINS-3	238	01	ROS/CTD	070701	0224	EN	62 30.33 N	34 00.76 W	GPS	2895						
06ME50/3		239	01	ROS/CTD	070701	1030	BE	63 27.83 N	36 17.85 W	GPS	2013		100				CO2
06ME50/3		239	01	ROS/CTD	070701	1048	EN	63 27.83 N	36 18.63 W	GPS	2007						
06ME50/3	VEINS-3	239	02	MOR	070701	1101	BE	63 28.40 N	36 17.90 W	GPS					Deployment of mooring UK1-2001		
06ME50/3	VEINS-3	239	02	MOR	070701	1135	EN	63 28.90 N	36 17.90 W	GPS							
06ME50/3	VEINS-3	240	01	MOR	070701	1221	BE	63 32.80 N	36 30.10 W	GPS					Deployment of mooring F2-2001		
06ME50/3	VEINS-3	240	01	MOR	070701	1413	EN	63 33.30 N	36 30.30 W	GPS							
06ME50/3	VEINS-3	241	01	MOR	070701	1445	BE	63 37.60 N	36 47.40 W	GPS					Deployment of mooring F1-2001		
06ME50/3	VEINS-3	241	01	MOR	070701	1515	EN	63 38.30 N	36 47.70 W	GPS							
06ME50/3	VEINS-3	242	01	MOR	070701	1551	BE	63 38.70 N	36 54.70 W	GPS					Deployment of mooring O1-2001		
06ME50/3	VEINS-3	242	01	MOR	070701	1611	EN	63 39.00 N	36 54.40 W	GPS							
06ME50/3		243	01	ROS/CTD	070701	1843	BE	63 36.53 N	35 58.27 W	GPS	2040						
06ME50/3		243	01	ROS/CTD	070701	1925	BO	63 36.31 N	35 58.44 W	GPS	2039	2005	2024	14			
06ME50/3		243	01	ROS/CTD	070701	2006	EN	63 36.34 N	35 58.74 W	GPS	2031						
06ME50/3		244	01	ROS/CTD	070701	2132	BE	63 45.69 N	35 39.85 W	GPS							
06ME50/3		244	01	ROS/CTD	070701	2219	BO	63 45.77 N	35 40.32 W	GPS	2144	2125	2146	14			
06ME50/3		244	01	ROS/CTD	070701	2300	EN	63 45.67 N	35 40.41 W	GPS	2147						
06ME50/3		245	01	ROS/CTD	070801	0020	BE	63 52.98 N	35 10.22 W	GPS	2021						
06ME50/3		245	01	ROS/CTD	070801	0111	BO	63 53.00 N	35 10.32 W	GPS	2032	2006	2028	14			
06ME50/3		245	01	ROS/CTD	070801	0147	EN	63 53.02 N	35 10.37 W	GPS	2022						
06ME50/3		246	01	ROS/CTD	070801	0314	BE	64 02.20 N	34 47.05 W	GPS	1973						
06ME50/3		246	01	ROS/CTD	070801	0354	BO	64 02.13 N	34 47.11 W	GPS	1973	1983	1977	14			
06ME50/3		246	01	ROS/CTD	070801	0430	EN	64 02.08 N	34 47.05 W	GPS	1976						
06ME50/3		247	01	ROS/CTD	070801	0551	BE	64 11.40 N	34 27.43 W	GPS	1971						
06ME50/3		247	01	ROS/CTD	070801	0633	BO	64 11.28 N	34 27.86 W	GPS	1982	1985	1982	14			
06ME50/3		247	01	ROS/CTD	070801	0715	EN	64 11.21 N	34 28.40 W	GPS	1984						
06ME50/3		248	01	ROS/CTD	070801	0837	BE	64 16.06 N	34 01.45 W	GPS	1974						
06ME50/3		248	01	ROS/CTD	070801	0918	BO	64 16.24 N	34 01.93 W	GPS	1972		1975	14			
06ME50/3		248	01	ROS/CTD	070801	0959	EN	64 16.56 N	34 02.34 W	GPS	1963						
06ME50/3		249	01	ROS/CTD	070801	1327	BE	64 10.65 N	32 38.67 W	GPS	2478		100				CO2
06ME50/3		249	01	ROS/CTD	070801	1344	EN	64 10.69 N	32 38.80 W	GPS	2478						
06ME50/3	VEINS-2	250	01	ROS/CTD	070801	2023	BE	64 00.07 N	30 00.18 W	GPS	2076						
06ME50/3	VEINS-2	250	01	ROS/CTD	070801	2105	BO	64 00.40 N	30 00.39 W	GPS	2038	2093	2066	14			
06ME50/3	VEINS-2	250	01	ROS/CTD	070801	2150	EN	64 00.71 N	30 00.82 W	GPS	2040						
06ME50/3	VEINS-2	251	01	ROS/CTD	070801	2306	BE	63 59.97 N	30 30.36 W	GPS	2500						
06ME50/3	VEINS-2	251	01	ROS/CTD	070801	2353	BO	64 00.12 N	30 30.40 W	GPS	2502	2469	2492	14			
06ME50/3	VEINS-2	251	01	ROS/CTD	070901	0041	EN	64 00.17 N	30 30.42 W	GPS	2499						
06ME50/3	VEINS-2	252	01	ROS/CTD	070901	0138	BE	63 59.96 N	30 50.11 W	GPS	2686						
06ME50/3	VEINS-2	252	01	ROS/CTD	070901	0230	BO	64 00.03 N	30 49.94 W	GPS	2684	2656	2685	14			
06ME50/3	VEINS-2	252	01	ROS/CTD	070901	0324	EN	64 00.08 N	30 50.21 W	GPS	2686						
06ME50/3	VEINS-2	253	01	ROS/CTD	070901	0421	BE	63 59.94 N	31 10.03 W	GPS	2717						
06ME50/3	VEINS-2	253	01	ROS/CTD	070901	0513	BO	63 59.99 N	31 10.00 W	GPS	2714	2684	2720	14			
06ME50/3	VEINS-2	253	01	ROS/CTD	070901	0606	EN	64 00.00 N	31 10.05 W	GPS	2722						
06ME50/3	VEINS-2	254	01	ROS/CTD	070901	0702	BE	63 59.95 N	31 30.23 W	GPS	2744						
06ME50/3	VEINS-2	254	01	ROS/CTD	070901	0756	BO	64 00.03 N	31 30.37 W	GPS	2744	2708	2746	14			
06ME50/3	VEINS-2	254	01	ROS/CTD	070901	0858	EN	63 59.89 N	31 30.58 W	GPS	2744						
06ME50/3	VEINS-2	255	01	ROS/CTD	070901	0953	BE	63 59.94 N	31 50.50 W	GPS	2732						
06ME50/3	VEINS-2	255	01	ROS/CTD	070901	1024	BO	64 00.09 N	31 51.09 W	GPS	2730	2693	2729	14			
06ME50/3	VEINS-2	255	01	ROS/CTD	070901	1136	EN	64 00.28 N	31 51.48 W	GPS	2727						
06ME50/3	VEINS-2	256	01	ROS/CTD	070901	1240	BE	63 59.77 N	32 10.11 W	GPS	2713						
06ME50/3	VEINS-2	256	01	ROS/CTD	070901	1331	BO	63 59.95 N	32 10.22 W	GPS	2689	2672	2700	14			
06ME50/3	VEINS-2	256	01	ROS/CTD	070901	1426	EN	64 00.20 N	32 10.53 W	GPS	2687						
06ME50/3	VEINS-2	257	01	ROS/CTD	070901	1543	BE	63 59.90 N	32 30.07 W	GPS	2644						
06ME50/3	VEINS-2	257	01	ROS/CTD	070901	1635	BO	64 00.00 N	32 30.60 W	GPS	2642	2620	2650	14			
06ME50/3	VEINS-2	257	01	ROS/CTD	070901	1726	EN	64 00.16 N	32 30.90 W	GPS	2639						
06ME50/3	VEINS-2	258	01	ROS/CTD	070901	1829	BE	63 59.96 N	32 50.22 W	GPS	2542						
06ME50/3	VEINS-2	258	01	ROS/CTD	070901	1921	BO	64 00.09 N	32 50.96 W	GPS	2530	2518	2542	14			
06ME50/3	VEINS-2	258	01	ROS/CTD	070901	2015	EN	64 00.13 N	32 51.70 W	GPS	2531						
06ME50/3	VEINS-2	259	01	ROS/CTD	070901	2117	BE	63 59.96 N	33 09.86 W	GPS	2443						
06ME50/3	VEINS-2	259	01	ROS/CTD	070901	2205	BO	64 00.14 N	33 10.54 W	GPS	2437	2419	2444	14			
06ME50/3	VEINS-2	259	01	ROS/CTD	070901	2251	EN	64 00.34 N	33 11.36 W	GPS	2434						
06ME50/3	VEINS-2	260	01	ROS/CTD	070901	2345	BE	64 05.04 N	33 17.51 W	GPS	2348						
06ME50/3	VEINS-2	260	01	ROS/CTD	071001	0031	BO	64 05.30 N	33 18.65 W	GPS	2337	2329	2341	14			
06ME50/3	VEINS-2	260	01	ROS/CTD	071001	0123	EN	64 05.66 N	33 19.50 W	GPS	2325						
06ME50/3	VEINS-2	261	01	ROS/CTD	071001	0208	BE	64 09.96 N	33 25.05 W	GPS	2228						
06ME50/3	VEINS-2	261	01	ROS/CTD	071001	0253	BO	64 10.21 N	33 25.56 W	GPS	2220	2214	2225	13			
06ME50/3	VEINS-2	261	01	ROS/CTD	071001	0331	EN	64 10.30 N	33 26.02 W	GPS	2220						
06ME50/3	VEINS-2	262	01	ROS/CTD	071001	0416	BE	64 14.95 N	33 32.42 W	GPS	2085						
06ME50/3	VEINS-2	262	01	ROS/CTD	071001	0455	BO	64 15.06 N	33 32.71 W	GPS	2082	2067	2085	14			
06ME50/3	VEINS-2	262	01	ROS/CTD	071001	0541	EN	64 15.07 N	33 32.96 W	GPS	2083						
06ME50/3	VEINS-2	263	01	ROS/CTD	071001	0629	BE	64 20.00 N	33 40.16 W	GPS	1928						
06ME50/3	VEINS-2	263	01	ROS/CTD	071001	0710	BO	64 20.01 N	33 40.37 W	GPS	1929	1899	1923	14			
06ME50/3	VEINS-2	263	01	ROS/CTD	071001	0753	EN	64 20.07 N	33 40.57 W	GPS	1927						
06ME50/3	VEINS-2	264	01	ROS/CTD	071001	0848	BE	64 25.04 N	33 47.42 W	GPS	1772						
06ME50/3	VEINS-2	264	01	ROS/CTD	071001	0923	BO	64 25.20 N	33 47.44 W	GPS	1770	1749	1764	14			
06ME50/3	VEINS-2	264	01	ROS/CTD	071001	0959	EN	64 25.23 N	33 47.28 W	GPS	1769						
06ME50/3	VEINS-2	265	01	ROS/CTD	071001	1111	BE	64 30.30 N	33 54.95 W	GPS	1599						
06ME50/3	VEINS-2	265	01	ROS/CTD	071001	1143	BO	64 30.37 N	33 54.74 W	GPS	1598	1615	1593	14			
06ME50/3	VEINS-2	265	01	ROS/CTD	071001	1219	EN	64 30.48 N	33 54.08 W	GPS	1597						
06ME50/3	VEINS-2	266	01	ROS/CTD	071001	1308	BE	64 35.03 N	34 02.45 W	GPS	1424						
06ME50/3	VEINS-2	266	01	ROS/CTD	071001	1338	BO	64 35.01 N	34 02.55 W	GPS	1424	1401	1414	14			
06ME50/3	VEINS-2	266	01	ROS/CTD	071001	1409	EN	64 35.01 N	34 02.54 W	GPS	1423						

06ME50/3	VEINS-2	267	01	ROS/CTD	071001	1500	BE	64 39.91 N	34 10.22 W	GPS	1244			
06ME50/3	VEINS-2	267	01	ROS/CTD	071001	1526	BO	64 39.82 N	34 11.09 W	GPS	1247	1231	1235	15
06ME50/3	VEINS-2	267	01	ROS/CTD	071001	1550	EN	64 39.80 N	34 12.67 W	GPS	1246			
06ME50/3	VEINS-2	268	01	ROS/CTD	071001	1643	BE	64 45.02 N	34 17.61 W	GPS	1116			
06ME50/3	VEINS-2	268	01	ROS/CTD	071001	1711	BO	64 44.93 N	34 18.25 W	GPS	1120	1098	1108	14
06ME50/3	VEINS-2	268	01	ROS/CTD	071001	1737	EN	64 44.82 N	34 18.94 W	GPS	1124			
06ME50/3	VEINS-2	269	01	ROS/CTD	071001	1833	BE	64 50.02 N	34 25.06 W	GPS	1047			
06ME50/3	VEINS-2	269	01	ROS/CTD	071001	1859	BO	64 50.07 N	34 25.07 W	GPS	1048	1031	1041	11
06ME50/3	VEINS-2	269	01	ROS/CTD	071001	1922	EN	64 50.03 N	34 25.03 W	GPS	1051			
06ME50/3	VEINS-2	270	01	ROS/CTD	071001	2016	BE	64 55.10 N	34 32.46 W	GPS	869			
06ME50/3	VEINS-2	270	01	ROS/CTD	071001	2040	BO	64 55.15 N	34 32.72 W	GPS	864	846	855	14
06ME50/3	VEINS-2	270	01	ROS/CTD	071001	2102	EN	64 55.13 N	34 33.00 W	GPS	863			
06ME50/3	VEINS-2	271	01	ROS/CTD	071001	2208	BE	65 00.03 N	34 40.02 W	GPS	373			
06ME50/3	VEINS-2	271	01	ROS/CTD	071001	2221	BO	65 00.00 N	34 40.29 W	GPS	376	372	374	14
06ME50/3	VEINS-2	271	01	ROS/CTD	071001	2230	EN	64 59.96 N	34 40.49 W	GPS	387			
06ME50/3	VEINS-2	272	01	ROS/CTD	071001	2316	BE	65 05.08 N	34 47.48 W	GPS	364			
06ME50/3	VEINS-2	272	01	ROS/CTD	071001	2331	BO	65 05.01 N	34 47.54 W	GPS	365	357	360	14
06ME50/3	VEINS-2	272	01	ROS/CTD	071001	2342	EN	65 05.00 N	34 47.53 W	GPS	364			
06ME50/3	VEINS-2	273	01	ROS/CTD	071101	0035	BE	65 09.96 N	34 54.91 W	GPS	282			
06ME50/3	VEINS-2	273	01	ROS/CTD	071101	0044	BO	65 10.02 N	34 54.92 W	GPS	282	272	274	14
06ME50/3	VEINS-2	273	01	ROS/CTD	071101	0053	EN	65 10.00 N	34 54.81 W	GPS	280			
06ME50/3		274	01	ROS/CTD	071101	0616	BE	64 23.96 N	33 17.97 W	GPS	1992			
06ME50/3		274	01	ROS/CTD	071101	0700	BO	64 24.10 N	33 18.29 W	GPS	1990	1969	1989	11
06ME50/3		274	01	ROS/CTD	071101	0740	EN	64 24.20 N	33 18.59 W	GPS	1985			
06ME50/3		275	01	ROS/CTD	071101	0858	BE	64 30.95 N	32 54.96 W	GPS	2086			
06ME50/3		275	01	ROS/CTD	071101	0938	BO	64 31.21 N	32 55.13 W	GPS	2081	2058	2087	5
06ME50/3		275	01	ROS/CTD	071101	1020	EN	64 31.32 N	32 55.64 W	GPS	2077			
06ME50/3		276	01	ROS/CTD	071101	1137	BE	64 38.96 N	32 31.98 W	GPS	2177			
06ME50/3		276	01	ROS/CTD	071101	1219	BO	64 39.15 N	32 32.05 W	GPS	2131	2154	2178	14
06ME50/3		276	01	ROS/CTD	071101	1257	EN	64 39.19 N	32 32.33 W	GPS	2171			
06ME50/3		277	01	ROS/CTD	071101	1409	BE	64 45.06 N	32 09.12 W	GPS	2243			
06ME50/3		277	01	ROS/CTD	071101	1454	BO	64 44.94 N	32 09.05 W	GPS	2246	2224	2248	12
06ME50/3		277	01	ROS/CTD	071101	1533	EN	64 44.86 N	32 08.87 W	GPS	2247			
06ME50/3		278	01	ROS/CTD	071101	1648	BE	64 51.04 N	31 46.01 W	GPS	2174			
06ME50/3		278	01	ROS/CTD	071101	1734	BO	64 50.88 N	31 46.28 W	GPS	2176	2155	2179	11
06ME50/3		278	01	ROS/CTD	071101	1818	EN	64 50.79 N	31 46.15 W	GPS	2178			
06ME50/3		279	01	ROS/CTD	071101	1929	BE	64 56.03 N	31 23.02 W	GPS	2065			
06ME50/3		279	01	ROS/CTD	071101	2013	BO	64 55.93 N	31 23.36 W	GPS	2071	2047	2073	11
06ME50/3		279	01	ROS/CTD	071101	2052	EN	64 55.89 N	31 23.57 W	GPS	2073			
06ME50/3		280	01	ROS/CTD	071101	2203	BE	65 02.09 N	30 59.72 W	GPS	1821			
06ME50/3		280	01	ROS/CTD	071101	2237	BO	65 02.08 N	30 59.93 W	GPS	1820	1804	1820	14
06ME50/3		280	01	ROS/CTD	071101	2317	EN	65 02.09 N	31 00.22 W	GPS	1818			
06ME50/3	VEINS-1	281	01	ROS/CTD	071201	0358	BE	65 45.05 N	31 25.07 W	GPS	367			
06ME50/3	VEINS-1	281	01	ROS/CTD	071201	0413	BO	65 45.16 N	31 25.22 W	GPS	360	343	344	23
06ME50/3	VEINS-1	281	01	ROS/CTD	071201	0422	BN	65 45.20 N	31 25.30 W	GPS	362			
06ME50/3	VEINS-1	282	01	ROS/CTD	071201	0517	BE	65 39.90 N	31 19.99 W	GPS	351			
06ME50/3	VEINS-1	282	01	ROS/CTD	071201	0533	BO	65 39.87 N	31 20.27 W	GPS	352	339	342	11
06ME50/3	VEINS-1	282	01	ROS/CTD	071201	0543	EN	65 39.94 N	31 20.39 W	GPS	350			
06ME50/3	VEINS-1	283	01	ROS/CTD	071201	0631	BE	65 34.99 N	31 15.03 W	GPS	362			
06ME50/3	VEINS-1	283	01	ROS/CTD	071201	0646	BO	65 35.03 N	31 15.21 W	GPS	359	350	355	11
06ME50/3	VEINS-1	283	01	ROS/CTD	071201	0658	EN	65 35.02 N	31 15.41 W	GPS	360			
06ME50/3	VEINS-1	284	01	ROS/CTD	071201	0745	BE	65 30.00 N	31 09.93 W	GPS	377			
06ME50/3	VEINS-1	284	01	ROS/CTD	071201	0800	BO	65 30.11 N	31 10.11 W	GPS	376	354	359	11
06ME50/3	VEINS-1	284	01	ROS/CTD	071201	0809	EN	65 30.17 N	31 10.42 W	GPS	378			
06ME50/3	VEINS-1	285	01	ROS/CTD	071201	0856	BE	65 25.00 N	31 04.78 W	GPS	670			
06ME50/3	VEINS-1	285	01	ROS/CTD	071201	0914	BO	65 25.33 N	31 04.55 W	GPS	644	657	640	14
06ME50/3	VEINS-1	285	01	ROS/CTD	071201	0930	EN	65 25.56 N	31 04.51 W	GPS	628			
06ME50/3	VEINS-1	286	01	ROS/CTD	071201	1027	BE	65 19.98 N	30 59.95 W	GPS	973			
06ME50/3	VEINS-1	286	01	ROS/CTD	071201	1047	BO	65 20.06 N	30 59.82 W	GPS	968	960	965	14
06ME50/3	VEINS-1	286	01	ROS/CTD	071201	1111	EN	65 20.20 N	30 59.81 W	GPS	961			
06ME50/3	VEINS-1	287	01	ROS/CTD	071201	1203	BE	65 15.05 N	30 55.11 W	GPS	1240			
06ME50/3	VEINS-1	287	01	ROS/CTD	071201	1229	BO	65 15.05 N	30 55.13 W	GPS	1240	1228	1234	14
06ME50/3	VEINS-1	287	01	ROS/CTD	071201	1258	EN	65 15.00 N	30 55.16 W	GPS	1243			
06ME50/3	VEINS-1	288	01	ROS/CTD	071201	1346	BE	65 10.00 N	30 50.02 W	GPS	1512			
06ME50/3	VEINS-1	288	01	ROS/CTD	071201	1417	BO	65 09.94 N	30 49.78 W	GPS	1515	1506	1508	13
06ME50/3	VEINS-1	288	01	ROS/CTD	071201	1449	EN	65 09.87 N	30 49.48 W	GPS	1516			
06ME50/3	VEINS-1	289	01	ROS/CTD	071201	1535	BE	65 05.08 N	30 44.98 W	GPS	1759			
06ME50/3	VEINS-1	289	01	ROS/CTD	071201	1612	BO	65 05.03 N	30 45.34 W	GPS	1757	1739	1753	13
06ME50/3	VEINS-1	289	01	ROS/CTD	071201	1651	EN	65 04.81 N	30 45.44 W	GPS	1763			
06ME50/3	VEINS-1	290	01	ROS/CTD	071201	1736	BE	64 59.88 N	30 39.97 W	GPS	1894			
06ME50/3	VEINS-1	290	01	ROS/CTD	071201	1817	BO	64 59.76 N	30 40.79 W	GPS	1901	1882	1898	11
06ME50/3	VEINS-1	290	01	ROS/CTD	071201	1855	EN	64 59.74 N	30 41.19 W	GPS	1899			
06ME50/3	VEINS-1	291	01	ROS/CTD	071201	1940	BE	64 54.88 N	30 34.82 W	GPS	2035			
06ME50/3	VEINS-1	291	01	ROS/CTD	071201	2024	BO	64 54.69 N	30 35.03 W	GPS	2020	2041	2041	11
06ME50/3	VEINS-1	291	01	ROS/CTD	071201	2112	EN	64 54.46 N	30 35.02 W	GPS	2046			
06ME50/3	VEINS-1	292	01	ROS/CTD	071201	2156	BE	64 49.86 N	30 29.93 W	GPS	2143			
06ME50/3	VEINS-1	292	01	ROS/CTD	071201	2236	BO	64 49.87 N	30 30.05 W	GPS	2144	2127	2147	14
06ME50/3	VEINS-1	292	01	ROS/CTD	071201	2320	EN	64 49.79 N	30 30.29 W	GPS	2144			
06ME50/3	VEINS-1	293	01	ROS/CTD	071301	0010	BE	64 44.94 N	30 24.93 W	GPS	2230			
06ME50/3	VEINS-1	293	01	ROS/CTD	071301	0055	BO	64 44.94 N	30 24.79 W	GPS	2228	2236	2236	14
06ME50/3	VEINS-1	293	01	ROS/CTD	071301	0133	EN	64 45.00 N	30 24.66 W	GPS	2227			
06ME50/3	VEINS-1	294	01	ROS/CTD	071301	0221	BE	64 45.08 N	30 12.66 W	GPS	2208			
06ME50/3	VEINS-1	294	01	ROS/CTD	071301	0303	BO	64 44.95 N	30 12.53 W	GPS	2208	2186	2214	13
06ME50/3	VEINS-1	294	01	ROS/CTD	071301	0350	EN	64 44.99 N	30 12.64 W	GPS	2207			
06ME50/3	VEINS-1	295	01	ROS/CTD	071301	0438	BE	64 44.98 N	30 00.15 W	GPS	2184			
06ME50/3	VEINS-1	295	01	ROS/CTD	071301	0523	BO	64 44.98 N	30 00.07 W	GPS	2183	2162	2189	11
06ME50/3	VEINS-1	295	01	ROS/CTD	071301	0610	EN	64 45.00 N	30 00.09 W	GPS	2180			
06ME50/3	VEINS-1	296	01	ROS/CTD	071301	0704	BE	64 44.94 N	29 44.94 W	GPS	2100			
06ME50/3	VEINS-1	296	01	ROS/CTD	071301	0749	BO	64 45.01 N	29 45.09 W	GPS	2114	2107	2133	18

```
06ME50/3  VEINS-1  296    01   ROS/CTD  071301  0834   EN   64 45.09 N  29 45.10 W  GPS    2114

06ME50/3  VEINS-1  297    01   ROS/CTD  071301  0934   BE   64 44.98 N  29 30.13 W  GPS    1843
06ME50/3  VEINS-1  297    01   ROS/CTD  071301  1011   BO   64 45.00 N  29 30.36 W  GPS    1843    1830    1851   14
06ME50/3  VEINS-1  297    01   ROS/CTD  071301  1045   EN   64 45.08 N  29 30.52 W  GPS    1847

06ME50/3  VEINS-1  298    01   ROS/CTD  071301  1152   BE   64 44.96 N  29 14.89 W  GPS    1405
06ME50/3  VEINS-1  298    01   ROS/CTD  071301  1220   BO   64 45.00 N  29 15.03 W  GPS    1384    1416    1429   14
06ME50/3  VEINS-1  298    01   ROS/CTD  071301  1253   EN   64 45.03 N  29 15.02 W  GPS    1383

06ME50/3  VEINS-1  299    01   ROS/CTD  071301  1348   BE   64 44.93 N  29 00.13 W  GPS    1064
06ME50/3  VEINS-1  299    01   ROS/CTD  071301  1413   BO   64 44.76 N  29 00.10 W  GPS    1066    1079    1088   12
06ME50/3  VEINS-1  299    01   ROS/CTD  071301  1438   EN   64 44.65 N  29 00.19 W  GPS    1062

06ME50/3  VEINS-1  300    01   ROS/CTD  071301  1548   BE   64 44.93 N  28 40.09 W  GPS    1266
06ME50/3  VEINS-1  300    01   ROS/CTD  071301  1617   BO   64 44.84 N  28 40.18 W  GPS    1266    1249    1269   13
06ME50/3  VEINS-1  300    01   ROS/CTD  071301  1644   EN   64 44.81 N  28 40.08 W  GPS    1270

06ME50/3  VEINS-1  301    01   ROS/CTD  071301  1753   BE   64 44.99 N  28 19.97 W  GPS    1133
06ME50/3  VEINS-1  301    01   ROS/CTD  071301  1829   BO   64 45.02 N  28 20.08 W  GPS    1136    1115    1127   11
06ME50/3  VEINS-1  301    01   ROS/CTD  071301  1843   EN   64 45.01 N  28 19.96 W  GPS    1130

06ME50/3  VEINS-1  302    01   ROS/CTD  071301  1953   BE   64 45.02 N  27 59.97 W  GPS    1022
06ME50/3  VEINS-1  302    01   ROS/CTD  071301  2017   BO   64 45.02 N  28 00.00 W  GPS    1023    1010    1017   11
06ME50/3  VEINS-1  302    01   ROS/CTD  071301  2040   EN   64 45.03 N  27 59.93 W  GPS    1021

06ME50/3  VEINS-1  303    01   ROS/CTD  071301  2147   BE   64 44.95 N  27 39.87 W  GPS     800
06ME50/3  VEINS-1  303    01   ROS/CTD  071301  2206   BO   64 44.95 N  27 39.96 W  GPS     804     768     795   14
06ME50/3  VEINS-1  303    01   ROS/CTD  071301  2220   EN   64 44.98 N  27 39.88 W  GPS     799

06ME50/3  VEINS-1  304    01   ROS/CTD  071301  2330   BE   64 44.86 N  27 19.84 W  GPS     545
06ME50/3  VEINS-1  304    01   ROS/CTD  071301  2346   BO   64 44.76 N  27 19.95 W  GPS     546     539     540   14
06ME50/3  VEINS-1  304    01   ROS/CTD  071301  2356   EN   64 44.73 N  27 19.96 W  GPS     547

06ME50/3  VEINS-1  305    01   ROS/CTD  071401  0109   BE   64 44.93 N  27 00.24 W  GPS     283
06ME50/3  VEINS-1  305    01   ROS/CTD  071401  0120   BO   64 44.87 N  27 00.13 W  GPS     281     273     275   12
06ME50/3  VEINS-1  305    01   ROS/CTD  071401  0126   EN   64 44.88 N  27 00.04 W  GPS     281

06ME50/3  VEINS-1  306    01   ROS/CTD  071401  0231   BE   64 44.88 N  26 39.99 W  GPS     249
06ME50/3  VEINS-1  306    01   ROS/CTD  071401  0242   BO   64 44.76 N  26 40.13 W  GPS     249     240     240   14
06ME50/3  VEINS-1  306    01   ROS/CTD  071401  0248   EN   64 44.75 N  26 40.20 W  GPS     248
```

Table 2: List of the alkenone samples and associated filters for chlorophyll, particulate organic carbon, SPM and nutrient samples. Water source was a seawater pump or CTD bottles.

Number	Date	Source	Chlorophyll	POC	SPM	Nutrients
1	22.06.2001	Pump	X	x	X	X
2	22.06.2001	Pump	X	x	X	-
3	23.06.2001	Pump	X	x	x	-
4	23.06.2001	pump	X	x	x	-
5	23.06.2001	pump	X	x	x	-
6	24.05.2001	pump	X	x	x	-
7	24.05.2001	pump	X	x	x	-
8	24.05.2001	pump	X	x	x	x
9	24.05.2001	pump	-	-	-	-
10	24.05.2001	pump	X	x	x	-
11	25.05.2001	pump	X	x	x	-
12	25.05.2001	pump	X	x	x	-
13	25.05.2001	pump	-	-	-	-
14	25.05.2001	pump	X	x	x	-
15	25.05.2001	pump	X	x	x	-
16	26.06.2001	pump	X	x	x	-
17	26.06.2001	pump	X	x	x	-
18	26.06.2001	pump	-	-	-	-
19	27.06.2001	pump	X	x	x	x
20	27.06.2001	pump	X	x	x	-
21	28.06.2001	pump	X	x	x	-
22	28.06.2001	pump	-	-	-	-
23	29.06.2001	pump	X	x	x	x
24	29.06.2001	pump	-	-	-	-
25	30.06.2001	pump	X	x	x	x
26	30.06.2001	pump	-	-	-	-
27	30.06.2001	pump	-	-	-	-
28	01.07.2001	pump	X	x	x	x
29	01.07.2001	pump	-	-	-	-
30	01.07.2001	pump	X	x	x	-

Number	Date	Source	Chlorophyll	POC	SPM	Nutrients
31	01.07.2001	pump	X	x	x	x
32	02.07.2001	pump	-	-	-	-
33	02.07.2001	pump	X	x	x	-
34	02.07.2001	pump	-	-	-	-
35	03.07.2001	pump	X	x	x	x
36	03.07.2001	pump	-	-	-	-
37	03.07.2001	pump	X	x	x	-
38	04.04.2001	pump	-	-	-	-
39	04.04.2001	pump	X	x	x	x
40	04.04.2001	pump	-	-	-	-
41	05.07.2001	pump	X	x	x	x
42	05.07.2001	CTD	X	x	x	x
43	05.07.2001	CTD	X	x	x	x
44	05.07.2001	CTD	X	x	x	x
45	05.07.2001	pump	-	-	-	-
46	06.07.2001	pump	X	x	x	x
47	06.07.2001	pump	-	-	-	-
48	07.07.2001	pump	X	x	x	x
49	07.07.2001	CTD	X	x	x	x
50	07.07.2001	CTD	X	x	x	x
51	07.07.2001	CTD	x	x	x	x
52	07.07.2001	pump	-	-	-	-
53	08.07.2001	pump	x	x	x	x
54	08.07.2001	pump	-	-	-	-
55	08.07.2001	CTD	x	x	x	x
56	08.07.2001	CTD	x	x	x	x
57	08.07.2001	CTD	x	x	x	x
58	08.07.2001	pump	-	-	-	-
59	09.07.2001	pump	-	-	-	-
60	09.07.2001	pump	-	-	-	-
61	10.07.2001	pump	x	x	x	x
62	10.07.2001	pump	-	-	-	-
63	10.07.2001	pump	-	-	-	-
64	11.07.2001	pump	x	x	x	x
65	11.07.2001	pump	x	x	x	x
66	12.07.2001	CTD	x	x	x	x
67	12.07.2001	pump	-	-	-	-
68	zu AF66	pump	-	-	-	-
69	12.07.2001	pump	x	x	x	x
70	12.07.2001	pump	-	-	-	-
71	12.07.2001	pump	-	-	-	-
72	12.07.2001	pump	-	-	-	-
73	12.07.2001	pump	x	x	x	x
74	12.07.2001	pump	-	-	-	-
75	13.07.2001	pump	-	-	-	-
76	13.07.2001	pump	-	-	-	-
77	13.07.2001	pump	x	x	x	x
78	13.07.2001	pump	-	-	-	-
79	13.07.2001	pump	-	-	-	-
80	13.07.2001	pump	-	-	-	-
81	13.07.2001	pump	-	-	-	-
82	13.07.2001	pump	-	-	-	-

3.7 Concluding Remarks

Sincere thanks goes to the crew of the RV METEOR for highly professional assistance and to the authorities of Greenland and Island for the research permission.

METEOR-Berichte 02-2

North Atlantic 2001

Part 4

Cruise No. 50, Leg 4

16 July – 12 August 2001, Reykjavik – Hamburg

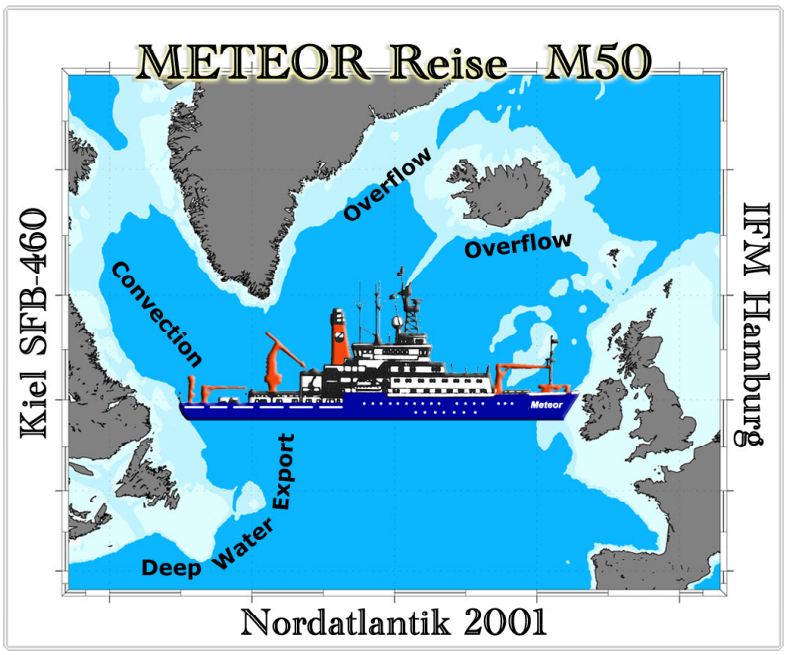

W. Zenk, J.D. Afghan, B. Bannert, M. Bleischwitz, K. Bulsiewicz, H. Cannaby, T. Csernok, U. Dombrowski, K. Friis, K. Fürhaupter, J. Greinert, J. Hauser, G. Karl, K. Lorbacher, H. Lüger, F. Malien, B. Marzeion, T. Müller, G. Niehus, M. Nielsen, W.-T. Ochsenhirt, J. Schafstall, R. Steinfeldt, T. Steinhoff

Editorial Assistance:

Frank Schmieder
Fachbereich Geowissenschaften, Universität Bremen

Leitstelle METEOR
Institut für Meereskunde der Universität Hamburg

2002

Table of Contents (M 50/4)

4.1 Participants of M50/4

1	Zenk, Walter, Dr.	Chief Scientist	IfMK
2	Afghan, Justine, D.	CO_2-Chemistry	IfMK/SIO
3	Bannert, Bernhard	UW Television	GEO/OKT
4	Bleischwitz, Marc	Tracer Physics	UBU
5	Bulsiewicz, Klaus	Tracer Physics	UBU
6	Cannaby, Heather	Coastal Oceanography Observer from Ireland	NUI
7	Csernok, Tiberiu	Marine Physics	IfMK
8	Dombrowsky, Uwe	Marine Physics	IfMK
9	Friis, Karsten, Dr.	CO_2-Chemistry	IfMK
10	Fürhaupter, Karin	Geochemistry	GEO/MaLi
11	Greinert, Jens, Dr.	Geochemistry	GEO
12	Hauser, Janko, Dr.	Oceanography	IfMK
13	Karl, Gerhard	Meteorology	DWD
14	Lorbacher, Katja, Dr.	Hydrography	BSH
15	Lüger, Heike	CO_2-Chemistry	IfMK
16	Malien, Frank	Marine Chemistry	IfMK
17	Marzeion, Benjamin	Marine Physics	IfMK
18	Müller, Thomas, Dr.	Marine Physics	IfMK
19	Niehus, Gerd	Marine Physics	IfMK
20	Nielsen, Martina	Marine Physics	IfMK
21	Ochsenhirt, Wolf-Thilo	Meteorology	DWD
22	Schafstall, Jens	Marine Physics	IfMK
23	Steinfeldt, Reiner	Tracer Physics	UBU
24	Steinhoff, Tobias	CO_2-Chemistry	IfMK

Participating Institutions

BSH Bundesamt für Seeschiffahrt und Hydrographie, Bernhard-Nocht-Str. 78, 20597 Hamburg – Germany, e-mail: koltermann@bsh.d400.de

DWD Deutscher Wetterdienst, Geschäftsfeld Schiffahrt, Bernhard-Nocht-Str. 76, 20359 Hamburg – Germany, e-mail: edmund.knuth@dwd.de

GEO Geomar Forschungszentrum für Marine Geowissenschaften, Wischhofstr. 1-3, 24148 Kiel – Germany, e-mail: rkeir@geomar.de

IfMK Institut für Meereskunde an der Universität Kiel, Düsternbrooker Weg 20, 24105 Kiel – Germany, e-mail: fschott@ifm.uni-kiel.de

MaLi MariLim, Büro für integrierte Meeres- und Küstenuntersuchungen, Wischhofstr. 1-3, Gebäude 11, 24148 Kiel – Germany, e-mail: tmeyer@marilim.de

NUI National University of Ireland, Newcastle Road, Galway - Republic of Ireland, e-mail: peter.bowyer@nuigalway.ie

OKT Oktopus, Gesellschaft für angewandte Wissenschaft, innovative Technologien und Service in der Meeresforschung mbH, Kieler Str. 51, 24594 Hohenwestedt – Germany, e-mail: schriever@biolab.com

SIO Scripps Institution of Oceanography, University of California, San Diego, 9599 Gilman Drive, La Jolla, CA 92093-0210 – USA, e-mail: jdafghan@pacbell.net

UBU Universität Bremen, Institut für Umweltphysik, Abt. Tracer-Ozeanographie, Bibliothekstraße, 28359 Bremen – Germany, e-mail: mrhein@physik.uni-bremen.de

4.2 Research Program

The fourth and last leg was again conducted by the *Institut für Meereskunde an der Universität Kiel*. SFB subproject A3 the revisited the Iceland Basin to continue measurements of the water mass variability in the subpolar gyre in the eastern basins of the North Atlantic. Research subjects are Labrador Sea Water penetrating from the west and Overflow Water entering from the northeast. Labrador Sea Water is generated annually by wintertime convection. Part of this water mass is advected eastward underneath the North Atlantic Current and over the Mid-Atlantic Ridge in the region of the Charlie Gibbs Fracture Zone at ~ 53°N. Its further penetration into the eastern basin is strongly influenced by mixing with Mediterranean Water, Subpolar Mode Water, and Overflow Water. Through these processes the low salinity tongue of Labrador Sea Water loses its prime characteristic properties while progressing northward into the Iceland Basin.

Water mass transformation processes also change the original properties of Iceland Scotland Overflow Water penetrating the Iceland Basin from the Norwegian Sea along the way southward. Then this partially mixed overflow water leaves the Iceland Basin for the Irminger Basin through gaps in the Reykjanes Ridge. Other diluted fractions follow the Mid-Atlantic Ridge as a deep western boundary current towards the Azores.

We aimed at making quantitative observations of transport fluctuations of the mentioned water masses. Such estimates are most relevant for the dynamics of the larger scale circulation of North Atlantic Deep Water. Modified Overflow Water, occasionally also called Charlie Gibbs Fracture Zone Water, is a main constituent of North Atlantic Deep Water. After leaving the subpolar gyre this water mass follows the continental slope of the Americas finally reaching the Antarctic Circumpolar Current. North Atlantic Deep Water is an integral limb of the global circulation and thus has a major impact on the global climate.

In cooperation with SFB subproject A1 moored equipment for monitoring the Denmark Strait Overflow Water had to be deployed during the beginning of the cruise. Like the Iceland Scotland Overflow, the Denmark Strait Overflow is another source for North Atlantic Deep Water.

Spreading paths of Labrador Sea and Overflow Waters in the Iceland Basin are subject to strong pulsations and shifts. These variations will be captured by eddy-resolving acoustically tracked RAFOS floats. Additional drifter launches support the newly initiated ARGO project.

The international ARGO Information Center has started to manage a sustained network of freely drifting ocean observing platforms. Their data are an essential part of future "ocean weather forecast". Within the next five years a fleet of 3000 deep sea drifters is planned. While drifting at 1500 m depth they cycle every ten days between 2000 m and the surface and transmit their data ashore. This information is broadcast via internet to operational oceanographers world wide within a day after the drifters reach the surfaces. The initial European contribution to ARGO is funded under GYROSCOPE by the European Commission in Brussels.

The return leg to Germany involved a repeat of WOCE section A2 between the Mid-Atlantic Ridge and the approaches of the European continent off Ireland. This work was conducted in co-operation with the Federal Maritime and Hydrographic Agency (BSH) in Hamburg. We completed the eastern part of A2 after its westward section had already been recorded during leg 1 in mid May 2001.

As part of the SFB project in Kiel the repeat hydrographic survey delivered chemical and tracer data with high vertical resolution and special consideration of pertinent CO_2 signals.

In addition, a group of geochemists from GEOMAR investigated methane sources. The latter were discovered during an earlier METEOR cruise at the Mid-Atlantic Ridge just south of Charlie Gibbs Fracture Zone. The group searched for the position and strength of a source in the region of the rift valley at 51°N and will determine the ratio of the stable carbon isotopes of the methane in its home laboratory in Kiel. In continuation of the geochemical water sampling the localizing of the sources was conducted by the Ocean Floor Observation System OFOS. It is hoped that the analysis phase will reveal the generation process (hydrodynamical smoker *versus* serpentination) in more detail.

4.3 Narrative of the Cruise

The majority of the scientific party arrived in Reykjavik on 16 July 2001. The day before the chief scientist Walter Zenk and a small group of technicians had taken over the ship from Jürgen Holfort and his team. Larger preparations of submersible gear were necessary for the sophisticated series of deep-sea moorings to be launched in Denmark Strait. The German ambassador to Iceland, Herr Dr Hendrik Dahne, visited METEOR twice while in port and arranged the visit of a team from the Icelandic National Television studios. As we were informed later by the embassy INT broadcast an extended report about the ship's mission on the day of departure.

On 17 July, 12:00, FS METEOR left Reykjavik and headed directly to the Denmark (or Greenland) Strait in good weather conditions and calm seas. On board were 24 scientists, technicians and students from eight institutions and companies plus two employees from the *Deutscher Wetterdienst (DWD).* Lists of personnel and contributing institutions are given in chapter 4.1, a list of stations in Table 4.3. After a transit of 27 hours we reached Sta. 307 on the afternoon of the next day. A cruise track chart is shown in Fig. 4.1.

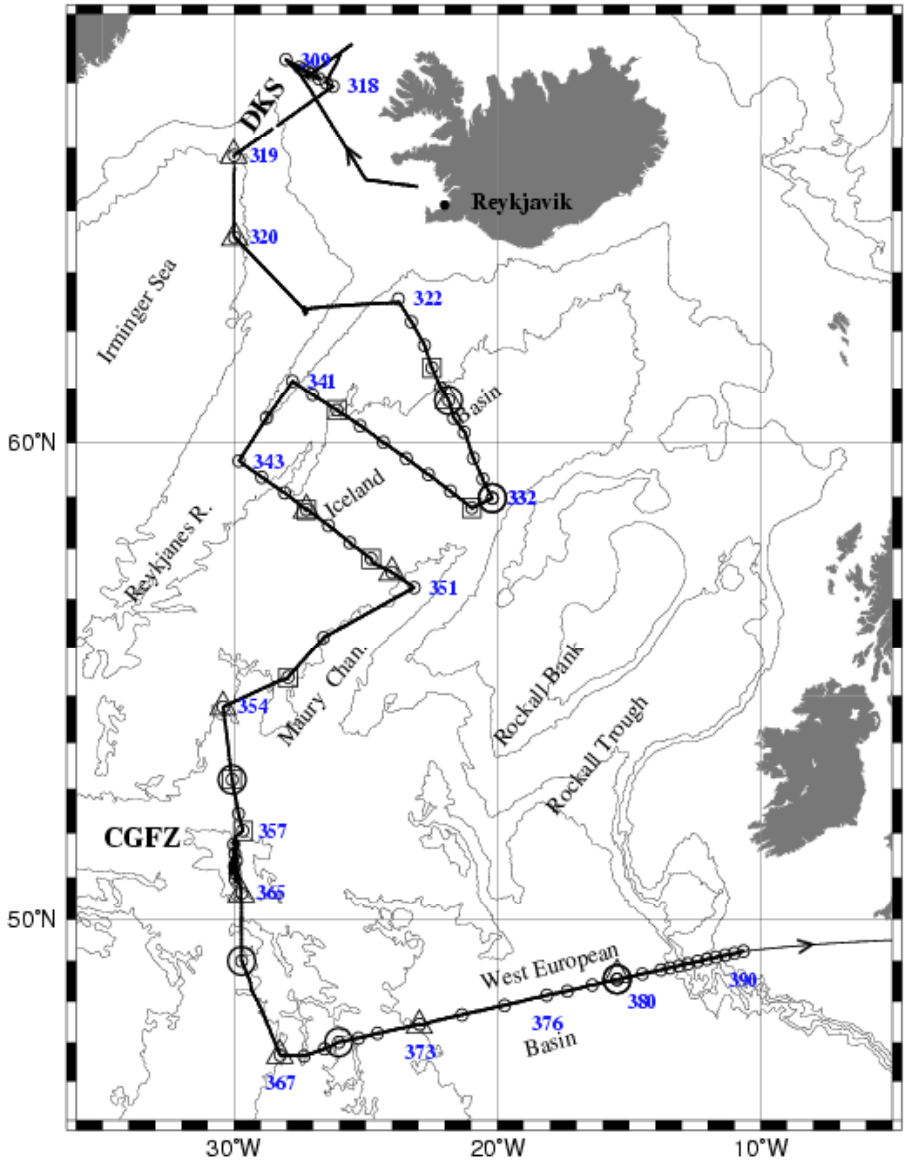

Fig. 4.1: Track chart METEOR cruise 50, leg 4. Legend: CTD stations (o), Thorium sites (O), APEX (triangles) & RAFOS launch sites (squares), Isobaths 1, 2, 3, 4 km.

We were pleased to find the site without ice and started primary functionality and handling trials with the **O**cean **F**loor **O**bservation **S**ystem (OFOS) and an acoustic release. This was a preparation exercise for the following deployment of the trawl resistant, remotely sensing current meter in the center of mooring gear V423_2 (SK). It comprises a hexagonal concrete shield housing and a modified **a**coustic **D**oppler **c**urrent **p**rofiling meter (ADCP). The device has been newly developed in Kiel to enable long-term observations of currents in bins of several hundred meters atop this near-bottom mooring. The test result was embarrassing because the auxiliary release for the joint deployment of the shielded ADCP and OFOS failed. It took several hours to reconstruct the OFOS frame for a spare release. Later in the evening we launched mooring V423 under permanent observation and documentation with the OFOS. We are sure to have it set on a flat bottom as confirmed by a short Hydrosweep survey prior to the station work.

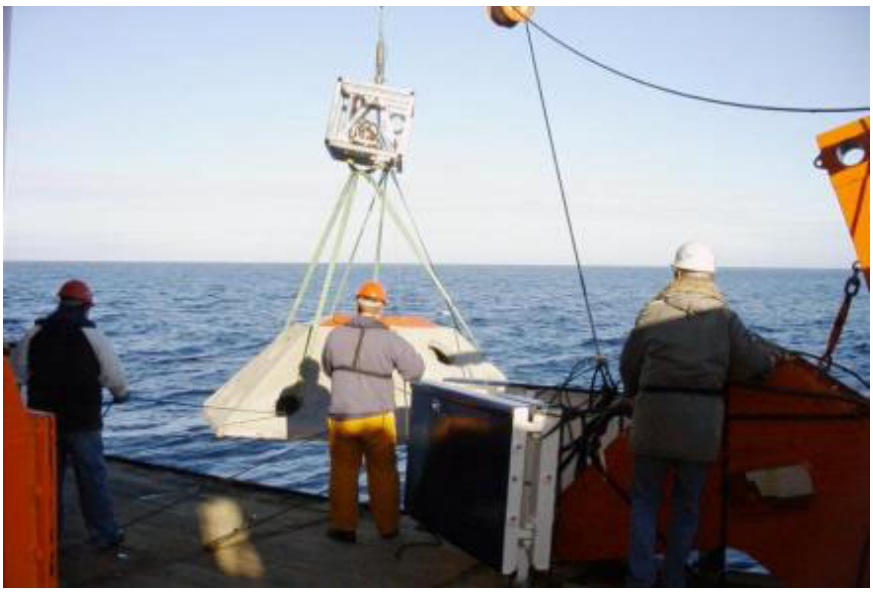

Fig 4.2: Deployment of shielded ADCP on Sta. 307.

Two additional moorings consisting of recording **P**ressure sensors and **I**nverted **E**cho **S**ounders (P/IES) were deployed on a section across the sill of Denmark Strait on Sta. 308 (Fig. 4.4) and 316. A final more conventional ADCP mooring without a shield was set on Sta. 315 in the deep out-flow channel where no fisheries activities are expected in contrast to the adjacent banks to both sites of the sill. All technical details on mooring work are summarized in Table 4.4. This table contains in its last row a remark on mooring V421_1 (TK). The latter was laid last summer by FS POSEIDON. While cautiously approaching the location on the afternoon of 19 July we realized that mooring TK apparently was situated just north of the closed ice margin as seen from our northern most position 66°34.5'N, 25°30.8'W. Hence, it was absolutely inaccessible for METEOR. Since more dense ice fields were drifting into the polar frontal region from the east (Fig 4.3), we were also unable to launch a prepared replacement mooring V421_2.

Without delay METEOR reversed its direction by 180°. We returned to the sill of Denmark Strait and supplemented the until then incomplete cross-sill CTD section (see inventory in Tab. 4.6) which includes lowered ADCP observations and regular water samples for analysis of numerous chemical substances including CFC, pCO_2, O_2 and nutrients. None of the ice barriers were forecast on the latest ices charts which we received from Greenland Command via IfM Kiel. After mid night of 19 July we had already settled the first phase of leg M50/4. The work load of the first phase was added relatively late in the planning stage of the expedition in due corse of the emergency case of FS POSEIDON. A multi-month long repair phase of this ship urged a complete revision of all IfM ship plans on which the field work of SFB 460 relies heavily.

Over the next few days the METEOR cruised southwestward into the Irminger Basin. There we launched two APEX drifters (see triangles in Fig 4.1). They are part of the internationally coordinated project ARGO. It aims at a future coverage of the world ocean with 3000 drifters for operational purposes. Our contribution at IfM Kiel is funded by the European Commission under GYROSCOPE. Initially METEOR carried ten APEX floats on board. Ten days later we received the first high quality up-cast CTD profiles from the first float cycles via satellite link from the CORIOLIS center in France.

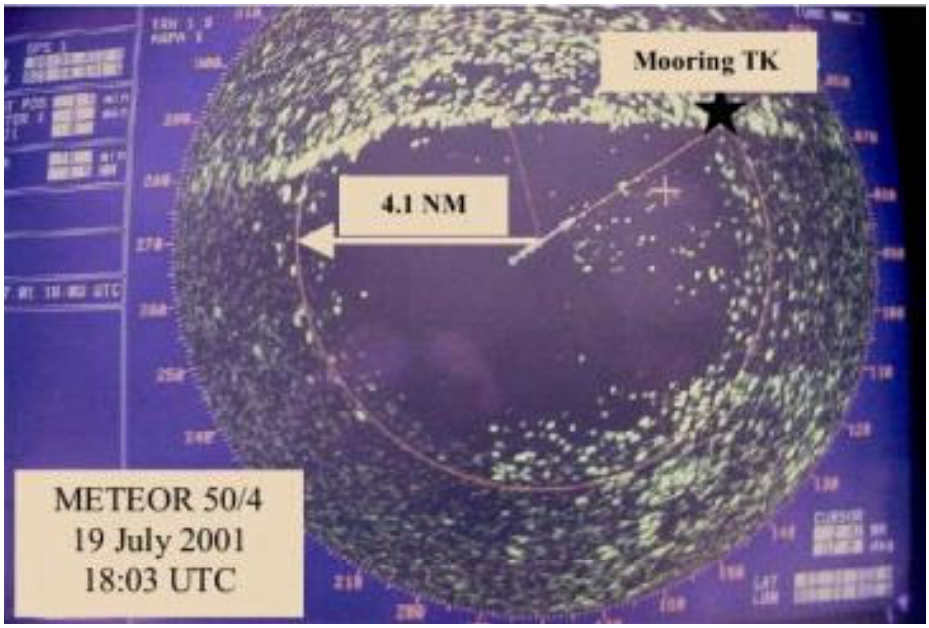

Fig. 4.3: Photograph of the icefield around mooring TK, taken from the radar screen of METEOR.

The second phase of M50/4 began on 21 July in the northern Iceland Basin after the vain search for a surfaced and transmitting RAFOS float on the Mid Atlantic Ridge (MAR) the day before. The sampling sites were targeted to cover CTD section **I** between the ridge and the more southeastward situated outskirts of Maury Channel, the deepest part of the Iceland Basin (Sta. 322-332). Station were located at near-by mooring positions which have been occupied since summer 2000. They were launched at strategic locations to monitor fluctuations of the Iceland Scotland Overflow entering the abyss of the Iceland Basin. Moorings along section **I** are planned for recovery in 2002.

Two more cross sections of the Iceland Basin were sampled (**A:** Sta. 333-341 and **B:** 343-351). In addition to APEX floats we launched eight eddy-resolving RAFOS floats in total (squares in Fig. 4.1). They are ballasted for the depth levels of the Labrador Sea Water (3 pieces) and the Overflow Water (5), respectively, and continue here and at more southerly situated positions earlier Lagrangian observations in the Iceland Basin (Davis & Zenk, 2001).

After repeat CTD/RO work north of Charlie Gibbs Fracture Zone (CGFZ) the remaining time was devoted to a detailed search for methane sources (Sta. 358-365) and to the subsequent repeat hydrographic section A2 of the **W**orld **O**cean **C**irculation **E**xperiment (WOCE). The core work of the GEOMAR group (see 4.4) on board concentrated on the meridionally oriented rift valley at 30°W south of the southern deep channel of the Fracture Zone. The expected occurrence of methane was confirmed at repeat and newly selected sampling sites. The 3-day sequence which included an intensive HYDROSWEEP survey of the valley, ended on 1 August with a 6 hour towed OFOS experiment showing excellent TV images from the eastern slope and the center of the rift valley.

After an additional station (366) for thorium samples METEOR reached the western end of the eastern half of WOCE A2. A series of full depth CTD stations with lowered ADCP obser-vations followed during the next five days. The 24 stations (367-390) were unevenly spaced with a more denser sampling on both sides of the crossed Western European Basin.

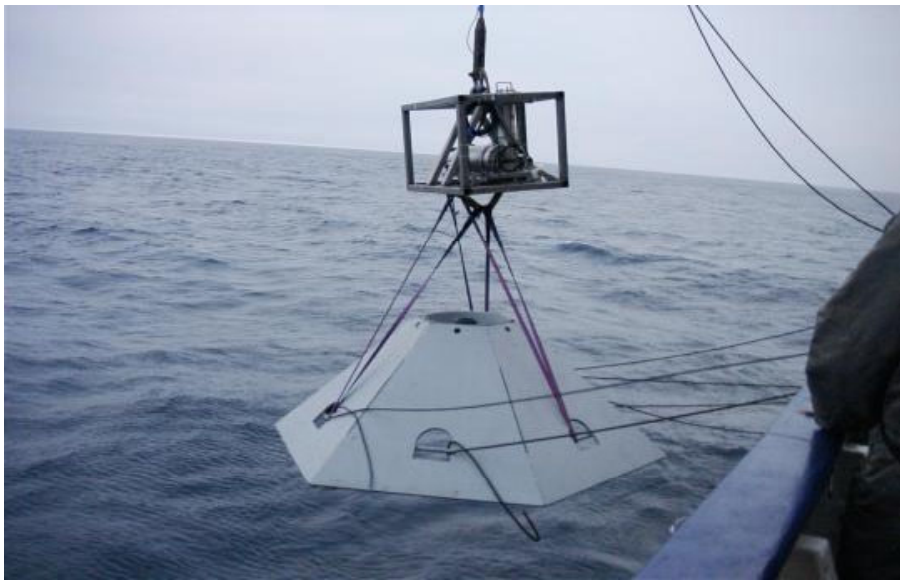

Fig. 4.4: Deployment of shielded echo sounder (P/IES06) by IfM Kiel in combination with video camera system OFOS (top) from GEOMAR.

The scientific work was terminated on 7 August at midnight and METEOR headed for her destination in Germany. We reached the shipyard in Rendsburg at noon on 12 August 2001.

4.4 Preliminary Results

4.4.1 Physical Oceanography

(J. Hauser, K. Lorbacher, F. Malien, T. J. Müller, W. Zenk)

Overview

The cruise covered a variety of different dynamic regimes of the northern North Atlantic. These can easily be distinguished by thermohaline records taken with the ship's thermosalinograph. In Fig. 4.5 we display sea surface temperature (T) and salinity (S). The diameters of the circles are proportional to the magnitudes of the parameters. We identify an arctic region that was covered at the beginning of the cruise. Temperatures dropped down to barely 0°C, the salinity decreased down to almost 31 at the ice edge. A subarctic region was crossed between the polar front in the Denmark Strait and the Reykjanes Ridge southwest of Iceland, marked by temperatures below and around 10°C. At ~52°N METEOR left the subpolar gyre and entered a domain with significantly warmer waters of mainly subtropical origin. The T/S data suggest a northward spreading of the North Atlantic Current focused and confined to the North by the Charlie Gibbs Fracture Zone. In the following paragraphs we present selected examples for the different oceanic regions as manifested in the hydrographic data. All profiles were collected by a Seabird CTD and 22 bottle rosette sampler. The CTD measurements were quality controlled onboard but not yet finally calibrated before arriving in Rendsburg.

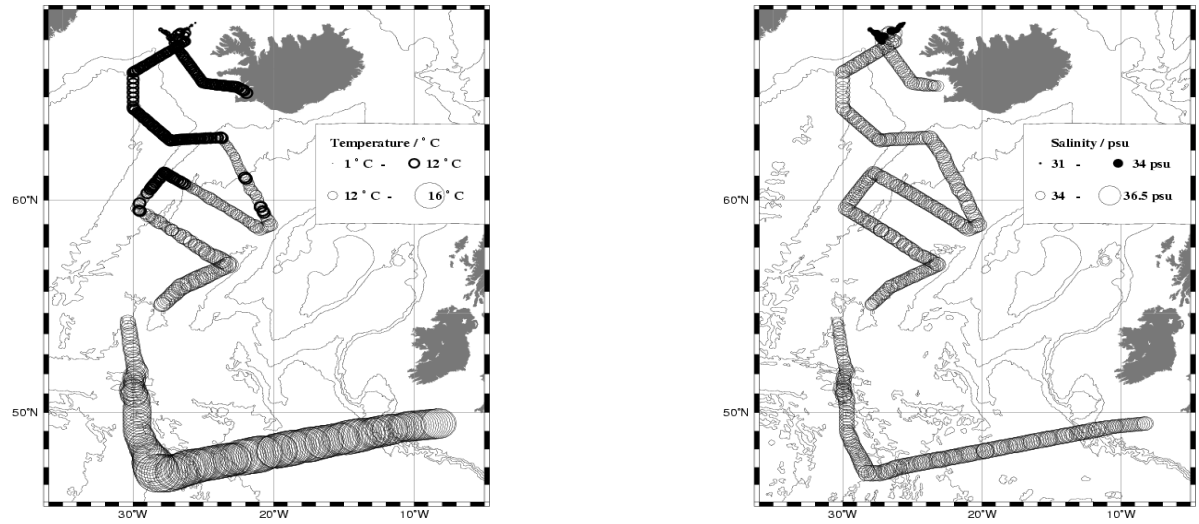

Fig. 4.5: Sea surface temperature (left) and salinity (right) from the ship mounted thermosalinograph. The diameter of the circles indicate magnitudes of the parameters.

CTD calibration and data processing

Temperature and pressure sensors

The CTD used on all stations on the cruise was a SeaBird 911 plus (internal IFM Kiel code SBE1) in conjunction with a SeaBird carousel. Due to external reasons, it was decided late in the planning phase for M50 that this instrument had to be the main one. Therefore, it had no fresh pre-cruise calibration for temperature and pressure sensors. However, during all stations, the pressure sensor read about –0.3 dbar (+/- 0.2 dbar) on deck immediately after a cast, indicating little drift, if any, in this sensor's calibration. As for the temperature sensor, experience with this type of sensor shows that it is stable also. Nevertheless, a post-cruise calibration of both sensors will be performed according to WOCE standards to allow for any significant corrections.

Salinity

The procedure was similar to that described by Müller (1999). Samples with rosette bottles were taken 20 m above the bottom, every 1000 dbar pressure levels and at 10 m depth. A Guildline AUTOSAL 8400B (internal IFMK code AS7) was standardized using standard seawater batch P137 (K15=0.99995, labelled S=34.998, ampoules filled December 1999). A drift of the salinomer's calibration of order 0.005 was confirmed independently by substandards taken from the deep sea and eliminated. This drift was not due to lab temperature which was recorded at 0.5 h intervals and was stable to within 0.2 K.

The resulting correction for the conductivity cell's output over leg M50/4 is linear in conductivity and time (cast). Recalculating salinity, the standard deviation of the residual SDIF is 0.0022 in salinity with most of the noise being associated with the 1000 dbar level where stratification is strong (cf. Fig. 4.6). In the deep sea of the eastern part of the WOCE section A2 the calibrated data match well the θ/S relation claimed to be stable by Saunders (1986) (Fig. 4.7).

As a secondary result note, that the ship-board thermosalinograph needs a salinity correction of 0.06 with standard deviation of 0.2 . No drift was obeserved here.

Processing

The CTD data were processed with the following steps (MÜLLER, 1999): range control; despiking; monotonizing with respect to inceasing pressure; minimum lowering velocity 0.2 dbar/s; median filter over 0.5 dbar intervals; interpolation to 0.5 dbar; calibration and recalculation of salinity; low pass cosine filter over 2.5 dbar; interpolation to 2 dbar. Later slight corrections for temperature and pressure sensor outputs will not affect salinity.

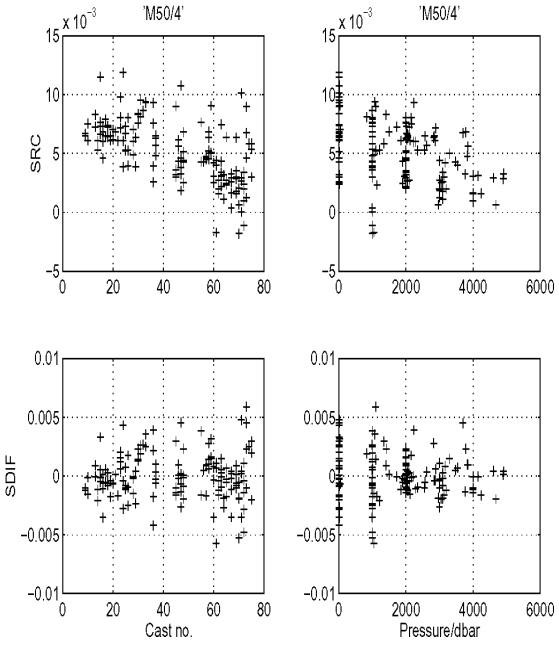

Fig. 4.6: Salinity correction for all CTD casts on cruise M50/4. Individual corrections SRC (upper panel) and residuals SDIF (lower panel) after calibration as functions of time (left: cast no.) and pressure (right). The standard deviation of the SDIF is 0.0022 in salinity.

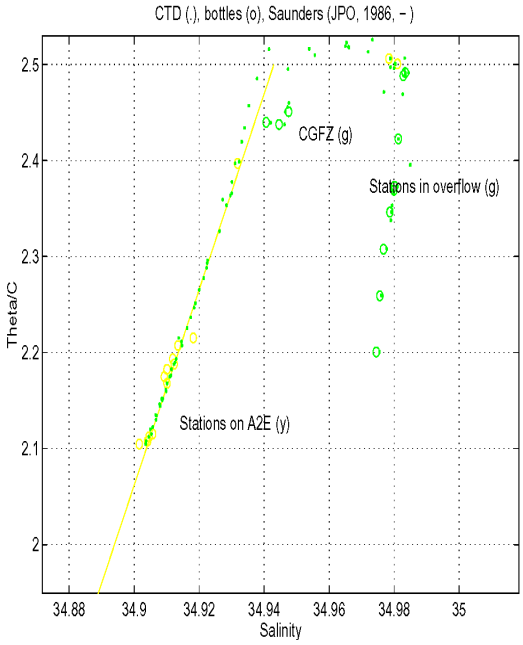

Fig. 4.7: Deep sea potential temperature/ salinity relation for all rosette samples (o) and CTD values (dots) at bottle depths. Three regimes appear clearly: Iceland Scotland overflow (ISOW) along the Reykjanes Ridge; CGFZ stations; eastern part of WOCE-section A2 stations further south.

Regional Hydrography

Arctic/Subartic Region: Denmark Strait

Although the main work in the Denmark Strait focused on the deployment and recovery of the moorings listed in Table 4.4, a complete hydrographic section across the Strait was recorded. Fig. 4.8 shows a section of salinity, temperature and density. It depicts the water mass characteristics of the typical current regime in the Strait with an almost vertical separation between the warm, saline water of the Irminger Current to the south-east and the colder water masses from the Greenland Sea to the north-western part of the Strait. The depth-range between 50 m and 150 m defines the East Greenland current, marked by an intermediate minimum in temperature and salinity compared to the centre of the Strait. Below 360 m there is a strong signal of the Denmark Strait Overflow water (DSOW), with higher salinity and temperatures below 0°C. The abrupt decline of the outflow bottom signal at the western end of the section can probably be an artefact of the increasing station-spacing and the resulting uncertainty in the

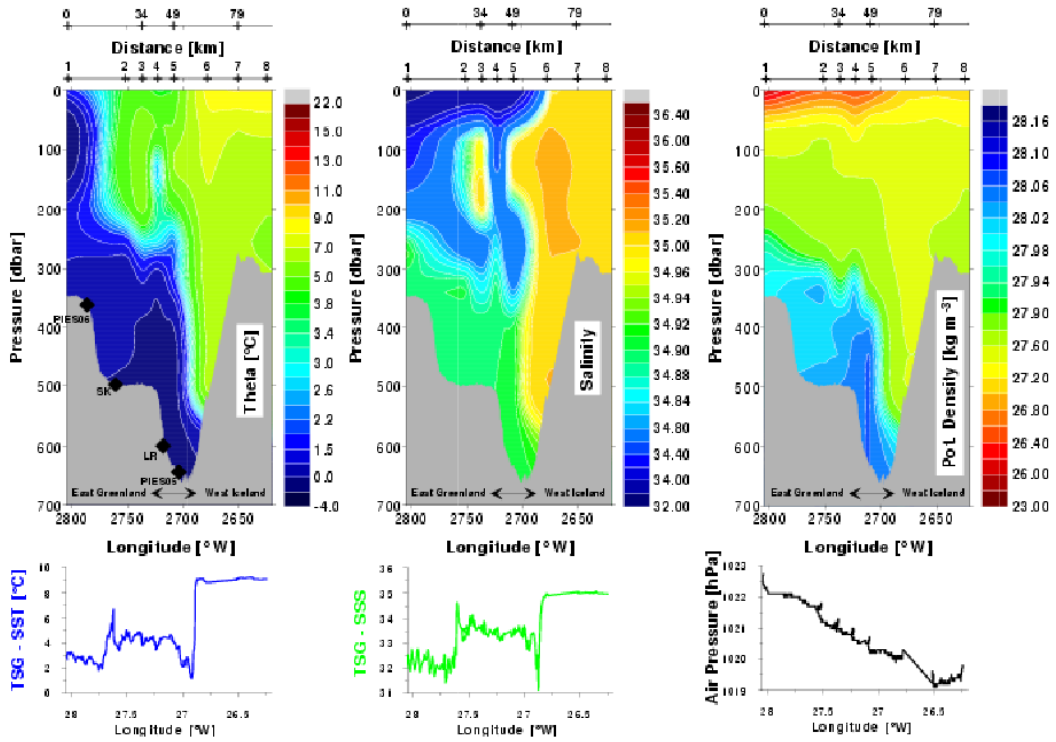

Fig. 4.8: Distribution of potential temperature, salinity and density across the Denmark Strait. In the left picture the longitudinal positions of the moorings deployed in the Strait are marked on the bottom topography, indicating that the outflow of DSOW may be well represented by the moored current meters.

interpolation. In the centre of the Strait the section runs through an eddy structure, which has a thickness of 125 m. This structure should also be visible in the measurements of the vessel mounted **A**coustic **D**oppler **C**urrent **P**rofile (ADCP) covering a depth range from 50 m to 700 m.

Subpolar Region: Iceland Basin

The main scope of the observations in the Iceland Basin was the identification of the pathway of Iceland-Scotland overflow water (ISOW). This water mass spreads along the south-eastern slope of the Reykjanes Ridge. We carried out three sections normal to the proposed pathway of the outflow. The sections are labeled from north to south as **I**, **A** and **B**. Specifically, section **I** covers a mooring line, which carries several recording devices at depth near to the bottom. The station-spacing varied from 30 km to 70 km, with a reduced spacing near the centre of the sections. In all three sections ISOW can clearly be identified by a relatively thin bottom layer, with several local minima, mainly in the potential temperature distribution (Fig.4.9).

The thickness of the bottom layer derived from the conservative tracer data varies between 150 m and 400 m, where the salinity shows a thickness of 150 m. In addition, the salinity distribution exhibits a clear separation of the outflow from the deep background field of the Iceland Basin, characterized by a lower salinity (Fig.4.10). The slope of the 27.99 neutral density surface marks the overflow by a lateral distribution in downward direction. This is also reflected in the disappearence of the 28.07 neutral density surface in the depth-range of 1500 m to 2500 m. Both, the disappearance of the high core densities and the corresponding broadening of the outflow, indicate the presence of active entrainment, enhanced over steep topography, whereas at greater depth the outflow remains a persistent signal on all three sections.

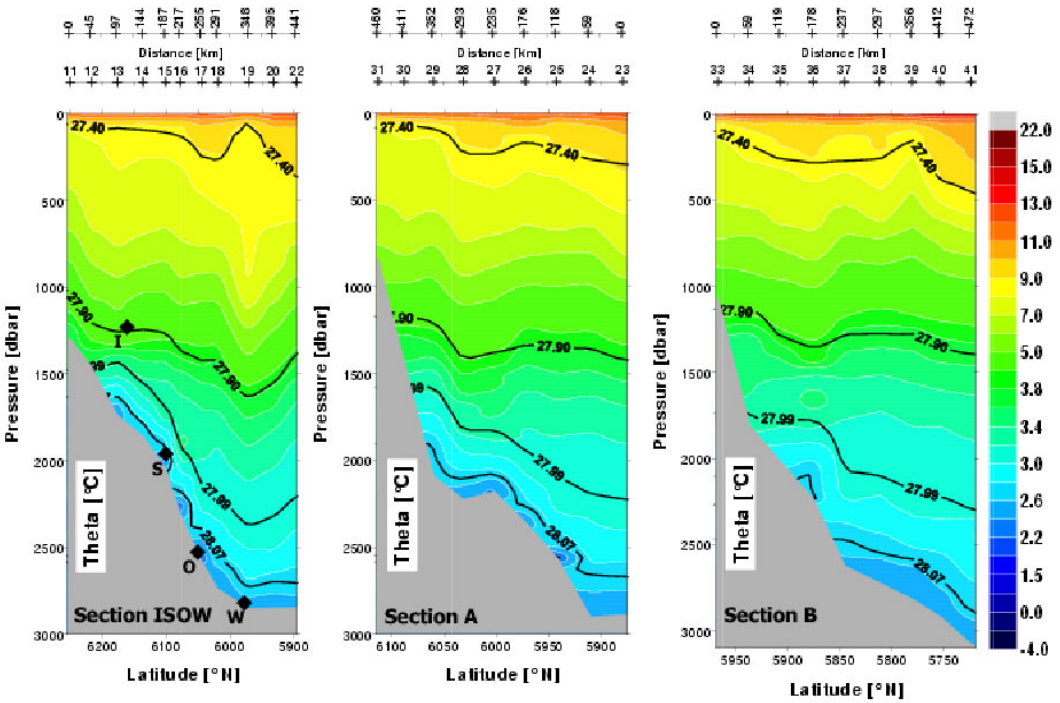

Fig. 4.9: Potential temperature sections in the Iceland Basin. In the left picture the locations of the moorings labeled as I, S, O, and W, are marked at the bottom. These four moorings were launched in spring 2001 and shall be recovered in summer 2002.

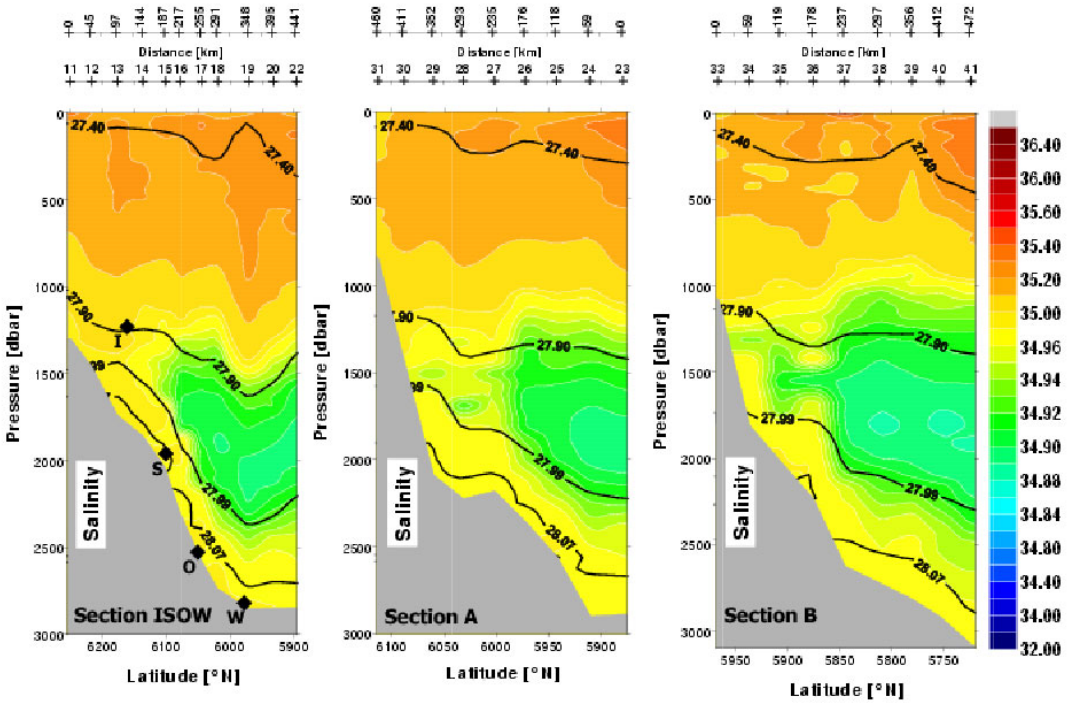

Fig. 4.10: Salinity sections I, A and B in the Iceland Basin.

The comparison of the tracer data of the three sections and the instantaneous velocity data, measured by a lowered ADCP (150 kHz), exhibits for the bottom layer a good agreement between the flow distribution and current direction (Fig.4.11). In general, the velocity data show a more barotropic, i.e. banded structure with local *maxima* at the bottom along the steep part of the topography. These are in good correspondence with the local *minima* in temperature. The maximum current velocity is around 30 cm/s and is directed south-westward. The velocity data were not detided, which accounts for an uncertainty in this region of up to 8 cm/s.

Section **I** runs through an intense eddy structure, with core velocities of up to 40 cm/s. The centre of the eddy is at 750 m. A corresponding local minimum appears in the oxygen data, indicating water masses inside the eddy from a different oceanic region. Fig. 4.12 shows the quasi-synoptic flow field at the bottom of the Iceland Basin. The vectors represent the mean of the lower 100 m of the LADCP profiles. The observed flow field is in good agreement with the current view of the spreading of the outflow along the Reykjanes Ridge. At section I there are high velocities in a relatively narrow region. Lower velocities were observed over a broader region further downstream of the outflow. The alignment of the vectors suggest a local recirculation at the south-eastern end of section **I**. However, as mentioned above, there is an intense eddy perturbation with different water masses at lower levels. This suggests an enhanced recirculation in the bottom layers by a barotropic signal of the eddy. It should be noted that the measurements of the downward looking LADCP do not cover the entire water column. The reflection of the acoustic pulses from the bottom prohibit the sampling in a column 50 m above the bottom. If an increasing velocity signal towards the bottom is detected, it can be assumed that the velocity underestimates the absolute velocity maximum of the bottom trapped outflow current.

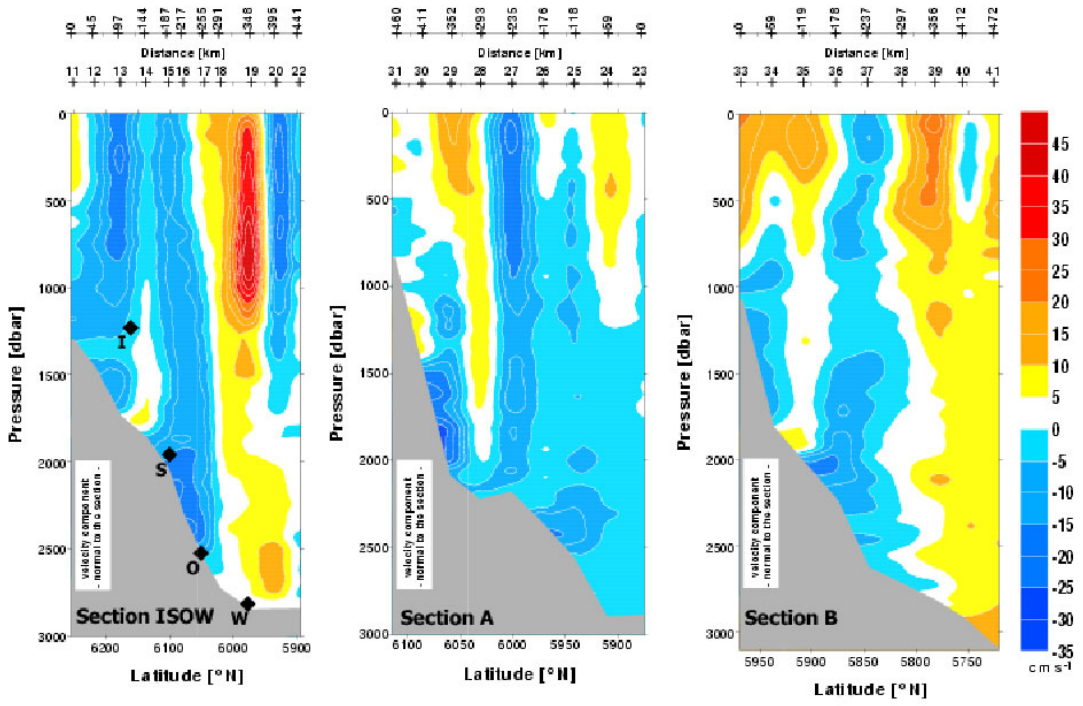

Fig 4.11: Horizontal velocity normal to the sections I, A and B measured by a lowered ADCP (data without compensation of a tidal signal).

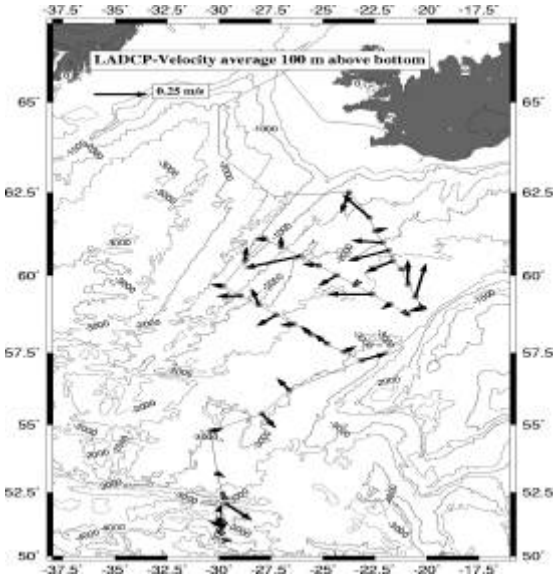

Fig 4.12: Horizontal map of the LADCP-bottom velocities in the Iceland Basin. The vectors define the mean velocity of the hundred metres above the bottom for each profile.

Subtropical Outskirts: Western European Basin

The fourth leg closed with the completion of the eastern part of the WOCE-section A2. This quasi-zonal section covers the North Atlantic from the Newfoundland Banks to the exit of the English Channel. The mean latitude of this section is 45°N. The western part of this section was occupied during leg 1 of this cruise. These two parts together represent the tenth realisation of the section A2 of the World Ocean Circulation Experiment (Fig.4.13 – 4.15). The eastern part of the WOCE/A2-section started at the western slope of the Mid-Atlantic Ridge (MAR). The station-spacing is reduced over both slopes of the Mid-Atlantic Ridge as well as in the eastern boundary current regime. The following water masses are defined by intervals of neutral density surfaces (cf. Lorbacher, 2000).

- SPMW Subpolar Mode Water
- MW Mediterranean Water
- LSW Labrador Sea Water
- ISOW Iceland Scotland Overflow Water
- NADW North Atlantic Deep Water
- AABW Antarctic Bottom Water

The SPMW shows both a negative zonal temperature and salinity gradient. The low-saline and high-oxygen tongue of LSW entering the Iceland Basin through the Charlie-Gibbs Fracture Zone (CGFZ) is best developed around 18°W at a depth of 2000 m. It is absent at the western slope of the MAR. The MW appears at two different depths. The salinity maximum is found at a depth of 1000 m. The lower, though less pronounced of high-saline water, spreads from the eastern boundary into the Iceland Basin within a depths range from 2500 m to 3000 m. This is the expected deep diffusive signal of MW at this latitude. We also found an additional unexpected strong signal of high salinity and higher temperatures directly along the European continental shelf at depths between 700 m and 900 m. The influence of possibly recirculated ISOW can be noticed at the eastern slope of the MAR by an increase in temperature, salinity and oxygen at a depth between 3000 m down to 3800 m.

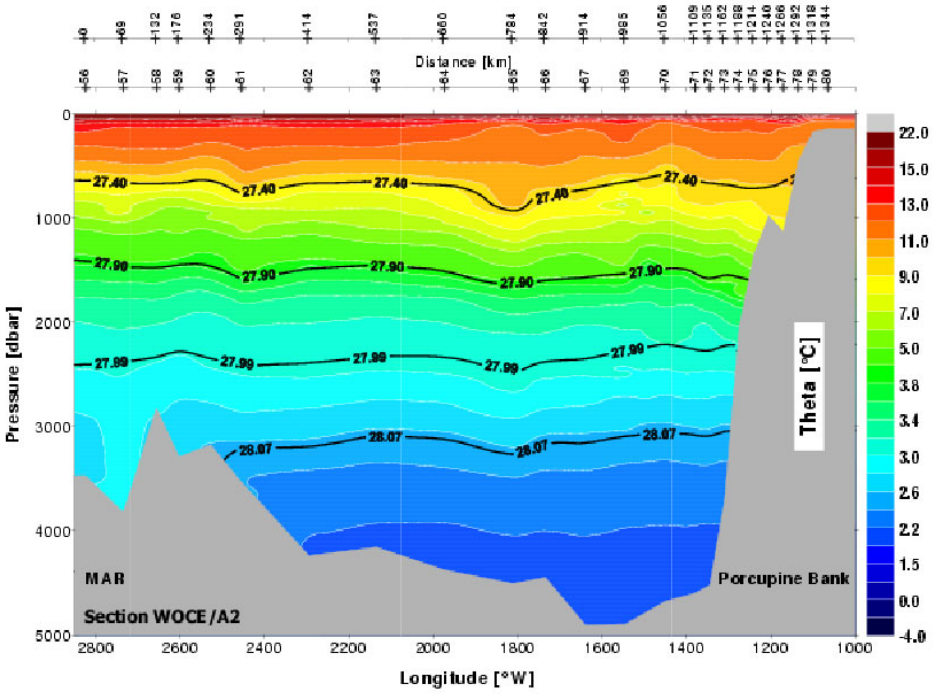

Fig. 4.13: Potential temperature of the eastern part of the WOCE-section A2.

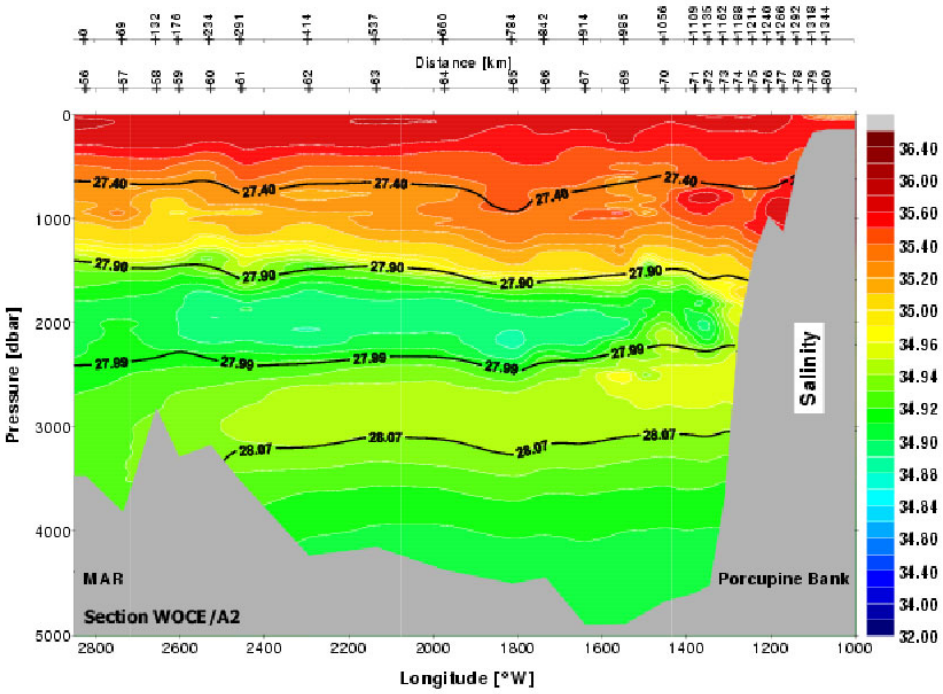

Fig. 4.14: Salinity of the eastern part of the WOCE-section A2.

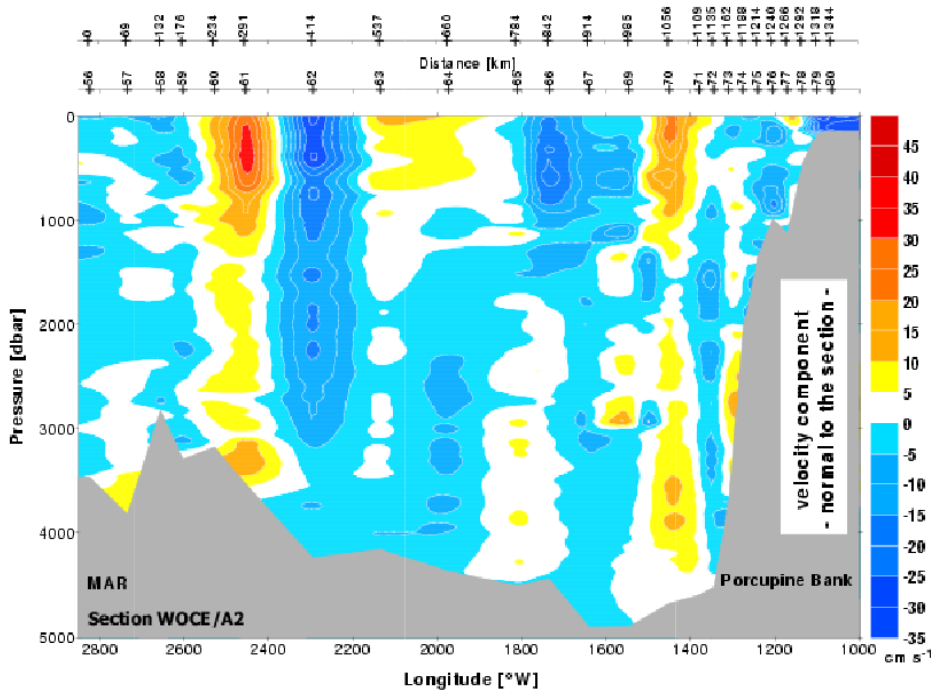

Fig. 4.15: Distribution of meridional velocity from the LADCP measurements for the eastern part of WOCE-section A2.

The instantaneous meridional velocity distribution observed with the LADCP across A2 (Fig. 4.15) shows various eddy structures in the upper water column. The velocities in the centre of the basin are negligible. There are velocity signals directly at the topography corresponding to the northward spreading deep MW at 3000 m at the eastern end of the section. Unexpectedly we also found a northward current at the depth range of ISOW on the eastern side of the MAR, which is in contradiction to the assumed southward spreading of the ISOW along the topography. Nevertheless, it should be noted that the velocities in general are rather low and, as already noted above, the velocity data do not incorporate a tidal correction. The latter may even lead to a reversal of the current direction is this area.

4.4.2 Tracer Oceanography

(M. Bleischwitz, K. Bulsiewicz, R. Steinfeldt)

Material and Methods

During legs 3 and 4 water samples have been collected from 10 liter-NISKIN bottles for the analysis of the **c**hloro**f**luoro**c**arbons (CFC-11 and CFC-12). Additionally on leg 4 Helium samples have been collected into copper tubes. These samples will be measured later with a specially designed noble gas mass spectrometer at the laboratory in Bremen. Measurements of the CFC-concentrations in the water samples have been performed on board using a gas chromatographic system with capillary column and Electron Capture Detector (ECD).

CFC sampling has been performed on 132 stations, and helium samples where taken on 9 stations (Fig. 4.16). A total of 2048 CFC data and 96 helium data have been obtained.

A detector drift affected the accuracy and precison for the CFC-11 data. The blank for CFC-11 and CFC-12 was negligable. Accuracy was checked by analysing 75 water samples at least twice. It was found to be 0.3% for CFC-12 and 0.6% for CFC-11. CFC-contamination of the Niskin bottles was checked at a test station in the deep eastern basin, where all bottles were tripped at the same depth. This water is 'old', exhibiting low CFC-concentrations. All measurements on this station show nearly the same data, which indicates clean Niskin bottles. The CFC concentration of the gas standard used to calibrate the water samples are not reported on the SIO93 scale. This standard gas will be recalibrated at the laboratory in Bremen.

The anthropogenic compounds CFC-11 and CFC-12 have been released into the environment since several decades. The atmospheric release of CFC-11 and CFC-12 started in the 1930s and showed initially exponential increase, since the 1980s the increase is slowing down. Because of their transient nature the CFCs provide time information on the ventilation of water masses.

Helium samples were taken near the Mid-Atlantic Ridge, were sources of methan had been detected. The data will show in how far ^{3}He is also released by these sources and if a correlation between anomalies of methane and ^{3}He exists.

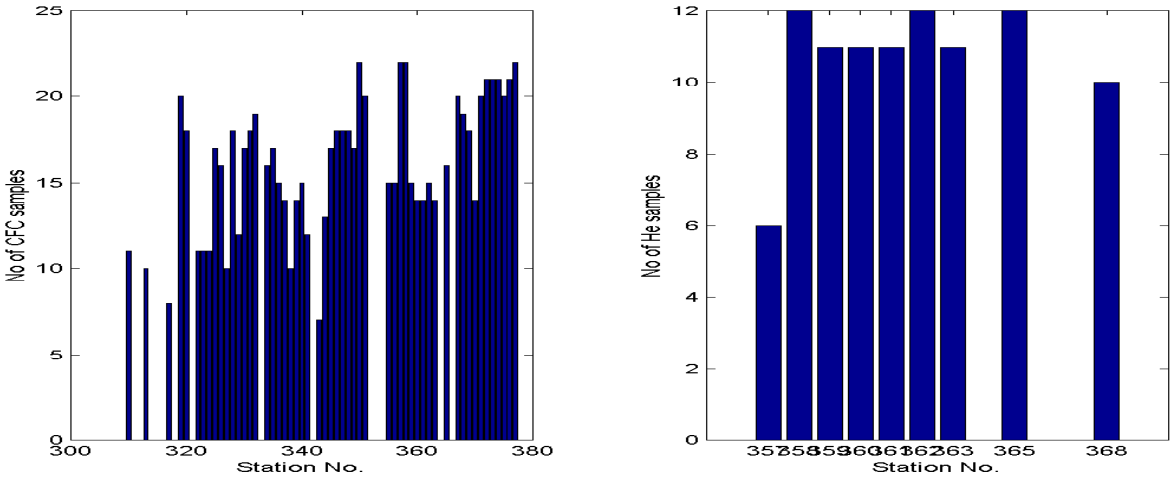

Fig 4.16: Number of tracer samples taken during M 50/4.

Preliminary Results

The tracer investigation along the East Greenland continental slope south of Denmark Strait dur ing leg 3 continues earlier investigations in 1997 and 1999. The main purpose of the sampling was to study the circulation and to analyze the variability of the composition of the Denmark Strait Overflow Water (DSOW).

Figure 4.17 shows the concentration of CFC-12 on the three sections throughout the Iceland Basin **(I**, **A** and **B** from north to south). Both deep water masses (ISOW and LSW) can be found on all three sections. The ISOW is confined to a terrain following boundary layer and shows maxima of CFC-concentration and salinity. It does not reach the deepest part of the Iceland Basin, but spreads along the Reykjanes Ridge. At the southernmost section B the CFC-

concentrations near the bottom are considerable lower (0.1 - 0.2 pmol/kg), supporting the finding that a great part of ISOW leaves the Iceland Basin through gaps in the Reykjanes Ridge into the Western Atlantic. The LSW (density range $27.74<\sigma_0<27.8$ kg/m³ indicated by isopycnals) is characterized by a salinity minimum (dashed line). Whereas temperature and salinity show a linear transition between the ISOW and the LSW, the CFC-data show that these two newly ventilated water masses are separated by older deep water.

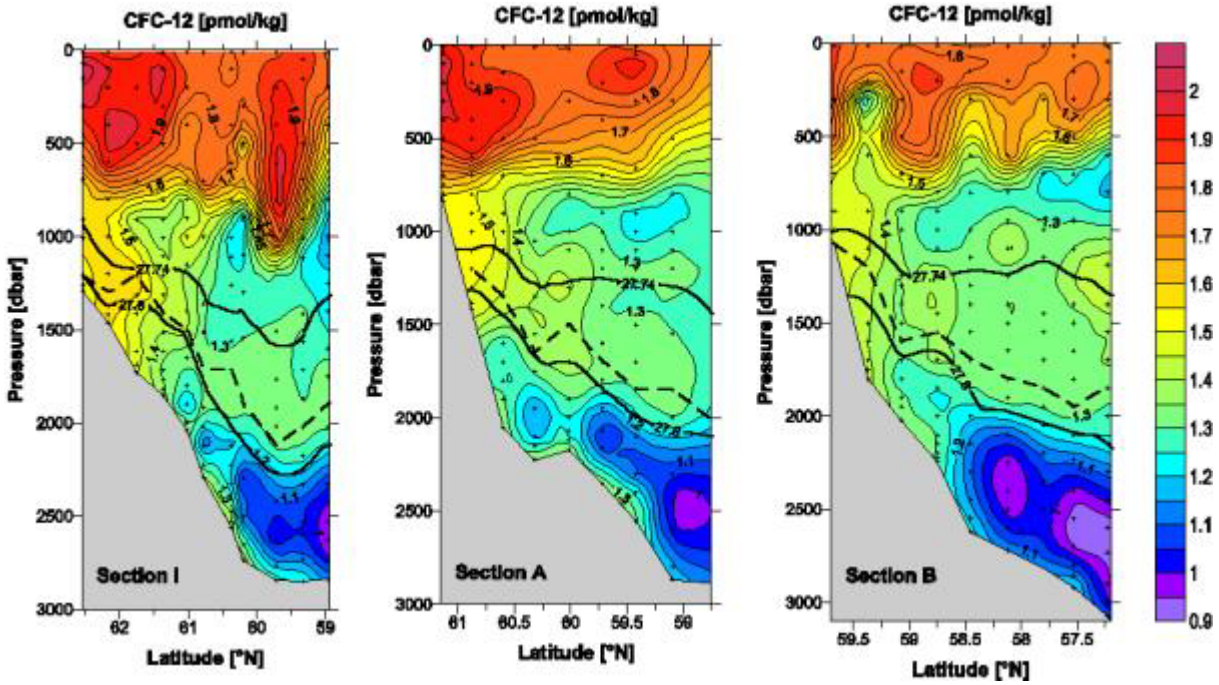

Fig. 4.17: CFC-12 distribution on sections I, A and B in the Iceland Basin.

LSW enters the Eastern Atlantic near the Charlie Gibbs Fracture Zone (CGFZ) and spreads in eastern and northern direction. The northern path can be traced from the comparison of CGFC-concentrations in the LSW-layer at the stations located near the GFZ and on the three sections inside the Iceland Basin (Figure 4.18). The concentrations are highest at the GFZ and decrease weakly from section **B** to sections **A** and **I**, indicating a short spreading time of LSW from the GFZ to the north of the Iceland Basin of only a few years. Not only the CFC-concentration inside the LSW, but also its volume decreases towards the north. Whereas at section **B** a marked core of LSW is present, at sections **A** and **I** a greater amount of more saline water influenced by ISOW can be found in the density range between $27.74<\sigma_0<27.8$ kg/m³.

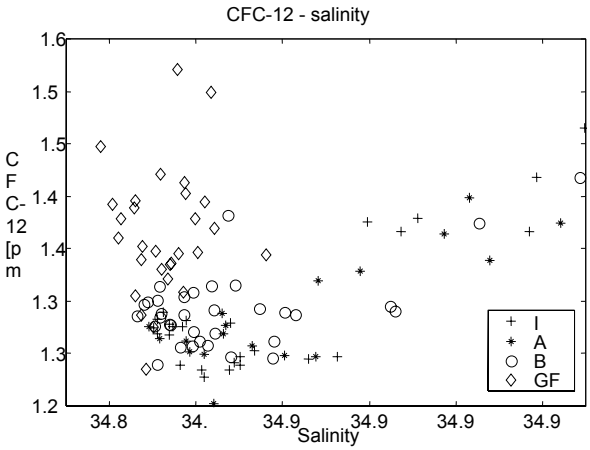

Fig. 4.18: CFC-12 vs salinity correlation in the LSW- density range 27.74<σ_θ <27.8 kg/m³ for different sets of stations. I, A and B: M50/4-sections in the Iceland Basin; GF: M50/4-stations near the Charlie Gibbs Fracture Zone.

4.4.3 Marine Chemistry

(K. Friis, J.D. Afghan, H. Lueger, F. Malien, T. Steinhoff)

On leg 4 the CO_2 group from Kiel (SFB 460, subprogram A5) continued the research program that started on leg 1 and is described above. The same analytical equipment was used and methodologies were applied.

C_T, A_T and pH Quality Control

The quality control of the various parameters of the carbonate system were performed by help of certified reference materials (CRM) and duplicate analysis that were taken approximately every tenth to twentieth sample. These standards are used to determine the accuracy and performance of the systems. The duplicates show the precision of the analytical instrument. For the pH quality control the CRM measurements allows assessment of the long term precision during the cruise as far, as a specific CRM batch is used for the whole cruise. An overview of the quality controls is shown in Tab. 4.1 and in Fig. 4.19 A-F. All controls show a very good agreement with the achievable accuracy and precision estimates according to Millero et al. (1993) (see also leg 1).

Tab. 4.1: M50/4 key data of the discrete C_T, A_T, pH analyses. The CRM measurements give an accuracy estimate, the duplicate measurements a precision estimate.

	C_T	A_T	pH_T $^{21\,°C}$
CRM: Analyzed bottles	50	80	37
Batches used	(52, 48, 36, 35)	(52, 35)	(52)
Mean deviation from certified CRM value	- 0.37 µmol/kg	0.34 µmol/kg	not certified for pH - 0.0023 compared to M50/1
(standard deviation)	(± 1.14 µmol/kg)	(± 2.41 µmol/kg)	(± 0.0023)
Duplicates: Analyzed pairs	81	82	83
Mean deviation from duplicate value	1.1 µmol/kg	2.9 µmol/kg	0.0009
(standard deviation)	(± 1.0 µmol/kg)	(± 2.6 µmol/kg)	(± 0.0009)

Fig. 4.19 shows the analytical C_T and A_T performance during leg 4. A mean deviation of the CRM measurements from the certified value is - 0.37 µmol/kg (C_T) and + 0.34 µmol/kg (A_T). The extreme outliers (station 345 and 351) in the A_T range chart (Fig. 4.19 C) are probably due to smaller instabilities of the emf at the reference electrode. Although the (A_T-) CRM measurements show no obvious deviations from the mean, the A_T profiles of both stations are not that smooth as can be expected from the C_T and pH_T measurements.

The quality control of the spectrophotometric pH determination shows a precision of about ± 0.001 pH units (Fig. 4.19 E and F and Tab. 4.1) and a slightly higher long term precision based on the CRM measurements of batch 52. The mean CRM pH is 0.0023 units lower than the mean pH on leg 1, but it is although comparable to the CRM pH in the end of leg 1. This holds on the speculation of an aged platinum resistance temperature probe, that has been mentioned above and will be controlled later. Nevertheless an uncertainty of ± 0.002 pH units corresponds with a C_T and A_T uncertainty of about ± 1 µmol/kg and seems to be acceptable with respect these parameters.

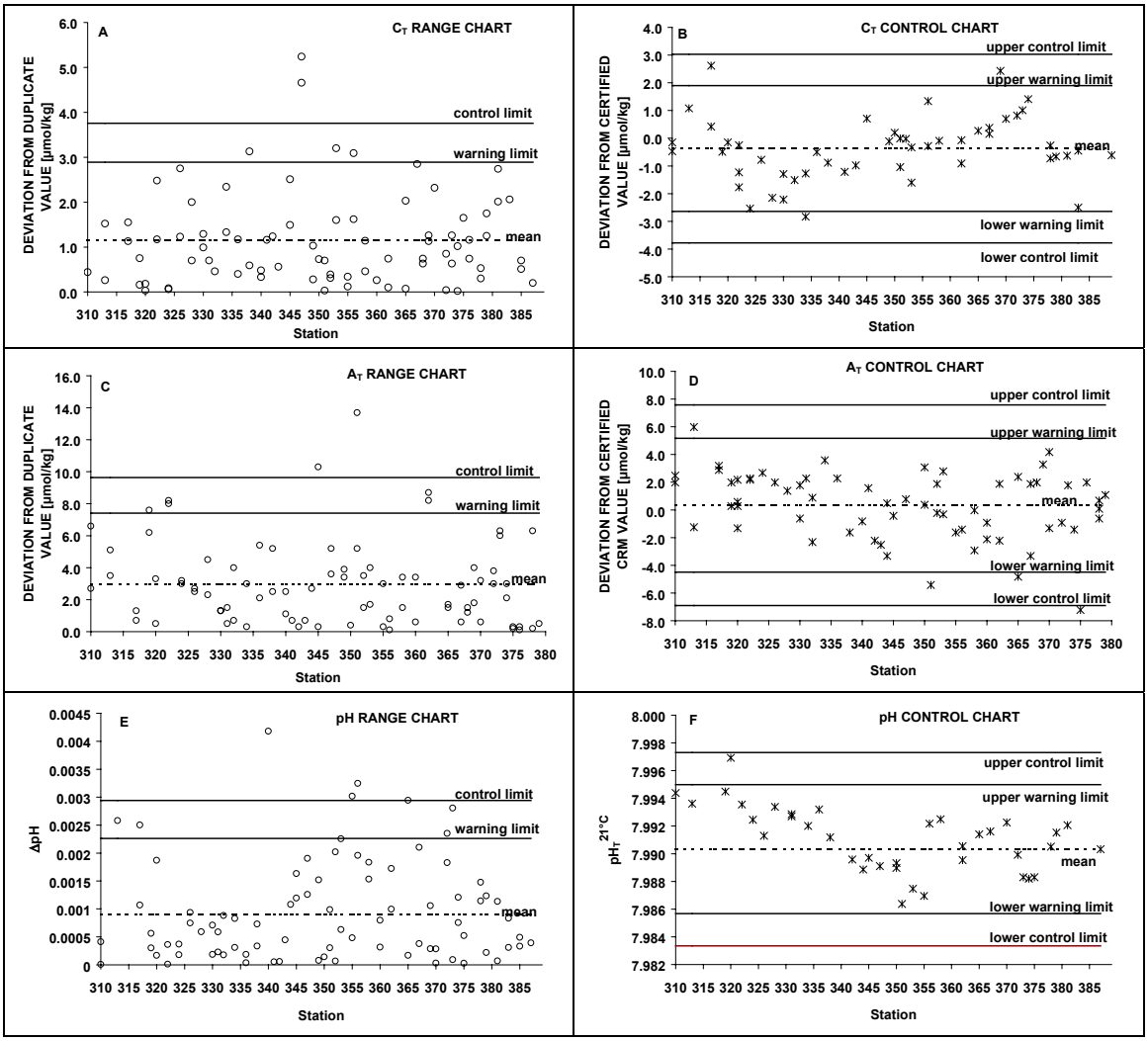

Fig. 4.19: A-F: Quality charts for C_T, A_T and pH_T analysis The range charts on the left-hand side are based on duplicate analysis of usually two niskin bottles per hydrocast. The control chart on the right-hand side are based on measurements of certified reference materials (CRM), that was at minimum one control measurement per hydrocast and parameter. Also shown are ‚warning' and ‚control limits', these are included according to a standard procedure for marine CO_2 parameter analysis in DOE (1994). The ‚warning limits' result in muliplying the standard deviation by two and the ‚control limits' by three. About 95 % of the plotted points should be within the warning limits.

Preliminary results of the C_T, A_T and pH analysis

A total number of 832 (n = 745) C_T samples, 798 (n = 723) A_T samples, and 850 (n = 768) pH samples we analyzed. A list of all stations where samples have been taken can be found in the listings.

For meridional transport calculations the transatlantic WOCE-A2 section has become a key section for the North Atlantic. The sections position is in between the subtropical and subpolar gyre at about 45 °N and describes the hydrographic situation of the meridional overturning cell near to regions of water mass formation. An overview of the A_T and C_T measurements on the quasi-zonal section is shown in Fig. 4.20. The **a**pparent **o**xygen **u**tilization [AOU = O_2^{sat} –

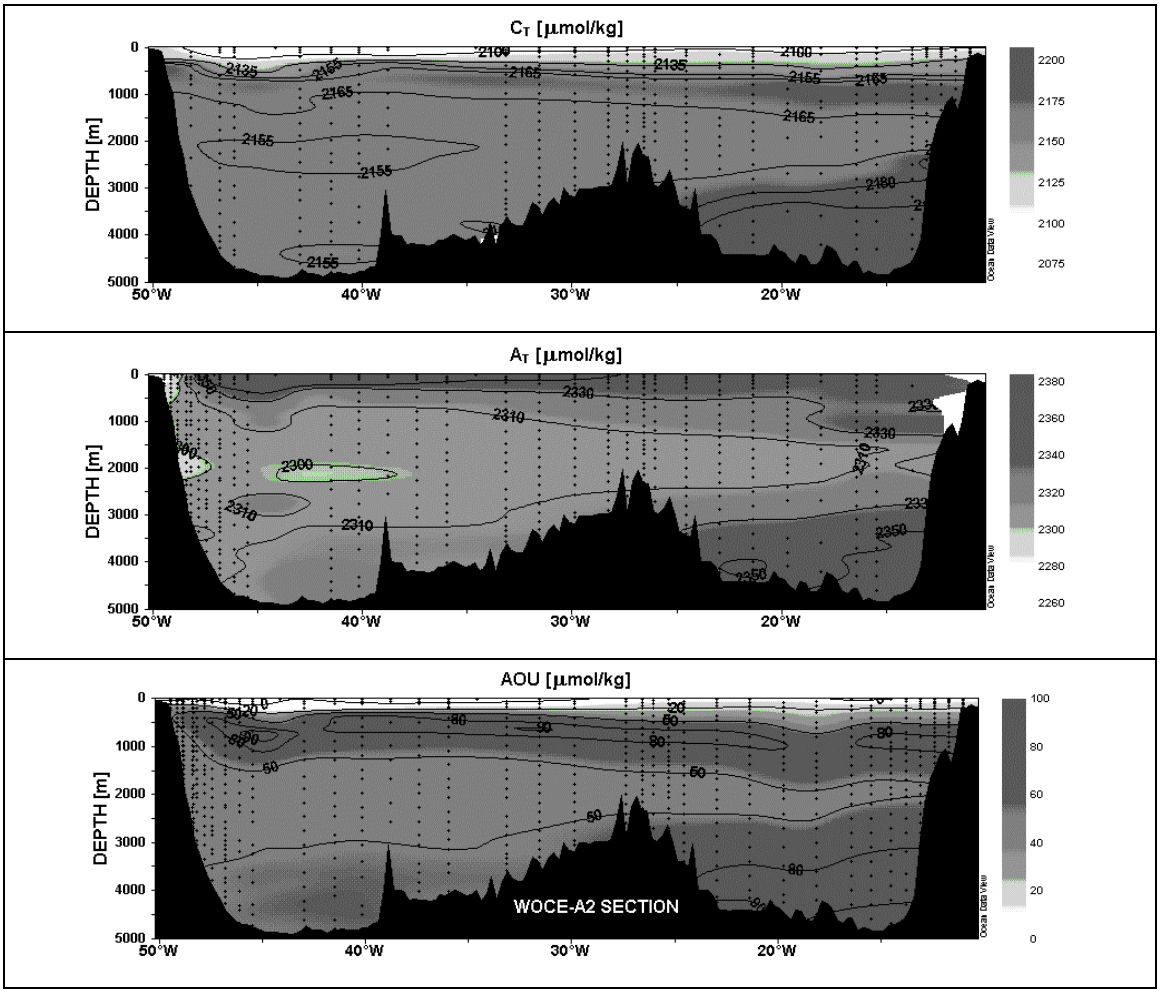

Fig. 4.20: Distribution of A_T and C_T and apparent oxygen utilization (AOU) on the transatlantic WOCE-A2 section. A back-calculation technique based on these parameters leads to an estimate of the ‚full' anthropogenic CO_2 signal, i.e. the additional CO_2 uptake from the beginning of the industrial revolution up to now (Poisson and Chen, 1987).

O_2^{meas}] in the third plot, is a direct measure of the respiration that took place in a water mass. High respiration (AOU) terms correspond with highest C_T and A_T values in the bottom waters of the eastern basin and indicate the old Antarctic Bottom Water component. Lowest AOU values at the sea surface agree with low C_T values and show the influence of photosynthesis on the carbonate system. CO_2 is transformed to organic carbon and therefore can not be seen by the inorganic C_T parameter. High A_T values in the sea surface express the minor influence of photosynthesis on this parameter. The surface near A_T values are mostly dependent on salinity (Friis, 2001) and in a minor part on temperature and biological processes of calcification and CO_2 assimilation/respiration. Below ~1000 m salinity changes are small with respect to carbonate chemistry and increasing A_T values with depth got an explanation by aragonite and calcite dissolution, that amplifies with depth and water mass age. In context of hydrology the three parameters in Fig. 4.20 mainly state the carbonate system. Therefore they are essential for different back-calculation techniques for the determination of anthropogenic CO_2 (Chen and Millero, 1979; Poisson and Chen, 1987; Gruber et al., 1996).

Preliminary results of the fCO_2 measurement

On leg 4 approximately 13.000 data points of sea surface (~5 m) pCO_2 and about 800 data-points of atmospheric pCO_2 were collected. Additionally ambient air pressure, sea surface temperature and sea surface salinity were measured. The results were already corrected on basis of three standards and transformed into the fugacity of CO_2 (fCO_2) in order to account for the non-ideal behavior of carbon dioxide as a gas. The fCO_2 of seawater is a function of temperature, total inorganic CO_2, alkalinity and salinity.

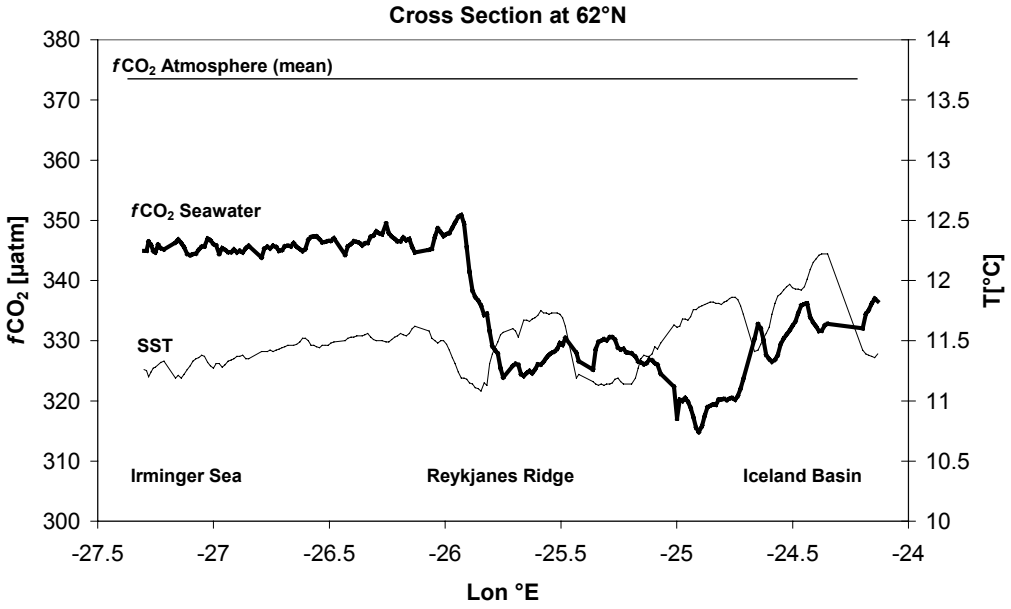

Fig. 4.21: Results of the continuous measurement crossing the Reykjanes Ridge at 62°N. The atmospheric fCO_2 data were averaged.

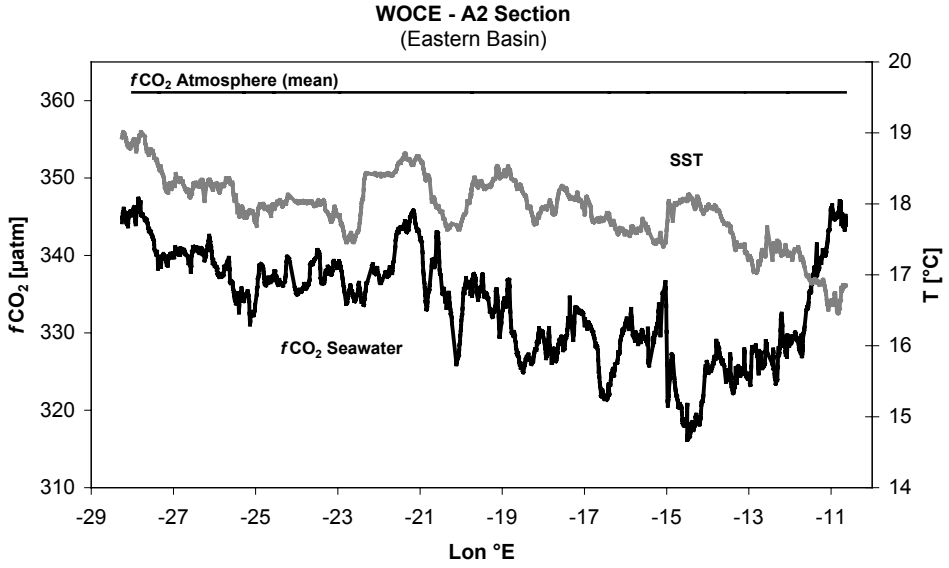

Fig. 4.22: Results of the fCO_2 measurement along 48°N. The first part of this section was measured during M50-1. The atmospheric fCO_2 data were averaged.

In open-ocean surface waters with only small changes in the alkalinity and salinity, the fCO_2 is primarily governed by changes in temperature and total inorganic CO_2 concentration (Stephens et al., 1995). The effect of temperature on the fCO_2 has been directly determined: the fCO_2 of seawater doubles for every 16°C increase in water temperature (Takahashi et al., 1993). In the North Atlantic one also finds that the fCO_2 varies over short distances. These variations can be attributed to patchiness in biological activity and episodic mixing events. The latter are correlated with chlorophyll concentrations and sea surface temperature, respectively.

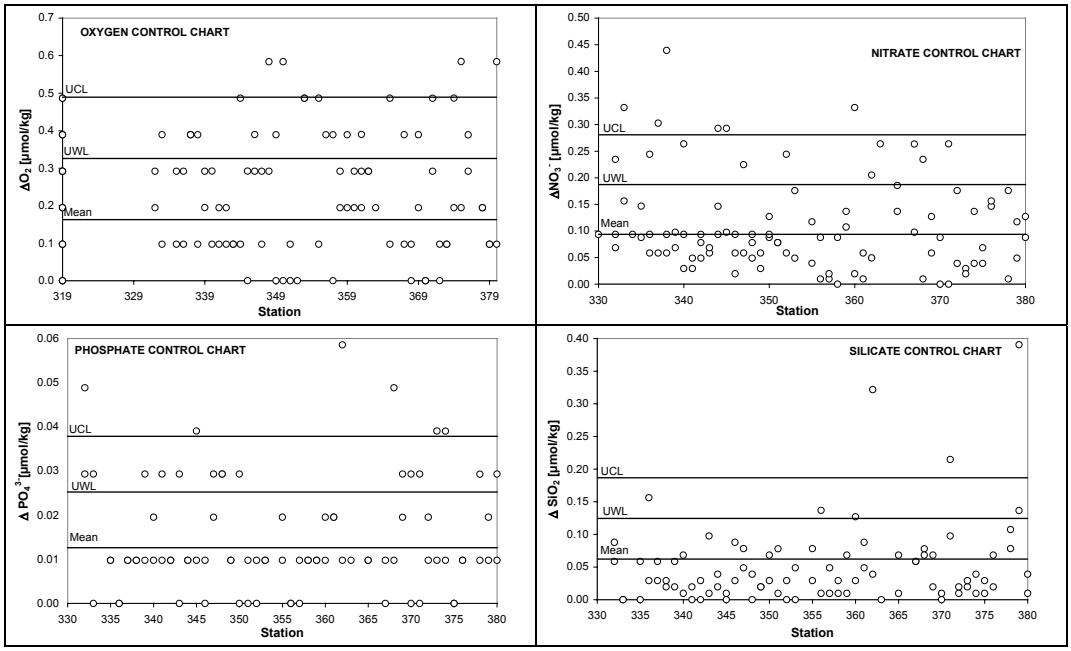

Fig. 4.23: Control charts for nutrients and oxygen (with mean deviations and control limits, see Fig. 4.20). The charts are based on measurements on duplicate samples.

The M50/4 cruise led us to the northern parts of the Irminger Sea, Iceland Basin and the eastern part of the WOCE-A2 section.

The section from the Irminger Sea to the Iceland Basin with a crossing of the Reykjanes Ridge is shown in Fig. 4.21. There is an obvious separation of the surface regimes of the two basins and the fCO_2 decreased by about 20 µatm in the Iceland Basin. The fCO_2 variability (differences of up to 50 µatm) is quite high and most of the time not thermo-dynamically related to the sea surface temperature.

The last part of the cruise went along the WOCE-A2 section. The corresponding fCO_2 results are shown in Fig. 4.22. Along this track there is a more or less constant undersaturation of about 30 µatm for the seawater fCO_2 compared to the atmosphere. The seawater fCO_2 follows most of the time the thermodynamic direction of sea surface temperature. The CO_2 fugacity reaches values as low as 316 µatm. Where a fCO_2 decrease does not have a counterpart in the sea surface temperature line probably biological activity is reflected. During a plankton bloom CO_2 fixation takes place and seawater fCO_2 values usually decrease to lower than 300 µatm. Hence Fig. 4.22 could record the beginning or the end a plankton bloom where the photosynthesis rate is reduced. The strong fCO_2 increase at about 14 °W to the European shelf can be explained by a inorganic (i.e. remineralized organic) freight along the continental margins.

Sample Collection and Storage of ^{13}C, ^{14}C, TOC and Chlorophyll Samples
On leg M50/4, 395 samples for ^{13}C mass spectrometer analysis were collected. Based on the ^{13}C data a priority list will be made for about 75 samples for ^{14}C mass spectrometer analysis, that can be done from the ^{13}C sample extract. Furthermore 194 TOC samples and 112 chlorophyll samples were stored.

Nutrients and Oxygen
Nutrients (nitrate, nitrite, phosphate, silicate) were determined from 1242 Niskin bottles. The nutrient analysis was made with an autoanalyzing system according to Grashoff et al. (1999). The accuracy for nutrient analysis was approximately 1 % of the nutrient standards. For precision estimates duplicate samples were taken and analyzed at about every tenth sample (Fig. 4.23). The corresponding accuracy and precision (± standard deviation / in brackets) estimates were 0.205 (± 0.09) µmol/kg for nitrate, 0.005 µmol/kg for nitrite, 0.025 (± 0.013) µmol/kg for phosphate and 0.5 (± 0.06) µmol/kg for silicate.

Oxygen was analyzed on 1270 niskin bottles according to a standard titration after Winkler (Grashoff et al., 1999). The measurements were done with a precision of ± 0.16 µmol/kg.

4.4.4 Methane analyses, seafloor observations and bathymetric mapping

(J. Greinert , K. Fürhaupter , B. Bannert)

The major task of the methane measurements during M50/4 was the study of methane plumes in the Mid-Atlantic-Rift Valley south of the Charlie-Gibbs-Fracture Zone (RV-CGFZ). Here, methane concentrations of 5 to 7 ppmv were observed between 2900 and 3200 m water depth during M39 and PO261 at two stations. These concentrations are up to four times enriched compared to the observed concentrations of approx. 1.5 ppmv usually found at this water depth. The higher concentrations were first discovered during METEOR cruise M39 in 1997 at station M39-260. Three years later the same position was sampled during cruise PO261 of FS POSEIDON (station 176), and equally high amounts of methane were found. At station PO261-170 further south, even higher concentrations of up to 7 ppmv were detected, and this raised questions: Where does the methane originate from, what is the source and are the methane expulsions permanent or temporary?

To get more information about the methane distribution, seven CTD casts were performed within the Rift Valley, two of them at the previously sampled stations. It was planned to use a TV-guided camera sled (OFOS) to observe the seafloor after the area with the strongest methane enrichment was found. Surveys with the multi-beam echosounder Hydrosweep were undertaken to map the seafloor where we hoped to find signs of the methane source during the OFOS observations. One possible methane source at mid ocean ridges is the mineral re-crystallisation of olivine to serpentine and magnetite which is called *serpentinisation*. This typical process at ultramafic rock hosted hydrothermal areas generates methane by CO_2 reduction with hydrogen released from the serpentinisation:

$$6[Mg_{0.5}Fe_{0.5}SiO_4] + 7\ H_2O \rightarrow 3[Mg_3Si_2O_5(OH)_4] + Fe_3O_4 + H_2$$

$$CO_2 + 4H_2 \rightarrow CH_4 + 2H_2O$$

In addition, the use of the OFOS system during M50/4 also served as a test for METEOR cruise M52 to the Black Sea during which seafloor observations will be an essential part.

In addition to our observations at the RV-CGFZ, we sampled and analysed CTD stations on all hydrographic sections, which were conducted in order to trace water masses using other chemical parameters as well. All in all we took samples from 50 CTD stations, deployed the OFOS once for a 2-mile long track and recorded multi beam data along approx. 200 miles at the RV-CGFZ.

Methods

Methane analyses

For the gas extraction we took water samples (1.2 l) from the CTD rosette in pre-evacuated 2 l glass bottles. In a degassing line these glass bottles were filled with supersaturated salt water and the escaping gas volume was measured in a burette. Gas samples were taken by gas-syringe and methane was analysed with a GC (*SHIMADZU*). The remaining gas was transferred to evacuated ampules for methane source reconstruction via isotope analyses which will be performed on shore. Before and after water samples from a CTD were measured we analysed at least three samples of a calibration gas which gave a accuracy of the GC analyses better than 0.05 ppmv or 3 %. The accuracy of the whole degassing method strongly depends on the goodness of the vacuum in the glass bottles for water sampling and their tightness. Unfortunately some samples were contaminated by atmospheric methane, which is particularly seen in higher gas volumes (> 24 ml). Those analyses were not used later.

OFOS

The Ocean Floor Observation System (OFOS) is used for TV-guided online observation of the seafloor. OFOS, an aluminium frame of 165 x 125 x 145 cm was equipped with a BW video camera, two Xenon lamps (OKTOPUS), an underwater slide camera with flash (BENTHOS), two laser pointers (OKTOPUS) and a FSI memory CTD. The telemetry works with 500 V and a separate cable for grounding was fixed between the telemetry and the wire and for additional security high voltage was switched on after the OFOS was in the water and was switched off before OFOS came on deck. For the seafloor observations themselves, OFOS is towed by the ship along a predefined track at less than 1 kn, and the distance to the bottom is manipulated by the winch. The observer can take slides manually via the deck unit and the video signal is permanently recorded on videotapes. Unfortunately the quality of the video signal was not as good as it could be. This depends on the electrical noise induced by electrical ship devices into the wire of winch 12. In particular we found a strong noise signal from the thermosalinograph in lab 7. Other possible sources of electrical noise could not be determined.

For further deployments and OFOS campaigns it is strongly recommended to shorten the wire of winch 12 to a maximum length of 8 km. Nevertheless, the deployment of OFOS showed that it and other TV-guided devices can be generally used successfully onboard FS METEOR.

HYDROSWEEP

One prerequisite for OFOS deployments is knowledge of the bathymetry. Thus we mapped the area at the R-GFZ where the OFOS might have been deployed by using the HYDROSWEEP system installed on FS METEOR. The data were roughly post processed using the software package 'HYDROMAP' and plotted with 'GMT'.

Results

Rift Valley south of the Gibbs-Fracture-Zone

The map in Fig. 4.24 shows the position of the CTD stations at the RV-CGFZ. At all stations higher methane concentrations were analysed between 2500 and 3600 m water depth with increasing concentrations to the south. In contrast to the former three stations, the concentrations did not exceed 4 ppmv and six of them did not even exceed 3.4 ppmv (Fig. 4.25). Nevertheless a significant methane signal was present at all stations. As shown by the methane distribution in Fig. 4.26, the rather equal methane signals below 2500 m water depth can be interpreted as methane generated further south, which slowly migrates to the north along the rift axis but below the rift crests, which form a 'methane-protecting' basin. The rift crest is generally above 2500 m water depth but shows a depression on the westward flank near 51.1°N were it drops down to 2700 m. This might be the reason for the depression of the upper 2 ppmv boundary in Fig. 4.26 at station M50-363 and may indicate that the bathymetry is an important factor for the methane distribution in rift valleys. The non-occurrence of higher methane concentrations further shows that methane generation by hydrothermal processes is not a permanent process and changes in time and space.

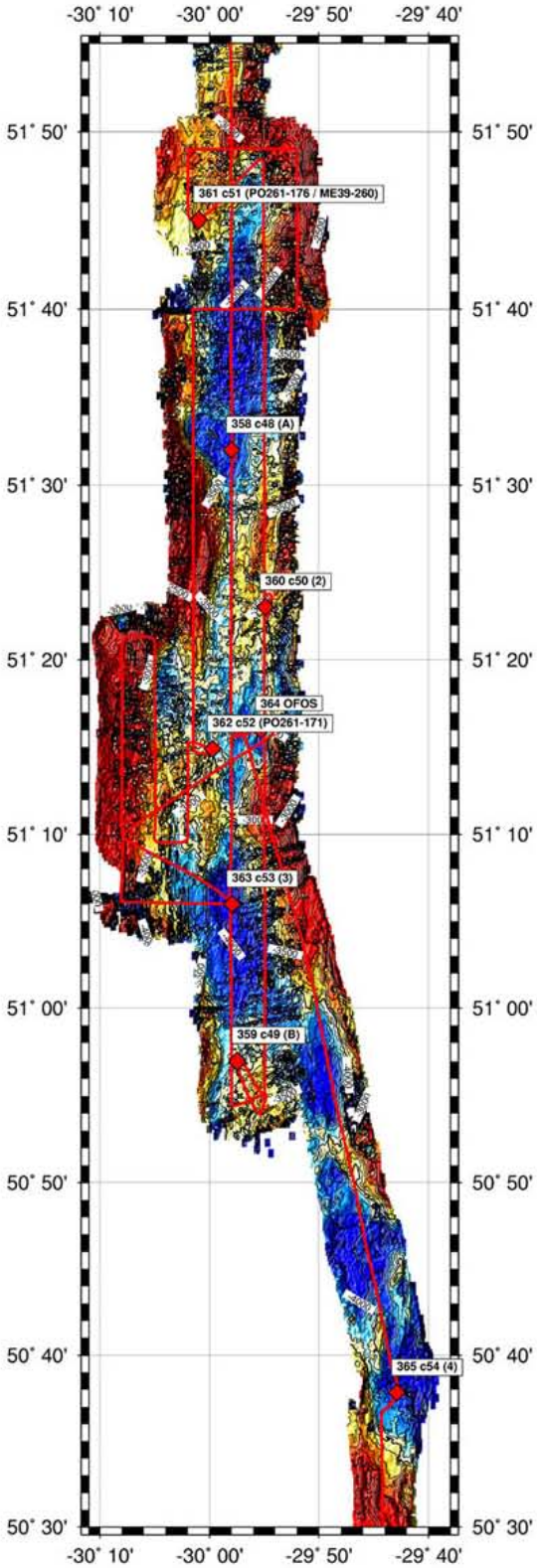

Fig. 4.24: Bathymetric map of the RV-CGFZ area with cruise track (red line) and CTD Stations. The bathymetric data are not yet edited.

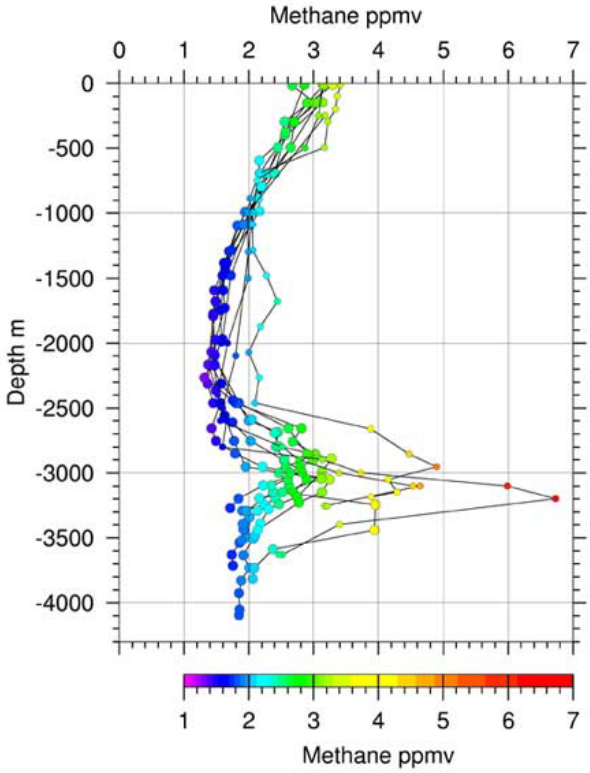

Fig. 4.25: Methane concentrations of all CTD stations at the RV-CGFZ. Smaller circles mark the samples from earlier soundings: PO261 and M39.

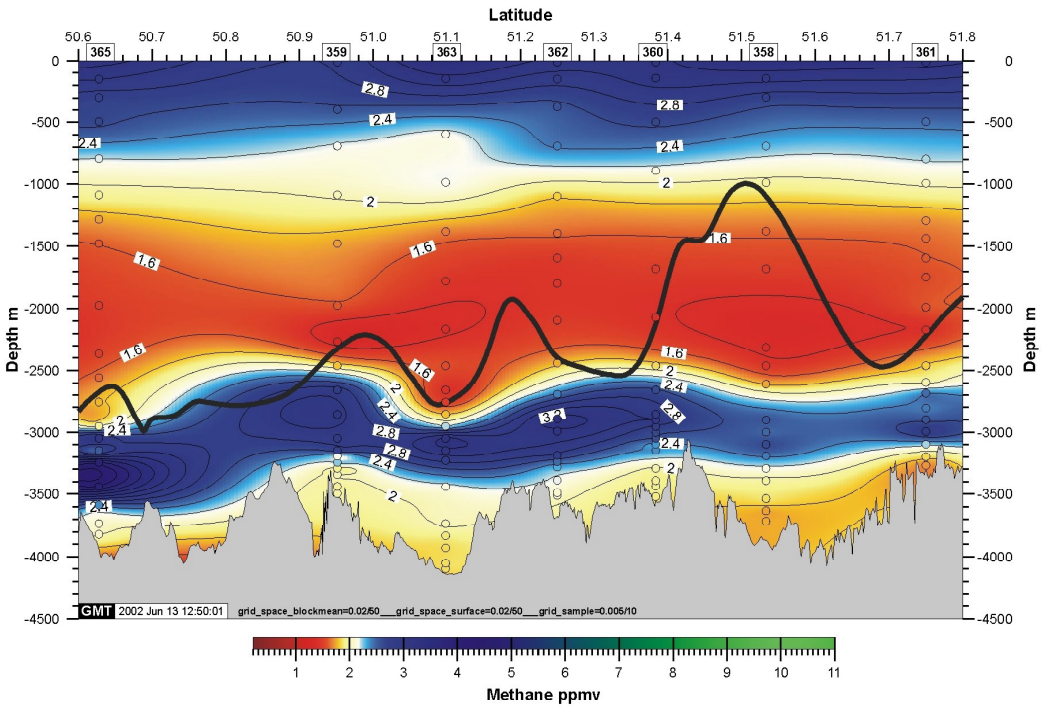

Fig. 4.26: Section of the methane distribution at the RV-CGFZ area, which shows significant methane enrichment below 2500 m water depth. The black line represents the western rift crest (taken from the gravimetric data published by Sandwell and Smith) indicating a relation between the seafloor morphology and the methane distribution.

After sampling CTD station 363 we deployed the OFOS at a rather shallow area at the eastward side of the rift valley, knowing that this area is below 3500 m water depth and thus below the methane maximum. However, we towed the OFOS for 2 miles above the bottom, which showed a small-scaled rough topography with up to 30 m high ridges build up by pillow lava (profile in Fig. 4.27). We found no visible signs of active hydrothermalism, but the OFOS system was successfully tested.

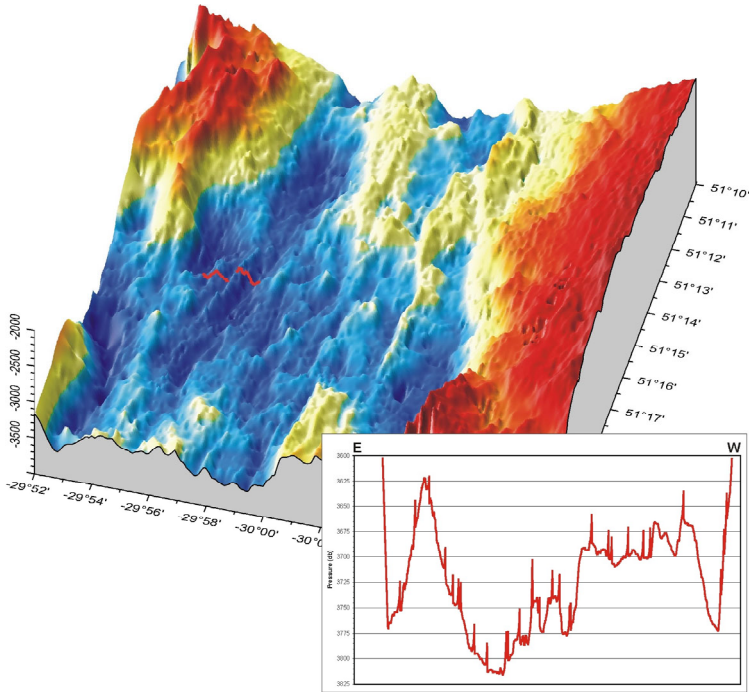

Fig. 4.27: 3D view of the Mid-Atlantic Rift valley (main figure) between 51°10' and 51°21' N showing axis parallel smaller ridges which were crossed by the OFOS deployment. The inserted pressure profile (right corner) was recorded by the FSI memory CTD. Spikes represent rapid heave movements.

Along section **A** in the Island Basin we sampled and analysed data from six CTD stations. The concentrations above 1500 m water depth appear to be typical for this area. The slightly increase below 1700 m at stations 336, 338 and 339 likely represent the ISOW correlating with increased salinity concentrations (Fig. 4.28).

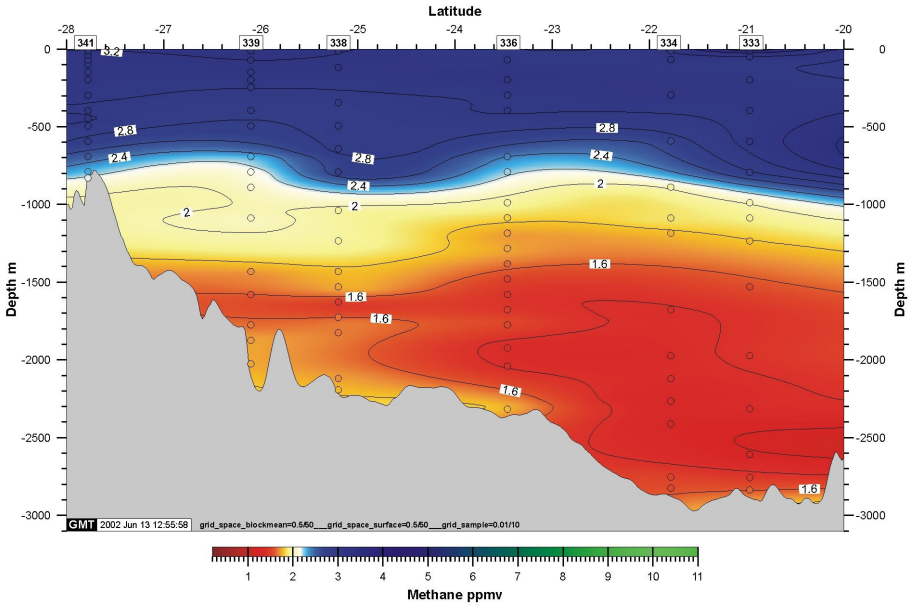

Fig. 4.28: Methane distribution at Section A, Island Basin.

Methane Distribution along WOCE A2

The general methane distribution at the WOCE A2 section shows a continuous decrease from 3 ppmv at the surface and 0.4 ppmv at the abyssal plain. At Station 368 located in the rift valley, we analysed again higher methane concentrations of up to 2.3 ppmv between 2000 and 3100 m water depth below the rift crest. This is similar to the concentrations from the RV-CGFZ area and likely represent a usual phenomena of elevated methane concentrations in rifts of mid ocean ridges. However, the highest methane concentrations during M50/4 were measured at the continental slope between 500 and 1000 m water depth at Station 387 with values of up to 10.14 ppmv. Up to now we do not know the source of these high methane concentrations. The forthcoming stable isotope analyses may provide an indication as to this methane source.

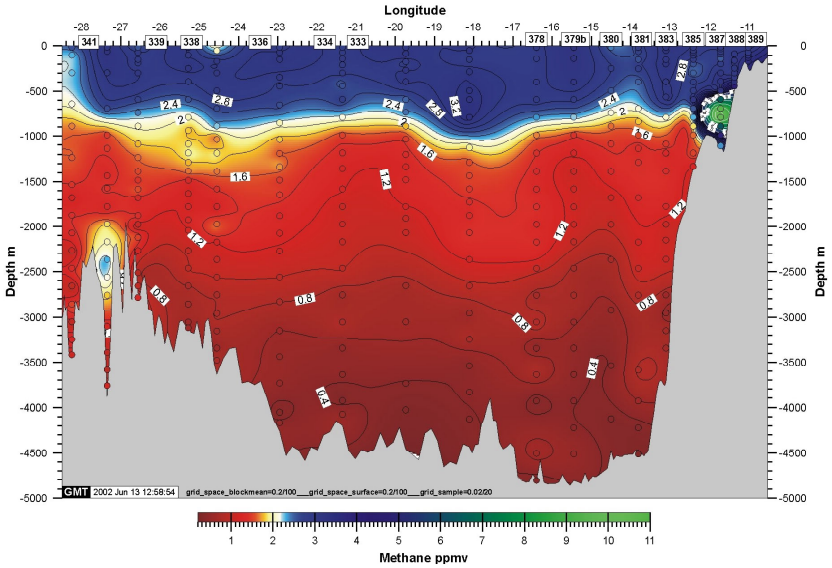

Fig. 4.29: Methane distribution at WOCE A2. Higher methane concentrations were analysed again in the rift valley and at the continental slope with more than 10 ppmv.

4.4.5 Natural Radionuclides

(J. Schaftstall, J. Scholten)

Natural radionuclide are useful tracers for the investigation of the pathways of particle reactive matter in the water column. Their major advantage is their well known production rate in the water-column; and information on particle residence times and scavenging rates can be obtained by comparing the concentration of e. g. ^{230}Th with its production rate from the decay of ^{238}U . In contrast to most of the oceanic environments the North Atlantic is characterised by relatively rapid ventilation of deep water masses which has a severe influence on the distribution of particle reactive elements.

In order to investigate the interannual changes in the concentration as well as the distribution of ^{230}Th along the flow path of the Labrador Sea and Island-Scotland Overflow water masses water samples were obtained during the Meteor cruise 50/4 in the Iceland Basin, near the Charlie-Gibbs Fracture Zone and on a transect along 48° N (cf large circles in Fig. 4.1).

Water samples were sampled in up to seven depth levels between 100m and 3000m. About 10 l of water were filled in pre-cleaned plastic containers, acidified and stored for further analyses in the home labs.

Table 4.2: Locations of radionuclide water samples

Station M50/4	No.	Bottle	Depth (m)	Station M50/4	No.	Bottle	Depth (m)
327	1	21	100	**332**	1	13	100
21°51.0E 60°46.9N	2	19	500	20°11.9E 58°58.9N	2	11	500
2292 m	3	17	700	2827 m	3	9	700
	4	14	1000		4	7	1000
	5	10	1500		5	5	1500
	6	6	2000		6	4	2000
355				**366**			
30°04.9E 53°12.2N	1	17	100	29°42.1E 48°59.7N	1	10	100
3116 m	2	20	500	3025	2	9	500
	3	15	700		3	8	700
	4	13	1000		4	7	1000
	5	10	1500		5	5	1500
	6	7	2000		6	4	2000
	7	3	2800		7	2	2800
370	1	21	100	**379**	1	6	100
26°02.1E 46°60.0N	2	17	500	15°26.9E 48°33.0N	2	5	500
3257	3	14	1000	4790	3	4	1000
	4	10	1500		4	3	1500
	5	7	2000		5	2	2000
	6	3	3000		6	1	3000

4.5 Weather and Ice Conditions during M50/4

When METEOR left Reykjavik heading for Denmark Strait on July 17, there was a gale center of 990 hPa near of Cape Clear, Eire, dominating all of the Western Approaches as well as the Bay of Biscay. A secondary low of 1009 hPa was situated at 58 North 24 West, whereas highs could be found of over 1025 in the Norwegian Sea and the Azores High of 1033 hPa, extending a wedge of 1025 hPa to 56 North 40 West. As the high over Greenland was not very strong, the ship experienced light easterly winds while working in Denmark Strait, these only temporarily being up to 6 Bft on July 19 and thus not hampering operations. The Ice Conditions were such that one of the mooring arrays to be retrieved and employed again could not be reached. An ice promontory rendered the ship's movement in that direction impossible so that the mooring array had to be left unserviced.

The next regions where hydrographic work was being carried out were the Reykjanes Ridge and the Iceland Basin. After retrieval of mooring arrays being deployed by POSEIDON a year earlier two hydrographic sections were made, these being repetitions of sections A and B done during M39 four years ago, thus enabling comparisons of conditions varying with time. The sections ranged from the Rift Valley of the Reykjanes Ridge through the Iceland Basin to its eastern margin. While the METEOR was working, winds were moderate, and direction was varying. The exception was July 26 when a complex gale center of 980 hPa had developed south of Greenland, extending a warm front to our research ship's position so that we observed

southeasterly gales up to 7 Bft, veering to strong southwesterly winds 6 Bft the next day. By then, one gale center had turned northeast into the Irminger Sea where is started to fill. The METEOR experienced lesser winds only on July 27 when a minor secondary low passed her. This was not the only one of its kind, however, for during July 28 another wave along the cold front developed quickly into a gale center of 988 hPa near southeastern Iceland so that at the vessel's position southwesterly gales up to 8 Bft were experienced. By July 29, winds were down to westerly 5 Bft again. The new gale center then dominated the Norwegian Sea for quite a few days.

The METEOR had by now reached her next area of investigation, the 'GEOMAR-Box' in the Charlie Gibbs Fracture Zone (CGFZ). The CGFZ has two abyssal channels connecting basins on both sides of the Mid Atlantic Ridge, and the GEOMAR-Box contains a valley connecting those two channels, thus separating the relative high elevation between the channels into two hills. So the CGFZ and the 'GEOMAR-Box' are key areas regarding exchange of water masses in the deep in a zonal direction. As the METEOR took her time probing this area, winds were light and variable during July 30 due to a wedge of high pressure extending from the Azores High. This prominent feature of the synoptic chart had strengthened to 1033 north of the archipelago so that the next low to migrate east from Labrador had to stay north of the 55th parallel, its intensity of 1010 hPa varying little. For our ship this meant moderate westerly winds during July 31 and August 01.

There was one task still to be done: During M50/1 a hydrographic section had been surveyed extending from about 42 North 46 West to 46 North 30 West. This had been the western part of the WOCE-Project A2 hydrographic section, and now in M50/4 the research vessel completed it across the West European Basin and up the shelf regions south of Eire. It took the METEOR up to August 07 to reach a position just east of where she had turned to Labrador during M50/1 and to complete that section. During these Days the Azores High concentrated on the Archipelago again and weakened somewhat. Meanwhile a low had formed on the U.S. Eastern Seaboard and moved northeast, its central pressure being down to 1015 hPa south of Newfoundland on August 02. Another Low moving east from the area west of the Hudson Bay had intensified to 995 hPa over Labrador. This one intensified further to 990 on August 03, and it managed to integrate the low from Newfoundland into its circulation. In this way it gained an influx of subtropical air masses, and therefore it intensified to 985 hPa on August 04 southwest of Greenland. Our ship experienced moderate westerly winds, backing during that day. The gale center stalled and began filling, and only when central pressure had reached 995 hPa again it continued to move east on August 05. The low slowly filled further, METEOR observing moderate to strong southwesterly winds until the low reached Eire on August 07, central pressure being 1000 hPa. By then its cold front had passed our ship so that strong westerly to northwesterly wind of 6 Bft gusting to 8 Bft in showers were reported when probing work ended late that evening.

The low was forecast to move past the North Sea into the Skaw and then on into northern Scandinavia, so that the METEOR would experience northwesterly winds right into the North Sea, but diminishing to 4 Bft there and backing while the ship reached the Elbe estuary.

4.6 Station List

Table 4.3: CTD inventory

Station	Cast	Date 2001	Time UTC	Latitude North	Longitude West	m	Inst. Depth (m)
309	1	19/07	00:19	66° 20.54’	028° -02.26’	348	319
310	2	19/07	02:19	66° 13.86’	027° 31.25’	502	477
311	3	19/07	04:02	66° 11.86’	027° 22.22’	499	477
312	4	19/07	05:13	66° 09.97’	027° 13.74’	515	489
313	5	19/07	06:28	66° 07.91’	027° 04.91’	638	610
314	6	19/07	08:11	66° 03.52’	026° 46.89’	533	519
317	7	19/07	22:12	65° 59.98’	026° 30.41’	275	265
318	8	19/07	23:59	65 56.98	026° 14.84’	308	294
319	9	20/07	10:34	64° 52.84’	029° 59.92’	2062	2040
320	10	20/07	20:10	63° 34.67’	029° 59.56’	2173	2145
322	11	21/07	22:00	62° 33.10’	023° 45.77’	1314	1280
323	12	22/07	01:42	62° 10.04’	023° 16.11’	1466	1461
324	13	22/07	05:45	61° 45.89’	022° 46.15’	1746	1741
325	14	22/07	09:36	61° 21.97’	022° 29.59’	1861	1833
326	15	22/07	13:34	61° 00.92’	022° 09.10’	2040	2022
327	16	22/07	16:40	60° 46.90’	021° 51.02’	2296	2266
328	17	22/07	20:18	60° 27.19’	021° 39.62’	2560	2535
329	18	23/07	00:20	60° 11.91’	021 -15.02’	2719	2703
330	19	23/07	05:17	59° 43.11’	020° 54.81’	2834	2810
331	20	23/07	09:42	59° 19.97’	020 33.11’	2828	2817
332	21	23/07	14:21	58° 58.02’	020 11.93’	2828	2000
332	22	23/07	16:48	58° 58.06’	020 11.89’	2829	2805
333	23	23/07	21:13	58° 46.94’	020° 57.87’	2871	2847
334	24	24/07	02:32	59° 06.08’	021° 46.72’	2883	2887
335	25	24/07	07:40	59° 24.99’	022° 37.03’	2549	2525
336	26	24/07	12:38	59° 43.00’	023° 27.96’	2357	2352
337	27	24/07	17:22	60° 00.98’	024° 20.21’	2180	2150
338	28	24/07	21:52	60° 18.99’	025° 12.75’	2123	2202
339	29	25/07	02:36	60° 36.00’	026° 06.16’	2083	2092
340	30	25/07	07:14	60° 52.90’	027° 01.11’	1431	1403
341	31	25/07	10:54	61° 07.76’	027° 46.73’	842	834
342	32	25/07	16:15	60° 27.87’	028° 45.99’	1147	1128
343	33	25/07	22:27	59° 40.06’	029° 48.95’	1060	1067
344	34	26/07	20:38	59° 22.00’	028° 57.07’	1801	1799
345	35	26/07	07:19	59° 04.07’	028° 05.09’	2020	2000
346	36	26/07	12:22	58° 45.08’	027° 15.18‘	2231	2240
347	37	26/07	18:20	58° 27.00’	026° 24.96‘	2615	2589

Station	Cast	Date 2001	Time UTC	Latitude North	Longitude West	WD m	Inst. depth (m)
348	38	26/07	23:25	58° 06.99’	025° 36.13’	2711	2693
349	39	27/07	05:43	57° 48.07’	024° 47.94’	2806	2775
350	40	27/07	11:27	57° 32.01’	023° 59.99’	2903	2887
351	41	27/07	16:50	57° 14.04’	023° 09.96‘	3055	3035
352	42	28/07	08:47	56° 12.88‘	026° 37.05‘	2992	2969
353	43	28/07	19:23	55° 23.61‘	027° 56.50‘	2801	2773
354	44	29/07	10:40	54° 45.94‘	030° 25.10‘	2871	2844
355	45	29/07	21:16	53° 12.01‘	030° 04.97‘	3116	3095
356	46	30/07	03:56	52° 26.42‘	029° 50.19‘	3814	3792
357	47	30/07	08:52	52° 03.85‘	029° 40.26‘	3722	3709
358	48	30/07	15:55	51° 31.98‘	029° 58.04‘	3749	3728
359	49	30/07	23:43	50° 57.06‘	029° 57.66‘	3516	3508
360	50	31/07	06:19	51° 23.01‘	029° 54.90‘	3768	3530
361	51	31/07	12:28	51° 45.00‘	030° 00.96‘	3276	3325
362	52	31/07	20:50	51‘ 14.98‘	029° 59.57‘	3467	3520
363	53	01/08	04:18	51° 05.88‘	029° 57.95‘	4138	4109
365	54	01/08	18:14	50° 37.80‘	029° 42.92‘	3822	3840
366	55	02/08	05:37	48° 59.94‘	029° 43.06‘	3025	2986
367	56	02/08	20:16	46° 39.94‘	028° 14.96‘	3431	3420
368	57	03/08	02:21	46° 39.02‘	027° 21.04‘	3864	3827
369	58	03/08	07:58	46° 49.88‘	026° 33.92‘	2903	2791
370	59	03/08	12:19	46° 59.94‘	026° 01.94‘	3257	3252
371	60	03/08	17:25	47° 05.98‘	025° 16.90‘	3149	3127
372	61	03/08	22:20	47° 12.99‘	024° 33.04‘	3487	3488
373	62	04/08	06:59	47° 26.89‘	022° 56.98‘	4177	4176
374	63	04/08	15:57	47° 41.00‘	021° 20.91‘	4109	4087
375	64	05/08	00:37	47° 54.96‘	019° 43.95‘	4289	4378
376	65	05/08	09:18	48° 10.04‘	018° 06.89‘	4417	4438
377	66	05/08	15:00	48° 15.98‘	017° 20.86‘	4350	4369
378	67	05/08	21:22	48° 25.03‘	016° 23.84‘	4792	4822
379	68	06/08	04:14	48° 33.04‘	015° 26.93‘	4790	3010
379	69	06/08	06:43	48° 33.01‘	015° 26.98‘	4788	4818
380	70	06/08	13:54	48° 40.98‘	014° 30.00‘	4589	4603
381	71	06/08	19:35	48° 46.99‘	013° 47.12‘	4501	4528

Station	Cast	Date 2001	Time UTC	Latitude North	Longitude West	WD m	Inst. depth (m)
382	72	07/08	00:15	48° 50.14‘	013° 26.82‘	4427	4452
383	73	07/08	04:35	48° 52.94‘	013° 05.77‘	3650	3643
384	74	07/08	08:28	48° 56.04‘	012° 45.02‘	2036	2025
385	75	07/08	11:28	48° 59.06‘	012° 23.93‘	1341	1335
386	76	07/08	14:18	49° 02.04‘	012° 03.14‘	982	980
387	77	07/08	16:45	49° 05.05‘	011° 42.15‘	1129	1112
388	78	07/08	19:17	49° 07.99‘	011° 20.98‘	469	446
389	79	07/08	21:16	49° 10.90‘	011° 00.05‘	177	168
390	80	07/08	23:19	49° 13.98‘	010° 38.84‘	158	145

Table 4.4: Mooring Activities

Sta. No.	Int. No.	IfM No.	Date	Time	Latitude North	Longitude West	Depth (m)	Instr. Type	Remarks incl. nominal instr. depth
307			18/07	15:25	66° 11.59‘	027° 35.59‘	501		Test OFOS ok, Benthos release failed., 499m
307	SK	V423_2	18/07	20:50	66° 11.60‘	027° 35.50'	498	WH-ADCP	V423_2/SK/shield with ADCP 150kHz set ARGOS - WD-ID: Dec: 9243 Hex: 906C0
308	PIES006	V421_2	18/07	22:46	66° 14.00‘	027° 45.00‘	487	P/IES	V421_2/PIES006/shield set, 472m
315	LR	V425_2	19/07	11:09	66° 07.60‘	027° 16.20‘	582	LR-ADCP	V425_2/LR set, ADCP 75 kHz set ARGOS - WD-ID: Dec: 1176 Hex: 12618
316	PIES005	V422_2	19/07	12:44	66° 06.50‘	027° 10.50‘	625	P/IES	V422_2/PIES005 set, 610m
	TK		19/07	1930	66° 31.50‘	025° 26.00‘			fail to recover V424_1 because of ice coverage

Table 4.5: APEX- and RAFOS Float Launches

Sta. No.	CTD Cast	IfM No.	Date 2001	Time (UTC)	Latitude North	Longitude West	Argos (Dec.)	Argos (Hex.)	WMO tag	Cycle (days)	WRC S/N	Surface Temperature [°C]	Salinity	Remarks
APEX float launches ↓														
319	9	313	20/07	12:12	64° 53.10‘	030° 00.29‘	12624	C5404	6900157	10	0570	11.3	34.97	Irminger Basin
320	10	323	20/07	21:57	63° 34.63‘	029° 57.61‘	12626	C54A2	6900158	10	0571	10.9	34.96	Irminger Basin
327	16	311	22/07	18:19	60° 46.89‘	021° 51.00‘	12622	C53AC	6900155	10	0568	12.2	35.13	Iceland Basin “I“
346	36	312	26/07	14:11	58° 44.89‘	027° 14.94‘	12623	C53FF	6900156	10	0569	13.2	35.12	Iceland Basin “B“
350	40	310	27/07	13:44	57° 31.78‘	023° 59.65‘	12614	C5192	6900154	10	0567	14.0	35.05	Maury Channel “B“
354	44	326	29/07	12:39	54° 45.80‘	030° 25.18‘	12629	C5548	6900161	10	0574	13.4	33.93	Central Iceland Basin
365	54	324	01/08	20:57	50° 36.88‘	029° 43.80‘	12627	C54F1	6900159	10	0572	15.8	35.36	Mid Atlantic Ridge
367	56	325	02/08	22:52	46° 40.00‘	028° 15.04‘	12628	C55IB	6900160	10	0573	19.4	35.68	
373	72	308	04/08	09:57	47° 25.08‘	022° 57.74‘	07467	74AE1	6900152	10	0565	18.3	35.73	
379	69	309	06/08	10:01	48° 32.69‘	015° 26.94'	12611	C50DE	6900153	10	0566	18.1	35.61	
RAFOS float launches ↓										Mission (month)	SeaScan S/N	***Nominal Depth*** (m)		
325	014	534	22/07	11:14	61° 22.29‘	022° 29.58‘	5462	55599		14	RF # 49	1500		Reykjanes Ridge “I“
333	023	532	23/07	23:27	58° 46.99‘	020° 58.03‘	4989	4DF63		21	RF # 47	2600		Maury Channel
339	029	536	25/07	04:13	60° 36.07‘	025° 06.15‘	5467	556EB		12	RF # 51	1500		Reykjanes Ridge “A“
346	036	537	26/07	14:06	58° 44.89‘	027° 14.98‘	5481	55A6F		12	RF # 52	1500		Reykjanes Ridge “B“
349	039	533	27/07	07:37	57° 47.97‘	024°.47.56‘	5460	5553F		21	RF # 48	2600		deep Iceland Basin
353	043	535	28/07	21:34	55° 22.34‘	027° 57.04‘	5463	555CA		21	RF # 50	2600		deep Iceland Basin
355	45	538	29/07	23:40	53° 12.25‘	030° 05.03‘	5482	55A9A		21	RF # 53	2600		Near mooring “C“
357	47	539	30/07	11:38	52° 03.52‘	029° 39.76‘	5486	55B85		21	RF # 54	2600		Near mooring “Z“

4.7 Concluding Remarks

Leg 4 of METEOR cruise 50 served a multi-disciplinary team, all involved research questions of the North Atlanic. It is our common pleasure to thank *Kapitän* N. Jakobi and *Koordinator* F. Schott and their crews for excellent cooperation and assistance. Our Irish observer H. Cannaby was of great help in support of the CTD group on board. Funding of ship time and logistics was kindly provided by the *Deutsche Forschungsgemeinschaft.* All APEX floats deployed during M 50/4 were financed by a grand from the European Commission, Research Directorate-General (contract no. EVK2-CT-2000-00087 – GYROSCOPE).

4.8 References

Davis, R. and W. Zenk, 2001: Subsurface Lagrangian Observations during the 1990s. In: Siedler, G., Church, J., Gould, J. (Ed), Ocean Circulation and Climate, Academic Press, pp. 123-139.

Dickson, A.G., 1990. The oceanic carbon dioxide system: planning for quality data, JGOFS News, (2): 2.

Doe, 1994. Handbook of methods for the analysis of various parameters of the carbon dioxide system in seawater. ORNL/CDIAC-74, U. S. Dep. of Energy, Oak Ridge Natl. Lab., Oak Ridge, Tenn., USA.

Friis, K., 2001. Separation von anthropogenem CO_2 im Nordatlantik – Methodische Entwicklungen und Messungen. Dissertation. Christian-Albrechts-Universität zu Kiel, Kiel, 137 pp.

Grasshoff, K., Kremling, K. and Ehrhardt, M. (1999): Methods of seawater analysis. 3rd edition, Wiley-VCH, Weinheim.

Johnson, K.M., Wills, K.D., Butler, D.B., Johnson, W.K. and Wong, C.S., 1993. Coulometric total carbon dioxide analysis for marine studies: Maximizing the performance of an automated gas extraction system and coulometric detector. Mar. Chem., 44(2-4): 167-188.

Körtzinger, A., Thomas, H., Schneider, B., Gronau, N., Mintrop, L. and Duinker, J.C., 1996. At-sea intercomparison of two newly designed underway pCO2 systems - encouraging results. Mar. Chem., 52(2): 133-145.

Lewis, E. and Wallace, D.W.R., 1998. CO2SYS - Program developed for the CO2 system calculations. Carbon Dioxide Inf. Anal. Center; Report ORNL/CDIAC-105, Oak Ridge, Tenn., U.S.A.

Lorbacher, K, 2000: Niederfrequente Variabilität meridionaler Transporte in der Divergenzzone des nordatlantischen Subtropen- und Subpolarwirbels. Berichte des BSH , 22, 156 pp.

Millero, F.J., Byrne, R.H., Wanninkhof, R., Feely, R., Clayton, T., Murphy, P. and Lamb, M.F., 1993. The internal consistency of CO2 measurements in the Equatorial Pacific. Mar. Chem., 44(2-4): 269-280.

Mintrop, L., Perez, F.F., Gonzalez-Davila, M., Santana-Casiano, J.M. and Körtzinger, A., 2000. Alkalinity determination by potentiometry: intercalibration using three different methods. Ciencias Marinas, 26(1): 23-37.

Müller, T.J. 1999: Determination of salinity. In: Grasshoff, K., K. Kremling and M. Erhardt (Eds.): Methods of seawater analysis, 3rd edition, ch. 3, pp 41-73, Wiley-VCH, Weinheim.

Stephens, M.P., G. Samuels, D.B. Olson, R.A. Fine, 1995. Sea-air flux of CO_2 in the North Pacific using shipboard and satellite data. J. Geophys. Res. III, 100 (7): 13,571-13,583.

Takahashi, T., J. Olafsson, J.G. Goddard, D.W. Chipman, and S.C. Sutherland, 1993. Seasonal variation of CO_2 and nutrients in the high-latitude surface oceans: A comparative study. Global Biogeochem. Cycles, 7: 843-878.